Biological hotspots in the deep sea

Environmental controls and interactions in deep-sea sponge and coral assemblages

Ulrike Beatrix Hanz

2021

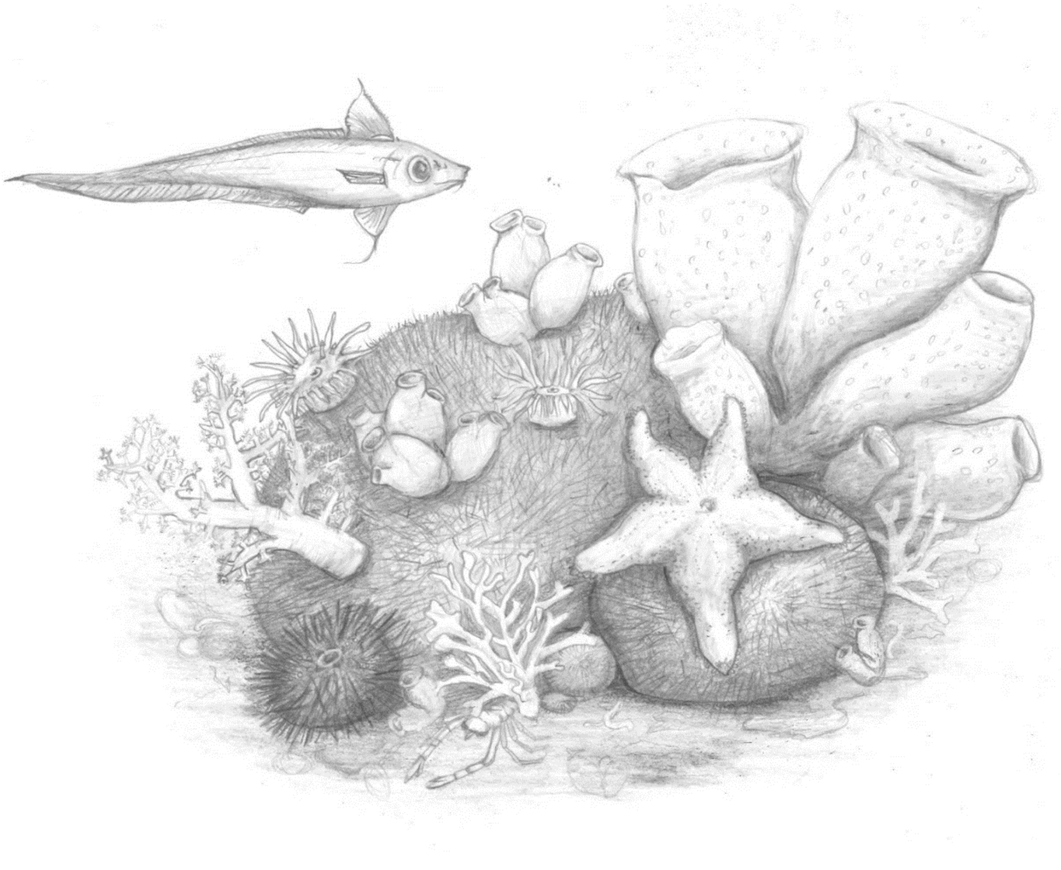

Members of the assessment committee:
Prof. dr. ir. S. Schouten, University Utrecht
Prof. dr. T. Murk, Wageningen University
Prof. dr. N.J. de Voogd, Naturalis/University Leiden
Prof. dr. U. Hentschel, GEOMAR Kiel
Dr. M. Maldonado, Centro de Estudios Avanzados de Blanes (CEAB)

ISBN : 978-90-6266-609-6

Cover design : Margot Stoete & Ulrike Hanz
Layout: Ulrike Hanz
Printing: Ipskamp Printing

Biological hotspots in the deep sea
Environmental controls and interactions in deep-sea sponge and coral assemblages

Biologische hotspots in de diepzee
Milieufactoren en interacties in diepzee spons- en koraal gemeenschappen
(met een samenvatting in het Nederlands)

Biologische Hotspots in der Tiefsee
Umweltkontrollen und Interaktionen in Schwamm- und Korallengemeinschaften der Tiefsee
(mit einer Zusammenfassung in Deutsch)

Proefschrift

ter verkrijging van de graad van doctor aan de
Universiteit Utrecht
op gezag van de
rector magnificus, prof.dr. H.R.B.M. Kummeling,
ingevolge het besluit van het college voor promoties
in het openbaar te verdedigen op

vrijdag 12 november 2021 des middags te 2.15 uur

door

Ulrike Beatrix Hanz

geboren op 1 april 1989
te Bonn, Duitsland

Promotor:
Prof. dr. G.J. Reichart

Copromotor:
Dr. F. Mienis

This research has been performed in the scope of the SponGES project, which received funding from the European Union's Horizon 2020 research and innovation program under grant agreement No. 679849.

Table of Contents

Summary 8

Samenvatting in het Nederlands 14

Zusammenfassung auf Deutsch 21

Chapter 1 29

Introduction

Chapter 2 53

Environmental factors influencing cold-water coral ecosystems in the oxygen minimum zones on the Angolan and Namibian margins
Ulrike Hanz, Claudia Wienberg, Dierk Hebbeln, Gerard Duineveld, Marc Lavaleye, Katriina Juva, Wolf-Christian Dullo, André Freiwald, Leonardo Tamborrino, Gert-Jan Reichart, Sascha Flögel and Furu Mienis

Chapter 3 89

Seasonal Variability in Near-bed Environmental Conditions in the *Vazella pourtalesii* Glass Sponge Grounds of the Scotian Shelf
Ulrike Hanz, Lindsay Beazley, Ellen Kenchington, Gerard Duineveld, Hans Tore Rapp† and Furu Mienis

Chapter 4 119

Long-term Observations Reveal Environmental Conditions and Food Supply Mechanisms at an Arctic Deep-Sea Sponge Ground
Ulrike Hanz , Emyr Martyn Roberts, Gerard Duineveld, Andrew Davies, Hans van Haren, Hans Tore Rapp†, Gert-Jan Reichart and Furu Mienis

Chapter 5 **151**

Are sponges at the top and bottom of the food web in a benthic deep-sea biological hotspot?
Ulrike Hanz, Philip Riekenberg, Anna de Kluijver,
Marcel van der Meer, Jack J. Middelburg, Jasper M. de Goeij,
Martijn C. Bart, Erik Wurz, Ana Colaço, Gerard Duineveld,
Gert-Jan Reichart, Hans-Tore Rapp† and Furu Mienis

Chapter 6 **177**

Oxygen uptake and inorganic nutrient dynamics in an Arctic deep-sea sponge ground: the sponge ground effect
Ulrike Hanz, Martijn Bart, Benjamin Mueller, Jasper M. de Goeij,
Kathrin Busch, Emyr Martyn Roberts, David Bowers,
Gert-Jan Reichart, Hans Tore Rapp† and Furu Mienis

Chapter 7 **213**

Synthesis

References **235**

Appendices

Co-authors & affiliations **272**

Bibliography **274**

Acknowledgements **277**

About the author **283**

Summary

The deep sea, starting below 200 m water depth, is one of the least studied habitats of our planet, while harbouring the largest ecosystem. With only a very small percentage of the deep sea being mapped in detail (~7%), even less is known about its biodiversity and ecosystem functioning. In general the deep sea can be considered unfavourable for most organisms, due to the inherent hostile conditions with immense pressure, darkness, and low temperatures. Moreover, food availability is very much limited. Life in the deep sea mainly relies on primary productivity at the ocean's surface, with only a small portion of the organic matter produced (1-3%) arriving in the deep ocean. Surprisingly we do find thriving communities like cold-water coral reefs and sponge grounds in specific places, similar to oases occurring in an otherwise water deprived desert. Both sponges and cold-water corals are so-called ecosystem engineers, increasing the local habitat heterogeneity and complexity, with their skeletons protruding from the otherwise muddy seafloor. This creates hotspots of biodiversity and biomass, whereby corals and sponges function like trees in a forest providing a habitat, nursery, shelter and foraging area for many other benthic and mobile species.

It has been shown that biological hotspots in the deep-sea often occur at sites with specific bathymetry and hydrography, whereby the seafloor topography is interacting with local and regional hydrodynamics. To understand why these hotspots grow where they grow and how they sustain themselves, environmental conditions and food supply mechanisms need to be determined. This thesis provides insight into the environmental variability near often vulnerable deep-sea biological hotspots, in particular deep-sea sponge grounds that so far have been overlooked. This is of vital importance with the deep sea more and more being impacted by anthropogenic pressures, like fisheries, deep-sea mining, ocean acidification and climate change. Due to its inaccessibility the deep sea can, however, only be studied using dedicated technology, like underwater robots and bottom observatories. The latter allow us for process-oriented studies continuously measuring environmental

conditions through time, while underwater robots provide us with the opportunity to collect discrete samples and carry out in situ experiments.

Both techniques are used in this thesis to establish and extent the knowledge on the functioning of biological hotspots in the deep sea, focusing on the environmental conditions influencing sponge grounds and cold-water coral reefs. This thesis can be divided in two major parts. The first chapters (2-4) focus on the environmental conditions and food supply mechanisms to cold-water coral and sponge hotspots in areas with different environmental characteristics, including the Angolan/Namibian margin, the Scotian Shelf and the Arctic Mid-Atlantic Ridge. Daily to seasonal variations of near-bed environmental conditions were measured using seabed observatories, measuring hydrodynamics, temperature, turbidity, fluorescence and oxygen, which were accompanied by hydrographic surveys with CTDs to study the water column bathing the reefs. Sediment traps attached to the deep sea landers provided insight in vertical and lateral particle and organic carbon fluxes reaching the reefs. In the second part of the thesis (Chapter 5 and 6) interactions between the environment and functioning of a sponge ground on the Mid-Atlantic Ridge are highlighted. Using a food web approach this shows how the sponge ground influences its environment and how the sponges associate with other deep-sea fauna.

Even though environmental ranges have been studied in detail in some cold-water coral areas, research along the Angolan and Namibian margin revealed so far unknown extreme environmental conditions in which cold-water coral reefs can thrive (Chapter 2), stretching the commonly anticipated environmental ranges. Dissolved oxygen levels were very low, resulting in fully anoxic conditions on the Namibian margin and hypoxic conditions on the Angolan reefs. In both areas tidally driven currents delivered water with enhanced amounts of food, also supplying limited amounts of oxygen to the local ecosystems. At the Angolan margin environmental conditions apparently met the minimum requirements to sustain a thriving cold-water coral reef, whereby the low oxygen concentrations were likely compensated by a sufficient supply of food of high enough quality. At the Namibian margin, in contrast, we observed only dead coral framework overgrown by fauna generally considered more environmentally robust such as bryozoans and sponges. Here the balance of oxygen stress and food availability did apparently not suffice, likely due to the somewhat lower oxygen concentrations, providing evidence for the rather fragile equilibrium conditions these systems are thriving in. This study provides insights into how unfavourable environmental conditions (e.g., low oxygen and high temperatures) are sometimes offset by favourable conditions (food supply).

In Chapter 3 the local environmental conditions of the Scotian Shelf were measured in the context of unravelling the food supply to a Vazella pourtalesii sponge ground for a period of 10 months using a bottom lander. The main finding is that these sponges live in an area where semi-diurnal tidal currents promote constant resuspension of particulate organic matter in the benthic boundary layer. This causes lateral particle transport, which likely forms an important food supply in addition to the vertical flux of settling organic matter during the spring bloom. Winter surface storm were observed to reach the sea bottom, episodically resulting in extremely turbid conditions at the seafloor that persisted for several days. These extreme episodic resuspension events may represent a major stress factor for sponges, clogging their filtration apparatus and thereby limiting their filtration capability as well as relocating them. However, these winter storms also play an important role in mixing of the water column, influencing primary productivity by mixing of the water column and enhancing food supply. Sponges seem to recover from these events relatively quickly, indicating their resilience to short term environmental disturbances, which might be beneficial for their survival under human induced threats that produce sediment plumes, like fisheries and deep-sea mining.

Environmental conditions on the Schulz Bank, a seamount belonging to the Arctic Mid-Atlantic Ridge, differed from what was observed on the Scotian Shelf. On the summit of the seamount a thriving sponge

ground was found, consisting of different cold-water sponge species and associated fauna, forming a reef like system. Here the sponge community lives in very cold temperatures of -0.5 to 1 °C. The summit of the seamount occurred at the interface of two water masses, which in combination with the occurrence of high internal waves produces strong currents and turbulent mixing. Amplification of internal waves is related to the interaction of the hydrodynamic conditions with the topography of the seamount. This vertically moves the water masses periodically by up to 200 m, causing changes in environmental conditions at the seafloor on a semi-diurnal time scale. This delivers particulate food from the surface and dissolved nutrients from the lower water column towards the filter feeding fauna. Still, the amount of fresh organic matter arriving from the surface ocean is not sufficient to sustain the demands of such a rich community. Hence it is likely that other food sources like for example bacteria and dissolved organic carbon also play an important role, since it was shown that sponges can additionally utilise these resources in contrast to other benthic fauna.

A food web study was conducted to determine what food sources the sponge ground at the Schulz Bank summit relies on (Chapter 5). Sponge ground fauna and primary food sources were collected and analysed for stable isotopes, fatty and amino acids. This showed that sponges have a very unique position in the food web. Sponges are divided into two groups depending on their microbial symbionts. One sponge group with high amounts of microbial symbionts takes up dissolved organic and inorganic carbon and transfers particulate carbon to higher trophic positions. The sponge group with little microbial symbionts had an extremely high trophic position, pointing towards unknown recycling mechanisms. Fatty acid analysis showed that both sponge groups transfer sponge derived organic matter to the wider food web (the so called sponge contribution). Our results show that sponges play a pivotal role in the sustenance of the deep-sea sponge ecosystem, shunting organic carbon to other trophic levels that would otherwise be inaccessible to other deep-sea fauna.

In-situ incubation experiments were performed to measure the oxygen, carbon and inorganic nutrient uptake at the Schulz Bank sponge ground (Chapter 6). These experiments were combined with sampling of the water column just above the sponge ground, to quantify fluxes between the sponge ground and the near-bed environment. In situ incubations showed that the sponge ground is a hotspot of carbon cycling, mainly driven by the presence of large sponge individuals. Measurements along a gradient in the benthic boundary layer showed that bacterioplankton was taken up by the sponge ground and nitrogen compounds were released, suggesting that the sponge ground plays an important role in benthic-pelagic coupling. In order to replenish the benthic boundary layer with fresh food, like for example bacterioplankton and dissolved organic carbon, high currents produced by the tidal waves are vital as described in Chapter 4. Our results show that sponge grounds are hotspots of carbon and nutrient cycling, comparable to other deep-sea biological hotspots like cold-water coral reefs.

Overall, long-term near-bed hydrodynamic conditions were measured successfully in two North Atlantic sponge grounds. These measurements provided valuable information about the environmental ranges and variability through time. Moreover, the research carried out in this thesis emphasizes the importance of the interplay between ecosystems and the near-bed hydrodynamic processes. Improved understanding of the environmental ranges suitable for the initiation, sustenance and development of biological hotspots will help to predict and model their distribution, which is vital information for marine management and policy making.

Even though the effects of climate change and anthropogenic pressures in the deep sea are difficult to observe, deep-sea biological hotspots are likely influenced by similar stressors as their shallow water counterparts. Modelled predictions show that circulation patterns and water mass properties will change in the future, exposing the deep-sea ecosystems to changing environmental conditions and influencing their food supply. The ability of cold-water coral reefs and sponge grounds to thrive over a large range of

environmental conditions, implies that they are likely rather resilient to environmental change. In addition, sponges can use a multitude of food sources, which might make them more competitive to other animals, that rely on one food source and therefore they might be able to cover an even larger surface area in the deep ocean compared to for instance cold-water coral reefs. However, it is also shown that these ecosystems often depend on a fragile equilibrium, whereby changes in a single factor can cause stress, especially since deep-sea species are growing slowly and generally long lived. Accordingly it is important to extend our knowledge about the critical factors for these ecosystems, as well as the goods and services they provide, or might provide in the future, for humankind. Scientists play an important role in creating awareness and conveying the importance of deep sea ecosystems to the wider public and policy makers.

Samenvatting

De diepzee, die begint bij 200 m waterdiepte, is een van de minst bestudeerde habitats, terwijl het plaats biedt aan het grootste ecosysteem van onze planeet. Tot nu toe is slechts een zeer klein deel van de diepzee in detail in kaart gebracht (ca. 7%), en is er nog minder bekend over de biodiversiteit en het functioneren van ecosystemen. In het algemeen kan de diepzee worden beschouwd als een ongunstige omgeving voor de meeste organismen door de inherente vijandige omstandigheden, vanwege de immense druk, totale duisternis en lage temperaturen. Bovendien is het voedselaanbod in de diepzee heel beperkt. Leven in de diepzee is voornamelijk afhankelijk van primaire productiviteit aan het oceaanoppervlak, waarbij slechts een klein deel van het organische materiaal wat daar wordt geproduceerd (1-3%), aankomt op de bodem van de oceaan. Desondanks vinden we op specifieke plekken in de diepzee bloeiende gemeenschappen, zoals koudwaterkoraalriffen en sponsgronden, die vergelijkbaar zijn met oases voorkomend in een droge woestijn. Sponzen en koudwaterkoralen zijn zogenaamde ecosysteem “engineers”, die hun directe leefomgeving beïnvloeden door hun driedimensionale skeletten, die boven de vlakke zeebodem uitsteken. Op deze manier ontstaat er een toename in heterogeniteit en complexiteit van de zeebodem. Koudwaterkoraalriffen en sponsgronden vormen hotspots van biodiversiteit en biomassa, waarbij de koralen en sponzen functioneren als bomen in een bos en een leefomgeving, kraamkamer, schuilplaats en foerageergebied voor vele andere benthische en mobiele diersoorten bieden.

In de diepzee komen biologische hotspots vaak voor op locaties met specifieke bathymetrie en hydrografie, waarbij de zeebodemtopografie in wisselwerking staat met de lokale en regionale hydrodynamiek. Om te begrijpen waarom deze hotspots groeien waar ze groeien en hoe ze zichzelf in stand houden, moeten de omgevingsomstandigheden en voedselaanvoer mechanismen worden bepaald. Dit proefschrift geeft ons inzicht in de variabiliteit van omgevingsfactoren van deze vaak kwetsbare biologische hotspots in de diepzee. In het bijzonder zijn de diepzee sponsgronden onderzocht, die tot nu toe weinig aandacht hebben gekregen. Deze gegevens zijn van groot belang, omdat de diepzee steeds ingrijpender wordt beïnvloed door de mens, door bijvoorbeeld visserij, diepzeemijnbouw, oceaanverzuring en klimaatverandering.

Vanwege de ontoegankelijkheid kan de diepzee alleen worden bestudeerd met behulp van speciale technologie, zoals onderwaterrobots en bodemobservatoria. Bodemlanders stellen ons in staat om procesgerichte studies uit te voeren waarbij de omgevingsomstandigheden door de tijd heen continu gemeten worden. Onderwaterrobots bieden ons de mogelijkheid om specifieke monsters te verzamelen en in situ experimenten uit te voeren. Beide technieken worden in dit proefschrift gebruikt om de kennis over het functioneren van biologische hotspots in de diepzee tot stand te brengen en te vergroten.

Dit proefschrift bestaat uit twee delen. Het eerste deel (Hoofdstukken 2-4) is gericht op de omgevingsomstandigheden en voedselvoorzieningsmechanismen in koudwaterkoraal- en spons-hotspots in gebieden met verschillende ecologische eigenschappen, waaronder de Afrikaanse continentale helling, de Scotian Shelf en de Arctische Mid-Atlantische Rug. Dagelijkse tot seizoensgebonden variabiliteit in omgevingscondities vlakbij de zeebodem zijn bestudeerd met bodemlanders, uitgerust met sensoren om temperatuur, troebelheid van het water, fluorescentie en het zuurstofgehalte te meten. Daarnaast is de waterkolom boven en rond de hotspots bestudeerd aan de hand van metingen met een CTD (conductivity-temperature-depth) sensor. Sedimentvallen bevestigd aan de bodemlanders geven ons inzicht in het verticale en laterale transport van deeltjes en de organische koolstof fluxen die de riffen bereiken. In het tweede deel van het proefschrift (Hoofdstukken 5 en 6) ligt de focus op de interacties tussen de omgeving en het functioneren van een sponsgrond op de Mid-Atlantische rug. Doormiddel van in situ experimenten en een voedselwebanalyse wordt aangetoond hoe de sponsgrond zijn omgeving beïnvloedt en hoe belangrijk de rol van sponzen is voor de andere aanwezige diepzee soorten.

Hoewel de omgevingsomstandigheden in een groot aantal koudwaterkoraalgebieden in detail zijn bestudeerd, onthulde onderzoek langs de Angolese en Namibische continentale helling tot nu toe onbekende extreme omgevingscondities waarin koudwaterkoraalriffen kunnen gedijen (Hoofdstuk 2). De zuurstofconcentraties in beide gebieden waren heel laag, wat resulteerde in volledig zuurstofloze omstandigheden op de Namibische helling en zuurstofarme omstandigheden in de Angolese riffen. Getijdestromingen in beide onderzoeksgebieden zorgden voor de aanvoer van water met grotere hoeveelheden voedsel en beperkte hoeveelheden zuurstof aan de lokale ecosystemen. Op de Angolese helling voldoen de omgevingscondities hierdoor aan de minimale eisen voor een bloeiend koudwaterkoraalrif. Hier worden de lage zuurstofconcentraties waarschijnlijk gecompenseerd door de aanwezigheid van voldoende voedsel van hoge kwaliteit. Op de Namibische helling daarentegen werden alleen dode koraalstructuren waargenomen die overgroeid waren door een andere fauna met bryozoën en sponzen, die over het algemeen als meer ecologisch robuust worden beschouwd. Hier is de balans tussen de extreem lage zuurstofconcentraties (zuurstof stress) en de beschikbaarheid van voedsel blijkbaar niet toereikend. Dit bevestigt dat de koudwaterkoraalriffen in een zeer fragiel evenwicht leven, waarbij de omgevingsomstandigheden exact moeten kloppen om een bloeiend ecosysteem in stand te houden. Deze studie biedt inzicht in hoe ongunstige omgevingsomstandigheden (bv., weinig zuurstof en hoge temperaturen) kunnen worden gecompenseerd door gunstige omstandigheden (voedselaanbod).

In Hoofdstuk 3 zijn de lokale omgevingscondities in een Vazella pourtalesii sponsgrond op de Scotian Shelf gemeten en is de voedselaanvoer ontrafelt met behulp van een bodemlander gedurende een periode van 10 maanden. De belangrijkste bevinding is dat deze sponzen in een gebied leven waarin semi-dagelijkse getijdenstromingen constant fijn organisch materiaal direct boven de zeebodem in suspensie houden. Dit veroorzaakt lateraal transport van deeltjes die waarschijnlijk een belangrijke bron van voedsel vormen, naast de verticale flux van organisch materiaal in het voorjaar. De landergegevens lieten zien dat winterstormen de zeebodem bereikten, wat soms resulteerde in extreem troebele omstandigheden, die enkele dagen aanhielden. Deze extreme episodische troebelheidswolken kunnen een belangrijke stressfactor vormen voor sponzen, omdat de poriën in hun skelet verstopt kunnen raken waardoor hun filtratievermogen wordt beperkt. Daarnaast werden de sponzen tijdens deze episodes ook verplaatst. De winterstormen spelen echter ook een belangrijke rol in het mengen van de waterkolom, en daarmee de primaire productiviteit en het verbeteren van de voedselvoorziening. Sponzen lijken relatief snel te herstellen van deze natuurlijke kortstondige verstoringen van hun omgeving, wat hun veerkracht aangeeft. Dit kan betekenen dat de sponzen ook een grotere kans hebben om te overleven tijdens door de mens veroorzaakte bedreigingen die sedimentpluimen produceren, zoals visserij en diepzeemijnbouw.

Omgevingsomstandigheden op de Schulz Bank (Hoofdstuk 4), een onderzeese berg (“seamount”) behorend tot de Arctische Mid-Atlantische Rug, verschilden van wat werd waargenomen op de Scotian Shelf. Op de top van de seamount werd een rifachtige sponsgrond gevonden, bestaande uit verschillende soorten koudwatersponzen en bijbehorende fauna. Hier leeft de sponsgemeenschap in zeer koude temperaturen van -0,5 tot 1 ° C. De top van de seamount bevindt zich op het grensvlak van twee watermassa's, die samen met het optreden van grote interne golven een sterke stroming en turbulente menging veroorzaken. Versterking van de interne golven is gerelateerd aan de interactie tussen de hydrodynamische omstandigheden en de topografie van de seamount. Hierdoor worden de watermassa's periodiek verticaal tot 200 m verplaatst, waardoor veranderingen in de omgevingscondities op de zeebodem op een semi-dagelijkse tijdschaal ontstaan. Dit zorgt voor de aanvoer van voedsel uit de hogere waterkolom en opgeloste voedingsstoffen uit de diepere waterkolom naar de sponsgemeenschap. De hoeveelheid verse organische stof die van het oceaanoppervlak naar beneden zinkt is echter niet toereikend om zo'n rijke gemeenschap in stand te houden. Derhalve is het waarschijnlijk dat andere voedselbronnen zoals bijvoorbeeld bacteriën en opgeloste organische koolstof ook een belangrijke rol spelen, aangezien studies hebben uitgewezen, dat sponzen deze voedselbronnen kunnen gebruiken in tegenstelling tot ander bodemleven in de diepzee.

Om te bepalen van welke voedselbronnen de sponsgrond op de Schulz Bank afhankelijk is, is er een voedselwebonderzoek uitgevoerd (Hoofdstuk 5). De meest voorkomende soorten en de primaire voedselbronnen zijn bemonsterd en geanalyseerd op stabiele isotopen, vetzuren en aminozuren. Hieruit bleek dat sponzen een unieke positie innemen in het voedselweb. Sponzen zijn verdeeld in twee groepen, afhankelijk van de aanwezigheid van microbiële symbionten. De sponsgroep met een hoog gehalte aan microbiële symbionten neemt opgeloste organische en anorganische koolstof op en verplaatst de koolstof als vaste deeltjes naar hogere trofische niveaus. De sponsgroep met weinig microbiële symbionten had een extreem hoge trofische positie, wijzend op onbekende recyclingmechanismen. Vetzuuranalyse toonde aan dat beide sponsgroepen van spons afkomstig organisch materiaal overbrengen naar het bredere voedselweb (de zogenaamde sponsbijdrage). Deze resultaten laten zien dat sponzen een cruciale rol spelen in het onderhoud van het diepzeesponsecosysteem, waarbij organische koolstof, die anders ontoegankelijk zou zijn voor andere diepzeefauna, wordt getransporteerd naar andere trofische niveaus.

In-situ incubatie-experimenten werden uitgevoerd om de zuurstof-, koolstof- en anorganische nutriëntenopname op de Schulz Bank sponsgrond te bepalen (Hoofdstuk 6). Deze experimenten werden gecombineerd met de bemonstering van de waterkolom boven de sponsgrond, om fluxen te kwantificeren tussen de sponsgrond en de naaste omgeving. In-situ incubaties toonden aan dat de sponsgrond een hotspot is van koolstof recycling, voornamelijk aangedreven door de aanwezigheid van grote sponsindividuen. Metingen langs een gradiënt in de benthische grenslaag toonden aan dat bacterioplankton door de sponsgrond werd opgenomen en stikstofverbindingen werden uitgescheiden, wat suggereert dat de sponsgrond een belangrijke rol speelt in de benthisch-pelagische koppeling. Om de benthische grenslaag aan te vullen met vers voedsel, zoals bijvoorbeeld bacterioplankton en opgeloste organische koolstof, zijn de sterke stromingen die door de getijdegolven worden geproduceerd van vitaal belang (zoals beschreven in Hoofdstuk 4). De resultaten laten zien dat sponsgronden hotspots zijn in de koolstof- en nutriëntenkringloop, vergelijkbaar met andere diepzee biologische hotspots, zoals de koudwaterkoraalriffen.

Over het algemeen werden de hydrodynamische omstandigheden in de buurt van de zeebodem over een lange tijdsperiode met succes gemeten in twee Noord-Atlantische sponsgronden. Deze metingen verschaffen ons waardevolle informaties over de natuurlijke omgevingsomstandigheden en hun variabiliteit door de tijd. Bovendien benadrukt het onderzoek in dit proefschrift het belang van de wisselwerking tussen de ecosystemen en de omgevingscondities en processen in hun directe omgeving. Een beter begrip van de omgevingsomstandigheden die geschikt zijn voor het ontstaan, het in stand houden en de ontwikkeling van biologische hotspots zal helpen bij het voorspellen en modelleren van hun verspreiding. Dit is essentiële informatie, die nodig is voor het beheer van en de beleidsvorming over onze oceanen.

Hoewel de effecten van klimaatverandering en antropogene druk in de diepzee moeilijk zijn waar te nemen, worden diepzee biologische hotspots waarschijnlijk beïnvloed door soortgelijke stressfactoren als hun tegenhangers in ondiep water. Gemodelleerde voorspellingen laten zien dat circulatiepatronen en watermassa eigenschappen zullen veranderen in de toekomst, waardoor diepzee-ecosystemen blootgesteld kunnen worden aan veranderende omgevingsfactoren, inclusief hun voedselvoorziening. Het vermogen van koudwaterkoraalriffen en sponsgronden om te gedijen onder een groot aantal omgevingsomstandigheden, impliceert dat ze behoorlijk veerkrachtig zijn als het aankomt op veranderingen in het milieu.

Bovendien kunnen sponzen een veelheid aan voedselbronnen gebruiken, waardoor ze waarschijnlijk meer concurrerend zijn dan andere dieren, die afhankelijk zijn van één voedselbron. Hierdoor zouden de sponsgronden mogelijk een nog groter oppervlak in de diepe oceaan kunnen begroeien in vergelijking met bijvoorbeeld koudwaterkoraalriffen. Het is echter ook aangetoond dat deze ecosystemen vaak voorkomen in een fragiel evenwicht, waardoor verandering in een enkele omgevingsfactor stress kan veroorzaken, te meer omdat diepzeesoorten langzaam groeien en doorgaans zeer oud worden. Het is daarom belangrijk om onze kennis uit te breiden over de mogelijk kritische factoren voor deze ecosystemen, evenals de toekomstige rol die ze zouden kunnen bieden voor de mensheid. Hier is een belangrijke taak weggelegd voor wetenschappers, om meer bewustzijn te creëren en het belang van diepzee ecosystemen te vertalen naar het grote publiek en beleidsmakers.

Zusammenfassung

Die Tiefsee, die jenseits von 200 m Wassertiefe beginnt, ist einer der am wenigsten erforschten Lebensräume unseres Planten, beherbergt jedoch gleichzeitig das größte Ökosystem der Erde. Bis heute ist nur ein sehr kleiner Teil der Tiefsee im Detail kartiert worden (~7%) und noch weniger ist über ihre Biodiversität und Ökosystemfunktionen bekannt. Im Allgemeinen kann man sagen, dass die Tiefsee durch ihre unvorteilhaften und lebensfeindlichen Bedingungen, wie ihren immensen Druck, Dunkelheit und niedrige Temperaturen für die meisten Organismen als unbewohnbar angesehen werden kann. Zusätzlich ist die Nahrungsverfügbarkeit stark eingeschränkt, da das Leben in der Tiefsee hauptsächlich von der Primärproduktion an der Meeresoberfläche abhängt. Von dieser organischen Substanz gelangt nur ein sehr kleiner Teil (1-3%) in die Tiefsee. Überraschenderweise finden wir an einigen Orten trotzdem florierende Gemeinschaften, wie zum Bespiel Kaltwasserkorallenriffe und Schwammriffe, ähnlich den Oasen in der Wüste. Sowohl Schwämme als auch Kaltwasserkorallen sind sogenannte Ökosystem-Ingenieure, welche die lokale Heterogenität und Komplexität des Lebensraumes erhöhen können. Ihre Skelete ragen aus dem ansonsten schlammigen Meeresboden heraus und bieten vielen anderen benthischen Arten Lebensraum, Kinderstube, Unterschlupf und Nahrung. Dadurch entstehen Hotspots der Biodiversität und Biomasse, ähnlich zu Bäume in einem Wald. Es hat sich gezeigt, dass biologische Hotspots in der Tiefsee häufig an Standorten mit spezifischer Bathymetrie und Hydrographie vorkommen, wo die Meeresboden Topography mit der lokalen Hydrodynamik interagiert. Um zu verstehen warum diese Hotspots dort vorkommen und um herauszufinden wie sie sich selbst erhalten, ist es wichtig die Umweltbedingungen und Mechanismen der Nahrungsmittelversorgung zu bestimmen. Diese Dissertation gibt Einblicke in die Umweltvariabilität in diesen empfindlichen biologischen Hotspots der Tiefsee, insbesondere von Tiefsee-Schwammriffen, welche bisher weitgehend unerforscht geblieben sind. Dies ist von entscheidender Bedeutung, da die Tiefsee immer

mehr von anthropogenen Belastungen wie Fischerei, Tiefseebergbau, Ozeanversauerung und Klimawandel bedroht wird. Aufgrund ihrer Unzugänglichkeit kann die Tiefsee jedoch nur mit speziellen Technologien wie Unterwasserrobotern und Bodenobservatorien, so genannten Landern, untersucht werden. Letztere ermöglichen uns prozessorientierte Studien, welche die Umweltbedingungen kontinuierlich messen, während Unterwasserroboter uns die Möglichkeit bieten, diskrete Proben zu sammeln und in-situ Experimente durchzuführen.

Beide Techniken wurden in dieser Arbeit verwendet um Wissen über die Funktionsweise von biologischen Hotspots in der Tiefsee zu etablieren und zu erweitern, wobei der Fokus auf den Umweltbedingungen liegt, die Schwamm und Kaltwasserkorallenriffe beeinflussen. Diese Arbeit lässt sich in zwei Teile gliedern: Die ersten Kapitel (2-4) konzentrieren sich auf die Umweltbedingungen und Nahrungsversorgungsmechanismen für Schwamm- und Kaltwasserkorallenriffe in Gebieten mit unterschiedlichen Umwelteigenschaften, einschließlich des angolanischen und namibischen Kontinentalrandes, des Scotian Shelf und des arktischen Mittelatlantischen Rückens. Tägliche bis saisonale Variationen der Umweltbedingungen dicht über dem Meeresboden wurden mit Meeresobservatorien gemessen, welche Hydrodynamik, Temperatur, Trübung, Fluoreszenz und Sauerstoff messen und von hydrographischen Untersuchungen der Wassersäule begleitet wurden. An den Tiefseeobservatorien angebrachte Sedimentfallen liefern dabei Einblicke in den vertikalen und lateralen Partikeltransport der organische Kohlenstoffflüsse. Im zweiten Teil der Arbeit (Kapitel 5 und 6) werden Wechselwirkungen zwischen der Umwelt sowie den Funktion des Schulz Bank Schwammriffes beleuchtet. Anhand des Nahrungsnetzes wird gezeigt, wie das Schwammriff seine Umwelt beeinflusst und wie Schwämme mit der übrigen benthischen Fauna interagieren.

Obwohl die Umweltbedingungen von Kaltwasser Korallenriffen bereits in einigen Studien im Detail untersucht wurden, ergaben Messungen entlang des angolanischen und namibischen

Kontinentalrandes bisher unbekannte extreme Bedingungen, unter denen Kaltwasserkorallen überleben können (Kapitel 2). Der Gehalt an gelöstem Sauerstoff war extrem niedrig, was zu vollständig anoxischen Bedingungen am namibischen Kontinentalrand und zu hypoxischen Bedingungen in den angolanischen Kaltwasserkorallenriffen geführt hat. In beiden Gebieten lieferten gezeitengetriebene Strömungen temporär Wasser mit erhöhten Nahrungsmengen und begrenzte Mengen an Sauerstoff an die lokalen Ökosysteme. Am angolanischen Kontinentalrand erfüllten die Umweltbedingungen offenbar die Mindestvorraussetzungen für ein gedeihendes Kaltwasserkorallenriff, wobei der Stress der geringen Sauerstoffkonzentrationen wahrscheinlich durch ein ausreichendes Nahrungsangebot an qualitativ hochwertiger Nahrung ausgeglichen wurden. Am namibischen Kontinentalrand hingegen wurden nur abgestorbene Korallengerüste beobachtet, die von einer allgemein robusten Fauna wie Bryozoen und Schwämme überwuchert wurden. Hier reichte das Gleichgewicht zwischen Sauerstoffstress und Nahrungsverfügbarkeit offenbar nicht aus, wahrscheinlich hervorgerufen durch die etwas geringere Sauerstoffkonzentration. Dies zeigt, in welch einem fragilen Gleichgewicht diese Systeme an einigen Standorten leben. Diese Studie gibt Aufschluss darüber, wie ungünstige Umweltbedingungen (wie zum Beispiel geringe Sauerstoffkonzentration und hohe Temperaturen) an einigen Orten durch günstige Bedingungen wie ein erhöhtes Nahrungsangebot ausgeglichen werden können.

In Kapitel 3 wurden die lokalen Umweltbedingungen auf dem Scotian Shelf über einen Zeitraum von 10 Monaten mit einem Unterwasserobservatorium gemessen um die Umweltbedingungen und Nahrungsmittelversorgung des *Vazella pourtalesii* Schwammriffes zu erkunden. Das Hauptergebnis dieser Studie ist, dass diese Schwämme in einem Gebiet leben, in dem halbtägige Gezeitenströmungen eine ständige Resuspension von partikulärem organischem Material in der benthischen Grenzschicht fördern. Dies verursacht einen lateralen Partikeltransport, der wahrscheinlich eine wichtige Nahrungsquelle darstellt. Es wurde beobachtet, dass winterliche Stürme an der Meeresoberfläche den Meeresboden erreichen, was episodisch für mehrere Tage zu extrem trüben Bedingungen am Meeresboden führte. Diese extremen episodischen Resuspensinonsereignisse können einen großen Stressfaktor für Schwämme darstellen, da ihr Filtrationsapparat verstopfen kann und starke Strömungen sie zusätzlich noch „entwurzeln“ und umwerfen können. Diese Winterstürme spielen jedoch auch eine wichtige Rolle bei der Durchmischung der Wassersäule und beeinflussen dadurch die Primärproduktion und Verbesserung der Nahrungsversorgung. Schwämme scheinen sich relativ schnell von diesen Extremereignissen zu erholen, was auf eine starke Widerstandsfähigkeit gegenüber kurzfristigen Umweltstörungen hinweist. Dies kann für ihr Überleben bei anthropogen verursachten Bedrohungen, wie zum Beispiel bodenberührender Fischerei und Tiefseebergbau, welche starke Resuspension verursachen, von Vorteil sein.

Die Umweltbedingungen im Schwammriff der Schulz Bank, einem arktischen Tiefseeberg des Mittelatlantischen Rückens, unterscheidet sich in einigen Punkten von dem, was auf dem Scotian Shelf beobachtet wurde. Auf dem Gipfel des Unterwasserberges wurde ein florierendes Schwammriff gefunden, welches aus verschiedenen Kaltwasserschwämmen und einer reichen assoziierten Fauna besteht. Hier leben die Gemeinschaften bei -0.5 bis 1 °C. Der Gipfel des Unterwasserberges befindet sich an der Grenzschicht zweier Wassermassen, was in Kombination mit dem Auftreten interner Wellen, starke Strömungen und eine turbulente Bedingungen erzeugt. Dadurch sinken und heben die Wassermassen sich periodisch um bis zu 200 m, was zu periodischen Veränderungen der Umweltbedingungen auf dem Meeresboden führt. Dadurch wird partikuläre Nahrung von der Oberfläche und gelöste Nährstoffe aus tieferen Wasserschichten zu der filtrierende Fauna geliefert. Dennoch reicht die Menge an der frischen organischen Substanz, die von der Meeresoberfläche geliefert wird, nicht aus um den Nährstoffbedarf dieser florierenden Gemeinschaft zu decken. Es ist daher wahrscheinlich, dass auch andere Nahrungsquellen wie beispielsweise Bakterien und gelöster organischer Kohlenstoff eine wichtige Rolle spielen, da gezeigt wurde, dass Schwämme diese

Ressourcen im Gegensatz zu anderen benthischen Tieren nutzen können.

Eine Nahrungsnetzstudie wurde deshalb durchgeführt um herauszufinden, auf welche Nahrungsquellen das Schulz Bank Schwammriff angewiesen ist (Kapitel 5). Die Schwammrifffauna und primären Nahrungsquellen wurden gesammelt und auf stabile Isotope, Fettsäuren und Aminosäuren untersucht. Dies zeigte, dass Schwämme eine ganz besondere Stellung im Nahrungsnetz einnehmen. Die verschiedenen Schwamm Arten können nach ihren mikrobiellen Symbionten in zwei Gruppen eingeteilt werden, Schwämme mit viel oder wenigen mikrobiellen Symbionten. Die Gruppe mit vielen mikrobiellen Symbionten kann gelösten organischen und anorganischen Kohlenstoff aufnehmen und transferiert partikulären Kohlenstoff an höhere trophische Level. Im Vergleich dazu hatte die Gruppe mit wenigen mikrobiellen Symbionten eine ungewöhnlich hohe trophische Position, was auf unbekannte Recyclingmechanismen hindeutet. Die Fettsäuren Analyse zeigte zusätzlich, dass beide Gruppen organisches Material auf das assoziierte Nahrungsnetz übertragen (der sogenannte Schwamm-Beitrag). Unsere Ergebnisse zeigen, dass Schwämme eine zentrale Rolle bei der Erhaltung dieses Tiefsee Ökosystem spielen, indem sie organischen Kohlenstoff auf höhere trophische Level transferieren. Dadurch stellen sie Nahrung für die assoziierte Tiefseefauna bereit, welche sonst unzugänglich wäre.

In-situ-Inkubationsexperimente wurden daraufhin durchgeführt um die Aufnahme von Sauerstoff, Kohlenstoff und anorganischen Nährstoffen im Schwammriff der Schulz Bank zu messen (Kapitel 6). Diese Experimente wurden mit einer Probenahme der unmittelbar darübergelegenen Grenzschicht kombiniert um die Flüsse zwischen dem Schwammriff und der bodennahen Umgebung zu quantifizieren. In-situ Inkubationen zeigten, dass der Schwammriff ein Hotspot des Kohlenstoffkreislaufs ist, der hauptsächlich durch die Anwesenheit großer Schwammindividuen angetrieben wird. Messungen entlang eines Gradienten in der benthischen Grenzschicht zeigten, dass Bakterioplankton vom Schwammriff aufgenommen und Stickstoffverbindungen freigesetzt wurden, was darauf hindeutet, dass das Schwammriff eine wichtige Rolle bei der benthisch-pelagischen Kopplung spielt. Um die benthische Grenzschicht mit frischer Nahrung, wie zum Beispiel Bakterioplankton und gelöstem organischem Kohlenstoff zu versorgen, sind starken Strömungen notwendig, welche in Kapitel 4 beschrieben wurden. Unsere Ergebnisse zeigen, dass Schwammriffe Hotspots des Kohlenstoff- und Nährstoffkreislaufs sind, vergleichbar mit anderen biologischen Hotspots wie zum Beispiel Kaltwasser-Korallenriffen.

Zusammenfassend, wurden für diese Arbeit langfristige hydrodynamische Bedingungen in Bodennähe in zwei nordatlantischen Schwammriffen gemessen. Diese Messungen lieferten wertvolle Informationen über die Umweltbedingungen und deren Langzeit Variabilität. Darüber hinaus betont die in dieser Dissertation durchgeführte Forschung die Bedeutung des Zusammenspiels zwischen Ökosystemen und hydrodynamischen Prozessen. Ein besseres Verständnis der Umweltbedingungen, die für die Entstehung, Erhaltung und Entwicklung biologischer Hotspots notwendig sind, wird dazu beitragen, die Ausbreitung von Schwammriffen vorherzusagen und zu modellieren, was für das Meeresmanagement und die Politikgestaltung von entscheidender Bedeutung ist.

Auch wenn die Auswirkungen des Klimawandels und der anthropogenen Belastungen in der Tiefsee schwer zu beobachten sind, werden biologische Hotspots in der Tiefsee wahrscheinlich von ähnlichen Stressoren beeinflusst wie ihre flachwasser Gegenstücke. Die Fähigkeit von Kaltwasserkorallenriffen und Schwammriffen unter einer Vielzahl von Umweltbedingungen zu gedeihen, impliziert dass sie wahrscheinlich relativ widerstandsfähig gegenüber Umweltveränderungen sind. Darüber hinaus können Schwämme eine Vielzahl von Nahrungsquellen nutzen, was sie gegenüber anderen Tieren, die auf eine Nahrungsquelle angewiesen sind, konkurrenzfähiger macht. Es zeigt sich aber auch, dass diese Ökosysteme oft von einem fragilen Gleichgewicht abhängen, wobei

Veränderungen eines einzelnen Faktors Stress verursachen können. Modellierte Vorhersagen zeigen, dass sich Zirkulationsmuster und Wassermasseneigenschaften in Zukunft ändern werden, welche die Umweltbedingungen in Tiefseeökosysteme verändern und ihre Nahrungsversorgung beeinflussen wird, was negative Auswirkungen auf diese Ökosysteme haben kann. Gleichzeitig ist es bekannt, dass Tiefseearten langsam wachsen und in der Regel langlebig sind. Dementsprechend ist es wichtig, die kritischen Bedingungen für diese Ökosysteme zu bestimmen. Zusätzlich sollten wir den Nutzen, den sie für die Menschheit leisten oder in Zukunft erbringen könnten, quantifizieren um zu vergegenwärtigen, dass diese Ökosysteme schützenswert sind. Nur so können Wissenschaftler eine wichtige Rolle bei der Bewusstseinsbildung und der Vermittlung der Bedeutung von Tiefseeökosystemen an die breite Öffentlichkeit und politische Entscheidungsträger spielen.

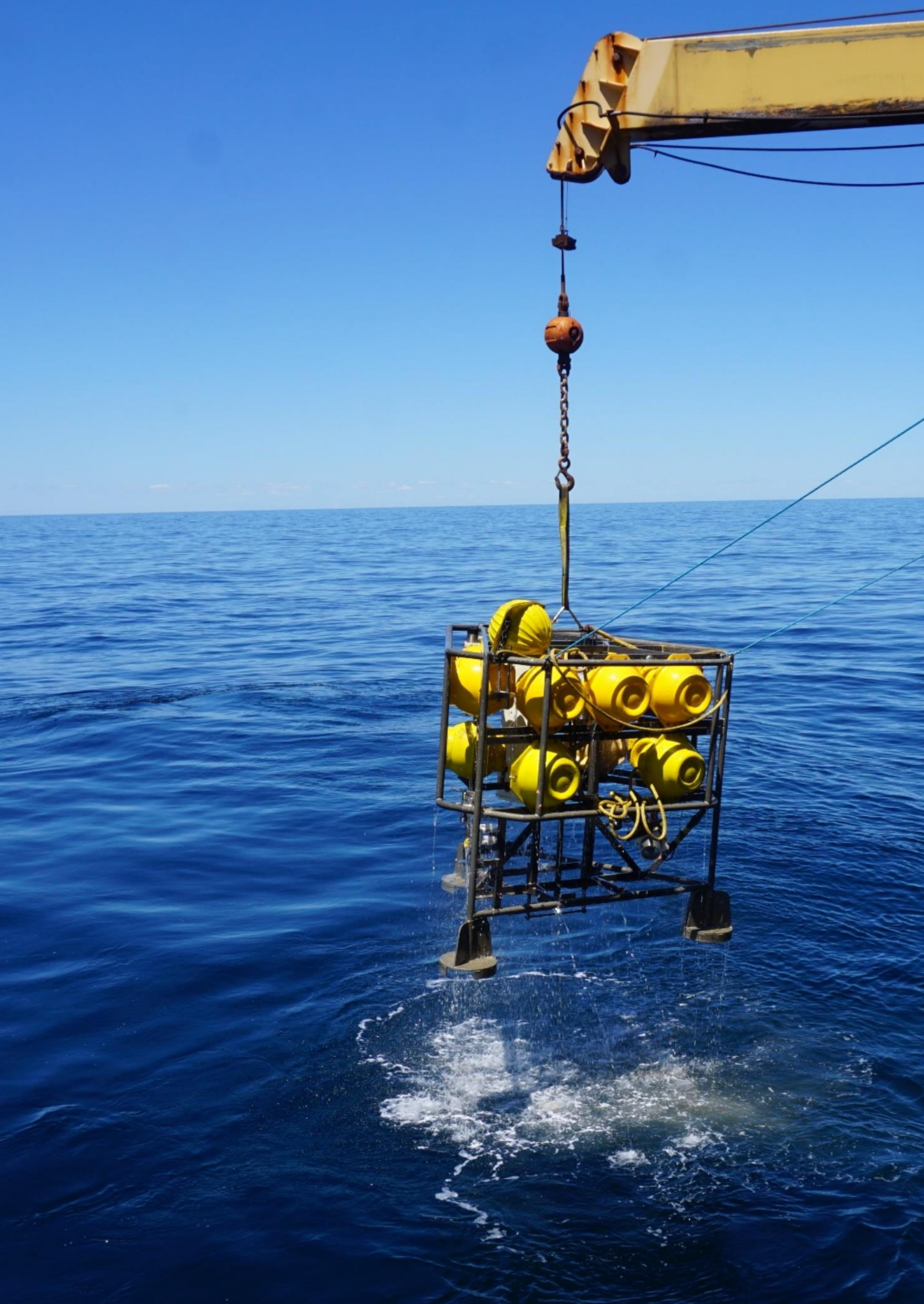

Chapter 1

Introduction

Picture to the left: Benthic ALBEX lander during recovery after a year-long deployment

1.1 The deep sea

One of the major concerns of our generations is climate change (Ahmed, 2020). Our planet is rapidly changing due to expanding human activities, which increasingly affect ecosystems with often-unknown consequences since large parts of our biosphere are still unknown. The oceans are one of the most overlooked parts of our planet even though they cover up to 70% of the surface and provide essential ecosystem services to mankind (Ramirez-Llodra et al., 2011). The deep sea starts where sunlight cannot penetrate far enough for photosynthesis to occur. It is an extreme environment in many ways, it is cold, dark and food deprived since primary production cannot take place anymore. Nevertheless, we know that the deep sea is a major sink for CO_2 and heat and it buffers multiple effects of climate change which influences marine as well as terrestrial ecosystems (Sweetman et al., 2017). This buffering capacity is vital for mitigating anthropogenic emissions and the climatic changes caused by carbon emissions. It is estimated that the deep sea absorbed already a quarter of the carbon released from human activities (Canadell et al., 2007) and 90% of the anthropogenic heat imbalance (Levitus et al., 2012). Additionally, the deep sea provides important ecosystem services by providing a habitat for a variety of economically important species and influences nutrient cycling and carbon sequestration. Next to this, it houses a wealth of energy, mineral and biological resources like massive reserves of oil, gas, precious metals and the rare minerals needed for modern electronics and batteries (Herzig and Hannington, 1995, Kato et al., 2011; Thurber et al., 2014; Levin et al., 2019). While increased knowledge on deep-sea biodiversity and ecosystem functioning is urgently needed, due to its inaccessibility, the deep sea largely remains a mystery (Ramirez-Llodra et al., 2011). Nevertheless, interest in services provided by deep-sea resources, as well as evidence for the effects of human activities have accumulated over the last decades (Armstrong et al., 2019).

The deep ocean starting at about 200 m depth, with an average depth of about 3800 m, is the least observed habitat of our planet and hides large areas of uncharted territory (Hedgpeth, 1957). Only roughly 7% of the deep ocean has been explored in detail by humans and only ~18% is mapped in a reasonable resolution (Mayer et al., 2018). For a long time anticipated that life in the deep sea was sparse (“Azoic Theory”; Forbes and Forbes, 1844). However, these views changed through time when in 1818 the first deep-sea fauna samples of echinoderms were collected from a depth of 1600 m (Menzies et al., 1973). This discovery was rapidly followed by many other deep-sea expeditions, whereby also species like cold-water corals and deep-sea sponges were observed (Figure 1.1; Gage and Tyler, 1991).

Figure 1.1 a) Expedition report of the deep-sea expedition "Valdivia" in 1895 and 1899 (Chun, 1903), b) early anthropogenic exploitation of sponges depicted in advertising prints for “Liebig's Extract of Meat” (c. 1900)

In the 1870s Sars and Sars (1872) were leading one of the first famous deep-sea expeditions, investigating the deep-sea fauna along the Norwegian coast. This important contribution to deep-sea science resulted in the naming of one of the Norwegian research vessels, the G.O. Sars after them (Figure 1.2a). This vessel was used for some of the research expeditions that form the basis of this thesis (Chapter 4-6). The first truly global deep-sea expedition was organized from 1872-1876, using H.M.S. Challenger, collecting physical, chemical and biological samples from the deep sea, including 4000 previously unknown species. Improved seafloor mapping opportunities and the development of new sampling equipment in the 1960s and 1970s such as multi corers, box corers, deep-sea sledges and trawls, revealed the tremendous heterogeneity present in the deep sea and resulted in the first quantitative analyses of deep-sea communities (Hessler and Sanders, 1967). The first ever live video footage of a cold-water coral reef was made in 1982 off northern Norway at a depth of 280 m, showing that the deep sea can also harbor reefs which are comparable to coral reefs in the shallow ocean (Hovland, 2008).

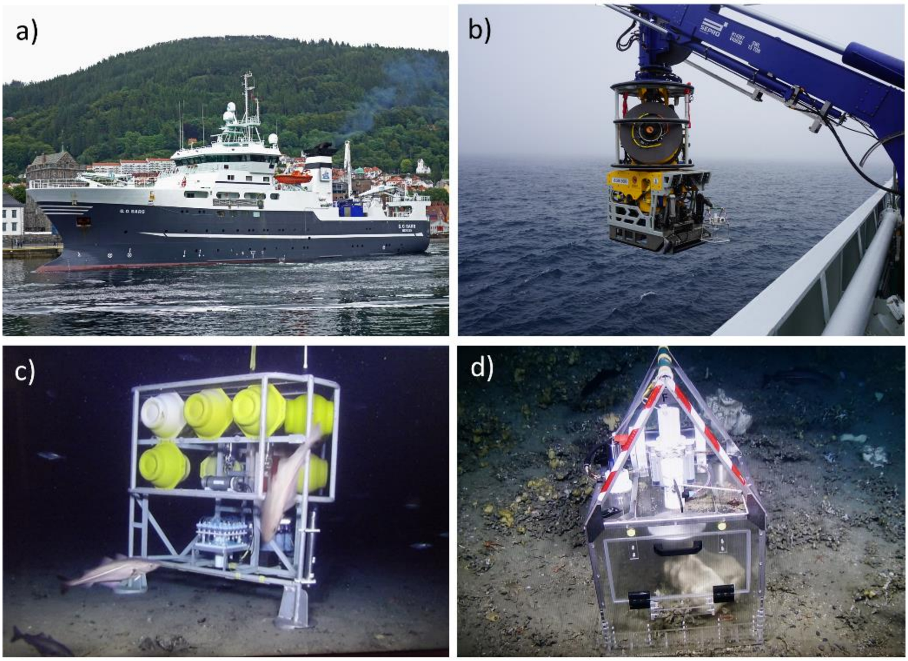

Figure 1.2 Examples of research vessel and sampling equipment for deep-sea studies a) RV G.O. Sars, b) deployment of the ROV Aegir, c) Benthic observatory (ALBEX lander) equipped with sensors to measure environmental conditions, d) In-situ incubation chamber, deployed inside a sponge ground.

Since the 1990s the invention of remotely operated- (ROVs, Figure 1.2b) and autonomous underwater vehicles (AUVs) as well as benthic observatories (e.g. landers, Figure 1.2c) allowed for targeted sampling, underwater in-situ experiments and process oriented studies (Figure 1.2c and 1.2d). This has shown that the deep sea hosts a variety of unique ecosystems, including hydrothermal vents, cold-seeps, whale falls, cold-water coral reefs, and sponge grounds. Although big steps in deep-sea exploration were made, major knowledge gaps on the occurrence and functioning of these deep-sea ecosystems still exist. For example, what is the role of the deep sea in global energy, nutrient and biological cycles (Sweetman et al., 2017)?

1.2 Biological hotspots in the deep sea

With changes in depth, food supply, the physical environment and reduced habitat complexity and heterogeneity, animal taxonomic composition and lifestyles are altered (Buhl-Mortensen et al., 2010; Levin and Sibuet, 2012). However, living organisms, so called ecosystem engineers can increase habitat heterogeneity with their structures protruding from the seafloor. Thereby they enhance biodiversity by providing shelter from predation, a spawning, nursery and foraging area for many (commercial) fish and invertebrate species, and hard substratum to settle on (Fuller and Cameron, 1998; Buhl-Mortensen et al., 2010; Maldonado et al., 2017; Hawkes et al., 2019; Meyer et al., 2019; Ramirez-Llodra, 2020). These often vulnerable hotspots of biomass and biodiversity (like cold-water coral reefs or sponge grounds) provide important ecosystem goods and services (Klitgaard and Tendal, 2004; Buhl-Mortensen et al., 2010), which are vital for the well-being of the entire ocean and biosphere (Sweetman et al., 2017; Levin et al., 2019).

Figure 1.3 (next page) a) & b) Cold-water coral reefs on the Angolan margin © MARUM ROV SQUID, Bremen, Germany, c) Sponge ground on the Schulz Bank seamount with its associated fauna, d) *Vazella pourtalesii* sponge ground on the Scotian Shelf © Bedford Institute of Oceanography Fisheries and Oceans Canada, e) Sponge ground on the Schulz Bank seamount with its associated fauna© University of Bergen.

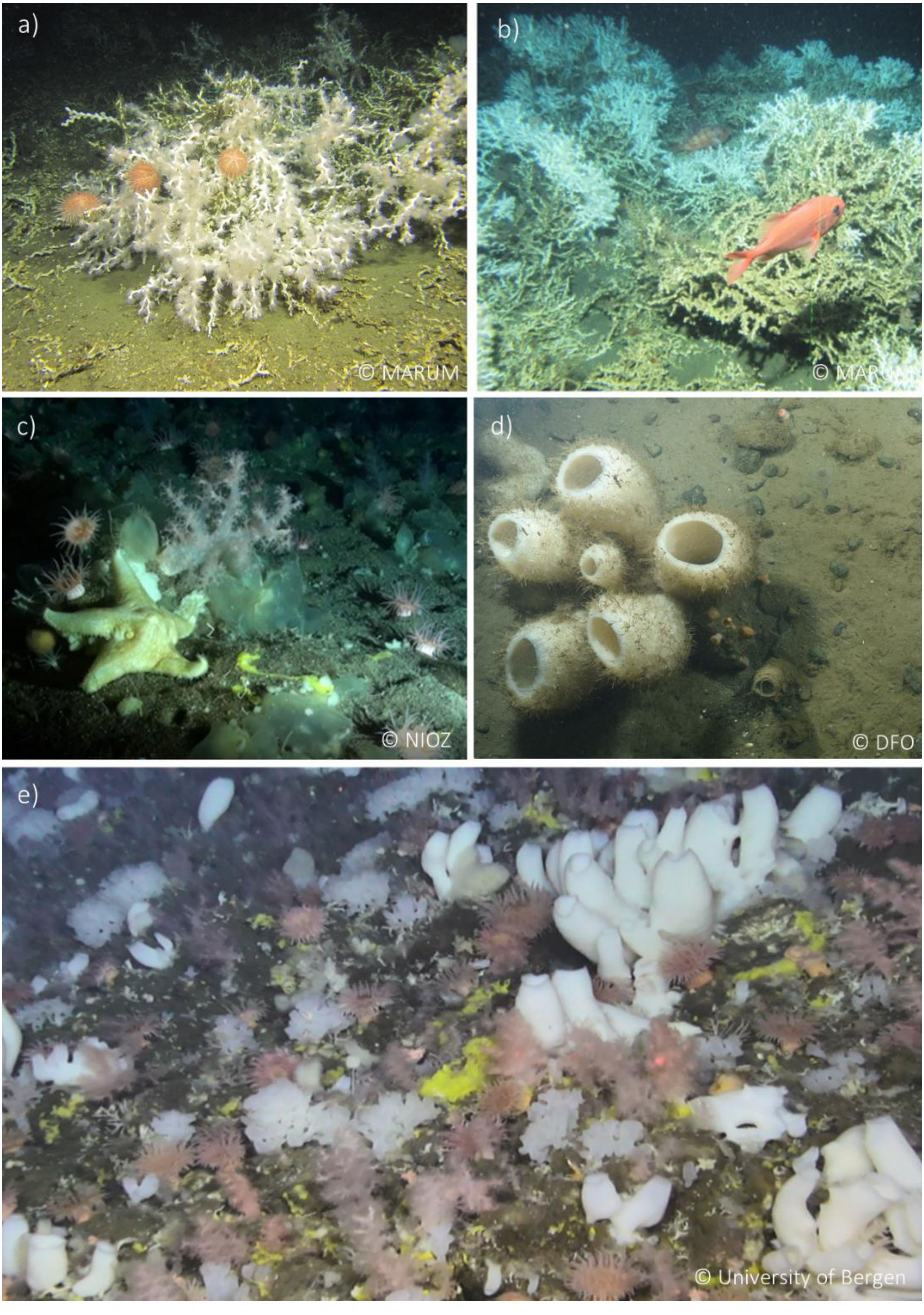
a)
© MARUM
b)
© MARUM
c)
© NIOZ
d)
© DFO
e)
© University of Bergen

1.3 Cold-water coral reefs

Cold-water coral reefs occur globally and are found at all latitudes and in all oceans, with most records reported from the continental margins of the North-East and North West Atlantic Ocean (Paull et al., 2000; Mortensen et al., 2001; De Mol et al., 2002; Roberts et al., 2006; Hebbeln et al., 2014). They occur in a depth range from 50–4000 m water depth and are estimated to cover a surface area of over 280,000 km^2, which is comparable to the surface area of tropical reefs (Roberts et al., 2006; Hebbeln et al., 2014; Davies et al., 2008; Mortensen et al., 2001; Freiwald et al., 2004; Freiwald, 2002; Grasmueck et al., 2006; Wheeler et al., 2007).

The most common framework building species in the Atlantic Ocean are the scleractinian corals *Lophelia pertusa* (Phylum Cnidaria, syn. *Desmophyllum dianthus;* Linnaeus, 1758; Addamo et al., 2016; *Madrepora oculate*, Phylum Cnidaria; Linnaeus, 1758), which are considered true ecosystem engineers (Figure 1.3a and 1.3b; Freiwald et al., 2004; White et al., 2005; Roberts et al., 2006; Cairns, 2007). Both species form bush like colonies of branches made of aragonite. Cold-water corals have been observed as single patches, as reefs and even can form large elevated structures, so-called coral mounds formed by the baffling of sediment in between the cold-water coral branches which can be several kilometers in diameter and hundreds of meters high (Wilson, 1979; Wienberg and Titschack, 2017; Titschack et al., 2015; De Haas et al., 2009).

Cold-water coral reefs have been identified as hotspots of biomass and biodiversity, comparable to shallow-water tropical reef systems (Roberts et al., 2006; Buhl-Mortensen et al., 2010; Cathalot et al., 2015), hosting a rich fauna with a high diversity of associated organisms, including sessile and mobile mega- to macrofauna (Henry and Roberts, 2007; van Soest et al., 2007) as well as fish (Costello et al., 2005). In addition they have been recognized as hotspots of carbon cycling (Oevelen et al., 2009; Cathalot et al., 2015). Habitat suitability of cold-water corals is mainly related to prevailing water masses and suitable environmental conditions (Davies et al., 2008).

Most cold-water coral reefs have been found between 300-1200 m water depth in waters with temperatures between 4-13°C, a salinity range between 32-38.8 (Freiwald, 2002) and oxygen concentrations > 2.1 ml l^{-1} (Davies et al., 2010). As sessile heterotrophic organism, cold-water corals are dependent on mechanism that transport food towards them. Therefore they appear often on topographic structures with enhanced currents and local hydrodynamic conditions that promote food supply (Davies, 2009; Mohn et al., 2014; van Haren et al., 2017). *L. pertusa* is an opportunistic feeder which uses different food sources (Mueller et al., 2014), mainly consisting of advected particulate organic matter (Duineveld et al., 2004; Duineveld et al., 2007; Davies et al., 2009) and small prey like crustaceans or krill (Roberts et al., 2009; Hebbeln et al., 2014). These reefs are often associated with sponges or are found adjacent to sponge grounds suggesting that similar environmental conditions are beneficial for CWC as well as sponges (van Soest and Lavaleye 2005; Cathalot et al., 2015), whereas compared to CWCs, deep-sea sponges (Phylum Porifera) received little attention so far.

1.4 Deep-sea sponge grounds

Like cold-water corals, sponges are cosmopolitan species, and are among the most common megafaunal organisms in bathyal and abyssal depths (>200 m; Tabachnick et al., 1994). Sponges can appear solitary or in high abundances, forming so called sponge grounds or even reef like systems in which they constitute 90% of the total invertebrate biomass (Figure 1.3c and 1.3d; Maldonado et al., 2017). Deep-sea sponge communities are represented by demosponges (Demospongiae, 1885) and glass sponges (Hexactinellidae, Figure 1.4; Schmidt, 1870). Both sponge classes have, with a few exceptions, a siliceous (SiO_2) skeleton of spicules that supports the soft body parts (Figure 1.4b). After the sponges die and decompose the spicules can remain on the seafloor as a so called spicule mat, which can form a 3D structure acting as a substrate and habitat for different organisms, as well as sponges themselves (Bett and Rice, 1992; Maldonado et al., 2017). The dominance of particular sponge species largely depends on environmental factors. Hexactinellida for example mainly occur in the deep oceans, where they are often found on steep rocky substrates with low amounts of suspended sediment and occur less often on flat shelves (Farrow et al., 1983; Maldonado et al., 2017). Some species (e.g. *Pheronema carpenteri*) are capable to build up a basal specular component (comparable to roots) enabling them to anchor in soft substrate (Barthel et al., 1996).

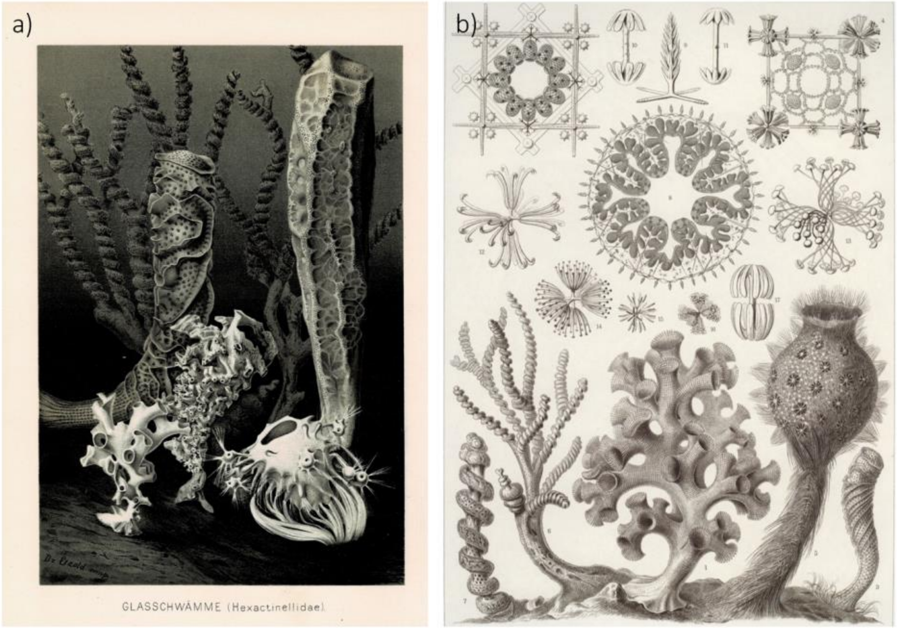

Figure 1.4 a) Glass sponges (*Hexactinellids*), Chromlithograph (Brockhaus c. 1892), b) Glass sponges (*Hexactinellids*) and their glass skeleton, the so-called spicules (Haeckel, 1904)

Sponges can also be grouped by the abundance of their associated microorganisms. They are known to contain an abundant and diverse community of microbial symbionts like bacteria, fungi, yeast and archaea (Hentschel et al., 2003; Taylor et al., 2007; Webster and Taylor, 2012). Based on differences in these symbionts, sponge species are classified as high microbial abundance (HMA) sponges or low microbial abundance (LMA) sponges (Vacelet and Donadey, 1977; Hentschel et al., 2006). In HMA sponges, symbionts account for up to 60% of the biomass and have 2–4 orders of magnitude higher microbial concentrations than the surrounding seawater. LMA sponges contain much lower microbial abundances at concentrations similar to that of the ambient seawater.

These sponge classes can build sponge grounds dominated by a single group or they can build sponge grounds with mixed sponge groups. In the North Atlantic several types of sponge-dominated communities have been discovered so far. Examples are the *Pheronema* sp. grounds in the northeast Atlantic Ocean (Rice et al., 1990), *Geodia* sp. grounds in the western Barents Sea (HMA, Klitgaard and Tendal 2004), *Vazella* sp. grounds in the northwest Atlantic along the Canadian continental shelf (LMA, Beazley et al., 2013), *Astrophorid* grounds of the Flemish Cap and Grand Banks (Murillo et al., 2018) or mixed assemblages on the Arctic Mid-Ocean Ridge (Figure 1.3, HMA and LMA; Meyer et al., 2019). The total surface area in the deep sea that these sponges cover is still unknown, since research on deep-sea sponge grounds is still in its infancy.

Additionally to the abovementioned role as habitat providers, sponges also have an important role in benthic pelagic coupling of carbon and nutrient cycling (Pile and Young, 2006; De Goeij et al., 2013; Rix et al., 2018). Sponges can filter up to 20 000 l of seawater per kg (dry weight) per hour and thereby ingest large amounts of carbon by removing bacteria, particulate and dissolved organic matter from the water column (Witte, 1996; Gili and Coma, 1998; Pile and Young, 2006; Kutti et al., 2013; Pham et al., 2019). Sponges take up carbon in the form of particulate organic matter (POM; Reiswig, 1971; Hadas et al., 2009), microbes (Pile and Young, 2006), but also to a significant amount from dissolved organic matter (DOM; Bart et al., 2021). Studies showed that sponges take up dissolved carbon (De Goeij et al., 2013; Bart et al., 2021) and nitrogen (Jiménez and Ribes, 2007; Morganti et al., 2017), which is generally not accessible for other heterotrophic organisms. In tropical reef systems they are able to transfer this DOM to the associated fauna in the form of particulate detritus, a pathway named the sponge loop (De Goeij et al., 2013). This bottom-up recycling of DOM into detritus has also been found in deep-sea coral reefs (Rix et al., 2016; Maier et al., 2020). So far, the budgets and fluxes of carbon and nutrients in deep sponge grounds remain largely unknown, even though they have the potential to significantly influence global biogeochemical cycles due to their global distribution (Figure 1.5).

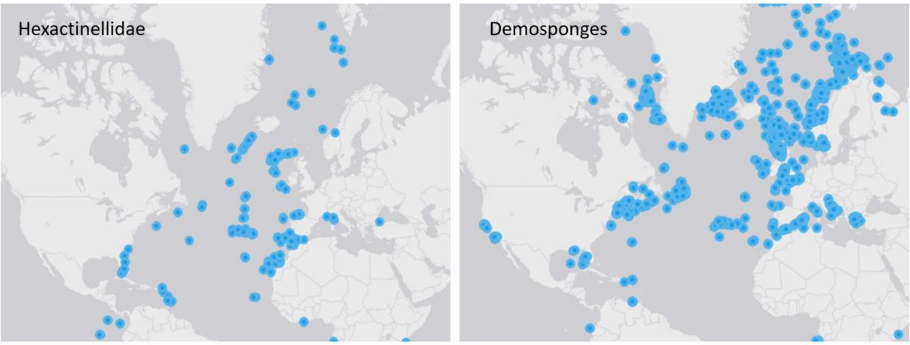

Figure 1.5 Known occurrences of Hexactinellidae and Demosponges in the North Atlantic (data from SponGIS; spongis.org).

1.5 Topographical features

Hotspots of deep-sea benthic fauna are often connected to specific bathymetry and hydrography. In these places, favourable hydrodynamic conditions are generated due to the seafloor topography interacting with local and regional hydrodynamics often in combination with high surface productivity. This is the case for example near continental margins, submarine canyons, seamounts, mid-ocean ridges, and trenches (Levin and Sibuet, 2012).

Continental margins constitute about 28% of the oceanic area and extend from the water surface towards more than 4000 m water depth. They are characterized by a multitude of habitats and ecosystems linked to geomorphological, geochemical, and hydrographic features (Freiwald et al., 2004; Levin and Sibuet, 2012). Continental margins can roughly be divided in the gently sloping continental shelves and the steeper continental slopes, which both have different geomorphological and physical characteristics. The shelf region, which is defined as the area above 200 m water depth, is often characterized by high productivity and has a vertically stratified water column depending on the season. The Norwegian and Canadian shelves for example are highly productive areas with large stocks of pelagic fish and plankton, harbouring vast complex benthic habitats of cold-water corals and demosponges (Mortensen et al., 2001; Klitgaard and Tendal, 2004; Fuller, 2011). The deeper and steeper continental slope (>200 m) is characterized by abrupt topography (e.g., canyons, ridges and mounds; De Mol et al., 2002; Harris and Whiteway, 2011) and is dominated by oceanic water masses and boundary currents (Huthnance, 1995). When this abrupt topography interacts with hydrography it can result in intensified ocean currents, which can enhance food particle supply as well as sediment redistribution (Figure 1.6). This was for example observed on the Rockall Trough margins where the occurrence of thriving cold-water coral reefs is related to physical processes which enhance downslope transport and retention of organic matter (White et al., 2005). The near bottom flow is strongly tidal and reflects the activity of internal waves and tides (Hosegood and van Haren, 2004), but also wind-induced up- and down welling can play a major role (Mooers, 1976).

Other deep-sea topographic features, which are characterized as biodiversity hotspots are seamounts, defined as topographically-isolated peaks rising more than 1000 m above the surrounding seabed (Rogers, 1994). There are more than 33,000 seamounts globally, which cover approximately 4.7% of the ocean floor (Yesson et al., 2011). Seamounts affect the general flow of water, causing eddies and increasing turbulence, which retains particles around the summit of the seamount in so called Taylor columns (Lavelle and Mohn, 2010; Figure 1.6). Tidal flow passing over the seamount summit may result in additional turbulence and vertical mixing (van Haren et al., 2017). These processes deliver water with higher nutrient concentrations towards the surface and thereby provide a nutrient source for phytoplankton. Enhanced phytoplankton blooms and related food supply not only attract higher trophic levels like fish and marine mammals (Jalali et al., 2017; Hosegood et al., 2019), but also increase the availability of food resources for the suspension feeding benthic fauna on the seamount itself (Taylor, 1923; Boehlert and Genin, 1987; Henrich et al., 1992; Lavelle and Mohn, 2010).

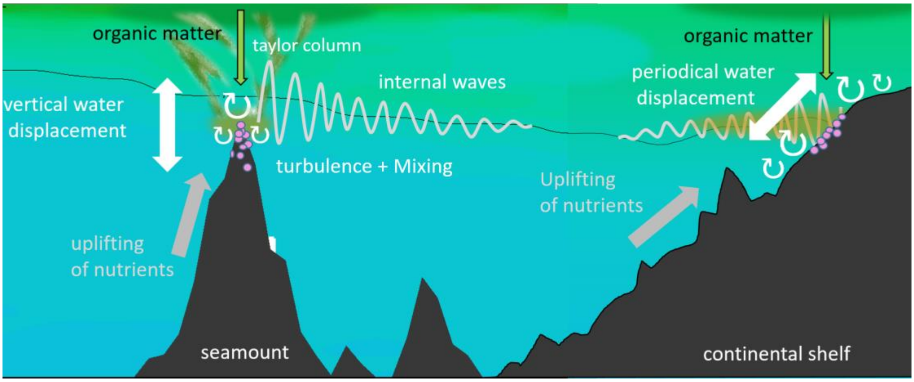

Figure 1.6 Hydrodynamic processes on two topographical features (seamounts and continental margin) that deliver organic matter from productive regions of the surface ocean to deep-sea benthic hotspots (indicated by pink dots).

1.6 Energy in the deep sea

Animals in the deep sea receive their energy from five major sources: plankton, carcasses of large nekton, marine macrophyte detritus, terrigenous organic matter and chemoautotrophic produced organic matter (Rowe and Staresinic, 1979). These sources vary regionally and seasonally. Allochthonous material from terrestrial sources is limited to the continental shelves and has a relatively small influence on the benthic fauna since it is mostly of a degraded nature. Sinking of large organisms (Smith and Baco, 2003) and plants (Krause-Jensen and Duarte, 2016) in contrast provide high quality organic matter, but are generally limited to very small spatial scales and do not have an influence on the majority of the seafloor for longer time scales. Hydrothermal vent or cold-seep communities are relying on chemical energy provided by chemicals dissolved in the vent fluids, where chemosynthetic bacteria build the base of the food web and provide energy to the associated fauna (Govenar, 2012). Still, such communities are generally considered exceptions bound to particular places, like for example mid ocean ridges (Sibuet and Olu-Le Roy, 2002; Baker and German, 2004). The main energy supply to the deep sea is hence derived from primary production in the surface ocean, which sinks to the seafloor as phytodetritus (Suess, 1980). Besides providing the deep-sea fauna with food, this solar energy-driven “biological pump” also plays an important role in the export and sequestration of CO_2 (Le Moigne, 2019). So called “sediment traps” collecting the sinking material or direct observations by cameras have been used to quantify the vertical flux of organic matter. Sediment trap studies have shown that below 2000 m water depth only about 1% of the sinking material reaches the seafloor (Martin et al., 1987; Buesseler et al., 2007). The majority of the organic matter is recycled by pelagic organisms (like zooplankton or large gelatinous fauna) or remineralized in the water column while settling before it reaches the seafloor (Carlson et al., 2010). Large particles (>32 µm) are known to sink faster and therefore account for most of the vertical flux, although the particle size and amount of vertical flux is highly variable in space and time. The amount of sinking material depends on the latitude, whereby the main pulses of organic matter occur during seasonal phytoplankton blooms (Billett et al., 1983; Duineveld et al., 2007; Maier et al., 2020). There are extreme temporal fluctuations in the oceanic carbon budget due to these phytoplankton bloom periods, which are a dependent on the temperature, stratification and light and nutrient availability (Boyd et al., 2019). Bloom periods amount up to ca. 40% of the annual particulate organic carbon flux to the deep sea (Smith et al., 2018). The organic carbon will not only passively travel to the deep sea by settling due to gravitational forces, but is also transported by physically mediated (for example downwelling) or biologically mediated processes like for example zooplankton vertical migration (Boyd et al., 2019). Physically mediated processes are often related to meteorological forcing as for example, convective overturning and storm events, which result in vertical mixing of the water column (Pedrosa-Pàmies et al., 2019) or tidally driven processes (e.g. internal waves) that increase turbulence and hence mixing of the water column like explained above (Frederiksen et al., 1992; Thiem et al., 2006). On the seafloor, this material will serve as a food source for the benthic fauna or will be buried in the sediment, removing CO_2 from the atmosphere for geological time scales.

1.7 Anthropogenic impacts and threats

Even though deep-sea ecosystems occur at great depths, they are vulnerable to anthropogenic impacts and threats like for example climate change, fishing or deep-sea mining activities (Rogers, 2004; Millennium Ecosystem Assessment, 2005; Hogg et al., 2010; Lubchenco and Petes, 2010). For instance, climate change due to rising atmospheric greenhouse gases is expected to significant change water column oxygenation, temperature, pH and food supply (Sweetman et al., 2017). This will expose deep sea ecosystems to critical changes in water temperature (+2 °C), reduce organic carbon fluxes by up to 50%, and decreased dissolved oxygen concentrations (>5%). On the other hand, physical disturbances by fisheries and deep-sea mining can have deleterious effects on coral and sponge ecosystems (Althaus et al., 2009; Pham et al., 2019). It has been recognized for example by the OSPAR Recommendation 2010/10 that key species like cold-water corals and sponges are "very sensitive to physical damage as a result of commercial bottom trawling and suffer significant declines as a result". Deep-sea species are slow-growing and long-lived and hence recover very poorly from stressors like for example physical damage. Next to the direct physical damage also climate change will have a major impact on deep-sea ecosystems, since it influences the physical and chemical properties of the ocean, including changes in oxygen and food supply (Sweetman et al., 2017). Therefore, serious actions are required to protect the functions and services that are provided by the deep-sea ecosystems that we are just getting to know (Armstrong et al., 2019).

1.8 Scope and framework of this thesis

This thesis intended to establish and extend the knowledge on deep-sea biological hotspots, especially focusing on the environmental conditions that influence and sustain cold-water corals and deep-sea sponges. It is divided in two major parts: The first part (Chapter 2-4) focuses on the recent hydrodynamic setting near biological hotspots, showing the hourly to seasonal variability in near-bed environmental conditions and food supply. In order to determine the environmental characteristics, landers were deployed inside coral reefs and sponge grounds, equipped with hydrodynamic sensors to measure the variability in near-bed environmental conditions (Figure 1.2c). Water column and sediment trap samples were analyzed to determine the available amount of particulate food received from the surface ocean throughout the year. In the second part of this thesis, it is shown if and how sponges influence their environment and what their association is with other deep-sea fauna (Chapter 5 and 6).

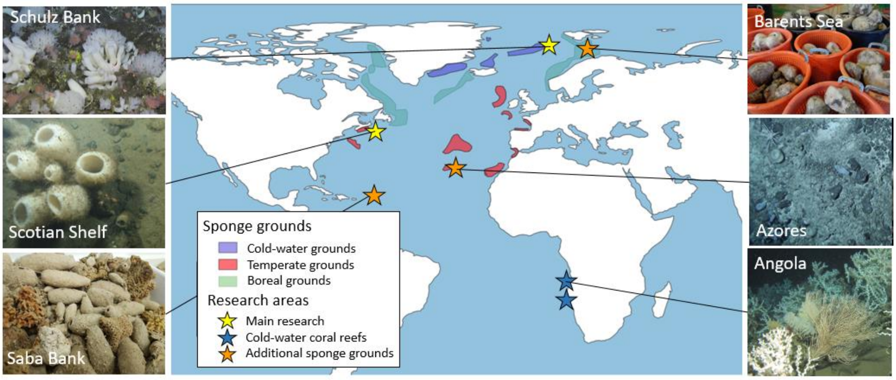

Figure 1.7 Distribution of sponge grounds in the North Atlantic. Research areas of this thesis are indicated by stars. Yellow= main research areas: Schulz Bank (mixed species assemblage, Chapter 4-6) and Scotian Shelf (*Vazella pourtalesii* grounds, Chapter 3), blue= Cold-water coral reefs at the Namibian and Angolan margins (Chapter 2), orange= Demosponge grounds in the Barents Sea, *Pheronema carpenteri* grounds around the Azores, Hexactinellid sponge grounds in the Caribbean on the Saba Bank.

In order to identify the food sources for deep-sea sponges and their position in the food web an extensive food-web study was performed on the Schulz Bank. In-situ incubation chambers were deployed (Figure 1.2d), which measured the oxygen consumption and nutrient exchange of the sponge ground on a shorter time scale (Chapter 6). Additionally, a profile pump was deployed on the Schulz Bank sponge ground to determine the effect of sponges and their associated fauna on the benthic boundary layer, the so-called “reef effect”. Several sponge dominated areas were studied in detail (Figure 1.6, yellow stars), including a multi specific sponge reef on the Schulz Bank seamount along the Arctic Atlantic Mid-Oceanic

Ridge (Chapter 4-6) and temperate monospecific sponge grounds on the Canadian Shelf (Chapter 3). Additionally, cold-water coral reefs in the oxygen minimum zones of the Namibian and Angolan margins were investigated (Figure 1.7, blue stars, Chapter 2).

In **Chapter 2** environmental factors influencing cold-water corals and sponges on the Angolan and Namibian margins were studied. Fossil cold-water coral mounds overgrown by sponges and bryozoans were observed in anoxic conditions on the Namibian margin, while mounds colonized by thriving cold-water coral reefs were found in hypoxic conditions on the Angolan margin. At the Angolan margin environmental conditions were sufficient for cold-water coral survival, whereas the anoxic conditions on the Namibian margin are inhibiting cold-water coral growth at present. In both areas, tidally driven water movements temporarily delivered food and water with more suitable characteristics to the deep-sea ecosystems from below and above the oxygen minimum zone. The high quantity and quality of organic matter served as an important food source, which on the Angolan margin likely counteracts the effect of the hypoxic conditions for cold-water corals. This study provides valuable insights in how cold-water coral communities as well as the associated fauna may compensate unfavourable conditions induced by (extreme) low oxygen levels and high temperatures with an enhanced availability of food.

In **Chapter 3** the seasonal variability in environmental conditions inside a monospecific sponge ground on the eastern Canadian shelf was investigated during a 10-month deployment of a benthic lander. The Scotian Shelf harbors unique aggregations of the glass sponge *Vazella pourtalesii*, at a depth between about 150 and 240 m with an average density of 3.8 ind. m^{-2} (Hawkes et al., 2019; Maldonado et al., 2020). Lander data showed that the sponges are bathed in a warm water mass and occur in an area of relatively strong bottom currents related to semi-diurnal tidal flow. Daily changes in current speed produced a constant resuspension of particulate matter in the benthic boundary layer, which likely acts as a food source for the filter feeding benthic fauna, since the flux of organic matter as collected by the sediment trap was not sufficient to cover the (particulate) energy demand of the sponge ground. Surface storm events were episodically causing extremely turbid conditions on the seafloor for several days, which are expected to be a major stressor for sponges. High amount of suspended matter might interfere with the pumping ability of sponges, however storm events in winter likely play an important role for the benthic ecosystem since they mix the water column, deliver food and replenishing oxygen in the deeper parts of the water column. This study indicated the resiliency of sponges to environmental changes and stressors over short time scales, which might be vital for their survival under human-induced threats such as bottom fishing and climate change.

Similar long term near-bed observations were made in a sponge ground on an Arctic Mid-Ocean Ridge seamount (Schulz Bank), to determine what is driving the distribution and sustenance of this deep-sea ecosystem (**Chapter 4**). Near-bed environmental conditions measured during a one year deployment with a bottom lander showed new insights on daily to seasonal fluctuations in environmental conditions. The deep-sea sponge ground is characterized by a mixed species assemblage of different sponge classes, which were thriving at temperatures of -0.5 to 1°C. The sponge ground was situated at the interface of two water masses at which inertial waves disseminate and interact with the seamount topography. This produces high currents and turbulent mixing, which resuspends organic matter as well as delivers organic matter from water layers above towards the sponge ground. In the benthic boundary layer these tidal currents are weakened, which allows organic material to remain suspended inside the benthic boundary layer throughout the year allowing an effective uptake of resuspended material by the abundant suspension feeders of the sponge ground. This system is only fuelled by a small amount of fresh particulate organic matter produced by the surface phytoplankton bloom in summer. This particulate carbon flux cannot sustain such a dense benthic ecosystem and likely sponges are able to exploit additional food resources. Therefore, the delivery of alternative food sources like dissolved organic matter and bacteria by tidal forced internal wave turbulence and transport by horizontal mean flows likely play an important role for the survival of this deep-sea sponge ground.

In **Chapter 5** we investigated the same sponge ground for its food web structure to identify the role of sponges in the provision of food for the associated fauna. In this study, the food-web interactions and potential food sources were identified by bulk and compound-specific stable isotope analysis of amino acids and fatty acids. The elevated bulk δ^{15}N values of sponges with relatively low abundance of associated microbes suggests a position at the top of the benthic food web, while the relatively high δ^{13}C and intermediate δ^{15}N values of high microbial abundance sponges suggest considerable reliance on an alternate resource. Trophic positions based on amino acid δ^{15}N values placed HMA sponges at the base of the food web, suggesting chemoautotrophic processes inside the sponge likely by their associated microbes. Fatty acid analysis of δ^{13}C indicated transfer of sponge derived organic matter to the wider food web. These results emphasize that sponges inhabit different positions in the food chain and play a unique and pivotal role in deep-sea food webs. Sponges likely drive both bottom-up and top-down processes, shunting particulate organic carbon to higher trophic levels that would otherwise be inaccessible to the associated fauna, enabling a thriving deep-sea ecosystem.

In order to determine the role of deep-sea sponge grounds in carbon and nutrient cycling, in-situ incubation experiments were performed in the sponge ground on the Schulz Bank seamount (**Chapter 6**). Oxygen, carbon and inorganic nutrient dynamics were measured with in-situ incubation chambers deployed amidst the sponge ground by an ROV. In addition, characteristics of the benthic boundary layer with regards to bacterioplankton and nutrient gradients were measured with a profile pump during different flow regimes. Oxygen consumption was mainly driven by the presence of large sponge specimens and was comparable to other deep-sea hotspots, like cold-water coral reefs. The vertical gradient of the bacterial concentrations revealed a flux of several millions of bacteria per m^2 per second towards the seafloor, probably acting as a food source for sponges. The sponge ground was measured to release inorganic nutrients (NO_3^-, NH_4^+, NO_2^-, PO_4^{3-}), whereas the kinetics of nitrogen were associated with the dominant sponge class in the incubation (HMA or LMA). This release of nutrients was also observed in the benthic boundary layer showing that sponges play an important role in benthic-pelagic coupling. The results of this study show that sponge grounds are hotspots of carbon and nutrient cycling in deep sea.

In **Chapter 7** the knowledge about the environmental conditions regulating the distribution of deep-sea sponge grounds are summarized, compared and discussed. For the first time long-term measurements of near-bed environmental conditions were collected in sponge dominated deep-sea ecosystems. Even though we only assessed the long term near-bed environmental conditions in two different areas in detail, comparison with literature shows that most sponge grounds are found at the interface of two water masses and at sites characterized by strong mixing and turbulence. Our data also showed that deep-sea sponges are very resilient and can thrive in a large range of environmental conditions compared to for instance cold-water coral reefs. The observation that they can thrive over these large environmental ranges and can utilize a multitude of food sources, implies that they might cover an even larger surface area in the Atlantic than so far known. Additionally, the unusual role of sponges in the deep-sea food web is discussed. Finally, the role and influence of sponge grounds is compared to other deep-sea ecosystems and their overall ecological role in the deep sea is assessed.

This thesis was written as part of the EU-funded SponGES project, which was aiming to develop an integrated ecosystem-based concept for the preservation and sustainable exploration of vulnerable deep-sea sponge ecosystems of the North Atlantic. By combining the results about past and present distribution, food web models and habitat suitability models the SponGES project will improve our understanding in how these ecosystems might change under climate change and other anthropogenic influences. SponGES has received funding from the European Union’s Horizon 2020 research and innovation programme under grant agreement No 679849.

This dissertation is dedicated to the memory of **Hans Tore Rapp**. He was a passionate sponge scientist and the initiator of the SponGES project. During the time we had the pleasure to work with him he inspired us all to have a closer look at the understudied sponges. Unfortunately he was unable to see the results of his project and our work, which would probably have made him proud. He is a very much missed member of the SponGES team since he was not only an excellent scientist but also the kindest and most helpful soul you can imagine.

Hans Tore Rapp

*22. January 1972 †07. March 2020

Chapter 2

Environmental factors influencing cold-water coral ecosystems in the oxygen minimum zones on the Angolan and Namibian margins

Ulrike Hanz, Claudia Wienberg, Dierk Hebbeln, Gerard Duineveld, Marc Lavaleye, Katriina Juva, Wolf-Christian Dullo, André Freiwald, Leonardo Tamborrino, Gert-Jan Reichart, Sascha Flögel and Furu Mienis

Published in Biogeosciences in 2019

Picture to the left: *Lophelia pertusa* on the Angolan margin ©MARUM

Abstract

Thriving benthic communities were observed in the oxygen minimum zones along the southwestern African margin. On the Namibian margin, fossil cold-water coral mounds were overgrown by sponges and bryozoans, while the Angolan margin was characterized by cold-water coral mounds covered by a living coral reef. To explore why benthic communities differ in both areas, present-day environmental conditions were assessed, using conductivity–temperature–depth (CTD) transects and bottom landers to investigate spatial and temporal variations of environmental properties. Near-bottom measurements recorded low dissolved oxygen concentrations on the Namibian margin of 0–0.15 ml l^{-1} (≙0 –9 % saturation) and on the Angolan margin of 0.5–1.5 ml l^{-1} (≙7 %–18 % saturation), which were associated with relatively high temperatures (11.8–13.2 °C and 6.4–12.6 °C, respectively). Semidiurnal barotropic tides were found to interact with the margin topography producing internal waves. These tidal movements deliver water with more suitable characteristics to the benthic communities from below and above the zone of low oxygen. Concurrently, the delivery of a high quantity and quality of organic matter was observed, being an important food source for the benthic fauna. On the Namibian margin, organic matter originated directly from the surface productive zone, whereas on the Angolan margin the geochemical signature of organic matter suggested an additional mechanism of food supply. A nepheloid layer observed above the cold-water corals may constitute a reservoir of organic matter, facilitating a constant supply of food particles by tidal mixing. Our data suggest that the benthic fauna on the Namibian margin, as well as the cold-water coral communities on the Angolan margin, may compensate for unfavourable conditions of low oxygen levels and high temperatures with enhanced availability of food, while anoxic conditions on the Namibian margin are at present a limiting factor for cold-water coral growth. This study provides an example of how benthic ecosystems cope with such extreme environmental conditions since it is expected that oxygen minimum zones will expand in the future due to anthropogenic activities.

2.1 Introduction

Cold-water corals (CWCs) form 3D structures in the deep sea, providing important habitats for dense aggregations of sessile and mobile organisms ranging from mega- to macrofauna (Henry and Roberts, 2007; van Soest et al., 2007) and fish (Costello et al., 2005). Consequently, CWC areas are considered as deep-sea hotspots of biomass and biodiversity (Buhl-Mortensen et al., 2010; Henry and Roberts, 2017). Moreover, they form hotspots for carbon cycling by transferring carbon from the water column towards associated benthic organisms (Oevelen et al., 2009; White et al., 2012). Some framework-forming scleractinian species, with *Lophelia pertusa* and *Madrepora oculata* being the most common species in the Atlantic Ocean (Freiwald et al., 2004; White et al., 2005; Roberts et al., 2006; Cairns, 2007), are capable of forming large elevated seabed structures, so-called coral mounds (Wilson, 1979; Wienberg and Titschack, 2017; Titschack et al., 2015; De Haas et al., 2009). These coral mounds, consisting of coral debris and hemipelagic sediments, commonly reach heights between 20 and 100 m and can be several kilometers in diameter. They are widely distributed along the North Atlantic margins, being mainly restricted to water depths between 200 and 1000 m, while records of single colonies of L. pertusa are reported from a broader depth range of 50–4000 m depth (Roberts et al., 2006; Hebbeln et al., 2014; Davies et al., 2008; Mortensen et al., 2001; Freiwald et al., 2004; Freiwald, 2002; Grasmueck et al., 2006; Wheeler et al., 2007)A global ecological-niche factor analysis by Davies et al. (2008) and Davies and Guinotte (2011), predicting suitable habitats for *L. pertusa*, showed that this species generally thrives in areas which are nutrient rich, well oxygenated and affected by relatively strong bottom water currents. Other factors potentially important for proliferation of *L. pertusa* include chemical and physical properties of the ambient water masses, for example aragonite saturation state, salinity and temperature (Davies et al., 2008; Dullo et al., 2008; Flögel et al., 2014; Davies and Guinotte, 2011). *L. pertusa* is most commonly found at temperatures between 4 and 12 °C and a very wide salinity range between 32 and 38.8

(Freiwald et al., 2004). The link of *L. pertusa* to particular salinity and temperature within the NE Atlantic led Dullo et al. (2008) to suggest that they are restricted to a specific density envelope of sigma-theta ($\sigma\Theta$)=27.35–27.65 kg m^{-3}. In addition, the majority of occurrences of live *L. pertusa* comes from sites with dissolved oxygen (DO) concentrations between 6 and 6.5 ml l^{-1}(Davies et al., 2008), with lowest recorded oxygen values being 2.1–3.2 ml l^{-1} at CWC sites in the Gulf of Mexico (Davies et al., 2010; Schroeder, 2002; Brooke and Ross, 2014) or even as low as 1–1.5 ml l^{-1} off Mauritania, where CWC mounds are in a dormant stage presently showing only scarce living coral occurrences (Wienberg et al., 2018; Ramos et al., 2017). Dissolved oxygen levels hence seem to affect the formation of CWC structures as was also shown by Holocene records obtained from the Mediterranean Sea, which revealed periods of reef demise and growth in conjunction with hypoxia (with 2 ml l^{-1} seemingly forming a threshold value for active coral growth; Fink et al., 2012).

Another essential constraint for CWC growth and therefore mound development in the deep sea is food supply. *L. pertusa* is an opportunistic feeder, exploiting a wide variety of different food sources, including phytodetritus, phytoplankton, mesozooplankton, bacteria and dissolved organic matter (Kiriakoulakis et al., 2005; Dodds et al., 2009; Gori et al., 2014; Mueller et al., 2014; Duineveld et al., 2007). Not only quantity but also quality of food particles are of crucial importance for the uptake efficiency as well as ecosystem functioning of CWCs (Ruhl, 2008; Mueller et al., 2014). Transport of surface organic matter towards CWC sites at intermediate water depths has been found to involve either active swimming (zooplankton), passive sinking, advection, local downwelling, and internal waves and associated mixing processes resulting from interactions with topography (Davies et al., 2009; van Haren et al., 2014; Thiem et al., 2006; White et al., 2005; Mienis et al., 2009; Frederiksen et al., 1992). With worldwide efforts to map CWC communities, *L. pertusa* was also found under conditions which are environmentally stressful or extreme in the sense of the global limits defined by Davies et al. (2008) and by Davies and Guinotte (2011). Examples are the warm and salty waters of the Mediterranean and the high bottom water temperatures along the US coast (Cape Lookout; Freiwald et al., 2009; Mienis et al., 2014; Taviani et al., 2005). Environmental stress generally increases energy needs for organisms to recover and maintain optimal functioning, which accordingly increases their food demand (Sokolova et al., 2012).

For the SW African margin one of the few records of living CWC comes from the Angolan margin (at 7°S; Le Guilloux et al., 2009), which raises the questions whether environmental factors limit CWC growth due to the presence of an oxygen minimum zone (OMZ; see Karstensen et al. 2008), or whether this is related to a lack of data. Hydroacoustic campaigns revealed extended areas off Angola and Namibia with structures that morphologically resemble coral mound structures known from the NE Atlantic (M76-3, MSM20-1; Geissler et al., 2013; Zabel et al., 2012). Therefore two of such mound areas on the margins off Namibia and Angola were visited during the RV Meteor cruise M122 “ANNA” (ANgola and NAmibia) in January 2016 (Hebbeln et al., 2017). During this cruise, fossil CWC mound structures were found near Namibia, while flourishing CWC reef-covered mound structures were observed on the Angolan margin. The aim of the present study was to assess present-day environmental conditions at the southwestern African margin to explore why CWCs thrive on the Angolan margin and are absent on the Namibian margin. Key parameters influencing CWCs, hydrographic parameters as well as chemical properties of the water column were measured to characterize the difference in environmental conditions and food supply. These data are used to improve understanding of the potential fate of CWC mounds in a changing ocean.

2.2 Material and Methods

2.2.1 Setting

2.1.1.1 Oceanographic setting

The SW African margin is one of the four major eastern boundary regions in the world and is characterized by upwelling of nutrient-rich cold waters (Shannon and Nelson, 1996). The availability of nutrients triggers a high primary production, making it one of the most productive marine areas worldwide with an estimated production of 0.37 Gt C yr^{-1} (Carr and Kearns, 2003). Remineralization of high fluxes of organic particles settling through the water column results in severe mid-depth oxygen depletion and an intense OMZ over large areas along the SW African margin (Chapman and Shannon, 1985). The extension of the OMZ is highly dynamic, being controlled by upwelling intensity, which depends on the prevailing winds and two current systems along the SW African margin, i.e., the Benguela and the Angola currents (Kostianoy and Lutjeharms, 1999; Chapman and Shannon, 1987; Figure 2.1).

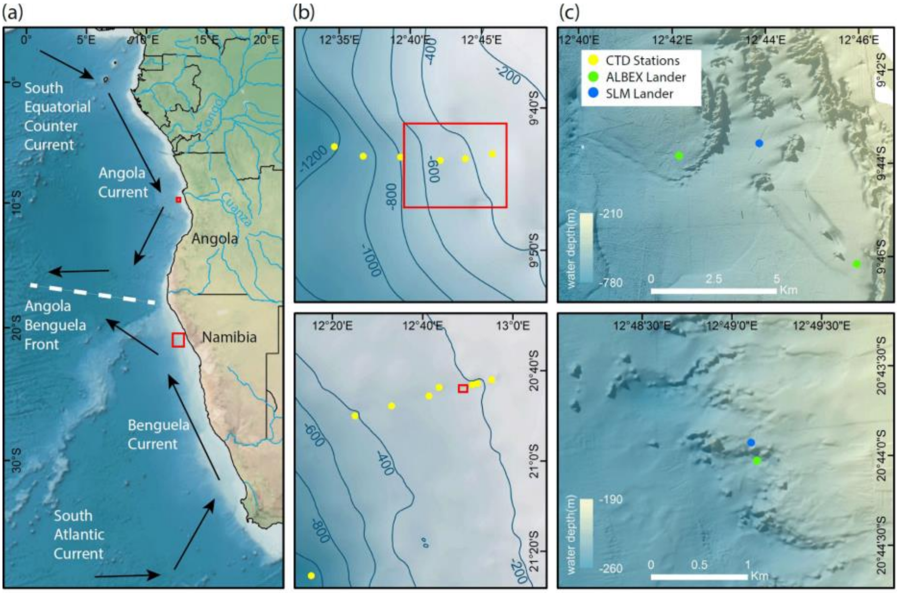

Figure 2.1 (a) Overview map showing the research areas off Angola and Namibia (red squares) and main features of the surface water circulation (arrows) and frontal zone (dashed line) as well as the two main rivers discharging at the Angolan margin. Detailed bathymetry maps of the Angolan (upper maps) and Namibian margins (lower maps) showing the position of (b) CTD transects (note the deep CTD cast down to 1000 m water depth conducted off Namibia) and (c) bottom lander deployments (red squares shown in (b) indicate the cutouts displayed in (c)).

The Benguela Current originates from the South Atlantic Current, which mixes with water from the Indian Ocean at the southern tip of Africa (Poole and Tomczak, 1999; Mohrholz et al., 2008; Rae, 2005) and introduces relatively cold and oxygen-rich Eastern South Atlantic Central Water (ESACW; Poole and Tomczak, 1999) to the SW African margin (Mohrholz et al., 2014). The Angola Current originates from the South Equatorial Counter Current and introduces warmer, nutrient-poor and less oxygenated South Atlantic Central Water (SACW; Poole and Tomczak, 1999) to the continental margin (Figure 2.1a). SACW is defined by a linear relationship between temperature and salinity in a T–S plot (Shannon et al., 1987). While the SACW flows along the continental margin the oxygen concentration is decreasing continuously due to remineralization processes of organic matter on the SW African shelf (Mohrholz et al., 2008). Both currents converge at around 14–16°S, resulting in the Angola–Benguela front (Lutjeharms and Stockton, 1987). In austral summer, the Angola–Benguela front can move southward to 23°S (Shannon et al., 1986), thus increasing the influence of the SACW along the Namibian coast (Junker et al., 2017; Chapman and Shannon, 1987), contributing to the pronounced OMZ due to its low initial oxygen concentration (Poole and Tomczak, 1999). ESACW is the dominant water mass at the Namibian margin during the main upwelling season in austral winter, expanding from the oceanic zone about 350 km towards the coast (Mohrholz et al., 2014). The surface water mass at the Namibian margin is a mixture of sun-warmed upwelled water and water of the Agulhas Current, which mixes in complex eddies and filaments and is called South Atlantic Subtropical Surface Water (SASSW) (Hutchings et al., 2009). At the Angolan margin the surface water is additionally influenced by water from the Cuanza and Congo rivers (Kopte et al., 2017, Figure 2.1). Antarctic Intermediate Water (AAIW) is situated in deeper areas at the African continental margin and can be identified as the freshest water mass around 700–800 m depth (Shannon and Nelson, 1996).

2.1.2.2 Coral mound provinces along the Angolan and Namibian margins

During RV Meteor cruise M122 in 2016, over 2000 coral mounds were observed between 160 and 260 m water depth on the Namibian shelf (Hebbeln et al., 2017). All mounds were densely covered with coral rubble and dead coral framework, while no living corals were observed in the study area (Hebbeln et al., 2017; Figure 2.2a, b). Few species were locally very abundant, viz. a yellow cheilostome bryozoan which was the most common species, and five sponge species. The bryozoans were encrusting the coral rubble, whereas some sponge species reached heights of up to 30 cm (Figure 2.2a, b). The remaining community consisted of an impoverished fauna overgrowing *L. pertusa* debris. Commonly found sessile organism were actiniarians, zoanthids, hydroids, some thin encrusting sponges, serpulids and sabellid polychaetes. The mobile fauna comprised asteroids, ophiuroids, two shrimp species, amphipods, cumaceans and holothurians. Locally high abundances of *Suffogobius bibarbatus*, a fish that is known to be adapted to hypoxic conditions, were observed in cavities in the coral framework (Hebbeln, 2017). Dead corals collected from the surface of various Namibian mounds date back to about 5 ka pointing to a simultaneous demise of these mounds during the mid-Holocene (Tamborrino et al., 2019).

On the Angolan margin CWC structures varied from individual mounds to long ridges. Some mounds reached heights of more than 100 m above the seafloor. At shallow depths (~250 m) some isolated smaller mounds were also present (Hebbeln et al. 2017). All mounds showed a thriving CWC cover, which was dominated by *L. pertusa* (estimated 99 % relative abundance), along with some *M. oculata* and solitary corals. Mounds with a flourishing coral cover were mainly situated at water depths between 330 and 470 m, whereas single colonies were found over a broader depth range between 250 and 500 m (Figure 2.2c, d; Hebbeln et al., 2017). Additionally, large aggregations of hexactinellid sponges (*Aphrocallistes, Sympagella*) were observed. First estimates for coral ages obtained from a gravity core collected at one of the Angolan coral mounds revealed continuous coral mound formation during the last 34 kyr until today (Wefing et al., 2017).

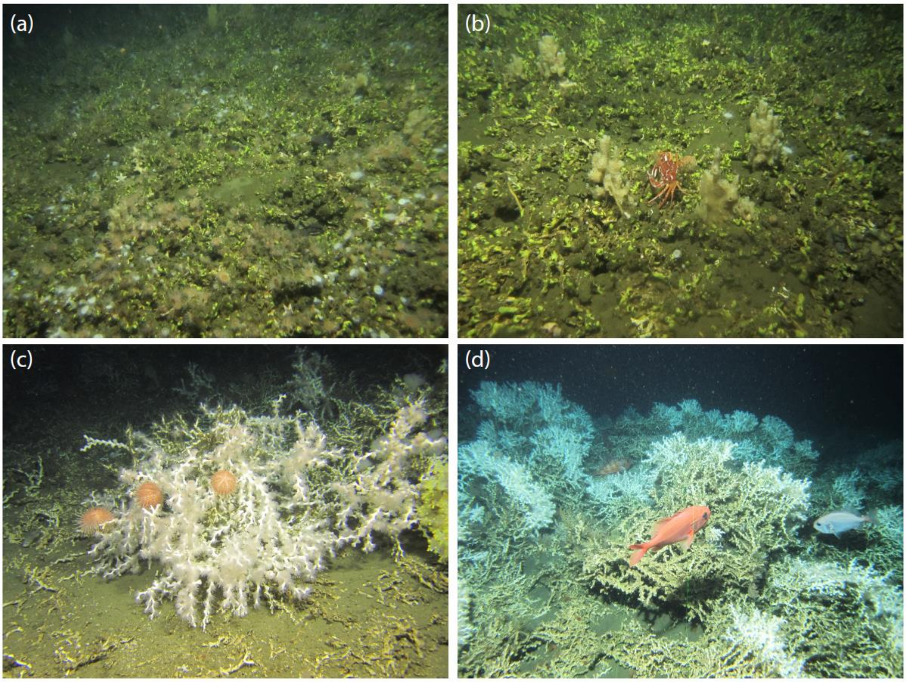

Figure 2.1 ROV images (copyright MARUM ROV SQUID, Bremen, Germany) showing the surface coverage of cold-water coral mounds discovered off Namibia (a, b) and Angola (c, d). Images were recorded and briefly described for their faunal composition during RV Meteor cruise M122 "ANNA" (see Hebbeln et al., 2017). (a) Sylvester mound, 225 m water depth. Dead coral framework entirely consisting of *L. pertusa*. The framework is intensely colonized by the yellow bryozoan *Metropriella* sp., zoanthids, actiniarians and sponges. Vagile fauna consists of asteroids and gobiid fishes (*Sufflogobius bibarbatus*) that hide in hollows in the coral framework. (b) Sylvester mound, 238 m water depth. Dense coral rubble (*L. pertusa*) heavily overgrown by *Metropriella* sp. and sponges. Note the decapod crab Macropipus australis (center of the image). (c) Valentine mound, 238 m water depth. Live *L. pertusa* colony being grazed by echinoids. Note the sponge *Aphrocallistes* sp. with its actiniarian symbionts (right side of the image). (d) Buffalo mound, 345 m water depth. Living CWC reef observed on top of an Angolan coral mound. Many fishes are present around the reef (*Helicolenus dactylopterus, Gephyroberyx darwinii*).

2.3 Methodology

During RV Meteor expedition M122 in January 2016, two conductivity–temperature–depth (CTD) transects and three short-term bottom lander deployments (Table 2.1, Figure 2.1) were carried out to measure environmental conditions influencing benthic habitats. In addition, weather data were continuously recorded by the RV Meteor weather station, providing real-time information on local wind speed and wind direction.

2.3.1 Lander deployments

Sites for deployment of the NIOZ-designed lander (ALBEX) were selected based on multibeam bathymetric data. On the Namibian margin the bottom lander was deployed on top of a mound structure (water depth 220 m). Off Angola the lander was deployed in the relatively shallow part of the mound zone at 340 m water depth and in the deeper part at 530 m (Figure 2.1, Table 2.1). Additionally, a GEOMAR satellite lander module (SLM) was deployed off-mound at 230 m depth at the Namibian margin and at 430 m depth at the Angolan margin (Figure 2.1, Table 2.1). The lander was equipped with an ARO-USB oxygen sensor (JFE Advantech™), a combined OBS-fluorometer (Wet Labs™) and an Aquadopp (Nortek™) profiling current meter. The lander was furthermore equipped with a Technicap PPS4/3 sediment trap with 12 bottles (allowing daily samples) and a McLane particle pump (24 filter units for each 7.5 L of seawater, 2 h interval) to sample particulate organic matter in the near-bottom water (40 cm above bottom).

Table 2.1 Metadata of lander deployments conducted during RV *Meteor* cruise M122 (ANNA) in January 2016. The deployment sites are shown in Figure 2.1.

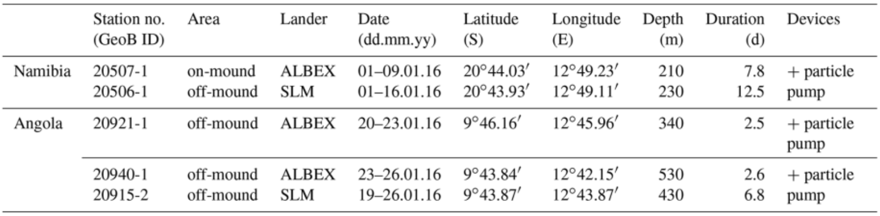

	Station no. (GeoB ID)	Area	Lander	Date (dd.mm.yy)	Latitude (S)	Longitude (E)	Depth (m)	Duration (d)	Devices
Namibia	20507-1	on-mound	ALBEX	01–09.01.16	20°44.03′	12°49.23′	210	7.8	+ particle pump
	20506-1	off-mound	SLM	01–16.01.16	20°43.93′	12°49.11′	230	12.5	
Angola	20921-1	off-mound	ALBEX	20–23.01.16	9°46.16′	12°45.96′	340	2.5	+ particle pump
	20940-1	off-mound	ALBEX	23–26.01.16	9°43.84′	12°42.15′	530	2.6	+ particle pump
	20915-2	off-mound	SLM	19–26.01.16	9°43.87′	12°43.87′	430	6.8	

The SLM was equipped with a 600 kHz ADCP Workhorse Sentinel 600 from RDI, a CTD (SBE SBE16V2™), a combined fluorescence and turbidity sensor (WET Labs ECO-AFL/FL), a dissolved oxygen sensor (SBE™) and a pH sensor (SBE™) (Hebbeln et al., 2017). From the SLM only pH measurements are used here, complementing the data from the NIOZ lander.

2.2.2 CTD transect

Vertical profiles of hydrographic parameters in the water column, viz. temperature, conductivity, oxygen and turbidity, were obtained using a Sea-Bird CTD–Rosette system (Sea-Bird SBE 9 plus). The additional sensors on the CTD were a dissolved oxygen sensor (SBE 43 membrane-type DO Sensor) and a combined fluorescence and turbidity sensor (WET Labs ECO-AFL/FL). The CTD was combined with a rosette water sampler consisting of 24 Niskin® water sampling bottles (10 l). CTD casts were carried out along two downslope CTD transects (Figure 2.1). Owing to technical problems turbidity data were only collected on the Angolan slope.

The CTD data were processed using the processing software Sea-Bird data SBE 11plus V 5.2 and were visualized using the program Ocean Data View (Schlitzer, 2011; Version 4.7.8).

Hydrographic data recorded by the landers were analyzed and plotted using the program R (R Core Team, 2017). Data from the different instruments (temperature, turbidity, current speed, oxygen concentration, fluorescence) were averaged over a period of 1.5 h to remove shorter-term trends and occasional spikes. Correlations between variables were assessed by Spearman's rank correlation tests.

2.2.4 Suspended particulate matter

Near-bottom suspended particulate organic matter (SPOM) was sampled by means of a phytoplankton sampler (McLane PPS) mounted on the ALBEX lander. The PPS was fitted with 24 GF/F filters (47 mm Whatman™ GF/F filters pre-combusted at 450 °C). A maximum of 7.5 l was pumped over each filter during a 2 h period, yielding a time series of near-bottom SPOM supply and its variability over a period of 48 h.

2.4.5 C/ N analysis and isotope measurements

Filters from the phytoplankton sampler were freeze-dried before further analysis. Half of each filter was used for phytopigment analysis and a 1⁄4 section of each filter was used for analyzing organic carbon, nitrogen and their stable isotope ratios. The filters used for carbon analysis were decarbonized by vapor of concentrated hydrochloric acid (2 M HCl supra) prior to analyses. Filters were transferred into pressed tin capsules (12 mm × 5 mm, Elemental Microanalysis), and $\delta^{15}N$, $\delta^{13}C$ and total weight percent of organic carbon and nitrogen were analyzed by a Delta V Advantage isotope ratio MS coupled online to an Elemental Analyzer (Flash 2000 EA-IRMS) by a ConFlo IV (Thermo Fisher Scientific Inc.). The reference gas was purified atmospheric N_2. As standards for $\delta^{13}C$ benzoic acid and acetanilide were used, for $\delta^{15}N$ acetanilide, urea and casein were used. For $\delta^{13}C$ analysis a high-signal method was used including a 70 % dilution. Values are reported relative to v-pdb and the atmosphere respectively. Precision and accuracy based on replicate analyses and comparison with international standards for $\delta^{13}C$ and $\delta^{15}N$ was ±0.15 ‰. The C⁄N ratio is based on the weight ratios between total organic carbon (TOC) and N.

2.4.6 Phytopigments

Phytopigments were measured by reverse-phase high-performance liquid chromatography (RP-HPLC, Waters Acquity UPLC) with a gradient based on the method published by Kraay et al. (1992). For each sample half of a GF/F filter was used and freeze-dried before extraction. Pigments were extracted using 95 % methanol and sonification. All steps were performed in a dark and cooled environment. Pigments were identified by means of their absorption spectrum, fluorescence and the elution time. Identification and quantification took place as described by Tahey et al. (1994). The absorbance peak areas of chlorophyll a were converted into concentrations using conversion factors determined with a certified standard. The ∑phaeopigment ⁄ chlorophyll a ratio gives an indication of the degradation status of the organic material, since phaeopigments form as a result of bacterial or autolytic cell lysis and grazing activity (Welschmeyer and Lorenzen, 1985).

2.2.5 Tidal analysis

The barotropic (due to the sea level and pressure change) and baroclinic (internal “free waves” propagating along the pycnoclines) tidal signals obtained by the Aquadopp (Nortek™) profiling current meter were analyzed from the bottom pressure and from the horizontal flow components recorded 6 m above the sea floor, using the T_Tide Harmonic Analysis Toolbox (Pawlowicz et al., 2002). The data mean and trends were subtracted from the data before analysis.

2.3 Results

2.3.1 Water column properties

2.3.1.1 Namibian margin

The hydrographic data obtained by CTD measurements along a downslope transect from the surface to 1000 m water depth revealed distinct changes in temperature and salinity throughout the water column. These are ascribed to the different water masses in the study area (Figure 2.3a). In the upper 85 m of the water column, temperatures were above 14 ◦C and salinities > 35.2, which correspond to South Atlantic Subtropical Surface Water (SASSW). SACW was situated underneath the SASSW and reaches down to about 700 m, characterized by a temperature from 14 to 7 ◦C and a salinity from 35.4 to 34.5 (Figure 2.3a). A deep CTD cast about 130 km from the coastline recorded a water mass with the signature of ESACW, having a lower temperature (Δ1.3 °C) and lower salinity (Δ0.2) than SACW (in 200 m depth, not included in CTD transects of Figure 2.4). Underneath these two central water masses Antarctic Intermediate Water (AAIW) was found with a temperature < 7 °C.

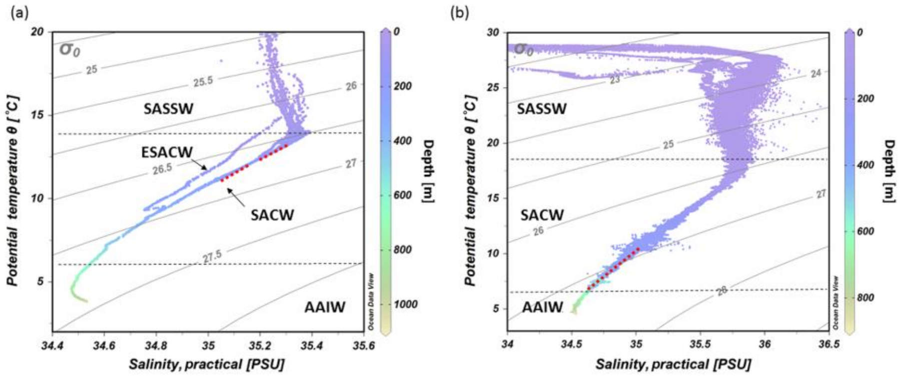

Figure 2.2 TS-diagrams showing the different water masses being present at the (a) Namibian and (b) Angolan margins: South Atlantic Subtropical Surface Water (SASSW), South Atlantic Central Water (SACW) and Eastern South Atlantic Central water (ESACW), Antarctic Intermediate Water (AAIW) (data plotted using Ocean Data View v.4.7.8; http://odv.awi.de; Schlitzer, 2011). Red dotted line indicates the depth range of cold-water coral mound occurrence.

The CTD transect showed decreasing DO (dissolved oxygen) concentration from the surface (6 mL l^{-1}) towards a minimum in 150 to 200 m depth (0 mL l^{-1}). Lowest values for DO concentrations were found on the continental margin between 100 and 335 m water depth. The DO concentrations in this pronounced OMZ ranged from < 1 mL l^{-1} down to 0 ml l^{-1} (≙9 % to 0 % saturation). The zone of low DO concentrations (< 1 ml l^{-1}) stretched horizontally over the complete transect from about 50 km to at least 100 km offshore (Figure 2.4c). The upper boundary of the OMZ was relatively sharp compared to its lower limits and corresponded with the border between SASSW at the surface and SACW below.

Within the OMZ, a small increase in fluorescence (0.2 mg m^{-3}) was recorded, whereas fluorescence was otherwise not traceable below the surface layer (Figure 2.4d). Within the surface layer, highest surface fluorescence (> 2 mg m^{-3}) was found ~40 km offshore. Above the centre of the OMZ fluorescence reached only 0.4 mg m^{-3}.

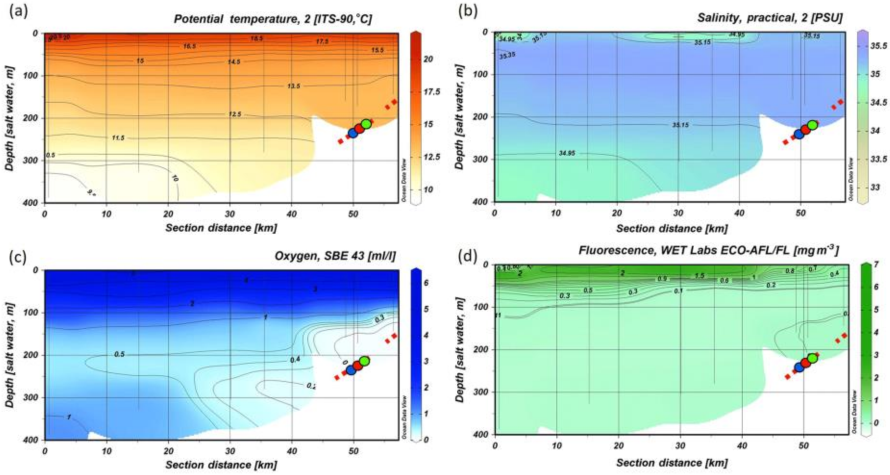

Figure 2.3 CTD transect across the Namibian margin (see Figure 2.1b for location). Data are presented for (a) potential temperature (°C), (b) salinity (PSU), (c) dissolved oxygen concentrations (ml l^{-1}), note the pronounced oxygen minimum zone (OMZ) between 100 and 335 m water depth, and (d) fluorescence (mg m^{-3}) (data plotted using Ocean Data View v.4.7.8; http://odv.awi.de, last access: 12 February 2016; Schlitzer, 2011). The occurrence of fossil CWC mounds is indicated by a red dashed line, colored dots indicate bottom lander deployments.

2.3.1.2 Angolan margin

The hydrographic data obtained by CTD measurements along a downslope transect from the surface to 800 m water depth revealed distinct changes in temperature and salinity throughout the water column, related to four different water masses. At the surface a distinct shallow layer (> 20 m) with a distinctly lower salinity (27.3–35.5) and higher temperature (29.5–27 °C, Figure 2.3b) was observed. Below the surface layer, SASSW was found down to a depth of 70 m, characterized by a higher salinity (35.8). SACW was observed between 70 and 600 m, showing the expected linear relationship between temperature and salinity. Temperature and salinity decreased from 17.5 °C and 35.8 to 7 °C and 34.6. At 700 m depth AAIW was recorded, characterized by a low salinity (< 34.4) and temperature (< 7 °C, Figure 2.3b).

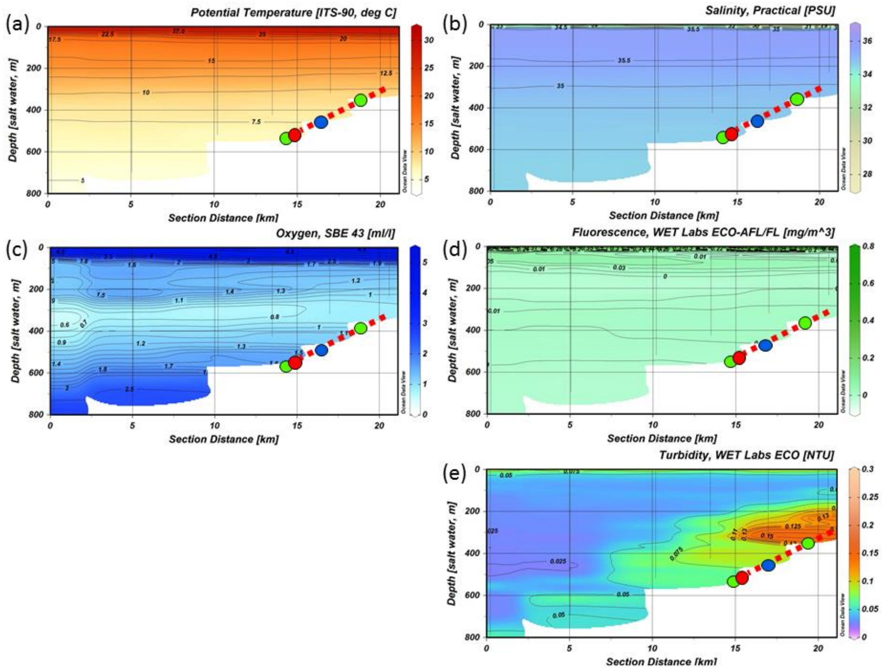

Figure 2.5 CTD transect across the Angolan margin. Shown are data for (a) potential temperature (°C), (b) salinity (PSU), (c) dissolved oxygen concentration (ml l^{-1}), (d) fluorescence (mg m^{-3}), (e) turbidity (NTU) (data plotted using Ocean Data View v.4.7.8; http://odv.awi.de; Schlitzer, 2011). The depth occurrence of CWC mounds is marked by a red, dashed line, the lander deployments are indicated by colored dots.

The CTD transect showed a sharp decrease in the DO concentrations underneath the SASSW from 5 to < 2 ml l^{-1} (Figure 2.5). DO concentrations decreased further to a minimum of 0.6 ml l^{-1} at 350 m and then increased to > 3 ml l^{-1} at 800 m depth. Lowest DO concentrations were not found at the slope but 70 km offshore in the center of the zone of reduced DO concentrations between 200 and 450 m water depth (< 1 ml l^{-1}). Compared to the Namibian margin (see Figure 2.4), the hypoxic layer was situated further offshore, slightly deeper, and overall DO concentrations were higher (compare Figure 2.4c). Also, the boundaries of the hypoxic zone were not as sharp. Fluorescence near the sea surface was generally low (around 0.2 with small maxima of 0.78 mg m^{-3}) and not detectable deeper than 150 m depth. A distinct zone of enhanced turbidity was observed on the continental margin between 200 and 350 m water depth.

2.3.2 Near-bottom environmental data

2.3.2.1 Namibian margin

Bottom temperature ranged from 11.8 to 13.2 °C during the deployment of the ALBEX lander (Table 2.2, Figure 2.6), showing oscillating fluctuations with a maximum semidiurnal (ΔT~6 h) change of ~Δ1 °C (on 9 January 2016). The DO concentrations fluctuated between 0 and 0.15 ml l^{-1} and were negatively correlated with temperature ($r=-0.39$, $p<0.01$). Fluorescence ranged from 42 to 45 NTU during the deployment and was positively correlated with temperature ($r=0.38$, $p<0.01$). Hence, both temperature and fluorescence were negatively correlated with DO concentrations ($r=-0.39$, $p<0.01$) and turbidity (optical backscatter, $r=-0.35$, $p<0.01$). Turbidity was low until it increased markedly during the second half of the deployment. During this period on the 6 January, wind speed increased from 10 m s^{-1} to a maximum of 17 m s^{-1} and remained high for the next 6 . The wind direction changed from counterclockwise cyclonic rotation towards alongshore winds. During the strong wind period, colder water (correlation between wind speed and water temperature, $r=-0.55$, $p<0.01$) with a higher turbidity (correlation of wind speed and turbidity, $r=0.42$, $p<0.01$) and on average higher DO concentrations was present. The SLM lander recorded an average pH of 8.01.

Maximum current speeds measured during the deployment period were 0.21 m s^{-1}, with average current speeds of 0.09 m s^{-1} (Table 2). The tidal cycle explained > 80 % of the pressure fluctuations (Table 3), with a semidiurnal signal, M2 (principal lunar semidiurnal), generating an amplitude of > 0.35 dbar and thus being the most important constituent. Before the 6 January, the current direction oscillated between SW and SE after which it changed to a dominant northerly current direction (Figure 2.6).

Table 2.2 Environmental properties at the Namibian and Angolan margins.

	Namibia	Angola
Temperature (°C)	11.8–13.2	6.73–12.9
DO concentration ($\mathrm{mL\,L^{-1}}$)	0–0.15	0.5–1.5
Fluorescence (NTU)	42–45	38.5–41.5
Current speed max. ($\mathrm{m\,s^{-1}}$)	0.21	0.3
Current speed average ($\mathrm{m\,s^{-1}}$)	0.09	0.1
Tidal cycle	Semidiurnal (0.37 dbar, 3 $\mathrm{cm\,s^{-1}}$)	Semidiurnal (0.6 dbar, 8.2 $\mathrm{cm\,s^{-1}}$)
Average pH	8.01	8.12

The observed fluctuations in bottom water temperature at the deployment site imply a vertical tidal movement of around 70 m. This was estimated by comparing the temperature change recorded by the lander to the respective temperature–depth gradient based on water column measurements (CTD site GeoB20553, 12.58 °C at 245 m, 12.93 °C at 179 m). Due to these vertical tidal movements, the oxygen-depleted water from the core of the OMZ is regularly being replaced with somewhat colder and slightly more oxygenated water (Δ up to 0.2 ml l^{-1}).

Table 2.3 Tidal analysis of the ALBEX lander from 6 m above the sea floor. Depth, mean current speed, current direction, tidal prediction of pressure fluctuations, two most important harmonics with amplitude, tidal prediction of horizontal current field, two most important harmonics with semi-major axes' amplitudes.

	Station no. (GeoB ID)	Depth (m)	Mean current speed ($\mathrm{cm\,s^{-1}}$)	Current direction (°)	Tides (%) (p)	Const. (dbar)	Tides (%) (u)	Const. ($\mathrm{cm\,s^{-1}}$)
Namibia	20507-1	430	9.34	221.6	81.8	M2: 0.37	10.5	M2: 3.1 M3: 0.8
Angola	20921-1	340	9.96	247.9	91.6	M2: 0.59 M3: 0.04	36	M2: 7.8 M8: 0.7
	20940-1	530	8.92	275.6	86.8	M2: 0.60 M8: 0.02	50.9	M2: 8.6 M3: 3.7

Figure 2.6 (next page) Data recorded by the ALBEX lander (210 m) at the Namibian margin in January 2016. Shown are data for temperature (°C; red), dissolved oxygen concentrations (ml l^{-1}; blue), optical backscatter (turbidity; moss green), fluorescence (counts per second; green), current speed (m s^{-1}; pink), current direction (°: 0–360°; dark red) as well as nitrogen (mg l^{-1}; pink dots), carbon (mg l^{-1}; purple dots), and chlorophyll a concentration (µg l^{-1}; green dots) of SPOM collected during the first 48 h by the McLane pump. These data are supplemented by wind speed and direction (small black arrows) recorded concurrently to the lander deployment by ship bound devices. Note that current directions changed from a generally south-poleward to an equatorward direction when wind speed exceeded 10 m s^{-1} (stormy period indicated by black arrow).

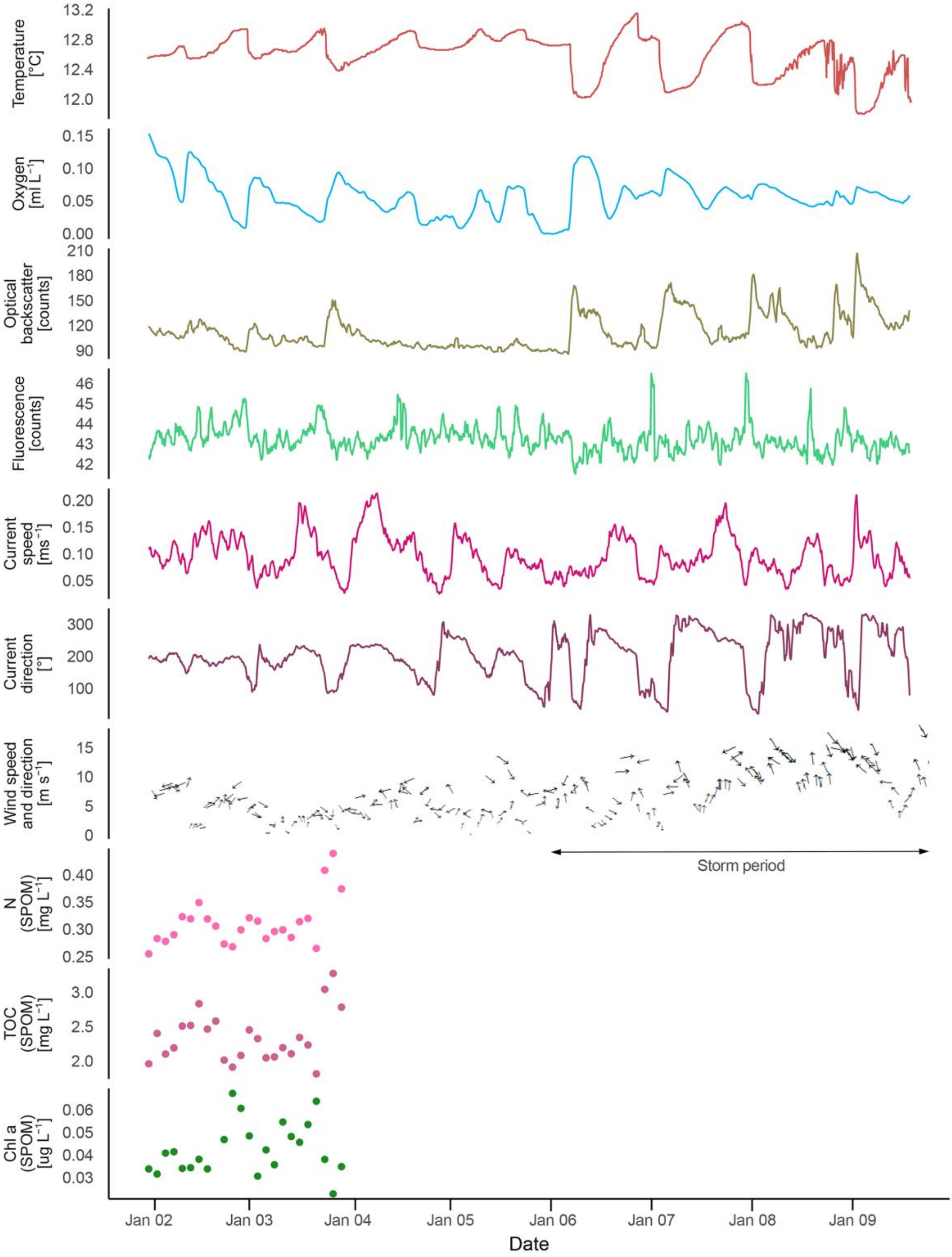
Temperature [°C]
13.2
12.8
12.4
12.0
Oxygen [ml L⁻¹]
0.15
0.10
0.05
0.00
Optical backscatter [counts]
210
180
150
120
90
Fluorescence [counts]
46
45
44
43
42
Current speed [ms⁻¹]
0.20
0.15
0.10
0.05
Current direction [°]
300
200
100
Wind speed and direction [m s⁻¹]
15
10
5
0
Storm period
N (SPOM) [mg L⁻¹]
0.40
0.35
0.30
0.25
TOC (SPOM) [mg L⁻¹]
3.0
2.5
2.0
Chl a (SPOM) [ug L⁻¹]
0.06
0.05
0.04
0.03
Jan 02
Jan 03
Jan 04
Jan 05
Jan 06
Jan 07
Jan 08
Jan 09
Date

2.3.2.2 Angolan margin

Mean bottom water temperatures were 6.73 °C at the deeper site (530 m) and 10.06 °C at the shallower site (340 m, Figure 2.7, Table 2.2). The maximum semidiurnal (ΔT~6 h) temperature change was Δ1.60 °C at the deepest site and Δ2.4 °C at the shallow site (Figure 2.7). DO concentrations at the deep site were a factor of 2 higher than those at the shallow site, i.e., 0.9–1.5 vs. 0.5–0.8 ml l^{-1} respectively (≙ range between 4 % and 14 % saturation of both sites), whereas the range of diurnal fluctuations was much smaller compared to the shallow site. DO concentrations were negatively correlated with temperature at the deep site ($r=-0.99$, $p<0.01$), while positively correlated at the shallow site ($r=0.91$, $p<0.01$). Fluorescence was low during both deployments and showed only small fluctuations, being slightly higher at the shallow site (between 38.5 and 41.5 NTU at both sites). Current speeds were relatively high (between 0 and 0.3 m s^{-1}, average 0.1 m s^{-1}) and positively correlated with temperature at the shallow site ($r=0.31$, $p<0.01$) and negatively correlated at the deep site ($r=-0.22$, $p<0.01$). Analysis of the tidal cycle showed that it explained 29.8 %–54.9 % of the horizontal current fluctuations. The M2 amplitude was 0.06–0.09 s^{-1} and was the most important signal (Table 3). A decrease in turbidity was observed during the deployment at the shallow station. This station was located directly below the turbidity maximum between 200 and 350 m depth as observed in the CTD transect (Figure 2.5). In contrast, a relative constant and low turbidity was observed for the deep deployment. Turbidity during both deployments was positively correlated to DO concentrations ($r=0.47$, $p<0.01$, shallow deployment and $r=0.50$, $p<0.01$, deep deployment). The SLM lander recorded an average pH of 8.12.

The short-term temperature fluctuations imply a vertical tidal movement of around 130 m (12.9–9.1 °C measured by lander, ≙ 218–349 m depth in CTD above lander at station GeoB20966).

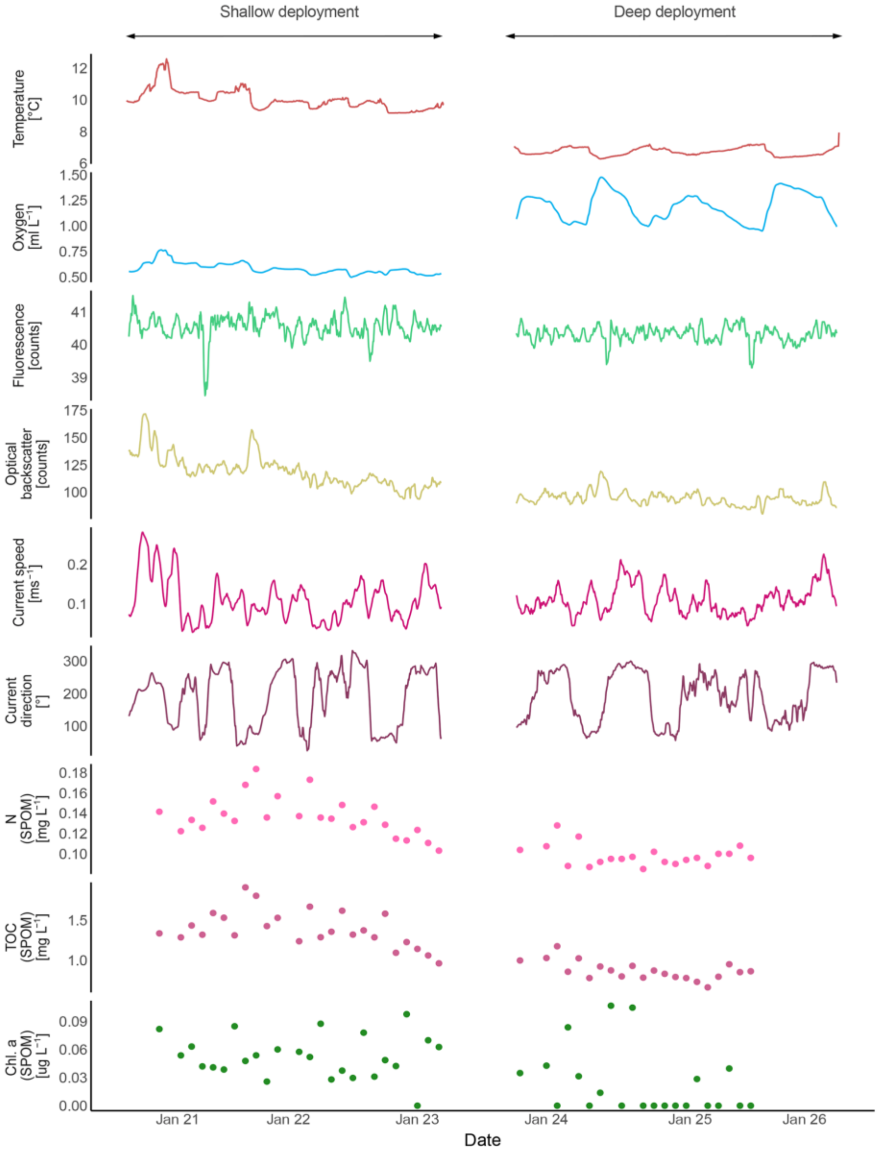

Figure 2.7 Lander data (ALBEX) recorded during at the shallow (~340 m water depth) and deep sites (~530 m water depth) off Angola (January 2016). Shown are temperature (˚C; red), dissolved oxygen concentration (ml l^{-1}; blue), fluorescence (counts per second; green), optical backscatter (turbidity; yellow), current speed (m s^{-1}; pink) and current direction (°: 0–360°; purple) as well as nitrogen (mg l^{-1}; pink dots), carbon (mg l^{-1}; purple dots), and chlorophyll *a* concentration (µg L^{-1}, green dots) of SPOM collected during the both deployments by the McLane pump.

2.3.3 Suspended particulate matter

2.3.3.1 Namibian margin

The nitrogen (N) concentration of the SPOM measured on the filters of the McLane pump fluctuated between 0.25 and 0.45 mg l^{-1}(Figure 2.8). The highest N concentration corresponded with a peak in turbidity ($r=0.42$, $p<0.01$). The $\delta^{15}N$ values of the lander time series fluctuated between 5.1 and 6.9 with an average value of 5.7 ‰. Total organic carbon (TOC) showed a similar pattern as nitrogen, with relative concentrations ranging between 1.8 and 3.5 mg L^{-1}. The $\delta^{13}C$ value of the TOC increased during the surveyed time period from −22.39 ‰ to −21.24 ‰ with an average of −21.7 ‰ (Figure 2.8a). The C⁄N ratio ranged from 8.5–6.8 and was on average 7.4 (Figure 2.8b). During periods of low temperature and more turbid conditions TOC and N as well as the $\delta^{13}C$ values of the SPOM were higher.

Chlorophyll a concentrations of SPOM were on average 0.042 µg l^{-1} and correlated with the record of the fluorescence ($r=0.43$, $p=0.04$). A 6 times higher amount of chlorophyll a degradation products was found during the lander deployment (0.248 µg l^{-1}) compared to the amount of chlorophyll a, giving a ∑phaeopigment ⁄ chlorophyll a ratio of 6.5 (not shown). Additionally, carotenoids (0.08–0.12 µg l^{-1}) and fucoxanthin (0.22 µg l^{-1}), which are common in diatoms, were major components of the pigment fraction. Zeaxanthin, indicating the presence of prokaryotic cyanobacteria, was only observed in small quantities (0.066 µg l^{-1}).

2.3.3.2 Angolan margin

In general TOC and N concentrations of SPOM were higher at the shallow site compared to the deep site. Nitrogen concentrations varied around 0.14 mg l^{-1} at 340 m and around 0.1 mg l^{-1} at 530 m depth (Figure 2.8b). The $\delta^{15}N$ values at the shallow site ranged from 1.6 ‰ to 6.2 ‰ (3.7 ‰ average) and were even lower deeper in the water column, viz. range 0.3–3.7 ‰ with an average of 1.4 ‰. The TOC concentrations were on average 1.43 mg l^{-1} at 340 m and

0.9 mg l^{-1} at 530 m, with corresponding $\delta^{13}C$ values ranging between −23.0 and −24.2 (average of −23.6 ‰) at the shallow, and between −22.9 and −23.9 (average −23.4 ‰) at the deep site.

The chlorophyll a concentrations of the SPOM collected by the McLane pump varied between 0.1 and 0.02 µg l^{-1}, with average ∑phaeopigment ⁄ chlorophyll a ratios of 2.6 and 0.5 at the shallow and deep sites, respectively. Phytopigments recorded by the shallow deployment included 0.3 µg l^{-1} of fucoxanthin, while at the deep site only a concentration of 0.1 µg l^{-1} was found. No zeaxanthin was recorded in the pigment fraction.

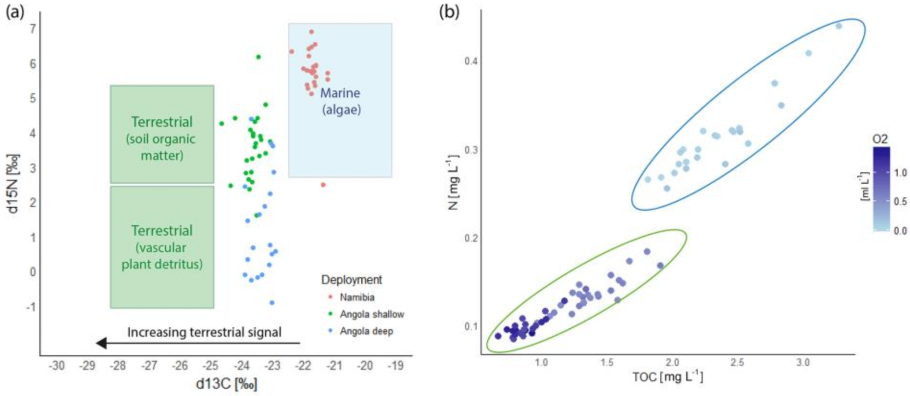

Figure 2.8 Composite records of SPOM collected by the McLane pump of the ALBEX lander at the Namibian and Angolan margins during all three deployments. **(a)** $\delta^{15}N$ and $\delta^{13}C$ isotopic values at the Namibian (red dots) and Angolan (blue and green dots) margins. Indicated by the square boxes are common isotopic values of terrestrial and marine organic matter (Boutton, 1991; Holmes et al., 1997; Sigman et al., 2009). The relative contribution of terrestrial material (green boxes) is increasing with a more negative $\delta^{13}C$ value. **(b)** Total organic carbon (TOC) and nitrogen (N) concentration of the SPOM. Values of the Namibian margin are marked by a blue circle (C⁄N ratio = 7.8), values of the Angolan margin are marked by a green circle (C⁄N ratio = 9.6). Dissolved oxygen concentrations are included to show the higher nutrient concentrations in less oxygenated water.

2.4. Discussion

Even though the ecological-niche factor analyses of Davies et al. (2008) and Davies and Guinotte (2011) predict *L. pertusa* to be absent along the oxygen-limited southwestern African margin, CWC mounds with two distinct benthic ecosystems were found. The coral mounds on the Namibian shelf host no living CWCs; instead the dead coral framework covering the mounds was overgrown with fauna dominated by bryozoans and sponges. Along the slope of the Angolan margin an extended coral mound area with thriving CWC communities was encountered. It is probably that differences in present-day environmental conditions between the areas influence the faunal assemblages inhabiting them. The potential impact of the key environmental factors will be discussed below.

2.4.1 Short-term vs. long-term variations in environmental properties

On the Namibian margin, seasonality has a major impact on local mid-depth oxygen concentration due to the periodically varying influence of the Angola current and its associated low DO concentrations (Chapman and Shannon, 1987). The lowest DO concentration is expected from February to May when SACW is the dominating water mass on the Namibian margin and the contribution of ESACW is smaller (Mohrholz et al., 2008). Due to this seasonal pattern, the DO concentrations measured in this study (January; Figure 2.4) probably do not represent minimum concentrations, which are expected to occur in the following months, but nevertheless give a valuable impression about the extent of the OMZ (February to May; Mohrholz et al., 2014). Interestingly, we captured a flow reversal after 6 January from a southward to an equatorward current direction during high wind conditions on the Namibian margin (Figure 2.6), leading to an intrusion of ESACW with higher DO concentrations (Δ 0.007 ml l^{-1} on average) and lower temperatures (Δ 0.23 °C on average, Figure 2.5) than the SACW. This led to a temporal increase in the DO concentrations. This shows that variations in the local flow field have the capability to change water properties on relatively short time scales, which might provide an analogue to the water mass variability related to the different seasons (Mohrholz et al., 2008). Such relaxations are possibly important for the survival of the abundant benthic fauna present on the relict coral mounds (Gibson et al., 2003). Other seasonal changes, like riverine outflow, do not have decisive impacts on the ecosystem since only relatively small rivers discharge from the Namibian margin. This is also reflected by the dominant marine isotopic signature of the isotopic ratios of $\delta^{15}N$ and $\delta^{13}C$ of the SPOM at the mound areas (Figure 2.8, cf. Tyrrell and Lucas, 2002).

Flow reversals were not observed during the lander deployments on the Angolan margin, where winds are reported to be weak throughout the year providing more stable conditions (Shannon, 2001). Instead river outflow seems to exert a strong influence on the DO concentrations on the Angolan margin. The runoff of the Cuanza and Congo river reach their seasonal maximum in December and January (Kopte et al., 2017), intensifying upper water column stratification. This stratification is restricting vertical mixing and thereby limits ventilation of the oxygen-depleted subsurface water masses. In addition rivers transport terrestrial organic matter to the margin, which is reflected by the isotopic signals of the SPOM (−1 ‰ to 3 ‰; Montoya, 2007) which is well below the average isotopic ratio of the marine waters of 5.5 ‰ (Meisel et al., 2011). Also $\delta^{13}C$ values are in line with the $\delta^{13}C$ values of terrestrial matter which is on average −27 ‰ in this area (Boutton, 1991; Mariotti et al., 1991). The C⁄N ratio of SPOM is higher compared to material from the Namibian margin, also confirming admixing of terrestrial matter (Perdue and Koprivnjak, 2007). This terrestrial matter contains suitable food sources as well as less suitable food sources, like carbon-rich polymeric material (cellulose, hemicellulose and lignin), which cannot easily be taken up by marine organisms (Hedges and Oades, 1997). The combined effects of decreased vertical mixing and additional input of organic matter potentially result in the lowest DO concentrations of the year during the investigated time period

(January), since the highest river outflow and therefore strongest stratification is expected during this period.

2.4.2 Main stressors – oxygen and temperature

Environmental conditions marked by severe hypoxia and temporal anoxia (< 0.17 ml l^{-1}) likely explain the present-day absence of living CWCs along the Namibian margin. During the measurement period the DO concentrations off Namibia were considerably lower than the thus far recorded minimum concentrations near living CWCs (1–1.3 ml l^{-1}), which were found off Mauritania where only isolated living CWCs are found (Ramos et al., 2017). Age dating of the Namibian fossil coral framework showed that CWCs disappeared about 5 ka which coincides with an intensification in upwelling and therefore most likely a decline of DO concentrations (Tamborrino et al., 2019), supporting the assumption that the low DO concentrations are responsible for the demise of CWCs on the Namibian margin. Although no living corals were observed on the Namibian coral mounds, we observed a dense living community dominated by sponges and bryozoans (Hebbeln et al., 2017). Several sponge species have been reported to survive at extremely low DO concentrations within OMZs. For instance, along the lower boundary of the Peruvian OMZ, sponges were found at DO concentrations as low as 0.06–0.18 ml l^{-1} (Mosch et al., 2012). Mills et al. (2018) recently found a sponge (Tethya wilhelma) to be physiologically almost insensitive to oxygen stress and respires aerobically under low DO concentrations (0.02 ml l^{-1}). Sponges can potentially stop their metabolic activity during unfavorable conditions and restart their metabolism when some oxygen becomes available, for instance during diurnal irrigation of water with somewhat higher DO concentrations. The existence of a living sponge community off Namibia might therefore be explained by the diurnal tides occasionally flushing the sponges with more oxic water, enabling them to metabolize, when food availability is highest (Figure 2.6). Increased biomass and abundances in these temporary hypoxic–anoxic transition zones were already observed for macro- and megafauna in other OMZs and is referred to as the “edge effect”

(Mullins et al., 1985; Levin et al., 1991; Sanders, 1969). It is very likely that this mechanism plays a role for the benthic communities on the Namibian as well as the Angolan margin.

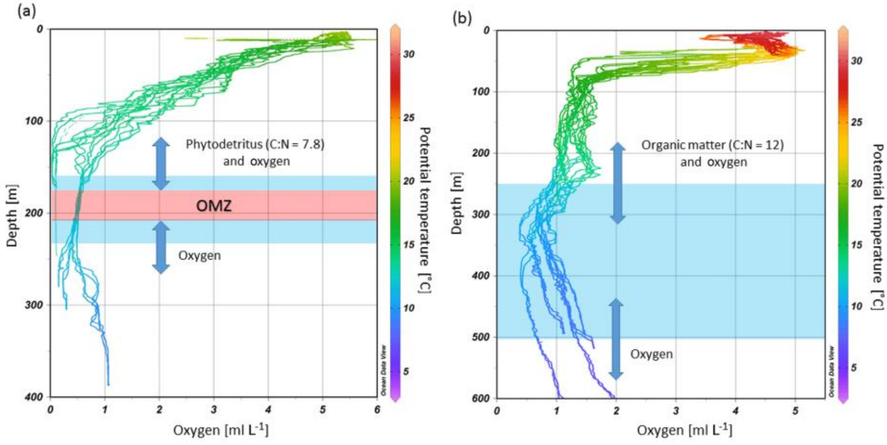

Figure 2.9 Depth range of cold-water coral mound occurrences (blue shaded areas) at the (a) Namibian and (b) Angolan margins in relation to the dissolved oxygen concentrations and potential temperature. Diurnal tides are delivering mainly phytodetritus (shown in a) and organic matter from the benthic nepheloid layer (shown in b) as well as oxygen from above and from below to the mound sites (indicated by blue arrows, the lengths of which indicate the tidal ranges).

Along the Angolan margin, low oxygen concentrations apparently do not restrict the proliferation of thriving CWC reefs even though DO concentrations are considered hypoxic ($0.5–1.5\ \mathrm{ml\ l^{-1}}$). The DO concentrations measured off Angola are well below the lower DO concentration limits for *L. pertusa* based on laboratory experiments and earlier field observations (Schroeder, 2002; Brooke and Ross, 2014). The DO concentrations encountered at the shallow mound sites ($< 0.8\ \mathrm{ml\ l^{-1}}$) are even below the so far lowest limits known for single CWC colonies from the Mauritanian margin (Ramos et al., 2017b). Since in the present study measured DO concentrations were even lower than the earlier established lower limits, this could suggest a much higher tolerance of *L. pertusa* to oxygen levels as low as $0.5\ \mathrm{ml\ l^{-1}}$ at least in a limited time period (4 % O_2 saturation).

In addition to oxygen stress, heat stress is expected to put additional pressure on CWCs. Temperatures at the CWC mounds off Angola ranged from 6.4 to 12.6°C, with the upper limit being close to reported maximum temperatures (~12–14.9 °C; Davies and Guinotte 2011) and are hence expected to impair the ability of CWCs to form mounds (see Wienberg and Titschack 2017). The CWCs were also occurring outside of the expected density envelope of 27.35–27.65 kg m^{-3} in densities well below 27 kg m^{-3} (Figure 2.3, Dullo et al., 2008). In most aquatic invertebrates, respiration rates roughly double with every 10 °C increase (Q_{10} temperature coefficient = 2–3, e.g., Coma, 2002), which at the same time doubles energy demand. Dodds et al. (2007) found a doubling of the respiration rate of *L. pertusa* with an increase at ambient temperature of only 2 °C (viz. Q_{10}=7–8). This would limit the survival of *L. pertusa* at high temperatures to areas where the increased demand in energy (due to increased respiration) can be compensated by high food availability. Higher respiration rates also imply that enough oxygen needs to be available for the increased respiration. However this creates a negative feedback, since with increased food availability and higher temperatures the oxygen concentration will decrease due to bacterial decomposition of organic substances.

Survival of *L. pertusa* under hypoxic conditions along the shallow Angolan CWC areas is probably positively influenced by the fact that periods of highest temperatures coincide with highest DO concentrations during the tidal cycle. Probably here the increase of one stressor is compensated by a reduction of another stressor. On the Namibian margin and the deeper Angolan mound sites the opposite pattern was found, with highest temperatures during lowest DO concentrations. However, at the deeper Angolan mound sites DO concentrations are higher and temperatures more within a suitable range compared to the shallow sites (0.9–1.5 ml l^{-1}, 6.4–8 °C, Figure 2.7). Additionally it was shown by ex situ experiments that *L. pertusa* is able to survive periods of hypoxic conditions similar to those found along the Angolan margin for several days, which could be crucial in periods of most adverse conditions (Dodds et al., 2007).

2.4.3 Food supply

As mentioned above, environmental stresses like high temperature or low DO concentration result in a loss of energy (Odum, 1971; Sokolova et al., 2012), which needs to be balanced by an increased energy (food) availability. Food availability therefore plays a significant role for faunal abundance under hypoxia or unfavorable temperatures (Diaz and Rosenberg, 1995). Above, we argued that survival of sponges and bryozoans on the relict mounds off Namibia and of CWCs, and their associated fauna at the Angolan margin, may be partly due to a high input of high-quality organic matter, compensating oxygen and thermal stresses. The importance of the food availability for CWCs was already suggested by Eisele et al. (2011), who mechanistically linked CWC mound growth periods with enhanced surface water productivity and hence organic matter supply. Here we found evidence for high quality and quantity of SPOM in both areas indicated by high TOC and N concentrations (Figs. 6 and 7) in combination with a low C⁄N ratio (Figure 2.8), a low isotopic signature of δ^{15}N and only slightly degraded pigments.

The Namibian margin is known for its upwelling cells, where phytoplankton growth is fueled by nutrients from deeper water layers producing high amounts of phytodetritus (Chapman and Shannon, 1985), which subsequently sinks down to the relict mounds on the slope. Benthic communities on the mounds off Namibia occur at relatively shallow depths, hence downward transport of SPOM from the surface waters is rapid and time for decomposition of the sinking particles in the water column is limited. The higher turbidity during lower current speeds provides additional evidence that the material settling from the surface is not transported away with the strong currents (Figure 2.6).

At the Angolan coral mounds, SPOM appeared to have a signature corresponding to higher quality organic matter compared to the

SPOM off Namibia. The phytopigments were less degraded and the $\delta^{15}N$, TOC and N concentrations of the SPOM were lower. However, here lower $\delta^{15}N$ and a higher ∑phaeopigment ⁄ chlorophyll a ratio are likely connected to a mixture with terrestrial OM input, which might constitute a less suitable food source for CWCs (Hedges and Oades, 1997). On the other hand, the riverine input delivers dissolved nutrients, which can support the growth of phytoplankton, indirectly influencing food supply (Kiriakoulakis et al., 2007; Mienis et al., 2012). Moreover, the variations in food quality at the shallow Angolan reefs, which were relatively small during this study, did not seem to be related to the presence of other environmental stressors. At the Angolan margin we see a rather constant availability of SPOM. The slightly higher turbidity during periods of highest DO concentrations (Figure 2.7) suggests that the SPOM on the Angolan margin originates from the bottom nepheloid layer on the margin directly above the CWC mounds (Figure 2.5e), which may represent a constant reservoir of fresh SPOM. This reservoir is probably fueled by directly sinking as well as advected organic matter from the surface ocean.

2.4.4 Tidal currents

The semidiurnal tidal currents observed probably play a major role in the survival of benthic fauna on the SW African margin. On the Namibian margin, internal waves deliver oxygen from the surface and deeper waters to the OMZ and thereby enable benthic fauna on the fossil coral framework to survive in hypoxic conditions (Figure 2.9a). At the same time these currents are probably responsible for the delivery of fresh SPOM from the surface productive zone to the communities on the margin, since they promote mixing between the water masses as well as they vertically displace the different water layers.

On the Angolan margin, internal tides produce slightly faster currents and vertical excursions of up to 130 m which are twice as high as those on the Namibian margin. Similar to the Namibian margin, these tidal excursions deliver oxygen from shallower and deeper waters to the mound zone and thereby deliver water with more suitable characteristics over the whole extent of the parts of the OMZ which otherwise may be unsuitable for CWCs (Figure 2.9b). Internal tides are also responsible for the formation of a bottom nepheloid layer at 200–350 m depth (Figure 2.5e). This layer is formed by trapping of organic matter as well as bottom erosion due to turbulence created by the interaction of internal waves with the margin topography, which intensifies near-bottom water movements. These internal waves are able to move on the density gradient between water masses, which are located at 225 and 300 m depth (Figure 2.3). Tidal waves will be amplified due to a critical match between the characteristic slope of the internal M2 tide and the bottom slope of the Angolan margin, as is known from other continental slope regions (Dickson and McCave, 1986; Mienis et al., 2007). As argued above, this turbid layer is likely important for the nutrition of the slightly deeper situated CWC mounds, since vertical mixing is otherwise hindered by the strong stratification.

2.5 Conclusions

Different environmental properties explain the present conditions of the benthic communities on the southwestern African margin including temperature, DO concentration, food supply and tidal movements. The DO concentrations probably define the limits of a suitable habitat for CWCs along the Namibian and the Angolan margin, whereas high temperatures constitute additional stress by increasing the respiration rate and therefore energy demand. On the Namibian margin, where DO concentrations dropped below 0.01 ml l^{-1}, only fossil CWC mounds covered by a community dominated by sponges and bryozoans were found. This benthic community survives as it receives periodically waters with slightly higher DO concentrations (> 0.03 ml l^{-1}) due to regular tidal oscillations (semidiurnal) and erratic wind events (seasonal). At the same time, a high quality and quantity of SPOM sinking down from the surface water mass enables the epifaunal community to survive despite the oxygen stress and to sustain its metabolic energy demand at the Namibian OMZ, while CWCs are not capable to withstand such extreme conditions. In contrast, thriving CWCs on the

Angolan coral mounds were encountered despite the overall hypoxic conditions. The DO concentrations were slightly higher than those on the Namibian margin but nevertheless below the lowest threshold that was so far reported for *L. pertusa* (Ramos et al., 2017; Davies et al., 2008, 2010). In combination with temperatures close to the upper limits for *L. pertusa*, metabolic energy demand probably reached a maximum. High energy requirements might have been compensated by the general high availability of fresh resuspended SPOM. Fresh SPOM accumulates on the Angolan margin just above the CWC area and is regularly supplied due to mixing by semidiurnal tidal currents, despite the restricted sinking of SPOM from the surface due to the strong stratification.

CWC and sponge communities are known to play an important role as a refuge, feeding ground and nursery for commercial fishes (Miller et al., 2012), and have a crucial role in the marine benthic pelagic coupling (Cathalot et al., 2015). Their ecosystem services are threatened by the expected expansion of OMZs due to anthropogenic activities like rising nutrient loads and climate change (Breitburg et al., 2018). This study showed that benthic fauna is able to cope with low oxygen levels as long as sufficient high-quality food is available. Further, reef-associated sponge grounds, as encountered on the Namibian margin could play a crucial role in taking over the function of CWCs in marine carbon cycling as well as in providing a habitat for associated fauna, when conditions become unsuitable for CWCs.

2.6 Data availability

CTD data presented in this work are available at https://doi.pangaea.de/10.1594/PANGAEA.904176 (Hebbeln, 2019). Lander time series data were submitted to Pangaea and are also available at the NIOZ data archive system (https://doi.org/10.25850/nioz/7b.b.q, Hanz, 2019).

2.7 Acknowledgements

We thank the captain of the RV *Meteor* cruise M122, Rainer Hammacher, his officers and crew, who contributed to the success of this cruise. We also would like to thank the scientific and technical staff for their assistance during the cruise and their work in the laboratory. Greatly acknowledged are the efforts from the German Diplomatic Corps in the German embassies in Windhoek and Luanda and in the Foreign Office in Berlin. We thank the German Science Foundation (DFG) for providing ship time on RV *Meteor* and for funding the ROV *Squid* operations to investigate the cold-water coral ecosystems off Angola and Namibia.

This research has been supported by the DFG Research Center/Cluster of Excellence “MARUM – The Ocean in the Earth System”. Ulrike Hanz is funded by the SponGES project, which received funding from the European Union's Horizon 2020 research and innovation program (grant no. 679849). Furu Mienis is supported by the Innovational Research Incentives Scheme of the Netherlands Organisation for Scientific Research (NWO-VIDI grant no. 016.161.360). Gert-Jan Reichart is supported by the Netherlands Earth System Science Centre (NESSC), financially supported by the Ministry of Education, Culture and Science (OCW). Katriina Juva is funded through the FATE project (Fate of cold-water coral reefs – identifying drivers of ecosystem change), supported by the Norwegian Research Council (NRC).

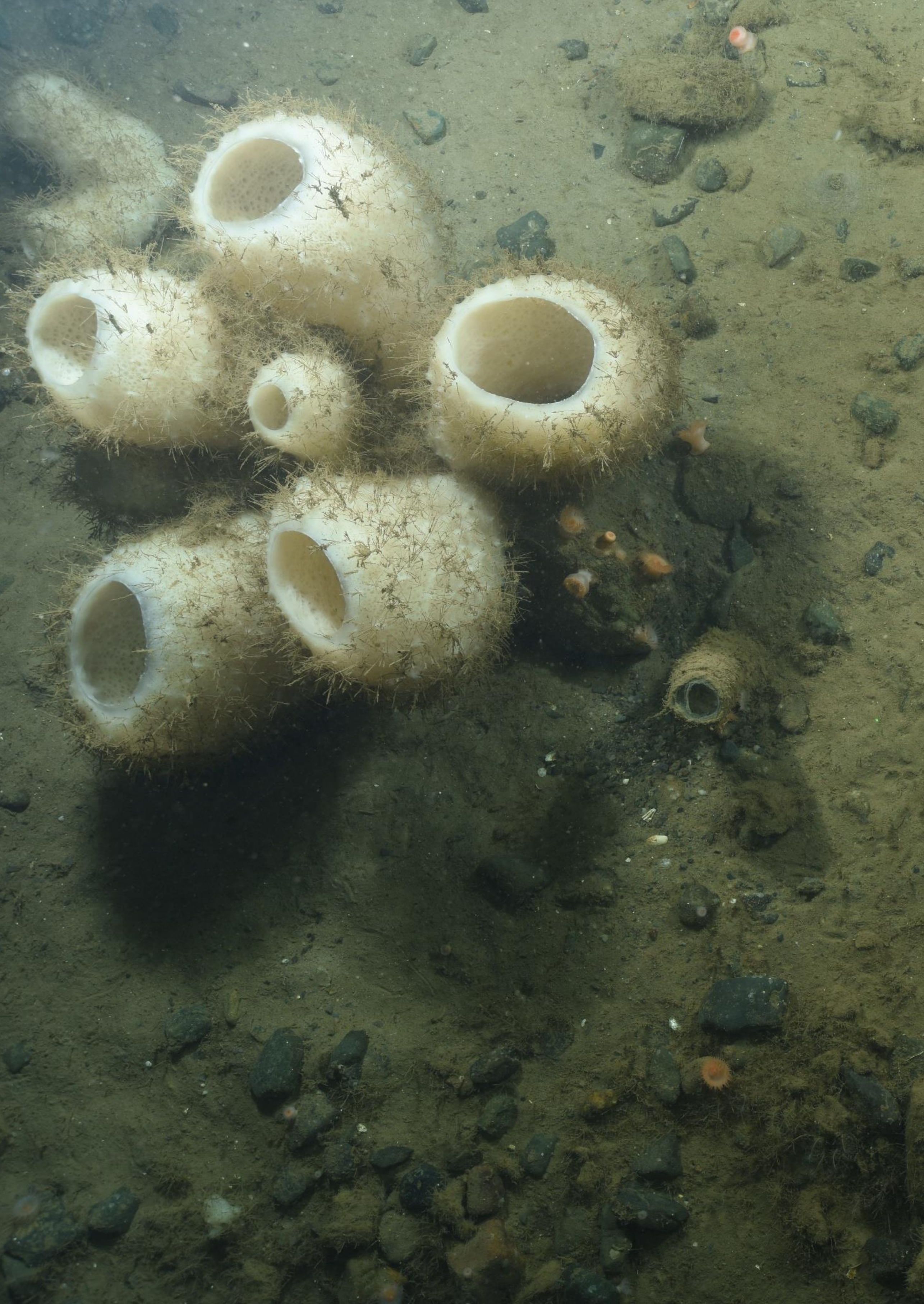

Chapter 3

Seasonal Variability in Near-bed Environmental Conditions in the *Vazella pourtalesii* Glass Sponge Grounds of the Scotian Shelf

Ulrike Hanz, Lindsay Beazley, Ellen Kenchington, Gerard Duineveld, Hans Tore Rapp† and Furu Mienis

Published in Frontiers in Marine Science in 2021

Picture to the left: *Vazella pourtalesii* on the Scotian Shelf ©DFO

Abstract

The Scotian Shelf harbours unique aggregations of the glass sponge *Vazella pourtalesii* providing an important habitat for benthic and pelagic fauna. Recent studies have shown that these sponge grounds have persisted in the face of strong inter-annual and multi-decadal variability in temperature and salinity. However, little is known of the environmental characteristics on hourly-seasonal time scales. This study presents the first hydrodynamic observations and associated (food) particle supply mechanisms for the *Vazella* sponge grounds, highlighting the influence of natural variability in environmental conditions on sponge growth and resilience. Near-bottom environmental conditions were characterized by high temporal resolution data collected with a benthic lander, deployed during a period of 10-months in the Sambro Bank Sponge Conservation Area. The lander was equipped with temperature and oxygen sensors, a current meter, a sediment trap and a video camera. In addition, water column profiles of temperature and salinity were recorded along a transect, conducted in a gradient from high to lower sponge presence probability. Over the course of the lander deployment, temperature fluctuated between 8.8-12 °C with an average of 10.6 °C ± 0.4 °C. The water contained on average 6.3 mg l^{-1} oxygen and near bottom current speed was on average 0.12 m s^{-1}, with peaks up to 0.47 m s^{-1}. Semi-diurnal tidal currents promoted constant resuspension of particulate matter in the benthic boundary layer. Surface storm events episodically caused extremely turbid conditions on the seafloor that persisted for several days, with particles being resuspended to more than 13 m above the seabed. The carbon flux in the near-bottom sediment trap peaked during storm events and also after a spring bloom in April, when fresh phytodetritus was observed in the bottom boundary layer. While resuspension events can represent a major stressor for sponges, limiting their filtration capability and remobilizing them, episodes of strong currents and lateral particle transport likely play an important role in food supply and the replenishment of nutrients and oxygen. Our results contextualize human-induced threats such as bottom fishing and climate change by providing more knowledge of the natural environmental conditions under which sponge grounds persist.

3.1 Introduction

Sponges are one of the most common megafaunal organisms in the deep sea (Tabachnick et al., 1994). They can have a scattered distribution with low abundances, but under certain environmental conditions may form dense monospecific or mixed sponge aggregations, and even reef-like ecosystems (Maldonado et al., 2017). Sponge aggregations provide ecosystem goods and services by providing shelter from predation, breeding grounds and substrate for many associated species including commercially important fish species (Kutti et al., 2015b), thereby enhancing biodiversity and biomass (Rice et al., 1990;Fuller and Cameron, 1998;Beazley et al., 2013;Beazley et al., 2015;Maldonado et al., 2017;Meyer et al., 2019). Moreover, sponges play a key ecological role in benthic-pelagic coupling by filtering substantial volumes of water (up to 24,000 L per kg^{-1} of sponge day^{-1} in temperate and tropical shallow-water sponge grounds; Leys et al., 2007;Maldonado et al., 2012;Pham et al., 2019). Furthermore, they can release particulate detritus to the associated benthic environment (Reiswig, 1971), a pathway referred to as the sponge loop (Rix et al., 2016). Consequently they transfer energy and nutrients from the pelagic to the benthic environment, and play an important role in carbon, nitrogen, phosphate and silicon cycling (Maldonado et al., 2012;Kutti et al., 2013;Cathalot et al., 2015;Maldonado et al., 2020).

In the North Atlantic, deep-sea aggregations of demosponges (especially Astrophorina) and glass sponges (Hexactinellida) have been found along continental shelves, slopes, seamounts, mid-ocean ridges and canyons, especially at depths between 200 to 3000 m (Tabachnick et al., 1994). These sponge ecosystems either occur as mono-specific or multi-species assemblages. At boreal and boreo-arctic latitudes mixed species assemblages have often been found, like for example on the Arctic Mid-Ocean Ridge (Meyer et al., 2019) and on the northwest Atlantic Canadian margin (Murillo et al., 2012;Murillo et al., 2018). At temperate latitudes monospecific aggregations of glass sponges seem to be a dominant feature, such as for example the *Pheronema carpenteri* grounds in the northeast Atlantic Ocean (Rice et al., 1990), *Geodia sp*. grounds in the western Barents Sea (Klitgaard and Tendal,

2004) and mono-specific *Vazella pourtalesii* grounds in the northwest Atlantic along the Canadian continental shelf (Beazley et al., 2013). The dominant presence of particular sponge species has been related to local environmental conditions such as substrate type, topography, as well as the hydrography (Rice et al., 1990;Chu and Leys, 2010;Murillo et al., 2018;Roberts et al., 2018;Davison et al., 2019). Hexactinellids are most abundant and diverse in the deep ocean on steep rocky substrates with low amounts of suspended sediment in the water column and occur less often on flat shelves (Farrow et al., 1983;Maldonado et al., 2017). Other species, such as *Pheronema carpenteri,* are able to build a basal specular component (comparable to roots) enabling them to anchor in soft substrate (Barthel et al., 1996).

The Scotian Shelf, the continental shelf off Nova Scotia, eastern Canada, harbors unique aggregations of the rosellid glass sponge *V. pourtalesii* (Schmidt 1870), commonly known as “Russian hats” (Fuller and Cameron, 1998). This species is distributed along the continental margin of eastern North America, from the Florida Keys in the southern US, where it occurs in low densities, to the Scotian Shelf, where it forms extensive monospecific aggregations between ~150 and 240 m depth in Emerald Basin, reaching average densities of 3.8 ind. m^{-2} (Hawkes et al., 2019;Maldonado et al., 2020). Single individuals were found in an even broader depth range between 75 to 498 m depth (Fuller, 2011;Beazley et al., 2018). High species abundance is likely linked to the high primary productivity on the Scotian Shelf (102 g C m^{-2}; Mills and Fournier, 1979), providing an important food source for the sponges and their associated fauna. Accumulations of *V. pourtalesii* harbor an enhanced biodiversity and species abundance of for example invertebrates such as shrimp, crabs and anemones. Furthermore, analysis of catch data revealed a significantly different fish community associated with the sponge grounds (Fuller, 2011;Hawkes et al., 2019). In order to protect these sponges from bottom fishing gear Fisheries and Oceans Canada (DFO) established two sponge conservation areas in 2013, the Emerald Basin Sponge Conservation Area (197 km^2) and the Sambro Bank Sponge Conservation Area (62 km^2) (referred to as the ‘closure areas’ thereafter).

Of 35 environmental predictor layers (representing ocean terrain, fishing effort, and physical oceanographic characteristics) minimum bottom temperature and summer primary production layers were most important in a random forest model used to predict the distribution of *V. pourtalesii* on the Scotian Shelf (Beazley et al., 2018). Variability of environmental factors (e.g. temperature) is defined by the variability of the main water masses entering the Scotian Shelf (McLellan, 1957;Urrego-Blanco and Sheng, 2014), which lies at the confluence of two large ocean gyre currents, the Gulf Stream flowing into a northward direction and the Labrador Current flowing in an equatorward direction (Drinkwater et al., 2003). The contemporary distribution of *V. pourtalesii* is associated with the deep basins and channels on the Scotian Shelf which are bathed by warm and saline slope waters (Smith, 1978;Loder et al., 1997).

In this study we present the first long-term results of near-bed hydrodynamic observations and (food) particle supply mechanisms to highlight the influence of natural fluctuating environmental conditions on sponge growth and resilience. Observational evidence of the hydrodynamic conditions of the *V. pourtalesii* sponge grounds on the Scotian Shelf was collected via a long-term deployment (10-month) of a benthic lander in the framework of the EU-SponGES project. Near-bed environmental conditions (e.g., temperature, current speed, turbidity) were measured at high-resolution to determine hourly to seasonal variability. In addition, the lander was equipped with a sediment trap to determine particle and carbon fluxes, which was used as a measure of food availability. Knowledge on the environmental requirements and natural variability experienced by these sponge grounds may help to improve knowledge of their resilience against environmental stressors, and their ability to recover after natural and anthropogenic-induced disturbances.

3.2 Material and Methods

3.2.1 Topographic and oceanographic setting

The Scotian Shelf is a 700 km long and 200 km wide section of the continental shelf off Nova Scotia, Canada, bounded by the Laurentian

Channel in the northeast, and the Northeast Channel and Gulf of Maine in the southwest. While the average depth of the shelf is 90 m, it is characterized by a heterogonous topography with several banks, channels, canyons and deeper basins (Figure 3.1; Han et al., 1997). The glass sponge *V. pourtalesii* is distributed in the Northeast Channel at the mouth of the Gulf of Maine in the west, and on the central Scotian Shelf in the Scotian Gulf, an inlet formed by a deeper cross-shelf channel situated between Emerald and LaHave Banks, which opens up to LaHave and Emerald Basin on the inner shelf (Beazley et al., 2018). The densest known concentration of *V. pourtalesii* is located above 200 m depth on a saddle between the two deep basins (>200 m water depth) that comprise Emerald Basin (Beazley et al., 2018), with a second notable concentration occurring on the eastern flank of Sambro Bank, Emerald Basin (Figure 3.1). These two concentrations are mostly encompassed by the Emerald Basin and Sambro Bank closures, respectively.

Two major ocean currents influence the sponge grounds; the Gulf Stream and the equatorward flowing subpolar Labrador Current (Hannah et al., 2001). The variability of the intensity of the Labrador Current influences all water masses on the shelf and results in the highest inter-annual variability of sea surface temperature (4.6°C) in the North Atlantic (Petrie and Drinkwater, 1993). When the Labrador Current (seasonally) reaches the seafloor it is known to be strong enough to displace organisms and matter, showing the largest volume transport (up to 0.6 Sv) in winter (Drinkwater et al., 1979;Hannah et al., 2001). The water column on the Scotian Shelf has a two-layered structure consisting of surface and slope waters (Drinkwater et al., 2003). The slope waters consist of two components with different signatures: the Warm slope Water (WSW) and the Labrador Slope Water (LSW). WSW originates from a mixture of Gulf Stream Water, deep North Atlantic Central Water and shelf waters and flows primarily north-eastward adjacent to the Gulf Stream. It is characterized by relatively high temperatures (12°C), high salinities (35.4, (Gatien, 1976;Mountain, 2012) and high nutrient concentrations (Townsend and Ellis, 2010). The LSW flows in an equatorward direction and is cold (2°C), less saline (32) and low in nutrients (with an exception of relatively high Si) (Petrie and Drinkwater, 1993;Petrie and Yeats, 2000; Mountain, 2012). Onshore movement of the warm slope waters through the major channels and gullies fills in the basins at the Scotian Shelf with in particular WSW, resulting in relatively warm waters bathing the sponges year round. The surface water layer (Scotian Shelf Waters (SSW) is mixed by winter winds and contains cold water (2°C) with a relatively fresh signature (32) resulting from terrestrial run-off (McLellan, 1957;Petrie and Drinkwater, 1993).

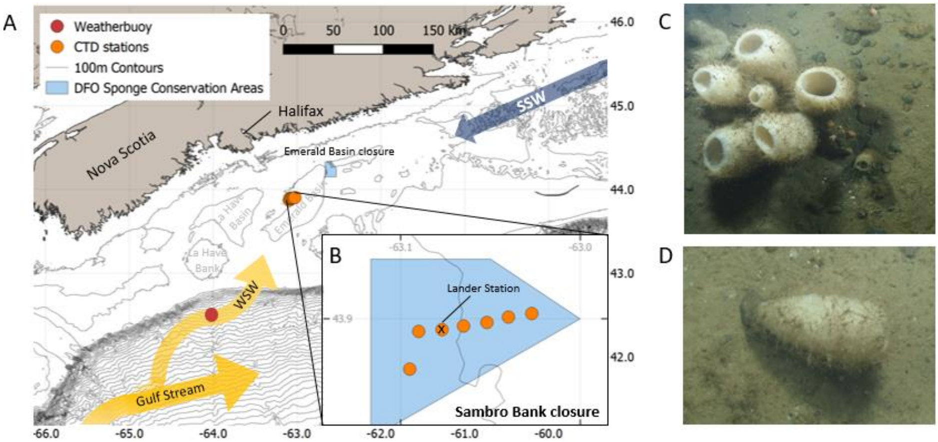

Figure 3.1 (A) Scotian Shelf with CTD, weather buoy stations and both DFO Sponge conservation areas indicated. The arrows indicate the flow of the slope waters, WSW (orange arrow) and SSW (dark blue arrow), (B) Sambro Bank closure with CTD and lander stations; (C) *V. pourtalesii* sponges inside the Sambro Bank closure, (D) some sponges were found in a horizontal position.

During summer winter cooled SSW is sitting in between a warmed up surface layer and the warmer WSW (Drinkwater et al., 2003). The water masses on the Scotian Shelf are influenced by seasonal warming and cooling , whereby the system is usually well stratified in late spring to early autumn, whereas it can be mixed over the shallow banks in winter (Smith et al., 1978). Vertical mixing occurs year round by internal tides, which are generated by the interaction of tidal flow of the stratified water masses over the abrupt bathymetry of the banks and basins (Han and Loder, 2003). This leads to vertical mixing of deep nutrient rich water into the surface waters (Townsend and Ellis, 2010), but also stirs up sediments and produces intermediate nepheloid layers (Azetsu-

Scott et al., 1995). In the Emerald Basin these nepheloid layers have been found at a depth of 140 to 200 m and occur when strong tidal currents flow in a northern direction (Azetsu-Scott et al., 1995). Tidal currents on the Scotian Shelf are dominated by semi-diurnal (M_2) tides (Chen et al., 2011).

3.2.2 Water column profiling

During a research cruise with the CCGS *Hudson* (HUD2018-021) in June 2018, water column profiles of Conductivity-Temperature-Depth (CTD) were recorded with a Sea-Bird SBE25 V 4.1c system along a transect in the Sambro Bank closure to collect CTD data (each CTD cast was ~1 km apart) inside and outside of the main sponge grounds (control station in the southwest, Figure 3.1B), which was based on abundance models from Beazley et al. (2018).

3.2.3 Lander

A NIOZ-designed ALBEX lander (Duineveld et al., 2004) was deployed at a depth of 154 m (43.898° N, 63.052° E) near the center of the Sambro Bank closure on September 6, 2017 with the CCGS *Martha L. Black*, and retrieved on June 22, 2018 with CCGS *Hudson* (Figure 3.1B). The lander was equipped with a CT sensor (Sea-Bird SBE37SM-RS232, sampling interval = 15 min, accuracy for temperature of 0.002°C and conductivity of 0.003 mS cm^{-1}), ARO-USB oxygen sensor (JFE-Advantech^{TM}, sampling interval = 15 min, accuracy of non-linearity ±2% of full scale (at 1 atm, 25 °C). A 2 point calibration was carried out before deployment to compensate for the time drift and ensure reliable and accurate DO data. An Aquadopp 2 MHz (Nortek™, sampling interval = 15 min) acoustic doppler current profiler (ADCP) was attached on the lander at a depth of 3 m above bottom (mab). The ADCP measured acoustic backscatter and velocity in 50 cm bins with an accuracy of ±1% of the measured value (0.05 cm s^{-1}). A NIOZ custom-made HD video camera with white lights recorded every 4 h a short video clip of 20 seconds of the seabed. The lander was also equipped with a Technicap PPS4/3 sediment trap with 12 bottles with the aperture at 3 mab. Sediment trap vials were filled with a pH-buffered mercury chloride ($HgCl_2$)

solution in filtered seawater collected from the deployment site and the carousel was programmed to rotate at 30-day intervals.

3.2.4 Sediment trap samples

Upon recovery of the lander, sediment trap samples were stored at 4 °C until they were split into five subsamples with a WSD10 McLane manual rotor splitter. Four of the subsamples were split and rinsed with MilliQ water and one subsample was washed with filtered seawater for pigment analysis. After splitting, samples were freeze-dried and weighed to calculate mass fluxes, whereby the average weights of two splits was used. It must be stressed that cylindrical traps tend to under-sample when current speed exceeds 15 cm s^{-1} (Gardner et al., 1983) . Therefore, trap fluxes presented here, especially during high current conditions, are likely underestimated with regards to the near-bed mass flux (Vangriesheim et al., 2001).

One split of each sample was used for isotope analysis. Half of the sample was used for organic carbon analysis and was first decarbonized by hydrochloric acid (2 M HCl supra) and afterwards transferred into pressed tin capsules (Elemental Microanalysis). The other half of the sample was used for nitrogen analysis and was directly transferred into pressed tin capsules. Stable isotopes $\delta^{15}N$, $\delta^{13}C$ and total weight percent of organic carbon and nitrogen were analyzed by a Delta V Advantage isotope ratio MS coupled to a Flash 2000 Elemental Analyzer (EA-IRMS) by a Conflo IV (Thermo Fisher Scientific Inc.). The reference gas was pure N_2. As a standard for $\delta^{13}C$ benzoic acid and acetanilide was used, for $\delta^{15}N$ acetanilide, urea and casein was used. For $\delta^{13}C$ analysis a high signal method was exercised including a 70% dilution. Precision for replicate measurements of $\delta^{13}C$ and $\delta^{15}N$ was ± 0.15 ‰.

The Chlorophyll-*a* (Chl-*a*) concentration of the sediment trap samples was measured by a Fluorescence Spectrometer (F-2500 Hitachi), by comparing the sample absorbance to the absorbance of a known Chl-*a* standard at two wavelengths (431.0/671.0 nm). Chl-*a* was extracted in 90% acetone and fluorescence was measured first on the intact extract and a second time after the extract was acidified with HCl (10 %) under dark and cold conditions. HCl was added to the sample to convert Chl-*a* into its degradation products (Phaeopigments). By this the amount of Chl-*a* can be deducted from its degradation products which otherwise interfere with the measurements since they absorb light at the same wavelength (for details Holm-Hansen et al., 1965).

3.2.5 Data analysis

Daily moving averages of all environmental variables of the long term data were calculated, as well as monthly averages that were related to the sediment trap sampling intervals. Correlations between the measured environmental variables were calculated using Pearson correlations (n= 27,384) in the program R (R Studio 1.2.1335). The pressure data and near-bed horizontal velocity components at 5 m mab obtained with the ADCP were analysed to determine the most important tidal constituents with the “tidem” package in the program R (R Studio 1.2.1335).

Velocity data of the ADCP at 5 mab were used to make a progressive vector diagram. A single passive particle representing a dissolved or suspended constituent was released and its transport simulated according to the horizontal velocities measured by the current sensor during a period of 30 days, corresponding to the intervals of sediment trap sampling (Duineveld et al., 2007). For this, the velocities per time step were added up in a two-dimensional space simulating the direction of transport. The released particle experiences in any new position the current of the initial position, independently of where the constituent went. Progressive vector diagrams accumulate errors and clearly cannot provide a real estimate of the particle position, but provide an estimate on how far particles or nutrients can disperse after they are released from their original position (Carlson et al., 2010).

3.3 Results

3.3.1 Environmental conditions on the Scotian Shelf

The CTD transect revealed a relatively fresh and solar heated upper layer reaching to a depth of about 20 m below the surface as shown by high temperature (>5°C) and low salinity (<32) (Figure 3.2). Underneath this layer colder winter cooled SSW water was found from 20 m until a depth of about 75 m (<5°C, Figure 3.2). Underneath the cold layer WSW was observed, which was characterized by a higher temperature (>6°C) and higher salinity (>33) (Figure 3.2A). Water stratification was very similar at all stations including the control station outside the sponge area, whereas the influence of the cold winter cooled SSW was decreasing towards the east.

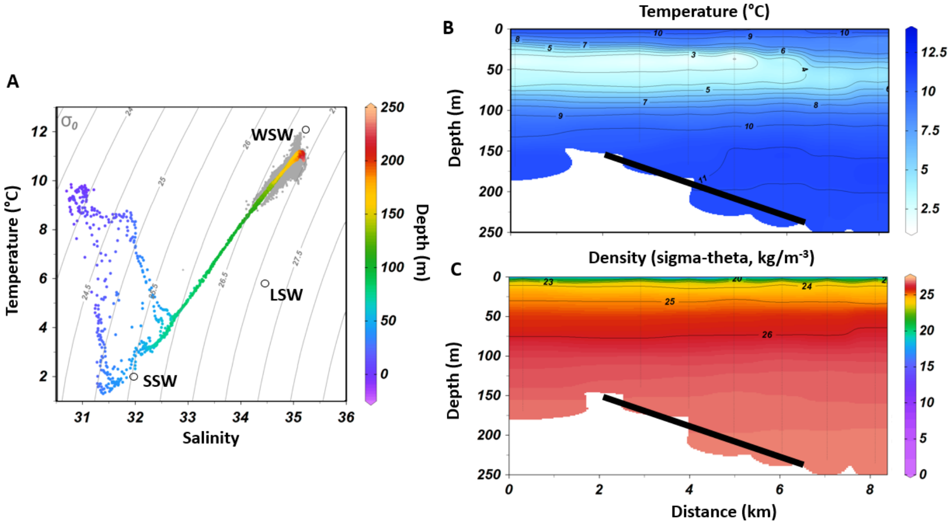

Figure 3.2 (A) T/S plot of CTD and lander data in grey. The characteristic end members of temperature and salinity for WSW, LSW and SSW are plotted (Mountain, 2012); (B) Temperature transect inside the Sambro Bank closure, with the westernmost station (on the left) located outside of the densest sponge area; (C) Density along the same transect. The black bars indicate the depth distribution of the sponge ground (150-250 m water depth).

3.3.2 Long-term environmental conditions in the Sambro Bank closure

The lander was deployed at a depth of 154 m and data were recorded during the whole deployment period of ten months (Figure 3.3). Average temperature (T) was 10.6 ± 0.4 °C and varied between 8.8 to 12°C. Average salinity was 35.0 ± 0.1 with a range between 34.1 and 35.3. As shown in Figure 3.3A and B, T and salinity were highly correlated (r^2=0.84, $p<0.001$, Pearsons product-moment correlation). The monthly temperature was on average highest in March and April (10.9 °C) and lowest in November (average 10.2°C).

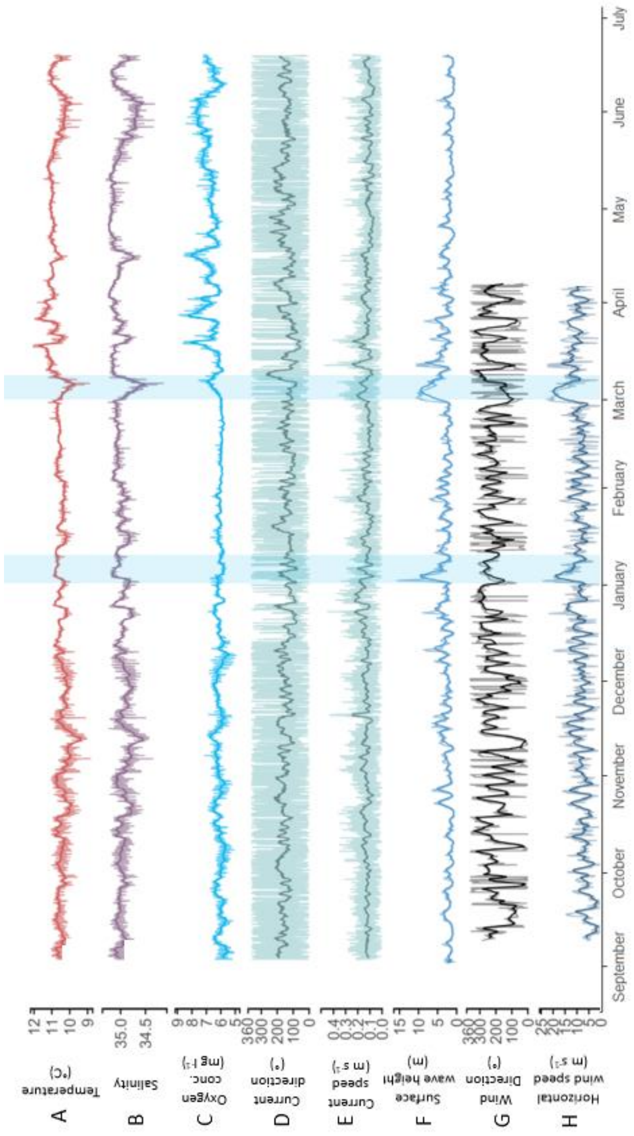

Figure 3.3 Near-bed hydrodynamic data, recorded by the lander from September 2017 to June 2018, with the daily moving average shown by thick lines. (A) Temperature, (B) Salinity, (C) Dissolved Oxygen concentration, (D) Current direction (5 mab) (E) Current speed (5 mab). Weather data from buoy: (F) Wave height; (G) Wind direction and (H) Wind speed (no continuous record) (DFO). Storm events are highlighted in light blue.

Salinity was on average highest in April (35.1) and lowest in November (34.8) (Figure 3.6A). The average dissolved oxygen (DO) concentration during the whole time period was 6.3 ± 0.5 mg l^{-1} with a range between 4.9 to 8.9 mg l^{-1}, corresponding to an oxygen saturation of on average 57 %. The dissolved oxygen (DO) concentration was negatively correlated with density (r^2=-0.52, p<0.001) and was on average highest in spring from March to June (6.7 - 7.1 mg l^{-1}), while lowest values were found from September to February (6.0 – 6.2 mg l^{-1}, Figure 3.6A). Currents at 5 mab were on average 0.12 m s^{-1} with peaks in current speed of up to 0.47 m s^{-1}. The direction of the large-scale sub-tidal flow was in a direction of 146°. Tidal flow oscillated between a NW and SE direction with the semi-diurnal tidal cycle. Current direction was not significantly correlated with temperature, salinity or oxygen concentration (Figure 3.1, supplements).

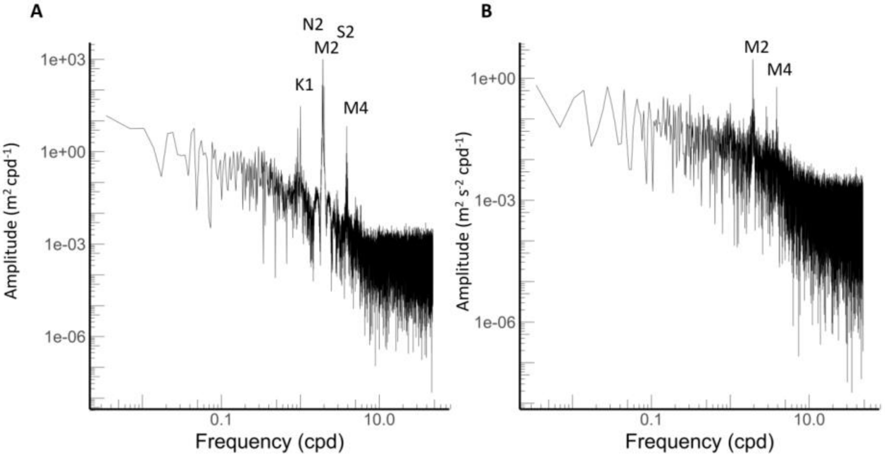

Figure 3.4 Energy spectra from (A) pressure and (B) velocity data. Main tidal frequencies are indicated.

The tidal analysis fitted to the pressure data and revealed that the biggest tidal constituent is the principal semi-diurnal lunar constituent (M_2) with an amplitude of 0.596 m, followed by the larger lunar elliptic semidiurnal (N_2) and principal solar semidiurnal constituents (S_2) with an amplitude of in each case of 0.13 m (Table 3.1). The tidal analysis fitted to the velocity data revealed that the M_2 tide produces the highest velocity with a current speed of 0.03 m s^{-1}. The second important constituent of the velocity data was the M_4 constituent producing a velocity of 0.01 m s^{-1} (Table 3.1). These tidal signals are evident in the energy spectra in which the largest peaks were found at the abovementioned frequencies (Figure 3.4).

The acoustic backscatter showed a permanently turbid benthic boundary layer up to a height of about 5 mab throughout the deployment period, whereas periodical peaks reached higher up in the water column, up to 13 mab (Figure 3.5A). Lowest backscatter was recorded from May to June 2018. The acoustic backscatter at 5 mab showed the strongest correlation with current speed ($r^2=0.25$, $p<0.001$), temperature and DO concentration (both $r^2=0.2$, $p<0.001$).

Table 3.1 Main tidal components with their frequencies and amplitudes of pressure and velocity data

Main tidal components	Frequency (cpd)	Amplitude (m)	Amplitude (m s^{-1})
M2	1.932	0.596	0.0294
N2	1.896	0.134	0.0048
S2	1.999	0.103	0.0065
K1	1.003	0.080	0.0061
M4	3.864	0.003	0.0089

Although several high turbidity events were observed throughout the year, two events are highlighted here in more detail, showing an altered daily amplitude of T, salinity, DO concentration (Figure 3.3), and corresponding peak in turbidity (Figure 3.5). Both events were correlated to storm events as observed by weather buoy data, being characterized by peaks in wave height at the 5th of January (max. 15.5 m at 4:20) and the 3th of March (max. 10.6 m at 21:20, Figure 3.3). Wind speed also peaked on these two days, reaching 24.2 m s^{-1} and 21.1 m s^{-1}, respectively, blowing into an eastern direction (DFO, 2020). Based on the acoustic backscatter data, the first extreme event in January resulted in a high load of particles in up to 13 mab for about 24 h (Figure 3.5). During this event three smaller turbidity peaks were found between the 05th of January and the 06th of January (Figure 3.5B), which were related to a change in current direction due to the semi-diurnal tides. The second storm event in March showed a slightly lower surface wave height, surface wind speed and turbidity than during the winter peak. Additionally, a temporal drop in temperature and salinity was observed during this event, where both parameters fell to a minimum of 8.8 °C and 34.1, respectively. On the contrary DO increased during the event. Several smaller events with similar characteristics were observed from March to May, showing the same alterations in T, salinity, DO and peaks in acoustic backscatter.

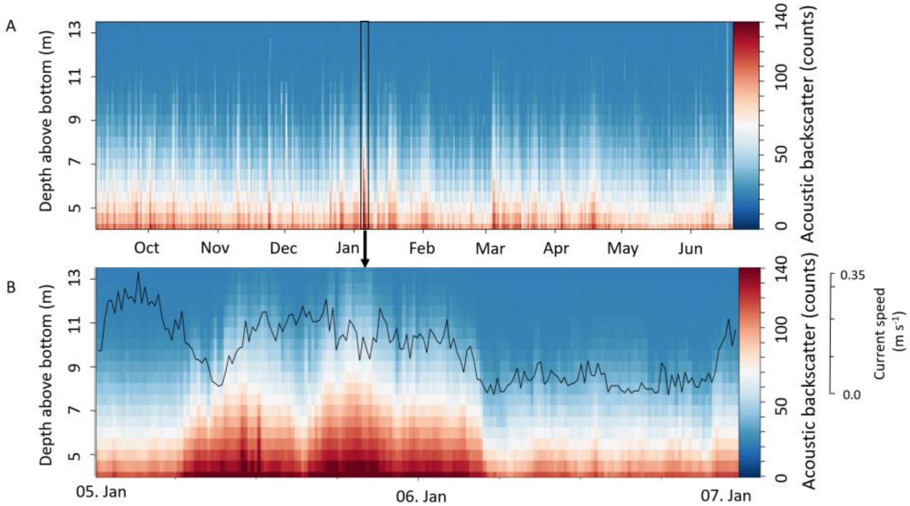

Figure 3.5 (A) Acoustic backscatter (counts) in 3.5 to 13 m above the sea bottom; (B) Resuspension event in January with current speed at 5 mab (bin2).

3.3.3 Sediment trap

The vertical mass flux during the deployment period was on average 3166 ± 3421 mg m^{-2} day^{-1} (Figure 3.6), while the average carbon flux was 100 ± 72 mg C m^{-2} day^{-1}. Highest vertical mass flux i.e., 12390 mg m^{-2} day^{-1}, was observed in the period from December 2017 to January 2018. Highest carbon flux was likewise found in December/January coinciding with the winter storm event (281 mg C m^{-2} day^{-1}, Figure 3.6). The C:N ratio was on average 8.3 ± 0.2, ranging from 7.8 to 8.6 and the δ^{15}N was 6.7 ± 0.4 ‰, ranging from 6.2 to 7.3‰. The δ^{13}C ratio ranged from -23.3 to -22.8 ‰ with an average of -23 ± 0.1 ‰.The Chl-*a* concentration was on average 2.1 ± 1.1 µg l^{-1}, with an average Chl-*a*: Phaeo ratio of 0.00069 ± 0.00077 (data not shown). The largest peak in Chl-*a* (4.05 µg l^{-1}), being two times higher than the average Chl-*a* concentration, was observed in March/April, indicating the arrival of fresh phytodetritus at the seafloor, which occurred after the second storm event in March.

The winter peak in mass flux (December/January) corresponded to a peak in acoustic backscatter (Figure 3.5B), which is likely the result of resuspension of bottom material as indicated by the presence of a large quantity of sponge spicules in the sediment trap sample. The quality of the organic matter flux in this period was low as indicated by the C:N ratio (8.4), the δ^{15}N (7.3 ‰) and the Chl-*a*: Phaeopigment ratio (0.000009), indicating that high amounts of more degraded organic matter are trapped. This is in contrast to the fresh organic matter observed in March/April with a C:N ratio of 7.9, the δ^{15}N of 6.3 ‰ and the Chl-*a*: Phaeopigment ratio of 0.003.

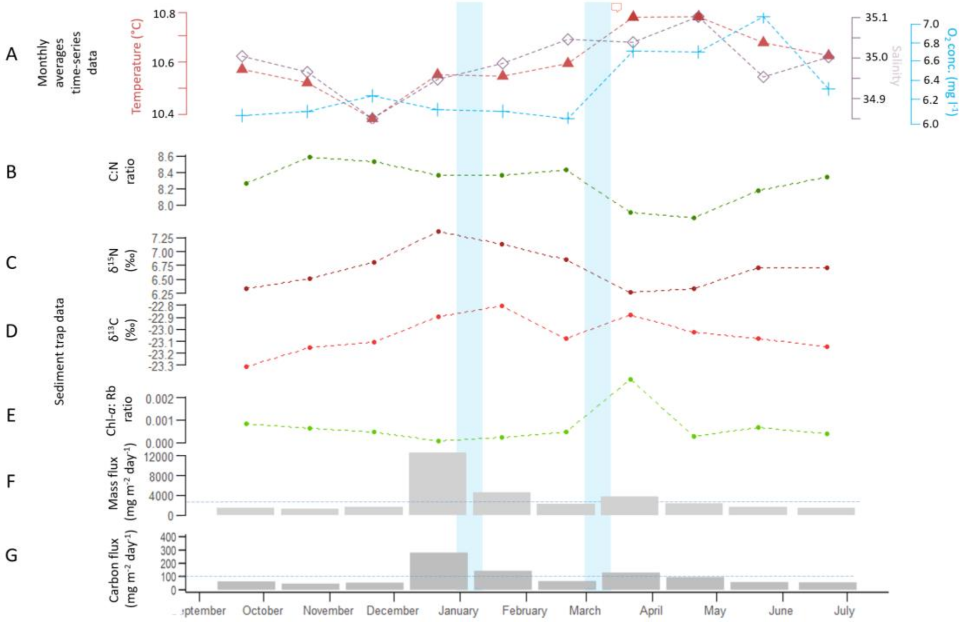

Figure 3.6 (A) Monthly averages of temperature, salinity and oxygen concentration recorded by the lander, Sediment trap data: (B) C:N ratio; (C) δ^{15}N; (D) δ^{13}C; (E) Chlorophyll-a: Phaeopigments ratio of the sediment trap material; (F) Mass and (G) Carbon flux recorded by the sediment trap. Blue horizontal lines are indicating the average mass and carbon flux. Line charts and histograms represent the average value during the 30-day sediment trap interval. Storm events are highlighted in light blue.

3.3.4 Particle displacement

The progressive vector plot showed that particulate suspended matter released at the deployment site was estimated to travel in a mainly southern direction (min. 71 km in June/July to a max. 233 km in December/January) during each 30-day sampling interval (Figure 3.7). SE-NW movements of particles are related to the semi diurnal tidal flow. In autumn, the particles generally travelled in a SSE direction, while after the storm event in January, the residual current direction shifted into a southern direction and showed the longest distance. After the storm event in spring (March/April) particles were transported relatively fast to the southwest. During spring residence time on the shelf was the longest as indicated by the shortest distances. With the shelf edge around 100 km to the south from the lander site, particles would be washed off the shelf in a period between 14 to >30 days.

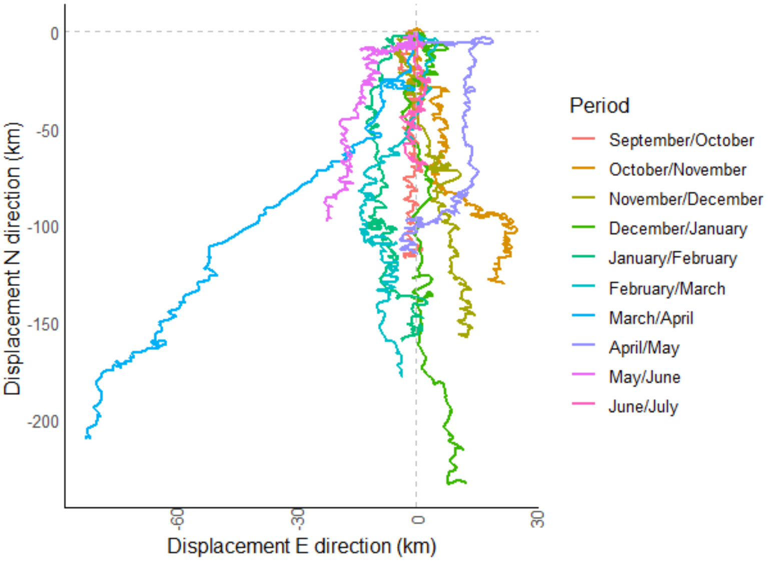

Figure 3.7 Progressive vector plot of 30-day intervals, corresponding to the sampling interval of the sediment trap. The site where the passive particle was released is the coordinate 0/0, the lander site.

3.3.5 Long-term seabed video observations in the Sambro Bank closure

The view of the camera showed several upright *V. pourtalesii* individuals as well as many anemones (Figure 3.8, 4th Jan.). Mobile species, such as pollock (*Pollachius virens*) and especially redfish (*Sebastes* spp.) also appeared in the recordings. Pollock were observed to swim relatively quickly through the video frame, mostly in groups of several individuals. Redfish were rather stationary or moving with the currents in a resting stage on the seafloor as single individuals or in small groups. The storm events were clearly captured by the video data. The video observations revealed that during the January storm event an extreme high load of particles was in resuspension for one day, whereas conditions gradually normalized within 2 days (Figure 3.8A), corresponding to the peaks in turbidity. After the water cleared up, sponges and anemones were observed to be dislocated, whereas the lander frame also moved during the storm and another view of the camera was visible. Sponges in the camera view did not appear to be negatively influenced by this dislodgement, since the sponges were white and unaffected in appearance. Nevertheless, some sponges transported in the view of the camera after a high current event, were observed to be dead (Figure 3.8B). Likely they have been ripped off from their initial position and substrate by the high currents. One of the bigger sponge individuals was observed to decompose in a time period of about three weeks (Figure 3.8B).

Figure 3.8 Photographs showing the camera view (A) before, during and after the storm event (4. January). Large amounts of suspended matter were observed in the benthic boundary layer from the 4. January to the 7. January; (B) Dead sponge in February indicated by a white arrow and its subsequent decomposition until its barely detectable at the 9th of March.

3.4 Discussion

To date the focus of most studies of the *V. pourtalesii* grounds has been on the spatial distribution of the sponge grounds, their associated fauna and biodiversity (Fuller and Cameron, 1998;Beazley et al., 2018;Hawkes et al., 2019). Little is known of the natural environmental characteristics and food supply mechanisms on short to seasonal time scales that influence these habitats. For the first time, we measured the environmental characteristics at high temporal resolution over a 10-month period in the *V. pourtalesii* sponge ground located in the Sambro Bank Sponge Conservation Area.

3.4.1 Environmental conditions on the Scotian Shelf

Based on the modelling results of Beazley et al. (2018), minimum bottom water temperature of 5°C is the most important determinant for the distribution of *V. pourtalesii* on the Scotian Shelf. In our study, bottom water temperature varied between 8.8 to 12.0 °C during the deployment period. The sponge grounds were observed below the boundary of two water masses, mainly bathed in WSW. During most of the year seasonal water column stratification on the Scotian Shelf prevents mixing of the WSW and SSW (McLellan, 1957), and in this study high and relatively stable bottom water temperatures were measured. Short-term daily fluctuations in temperature and salinity were linked to internal tides (M_2) moving stratified waters up and down the sloping topography of the Emerald Basin (Wunsch, 1975;van Haren et al., 1994). Extreme temperature fluctuations during the lander deployment were only observed during some of the storm events in spring, when colder, less saline and oxygen-rich water, typical for the winter cooled surface waters was observed near the bottom (Fig 3.3). These events resulted in abrupt fluctuations in bottom water temperature of up to 3.2 °C, which might be related to wind driven downwelling on the shelf (Greenberg et al., 1997). These fluctuations did not exceed multi-decadal variability (4-12 °C), which is even higher with bottom temperatures varying by up to 8°C and being as low as 5°C (Beazley et al., 2018). That sponges can thrive in a large temperature range was also observed in other studies: glass sponge accumulations in

Norway were correlated with temperatures below 12°C (Strand et al., 2017) and even as low as -0.5 °C along the arctic mid-Atlantic Ridge (Roberts et al., 2018), whereas *P. carpenteri* was found over a temperature range of 2.7-20.9 °C (Howell et al., 2016). Even though lower and upper temperature ranges of most sponge species are still largely unknown, it seems that they can thrive at larger temperature ranges than other deep-sea species forming hotspots like cold-water coral reefs (4-12 °C) (Roberts et al., 2006).

The DO concentration of 6.3 ± 0.53 mg l^{-1} measured in this study was about three times higher than the DO concentration (2.05 mg l^{-1}) measured in a sponge reef on the western Canadian margin (Whitney et al., 2005). So far it is not evident which DO concentrations are suitable for sponges. They seem very resilient even at low DO concentrations, as observed at the Namibian margin where DO concentrations were far below 2 mg l^{-1} (Hanz et al., 2019), which seems to be the threshold for growth and survival of many other marine organisms (Gray et al., 2002).

Another important environmental factor for the occurrence and sustenance of sponge grounds is the interaction between hydrography and seafloor topography (van Haren et al., 2017;Davison et al., 2019). Sponge grounds are often associated with areas, where the slope angle of the bottom matches the slope of internal tides, producing internal waves. Internal waves, generated by wind or flow over topography are the main causes of strong bottom currents, enhanced turbulence and mixing and resuspension of particulate matter near the seafloor (Garrett and Laurent, 2002;Hosegood and van Haren, 2004), thereby influencing food supply by increasing the vertical and lateral flux (Davison et al., 2019) as has also been observed in cold-water coral ecosystems (Cyr et al., 2016). An example is the *P. carpenteri* belt along the slope of the Porcupine Seabight in the NE Atlantic (Rice et al., 1990) or the Faroe Shetland channel where sponges were observed in regions with intensified internal wave activity and associated with pronounced changes in temperature (Davison et al., 2019). Such conditions have also been found on seamounts and canyons, where sponge aggregations have been observed in areas of critical slope in the Arctic

(Schulz Bank seamount; Busch et al., 2020) and the Azores (Rainbow Basin; van Haren et al.,2017). Based on our data we can only link the environmental fluctuations to the presence of tidal currents. However, other studies have described the presence of internal wave activity in the Emerald Basin (van Haren et al., 1994). Intermediate nepheloid layers were found to coincide with the critical depth for possible generation and amplification of internal waves with semi-diurnal (M2) internal tidal frequency (Azetsu-Scott et al., 1995). The nepheloid layers observed by Azetsu-Scott et al. (1995) in their vertical profiles had an intermittent character that was explained by recurrent resuspension and variable currents. This intermittency was also clearly visible in the near-bed data (current data and video) from this study (Figure 3.5 and 3.8) showing pulse-like increases of particulate matter concentrations in the benthic boundary layer pointing to local resuspension. These frequent resuspension and subsequent lateral transport of high near-bed particle concentrations might be an important driver of food supply for *V. pourtalesii* sponge grounds on the Scotian Shelf.

3.4.2 Food supply

Sponges are very efficient filter feeders and feed on particulate as well as dissolved resources (Reiswig, 1971;Pile and Young, 2006). While the average daily carbon flux in the near-bed sediment trap was 100 ± 72 mg mg m^{-2} day^{-1} during the deployment period, carbon flux was highly variable and peaked in December/January (281 mg C m^{-2} day^{-1}) and March/April (130 mg C m^{-2} day^{-1}). During the December peak no major fluctuations in temperature, salinity or DO concentration were observed which is likely indicating that the organic matter is not delivered from the surface but rather due to resuspension events inside the bottom boundary layer. Even though this winter event was characterized by a high carbon flux, mainly degraded organic matter was resuspended as shown by the low concentration of Chl-*a* and a high C:N ratio (Figure 3.6), likely related to resuspension and lateral transport of more degraded material from the seafloor. Hill and Bowen (1983) calculated that a current speed of 0.15 m s^{-1} is required to resuspend the coarser sand, whereas fine sand and mud is transported at a speed of 0.11 m s^{-1}. Current speed as measured in this study would be sufficient to resuspend coarse sediment during 31 % of the time and 56 % for the finer fraction. This was also apparent in the ADCP turbidity data (Figure 3.5) which showed an almost permanent turbid layer close to the bottom. The video recordings showed that during storm-induced resuspension events, particularly the event that occurred during winter, particles stayed in resuspension for several days, which was however not detected in the acoustic backscatter data of the ADCP, implying that turbidity close to the bottom might be even more persistent. This could possibly be due to the particle size of the particles in resuspension, whereby the finer particles are not resolved by measurements of the ADCP (Bunt et al., 1999).

In March/April the highest amounts of fresh (high concentration of Chl-*a* and lower C:N ratio) organic matter were observed , likely related to a surface algal bloom. The algal bloom period seems indirectly related to the mixing of the water column during the storm event in March (Figure 3.6), when nutrients are stirred up to the surface. Our data on the importance of a mixed water column for the surface productivity was confirmed by an ecosystem model, which predicted highest primary production to appear in the beginning of April (Song et al., 2011).

Taking the estimated carbon demand of a deep-water glass sponge reef (ca. 160 m depth, ~10°C) at the Canadian coast (1800-4100 mg C m^{-2} day^{-1}, Kahn et al. 2015), the carbon derived from the vertical flux would provide on average approximately <8 % of the required carbon demand. Ex situ experiments have shown that in the Canadian sponge reefs carbon consumption was much higher (360 mg m^{-2} day^{-1}), compared to the average carbon flux (100 mg m^{-2} day^{-1}), showing that the carbon demand of the Vazella grounds will not be covered (Bart et al., 2020b). A potential carbon deficit may be alleviated from the resuspended organic-rich sediment itself (Grant et al., 1987), but also from the filtration of bacteria and uptake of DOC from the water column (Bart et al., 2020a). Bacteria are expected to be an even more important food source than suspended particulate matter for some glass sponges and will be assimilated efficiently (Pile and Young, 2006;Kahn et al., 2015;Bart et al., 2020a). On the Scotian Shelf an important source of bacteria can be the resuspended sediments, which are 100-1000 times enriched in heterotrophic bacteria compared to the overlaying water (Kuwae and Hosokawa, 1999a). These benthic bacteria are attached to sediment particles with extracellular polymeric substances and can be taken up by the ingestion of sediment particles (Kuwae and Hosokawa, 1999b). It was also shown that particles remaining in suspension become more densely packed with bacteria (Wainright, 1987). This was suggested to occur on the Scotian Shelf by Grant et al. (1987), who found a high N content in sand particles, which they hypothesized was due to attachment by bacteria. Considering the fact that several large resuspension episodes were observed during the deployment period, the resuspended sediment with microbes attached and subsequent lateral transport might constitute a major food source for the sponges. The fine carbon- and nitrogen-rich suspended material and even the coarse sandy fraction is constantly resuspended and transported over the shelf (Grant et al., 1987) in a mainly southern direction as was also shown by the progressive vector analysis (Figure 3.7). Even though this type of analysis only provides an estimate, we showed that suspended matter stays on the shelf for 14->30 days. During the event in March the wind direction was towards the east and the residual current direction changed to the SW in an along slope direction that likely has resulted in downwelling (Greenberg et al., 1997;Li et al., 2014), which was indicated by a decrease in temperature related to the cooler SSW. Due to the occurrence of natural resuspension events throughout the 10-month lander deployment, the question arises if these events and resulting lateral transport of (food) particles are essential for the occurrence of *V. pourtalesii* on the Scotian Shelf.

3.4.3 Events

The extreme events at the seafloor at the 154 m deep lander site were mainly driven by storm events and occurred predominantly in the winter and spring months, influencing the water column structure and particle distribution on the shelf. Only the storm events in spring were observed to introduce colder and less saline water to the sponge ground, which was during the event in March coinciding with a peak in surface wave height as well as an on average more easterly wind direction (Figure 3.3). Water column mixing will result in an increased availability of nutrients from the deeper water masses towards the surface (Townsend et al., 2006), triggering primary productivity and increased benthic-pelagic coupling (Ji et al., 2006). Topography-hydrography interactions can also influence biogeochemistry and microbiology either by mixing or by resuspension as described above, which can result in different sponge associated microbial communities defined by the surrounding near-bed environment (Busch et al., 2020). This mixing will indirectly promote an increased vertical flux and therefore food supply to the sponge grounds and their associated fauna, as was also observed in the Gulf of Mexico and on the Namibian margin (Mienis et al., 2012;Hanz et al., 2019). Wind-induced mixing also can play a major role in the replenishment of for instance oxygen as was observed during the spring storm events, where colder SSW with a lower salinity and higher DO concentration was observed amidst the sponge ground. Replenishment of nutrients and DO have shown to be vital for the occurrence of sponges as well as other deep-sea ecosystems, like cold-water coral reefs (van Haren et al., 2014;Hanz et al., 2019).

However, these events can also act as stressors for the sponge ground. During periods of high current speed sponges and anemones were observed to be dislocated and tipped over into a horizontal position and a dead individual was observed in front of the camera in late winter (February-March). Accumulations of dead individuals have been observed in the Sambro Bank Sponge Conservation Area (Hawkes et al., 2019), caused either by the displacement by high currents or by fishing activities and subsequent transport by the current (trawling and dumping). Our video data showed that large dead individuals were disintegrating in a period of several weeks, which might be important for the silicon cycling on the Scotian Shelf (Maldonado et al., 2020).

Besides the observed events, the Labrador Current which varies seasonally in extent, is in general known for the displacement of biological organisms and materials to the southwest (Hannah et al., 2001). The association of the *V. pourtalesii* with movable hard substrate like stones and pebbles might hence have a benefit for the sponges at the Scotian Shelf. The strong currents during winter and spring storm events might be destructive if sponges would be attached to non-movable hard substrate since they can be ripped off their attachment. Additionally, small stones and pebbles might play a role in helping the sponges to stay upright or regain an upright position after being moved by transferring their mass centre to their bottom. That would also explain why only in deeper areas in the Fundian Channel, which are likely less affected by storm activity and high current speeds, sponges are also found on bigger boulders (Fuller and Cameron, 1998;Lacharité and Metaxas, 2017).

High amounts of resuspended material can also be a stressor for *V. pourtalesii* since high amounts of suspended sediment or larger particles can clog the aquiferous system of sponges and could negatively impact their filtering ability and even their survival (Maldonado et al., 2008;Tjensvoll et al., 2013;Kutti et al., 2015a). To avoid complete clogging, sponges exhibit adaptations to high particle loads and can arrest pumping and 'cough' (a clearing response) when exposed to high concentrations of suspended sediment. The exact concentration of suspended particulate matter in the water column during the winter storm events was not measured in this study. However, video observations showed that the extreme conditions in the benthic boundary layer lasted up to several days (Figure 3.8). If *V. pourtalesii* arrest their pumping activity during these periods they would need to do so for a much longer time than has been shown so far in other studies (Tjensvoll et al., 2013;Kutti et al., 2015a;Grant et al., 2019). The Scotian Shelf is subject to severe storms as well as hurricanes on a regular basis, caused by extratropical cyclonic storms that develop along the U.S. east coast and travel northward (Anderson et al., 1989). Modelling studies have indicated that with predicted climate change storm intensity will increase, which likely will have an effect on the sponge grounds situated on the Scotian Shelf (Knutson et al., 2010).

Besides naturally driven suspension events, sponges on the Scotian Shelf are also influenced by anthropogenic impacts like fishing activities that can also resuspend large amounts of particulate matter. The

Vazella grounds on the Scotian Shelf are situated in traditional fishing grounds for groundfish (Beazley et al., 2018). Bottom-tending fishing gears can directly impact sponge grounds through removal and incidental damage, or through indirect effects such as resuspension of sediment and smothering (Tjensvoll et al., 2013), whereby impacts of plumes were observed kilometres away from the source of the plume (Grant et al., 2019). As mentioned above, resuspension events and lateral transport of particles can positively and negatively influence sponges. Particles suspended by fishing activity are known to decrease the filtering capacity and efficiency in many species which can result in adverse effects on overall metabolism and health of sponges (Bell et al., 2015;Grant et al., 2019). How the concentration of suspended sediment observed during storm events compares to resuspension induced from bottom trawling remains unknown. Nevertheless, *V. pourtalesii* do overall not seem to suffer from the natural resuspension events and showed healthy appearances after the events. Results from this study contextualize the response of sponges to human-induced threats such as bottom fishing and climate change by providing detailed site-specific knowledge of the natural conditions under which these sponges persist and their resilience during changing environmental conditions.

3.5. Conclusion

In order to be resilient to environmental and anthropogenic stressors environmental factors like temperature, DO concentrations and food supply need to be in an optimal range (Odum, 1971;Sokolova et al., 2012). Overall the near-bed environmental conditions in the *Vazella* grounds fitted in the ranges as described for glass sponge species. *V. pourtalesii* experienced temperature fluctuations of up to 3.2°C on seasonal timescale, with maximum temperatures of 12°C in spring and on average lowest temperatures in autumn (November), which fits in the inter-annual temperature range as described before. Major storm events in winter and spring were additionally observed to cause extreme resuspension events, which were expected to exhibit a stressor but also an important mechanism for food supply *V. pourtalesii* appeared to withstand these events, even for several days, suggesting that sponges are resilient to natural as well as anthropogenic (e.g., fishing) resuspension events. The vertical flux of organic matter was estimated to not cover the food demand of the sponges as was also observed in other sponge areas, whereas the semi-diurnal tidal currents play an important role in the resuspension of sediments, which likely constitute a constant source of particulate food for the sponges. The only directly observed stressor was high currents, which relocated benthic fauna and sometimes lead sponges to loosen their upright position. Our findings show how resilient these sponges are to environmental changes over short time scales, which might be vital for their survival under human-induced threats such as bottom fishing and climate change.

3.6 Funding

This research has been performed in the scope of the SponGES project, which received funding from the European Union's Horizon 2020 research and innovation programme under grant agreement No. 679849. Canadian cruises and contributions were funded by Fisheries and Ocean’s Canada’s International Governance Strategy Science Program through project “Marine Biological Diversity Beyond Areas of National Jurisdiction (BBNJ): 3-Tiers of Diversity (Genes-Species-Communities)” led by EK (2017-2019) and Strategic Program for Ecosystem-Based Research and Advice (SPERA) project “Evaluation of the Effectiveness of Two Sponge Conservation Areas in the Maritimes Region: Identifying Patterns of Dispersal, Connectivity, and Recovery Potential of the Russian Hat Sponge Vazella pourtalesii” led by L. Beazley and E. Kenchington. FM was supported financially by the Innovational Research Incentives Scheme of the Netherlands Organisation for Scientific Research (NWO-VIDI grant 016.161.360).

3.7 Acknowledgements

We thank the captain and crew of the CCGS Martha L. Black and CCGS Hudson for their help with the deployments and recoveries of the research gear. We also thank Barry MacDonald, Francisco Javier Murillo and the scientific party of both cruises for their help in collecting the samples.

3.9 Supplements

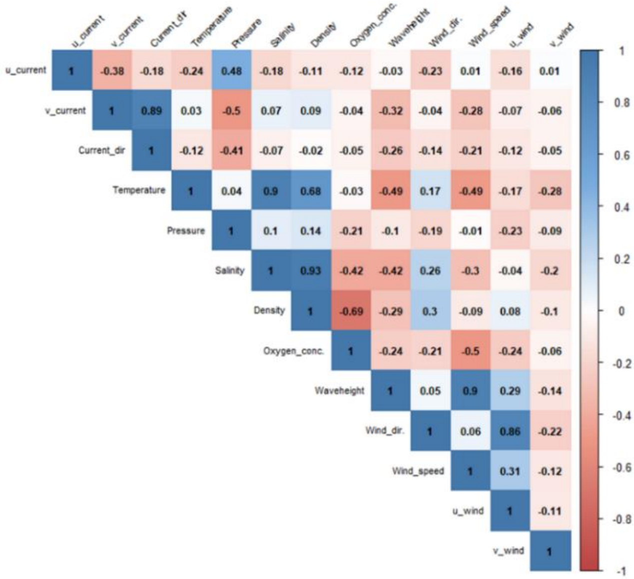

	u_current	v_current	Current_dir	Temperature	Pressure	Salinity	Density	Oxygen_conc.	Waveheight	Wind_dir.	Wind_speed	u_wind	v_wind
u_current	1	-0.38	-0.18	-0.24	0.48	-0.18	-0.11	-0.12	-0.03	-0.23	0.01	-0.16	0.01
v_current		1	0.89	0.03	-0.5	0.07	0.09	-0.04	-0.32	-0.04	-0.28	-0.07	-0.06
Current_dir			1	-0.12	-0.41	-0.07	-0.02	-0.05	-0.26	-0.14	-0.21	-0.12	-0.05
Temperature				1	0.04	0.9	0.68	-0.03	-0.49	0.17	-0.49	-0.17	-0.28
Pressure					1	0.1	0.14	-0.21	-0.1	-0.19	-0.01	-0.23	-0.09
Salinity						1	0.93	-0.42	-0.42	0.26	-0.3	-0.04	-0.2
Density							1	-0.69	-0.29	0.3	-0.09	0.08	-0.1
Oxygen_conc.								1	-0.24	-0.21	-0.5	-0.24	-0.06
Waveheight									1	0.05	0.9	0.29	-0.14
Wind_dir.										1	0.06	0.86	-0.22
Wind_speed											1	0.31	-0.12
u_wind												1	-0.11
v_wind													1

Figure S3.1 Correlations between factors measured by the lander and factors measured by the surface buoy.

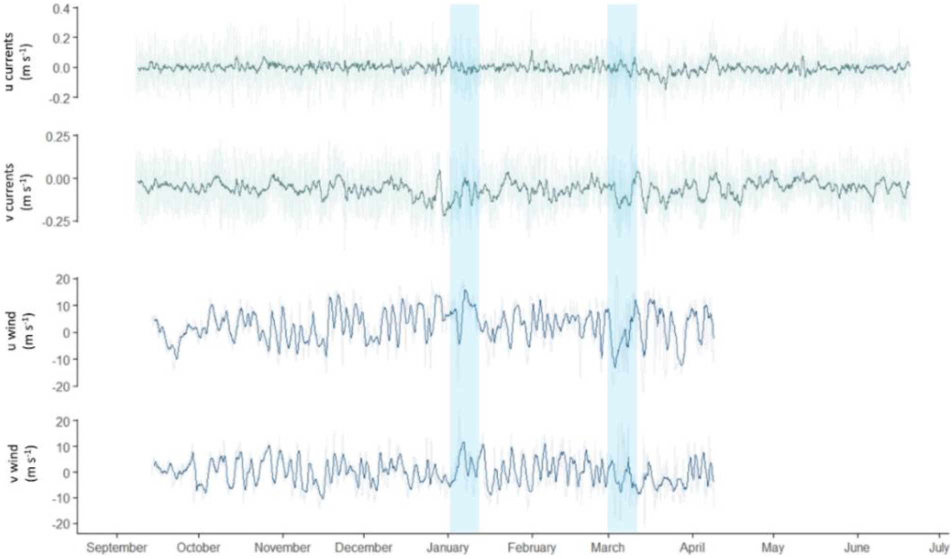

Figure S3.2 u and v components of the bottom currents and surface wind data during the investigated time period.

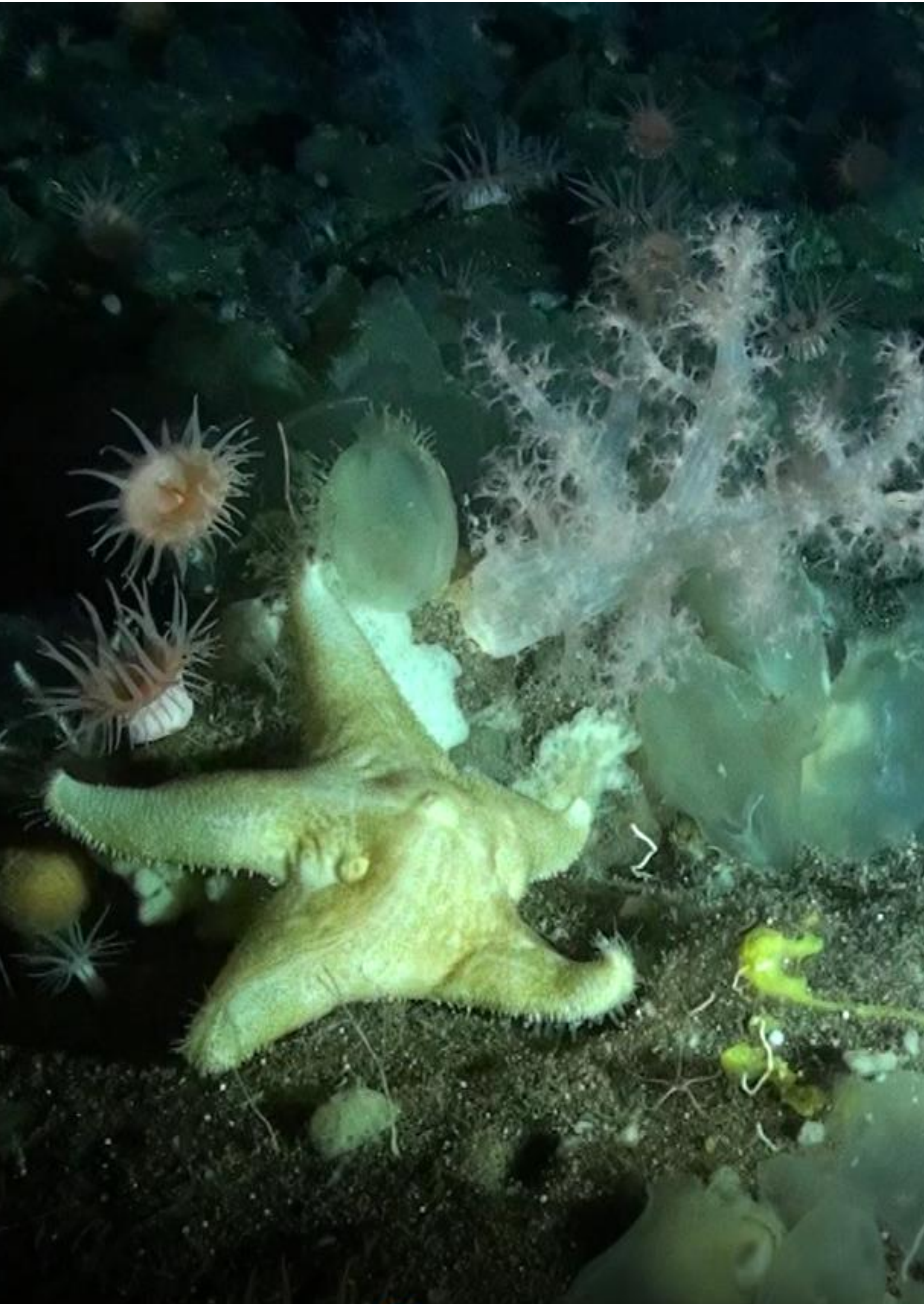

Chapter 4

Long-term Observations Reveal Environmental Conditions and Food Supply Mechanisms at an Arctic Deep-Sea Sponge Ground

Ulrike Hanz, Emyr Martyn Roberts, Gerard Duineveld, Andrew Davies, Hans van Haren, Hans Tore Rapp†, Gert-Jan Reichart and Furu Mienis

Published in Journal of Geophysical Research: Oceans in 2021

Picture to the left: Schulz Bank sponge ground with *Tylaster willei* sitting on *Geodia* sp. ©NIOZ

Abstract

Deep-sea sponge grounds are hotspots of benthic biomass and diversity. To date, very limited data exists on the range of environmental conditions in areas containing deep-sea sponge grounds and which factors are driving their distribution and sustenance. We investigated oceanographic conditions at a deep-sea sponge ground located on an Arctic Mid-Ocean Ridge seamount. Hydrodynamic measurements were performed along CTD transects and a lander was deployed within the sponge ground that recorded near-bottom physical properties as well as vertical fluxes of organic matter over an annual cycle. The data demonstrate that the sponge ground is found at water temperatures of -0.5 to 1 °C and is situated at the interface between two water masses at only 0.7° equatorward of the turning point latitude of semidiurnal lunar internal tides. Internal waves supported by vertical density stratification interact with the seamount topography and produce turbulent mixing as well as resuspension of organic matter with temporarily very high current speeds up to 0.72 m s^{-1}. The vertical movement of the water column delivers food and nutrients from water layers above and below towards the sponge ground. Highest organic carbon flux was observed during the summer phytoplankton bloom period, providing fresh organic matter from the surface. The flux of fresh organic matter is unlikely to sustain the carbon demand of this ecosystem. Therefore, the availability of bacteria, nutrients and dissolved and particulate matter, delivered by tidally-forced internal wave turbulence and transport by horizontal mean flows, likely plays an important role in meeting ecosystem-level food requirements.

4.1. Introduction

Benthic organisms in the deep sea largely depend on the vertical flux of organic matter from productive surface waters. Much of this vertical flux is remineralized during downward transport to the sea bottom, reducing the quantity and quality of the organic matter (Davies et al., 2009; Gooday, 2002; Kiriakoulakis et al., 2001; Lampitt and Antia, 1997; Smetacek, 1984). Still, flourishing ecosystems such as cold-water coral (CWC) reefs and sponge grounds, have been discovered in areas of the deep sea, where their presence cannot be explained by the amount of energy supplied by vertical flux alone (Kahn et al., 2015; Oevelen et al., 2009). For example on the Canadian shelf, it was estimated that sponges consume seven times more carbon than provided by the vertical flux of organic matter (Kahn et al., 2018). Therefore, additional food supply mechanisms and efficient recycling of resources must exist to fulfil this deficit.

Recently sponge grounds have become a focus of deep-sea research since they can form hotspots of biomass and biodiversity in the deep sea similar to CWC reefs (Beazley et al., 2013; Hogg et al., 2010; Maldonado et al., 2017). At bathyal and abyssal depths sponges, specifically hexactinellids (glass sponges), belong to the most common megafaunal organisms (Tabachnick et al., 1994). Together with other sponge groups (demosponges) they are able to form extensive grounds and even reef-like habitats that cover large areas of the seafloor on shelves, slopes, seamounts, plains and even hadal bottoms (Barthel and Gutt, 1992; Cathalot et al., 2015; Kahn et al., 2015; Klitgaard and Tendal, 2004; Murillo et al., 2012). Sponges are considered ecosystem engineers since they build 3D-structures providing a habitat for sessile and mobile fauna, which can persist beyond their lifetime (Buhl-Mortensen et al., 2010; Meyer et al., 2019). Components of the sponge glass skeleton (so-called spicules) remain on the seafloor after their death, creating structures from several centimetres up to several meters. These spicule mats provide an important substrate for living sponges and associated fauna (Bett and Rice, 1992; Conway et al., 2005). These structures as well as the sponges themselves interact with the flow of water, leading to a modification of flow in the benthic boundary layer (BBL) which likely influences food and particle supply as well as the retention and availability of food for sponges and other suspension feeding organisms (Culwick et al., 2020; Maldonado et al., 2015; Mienis et al., 2019).

Sponges display a wide variety of feeding behaviour that match the extreme conditions they inhabit. In addition to very specific mechanisms such as carnivory in some deep-sea sponge species (Vacelet et al. 1995), they are known to be associated with microorganisms like bacteria, viruses, and archaea which transfer food to the sponge (Hentschel et al., 2006), feed directly on bacteria from the water column (Yahel et al., 2006) or even directly take up dissolved organic carbon (DOC) as shown for tropical reef sponges (de Goeij et al., 2008; Rix et al., 2017). Therefore, they play a major role in biogeochemical cycling, for example carbon cycling, and are able to transfer organic matter from the pelagic to the benthic environment (Beazley et al., 2013; Cathalot et al., 2015).

Sponge grounds are commonly associated with increased near-bottom current velocities due to the seafloor topography interacting with local and regional hydrodynamics, similar to CWC ecosystems (Chu and Leys, 2010; Davies et al., 2009; Frederiksen et al., 1992; Rice et al., 1990). This interaction often comprises internal tidal waves enhancing currents and increasing turbulence in regions where the bed slope is comparable to the ray-path slope of the internal wave propagation (e.g. Eriksen, 1982; Jalali et al., 2017; Müller and Liu, 2000; van Haren et al. 2017). Particularly at seamounts, but also on shelves turbulence and vertical mixing have been observed and enhanced by shear, convective instabilities from the rebounding tidal flow and breaking of transient lee waves (Davison et al., 2019; Lavelle and Mohn, 2010). Around seamounts this has led to accumulations of pelagic as well as benthic biomass (Clark et al., 2010; Hosegood et al., 2019; Jalali et al., 2017). These processes also impact food supply from surface waters to the deep sea, increasing delivery and retention of suspended particulate matter (SPM) (Duineveld et al., 2007). Seamounts can also induce a closed circulation above their summits (e.g. Taylor Columns), which leads to trapping of organic material or retention of resuspended organic material (Boehlert and Genin, 1987; Henrich et al., 1992; Lavelle and Mohn, 2010; Taylor, 1923).

The distribution of CWCs and sponges overlap in many areas, suggesting that similar environmental conditions are beneficial for both groups of species. However, areas consisting primarily of sponges also occur, such as for example in the NE Atlantic (e.g. Western Barents Sea, along the Norwegian Shelf to the Faroes), south of Iceland (Klitgaard and Tendal, 2004; Roberts et al., 2018), on seamounts in the Alboran Sea in the Mediterranean (Maldonado et al., 2015), the Flemish Cap, and Scotian Shelf on the Canadian shelf (Chu and Leys, 2010).

A recent short-term study on the environmental conditions at an Arctic seamount, the Schulz Bank, suggested that the hydrodynamic regime produces favourable conditions for the appearance of dense sponge grounds (Roberts et al., 2018). The aim of the current study was to extend these short-term observations to determine the long-term environmental drivers and their temporal variability as well as the food supply mechanisms that support the presence of a dense deep-sea sponge ground on the summit of the Schulz Bank. For this purpose long-term near-bed observations of environmental conditions were combined with measurements of deep sea particle fluxes. In addition, CTD profiles were recorded along transects to study the water column structure around the Schulz Bank. The ensuing data form a comprehensive set of continuous, high-resolution, long-term records of near-bed environmental conditions at a sponge ground, shedding light on the environmental ranges in which sponges are found. This study provides insight on the hydrodynamic processes that influence the sponge grounds so they can meet their energy demand in the food-limited deep sea.

4.2. Study site and methods

4.2.1 Regional setting

The Schulz Bank (73° 50’ N, 7° 34’ E, Figure 4.1, earlier also described as the Schulz Massif seamount in Roberts et al. 2018) is part of the Arctic Mid-Ocean Ridge (AMOR). It is approximately 22 km wide and rises to about 1900 m above the plain of the Lofoten Basin in the south and the Greenland Basin in the north. The Schulz Bank is situated between two sub-ridges, the Mohn Ridge and the Knipovich Ridge. The summit is oriented in a NE-SW direction and is situated at 600 m below the sea surface. The slope is largely dominated by soft sediments with local rocky outcrops; the summit is known to be covered by sponge spicule mats of up to 20 cm thick, overgrown by living sponges and associated fauna (Roberts et al., 2018). The highest abundance of sponges and associated fauna was found on the summit at depths above 600-800 m, below that, sponge occurrences were patchier and sponge density was significantly lower. The flanks and deeper plains showed only a sparse sponge cover. A more detailed description of sponge occurrences is presented in Roberts et al. (2018) and Meyer et al. (2019).

The water masses surrounding the Schulz Bank in the Greenland, Iceland and Norwegian (GIN) seas have been described in detail by Hopkins (1991). The area is influenced by North Atlantic Water which is characterised by salinities > 35 and temperatures > 2 °C (Helland-Hansen and Nansen, 1909). These waters enter from the south as a surface water mass (NwAtW, Norwegian Atlantic water). The intermediate water mass around the Schulz Bank is Norwegian Arctic Intermediate Water (NwArIW) which originates in the GIN seas and is derived by convection from surface waters exposed to atmospheric exchange (Hopkins, 1991; Jeansson et al., 2017). Beneath this, Norwegian Sea Deep Water (NwDW) in the east and Greenland Sea Deep Water (GSDW) in the west are present (Rudels et al., 2002).

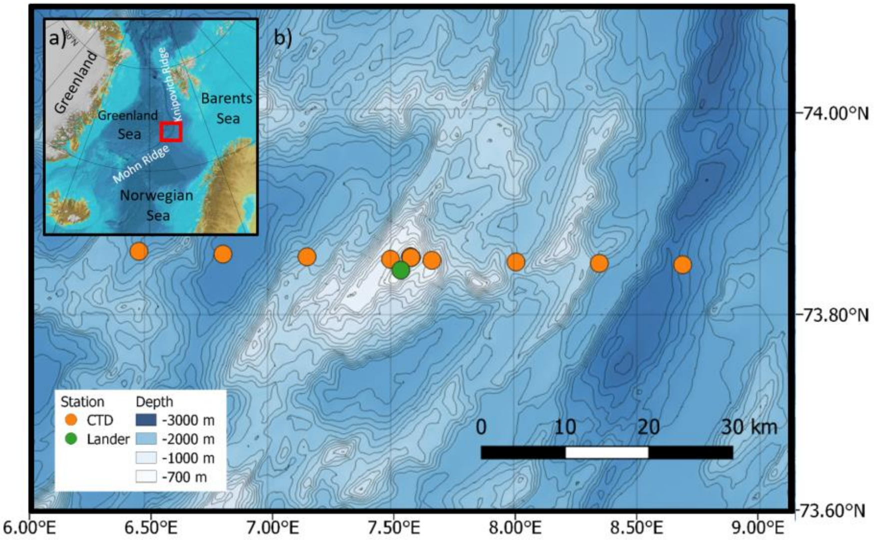

Figure 4.4 a) Inset: the Schulz Bank as part of the AMOR (adapted from Jakobsson et al., 2012), b) Map of the Schulz Bank region (contour interval 100 m) with CTD stations and position of the lander (bathymetry from Consortium, 2016).

4.2.2 Data collected in the field

Fieldwork was conducted as part of three multi-disciplinary research cruises to the Schulz Bank (GS2016109, GS2017110 and GS2018108) with the Norwegian vessel RV *G.O. Sars* in the frame of the Horizon 2020 project SponGES. The fieldwork for the present study consisted of the deployment of a benthic lander (see below) in 2016 amidst the sponge ground for the period of one year and a Conductivity-Temperature-Depth (CTD) transect at the end of the deployment to determine water column characteristics around Schulz Bank (Table 4.1). During CTD casts different samples were collected from the water column (Table 4.1).

A CTD transect conducted in 2018 covered the deep Norwegian and Greenland basins in the east and west as well as the seamount summit to characterize the water column structure (Figure 4.1). The CTD profiler used was a Seabird “SBE 9 plus” underwater unit and a Seabird “SBE 11 plus V2” deck unit, equipped with a dissolved oxygen sensor (SBE 43), a chlorophyll-*a* sensor (Chelsea Aqua 3), and a rosette water sampler of 12x 10 L Niskin® water sampling bottles, triggered to close at given depths during the up-cast. For the analysis and interpretation of the measured profiles, the downcast raw data were processed with “SBE Data Processing” software.

Table 4.1 Overview of lander and CTD stations surveyed on the Schulz Bank from cruises GS2016109, GS2017110 and GS2018108.

Station	Device	Date	Latitude	Longitude	Depth [m]
GS2016109-07 to GS2017110-17	Lander	21.06.2016 until 27.07.2017	73.816	7.55234	668
GS2018108-02	CTD	31.07.2018	73.83067	7.55917	584
GS2018108-12	CTD	01.08.2018	73.82733	7.642	1056
GS2018108-13	CTD	01.08.2018	73.82733	7.96467	2057
GS2018108-14	CTD	01.08.2018	73.82716	8.28483	2190
GS2018108-15	CTD	02.08.2018	73.8265	8.60483	3000
GS2018108-22	CTD	03.08.2018	73.82983	7.56233	582
GS2018108-28	CTD	04.08.2018	73.82684	6.51617	2479
GS2018108-29	CTD	04.08.2018	73.82733	6.839	2972
GS2018108-30	CTD	05.08.2018	73.8275	7.162	2111
GS2018108-31	CTD	05.08.2018	73.82733	7.48283	994
GS2018108-37	CTD	06.08.2018	73.82983	7.561	580

4.2.3 Near-bed environmental conditions

A BOBO (BOttom BOundary) lander was deployed on the summit of the Schulz Bank on the 21st July 2016 and successfully recovered on the 5th August 2017 (Figure 4.1, Table 4.1). The BOBO-lander was equipped with an Acoustic Doppler Current Profiler (ADCP; Teledyne-RDI, 1200 kHz, recorded 13 bins of 1 m between 3.55 and 15.55 m above bottom (mab)), a combined Wetlabs turbidity and fluorometer (Wetlabs-FLNTU), a Seabird CT sensor and a combined temperature and oxygen sensor (Advantech RINKO). The ADCP sensor was attached at the top of the lander at 2 mab, all other sensors were attached around 1 mab. An HD video camera (Sony) with LED illumination was directed at the seafloor recording 30 s of video every 2 h. During the deployment all instruments were programmed at a sample interval of 15 min, except the oxygen sensor which was set to a 30 min interval. All instruments measured during the whole deployment period, except the oxygen sensor, which stopped recording on the 01.06.2017 due to power failure. The lander was also equipped with a sediment trap (Technicap PPS4/3) with a rotating carousel of 12 bottles. The trap aperture (0.05 m^2) was at 2 mab. Sediment trap bottles were filled with a pH-buffered mercury chloride ($HgCl_2$) solution in filtered seawater collected from the deployment site and the carousel was programmed to progress in 30 day intervals. The sediment trap material was filtered over a 1 mm sieve to remove bigger particles and zooplankton. Samples were split into 5 sub-samples with a rotor splitter: four sub-samples were rinsed with demineralized water to remove salts and $HgCl_2$; and one sub-sample was rinsed with bottom water to keep pigments intact. All samples were freeze-dried and weighed to measure mass fluxes (Mienis et al., 2012).

In this study data of two backscatter sensors were used to identify the presence of different particle sizes. As the wavelength of sound is larger than that of light, acoustic backscatter showed the presence of larger grain sizes, about 1 mm at 1200 kHz, while optical backscatter recorded a smaller range of particle sizes (Fugate and Friedrichs, 2002). For the time series of the acoustic backscatter signal, raw data were transferred to mean volume backscatter using the noise- and attenuation-correction of Gostiaux and Van Haren (2010). Data from bin 4 were selected, which corresponded to a height of 6.5 mab. This bin was chosen as it is close to the bottom, but high enough above the lander to minimize the effects of any flow alteration caused by the lander structure.

The near-bed horizontal velocity components obtained with the ADCP were analyzed to determine the tidal constituents contributing to currents at the Schulz Bank. The method used is an extension of the one-dimensional harmonic analysis (least squares) method commonly applied to sea-level time series data. The two velocity components were analyzed separately as a one-dimensional time series and the resulting amplitudes and phases used to define tidal current ellipses for each constituent. Top contributing constituents were assessed based on current speeds and percent energy contribution to the tidal model solution. The analyses were conducted on the horizontal velocity components averaged vertically over 7 ADCP depth bins (3.5-9.5 mab) using the ‘UTide’ package functions in MATLAB (Codiga, 2011). The length of the time-series allowed a resolution of 67 constituents. Spectral analysis was performed to demonstrate the most energetic motions.

In order to assess the likelihood that the Schulz Bank sponge ground experiences intensified near-bed currents arising from incident internal tides (*sensu* Huthnance, 1989; see also Frederiksen et al.,1992), the ray slope s for an internal wave with the frequency of the dominant semi-diurnal lunar tidal constituent (M_2) was calculated according to:

$$s^2 = \frac{(\sigma^2 - f^2)}{(N^2 - \sigma^2)}$$

where f is the local inertial (Coriolis) frequency ($1.4007\text{x}10^{-4}$ rad s^{-1} at the latitude of the Schulz Bank), N the buoyancy frequency ($9.6\text{x}10^{-4}$ rad s^{-1}; representative value from below the permanent pycnocline) and σ the frequency of the internal tide ($1.4053\text{x}10^{-4}$ rad s^{-1} for an internal tide with semidiurnal lunar M_2 periodicity).

The resulting ray slope (0.68°) was compared to the bottom slopes at the Schulz Bank on the basis of multibeam data (see Figure 4.11, Roberts et al. 2018).

Vertical water displacement was estimated by comparing the CTD profile with the lander time series. The recorded temperature change during one day (ΔT; determined from maximum and minimum temperatures) measured by the lander was compared with the corresponding temperatures and depths in the CTD transect during the same time interval.

4.2.4 Suspended Particulate Matter: C/N analysis, isotope and chlorophyll measurements

Sediment trap material was transferred into silver cups and the material was acidified inside the cups (2 M HCl). $\delta^{15}N$ ($^{15}N/^{14}N=\delta^{15}N$), $\delta^{13}C$ ($^{13}C/^{12}C=\delta^{13}C$) and total weight percent of organic carbon and nitrogen were analyzed on an Elemental Analyzer (EA; Flash 2000) coupled via an open split (Conflo IV, Thermo Fisher Scientific Inc.) to an Isotope Ratio Mass Spectrometer (IRMS; Thermoscientific, Delta V Advantage). For nitrogen stable isotope analyses pure N_2 was used as a reference gas. As a standard for $\delta^{13}C$ benzoic acid and acetanilide was used, while for $\delta^{15}N$ acetanilide, urea and casein were used. Values are reported in per mille relative to air (N_2) and VPDB (C) respectively. For $\delta^{13}C$ analysis a high signal method was exercised including a 70% dilution. Precision and accuracy based on replicate analyses and comparison of standards to their certified values was better than 0.15 ‰ for both $\delta^{13}C$ and $\delta^{15}N$. Chlorophyll-*a* was extracted from sediment trap samples by adding 90% acetone under dark and cool conditions (Wakeham et al., 1993). The concentration was measured by a Fluorescence Spectrometer (F-2500 FL Hitachi) by comparing the sample absorbance to the absorbance of a known chlorophyll-*a* standard at two wavelengths (431.0 and 671.0 nm). Afterwards HCl was added to the sample to break down chlorophyll-*a* and measure degradation products (phaeophytin-*a*). The amount of chlorophyll-a compared to degradation products was then calculated (for details see Holm-Hansen et al., 1965).

4.3 Results

4.3.1 Water column data

At the surface NwAtW was observed and reached depths deeper than 700 m in the basin east of Schulz Bank while the thickness of the NwAtW gradually decreased in extent towards the west (Figure 4.2). East of the summit of Schulz Bank NwArIW is constrained at a depth of 1000-1500 m which is in contrast with the western side where it is also located shallower. NwArIW has a density anomaly between 27.70 and 27.97 kg m^{-3} (Rudels et al. 2002; Figure 2a). NwArIW features a local dissolved oxygen (DO) concentration maximum between 500 to 1000 m water depth (Figure 4.2e). Below about 1000 m and at a density anomaly > 28.05 kg m^{-3} NwDW ($T < -0.5$ °C, salinity of 34.91-34.92) was observed. In 2018, the summit of the seamount was somewhat above the interface between NwArIW and NwDW, where it was observed in 2016 (Roberts et al., 2018). As NwArIW contained more oxygen than NwDW, the oxygen data provide good insight into the characteristics of the interface between the two water masses. Fluorescence maxima were observed at approximately 50 m water depth, declining to < 0.1 µg l^{-1} below (data not shown) as was also observed by Roberts et al. (2018).

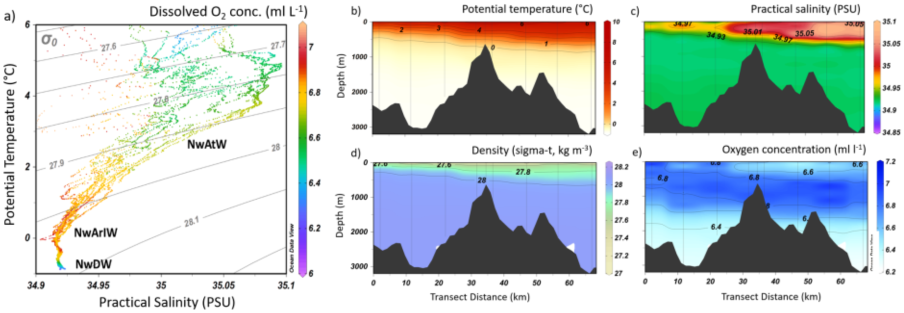

Figure 4.2 a) TS diagram including isobars and water masses indicated. CTD transect cross-sections of b) potential temperature, c) salinity, d) density anomaly (sigma-t), e) DO concentration in August 2018. Vertical lines indicate CTD locations (data plotted using Ocean Data View v.4.7.8; Schlitzer, 2015).

The square of the buoyancy frequency, N^2, is a measure of stratification stability, and was calculated from the density profile at a CTD station on the eastern side of the Schulz Bank. In this case, two maxima in N^2 were observed (Figure 4.3). A strong stratification was found underneath the surface mixed layer at about 50 m and a second, weaker pycnocline was identified at a depth of 500 m (N^2 =0.00001 s^{-2}, Figure 4.3b). The deeper pycnocline was situated at the interface between NwAtW and NwArIW. No N^2 peak was situated at the interface of intermediate and deeper water masses.

The height of internal waves was estimated by comparing temporal and spatial measurements of temperature (see methods). In July 2017 the maximum isopycnal displacement was calculated to be around 210 m (-0.2 to 0.1 °C temperature fluctuations during one day corresponds to 870 and 660 m depth in the water column, respectively).

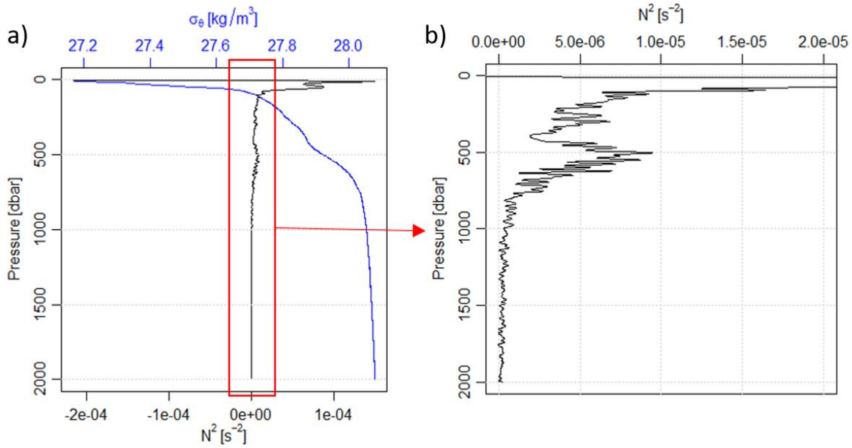

Figure 4.3 a) Buoyancy frequency N^2 (black) and density (blue) of CTD station slightly east of the seamount, b) zoomed-in view of the second peak around 500 dbar.

4.3.2 Lander data

4.3.2.1 Setting

Visual information recorded by the camera on the BOBO lander confirmed that the lander was deployed within an area densely covered with sponges and associated fauna, including anemones, soft corals, tunicates (Figure 4.4) as well as mobile fauna like sea urchins, brittle stars, starfish, and Grenadier fish, which appeared temporarily in some videos. Analysis of the video clips taken by the lander demonstrated that there were no major changes in benthic cover, size of the organisms and species abundance during the deployment. Several events with strong currents were observed, whereby some benthic organisms were affected. For example, anemones and soft corals retracted their tentacles and some anemones, tunicates and larger sponges (likely *Schaudinnia rosea*) were observed to be relocated by the currents (Hanz, 2019).

Figure 4.4 Camera view from the lander showing sponges as well as associated fauna, including anemones, soft corals, tunicates on top of a dense spicule mat. a) Video still captured at the start of the deployment 04.06.2016, b) Video still captured at the end of the deployment at 15.07.2017

4.3.2.2 Long-term records

The most striking observation of the long-term record was that near-bed water temperatures were low throughout the year, varying around a mean of 0 °C (-0.5 to 1°C, Figure 4.5a). The highest temperatures were observed in November-December, while lowest temperatures were recorded in March, April and August (min. of -0.5 °C). Spring and neap tidal cycles were observed in the temperature record from March to August. From September to December temperature increased towards a maximum of 1 °C. In December short-term temperature fluctuations were largest and sometimes were as large as 1 °C during one day, which coincided with high current speed. DO concentrations decreased from October to January until they increased in January (Figure 4.5b). After late March periodical fluctuations of DO concentrations were recorded. The oxygen concentration was varying between 8.4 and 9.1 ml l^{-1}. Fluorescence was in general low and showed only one major peak at the end of May (Figure 4.5c). Turbidity (based on acoustic backscatter measurements) increased from September to October and also during a short period in December (Figure 4.5e). In December, higher turbidity was corresponding to periods of high current speed.

Figure 4.5 Time series of a) temperature, b) oxygen concentration, c) fluorescence, d) optical- and e) acoustic backscatter and f) current speed with 0.3 cycles per day cut-off low-pass filtered current speed, measured by the lander on the summit of the Schulz Bank from July 2016 to August 2017.

The acoustic backscatter recorded constantly elevated values in the benthic boundary layer up to about 6 mab (Figure 4.5e and 4.6). This turbid layer was thinner from April to June (up to 4 mab) and thicker during resuspension events in autumn and winter (over 10 mab, Figure 4.6). Periods of high turbidity in the benthic boundary layer were connected to slow southwestward currents in the first 5 mab (<0.07 m s^{-1}). Water flow at the summit of the seamount exhibited an asymmetry in the tidal transport, with net residual transport in the WNW (290°) direction over the summit (Figure 4.7). Current speed at a depth of 6.5 mab showed daily fluctuations of about 0.4 m s^{-1} around an average of 0.14 m s^{-1}, whereas highest current speeds of up to 0.76 m s^{-1} were recorded in December (Figure 4.5f). Slowest current speeds were related to a southward directed flow.

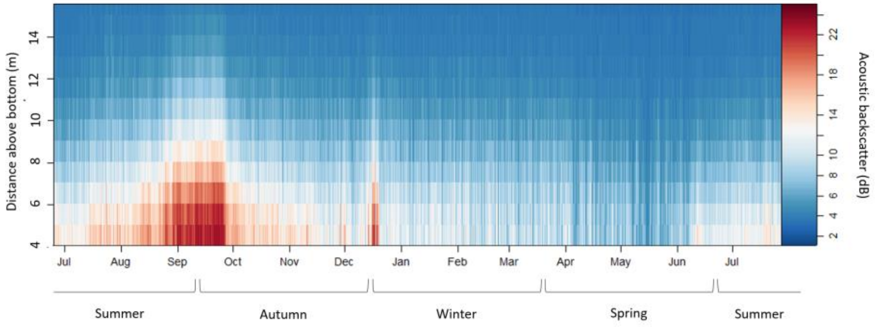

Figure 4.6 Acoustic backscatter intensity at 4-15 m above bottom during the period July 2016 until August 2017.

The optical backscatter sensor at 1 mab recorded only one major turbidity peak in December (Figure 4.5d) and a smaller peak after the peak in fluorescence in May 2017, indicating an increase of smaller particles in the SPM fraction, while mostly larger particles predominate at the end of summer/autumn as shown by the acoustic backscatter record. This was confirmed by comparing the video observations for the different time intervals, with large, slow moving marine snow being observed at the end of summer and fast moving particle aggregates and sponge spicules being observed in winter, specifically during the high current speed events.

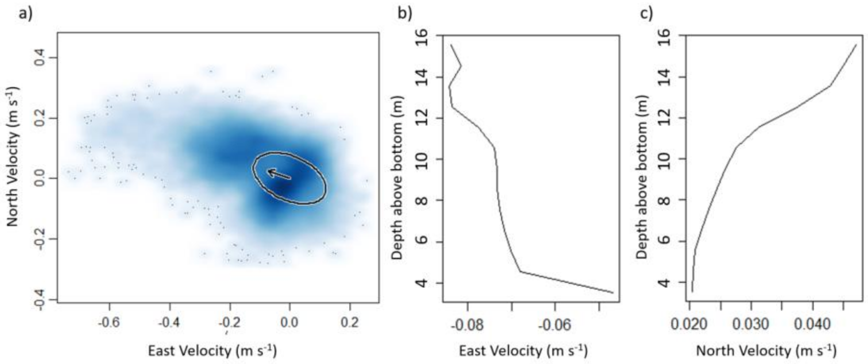

Figure 4.7 a) Time-averaged flow velocity in the horizontal at the Schulz Bank summit during one year with the tidal ellipse and residual current indicated by an arrow, b) Time-averaged eastward flow velocity per depth above the bottom during one year, c) Time-averaged northward flow velocity per depth above the bottom.

4.3.2.3 Tidal analysis

The primary astronomical constituents determined for the observed current signal were the principal lunar semi-diurnal (M_2) constituent, contributing about 38% energy to the tidal model solution, and the luni-solar declinational diurnal (K_1) constituent, contributing 24% energy. This is evident in the kinetic energy spectrum, in which the largest peaks were found at these frequencies (Figure 4.8). The local inertial frequency is very close to M_2 and does not show a separate distinguishable peak. In terms of internal waves, $K_1 < f$ and thus waves are non-propagating or trapped, while $f \leq M_2 \leq N$ permits freely propagating waves with the notion that M_2-waves propagate near-horizontally.

The M_2 satellite constituents H_1 and H_2 (with frequencies very close to that of M_2) were indicating seasonal modulation of the amplitude and phase of the M_2 harmonic. Some variations on seasonal timescales captured by the fitting procedure (including the M_2 modulation and solar semi-annual constituent) may be the result of non-tidal processes (e.g. seasonal changes in stratification and associated changes in tidal currents through internal tides). The compound tide MKS_2 contributes 6.7% energy to the tidal model solution, and thus the nonlinear interaction of astronomical tides that this harmonic represents is relatively important.

The superposition of all 67 constituents in the fit explained 44.3% of the observed variance in the original currents record (i.e., 44.3% tidal variance, *sensu* Codiga, 2011). The mean current components were found to be 0.022 m s^{-1} and -0.067 m s^{-1} for the north and east components, respectively, confirming a mean current of 0.071 m s^{-1} flowing west-northwest (288.2°).

The residual or ‘de-tided’ signal in the horizontal velocity data was computed by subtracting the reconstructed tidal signal (based on the amplitudes and phase lags determined by harmonic analysis) from the original record. It revealed that high current events, particularly those in December, were not well captured by the tidal model (i.e., they remained strongly present in the residual component of the time series and were thus non-tidal in nature) - see the tidally low-pass filtered record in Figure 4.5f. Sub-tidal flows are dominated by a small peak at 0.2 cpd (cycles per day), implying a 5 day periodicity. Larger broadband ‘peaks’ are found at 0.02 cpd (50 day periodicity) and 0.005 cpd (200 day periodicity), see Figure 4.8. The direction of the large-scale sub-tidal flows is mainly east-west (cf. Figure 4.7a), or about a 45° angle with the main ridge of Schulz Bank.

Intensified near-bed currents, caused by internal tides being amplified by the topography, are generated most effectively where the bottom slope is equal to or larger than the ray slope of the internal wave. These intensified currents were calculated to appear in areas where the slope of the Schulz Bank exceeds 0.68°, for the dominant M_2 constituent (for calculation see Methods).

At the lander site, bottom slopes are about 7° and are thus supercritical for M_2 propagating internal waves. The site of Schulz Bank is very close to the turning point latitude for M_2 internal tidal waves, which become evanescent poleward of 74.5°N and thus reflect equatorward. At the turning point latitude, which is only 0.7° poleward of the lander site, internal wave energy is expected to be enhanced (e.g., Munk, 1980) and internal tides propagate near-horizontally like inertial waves.

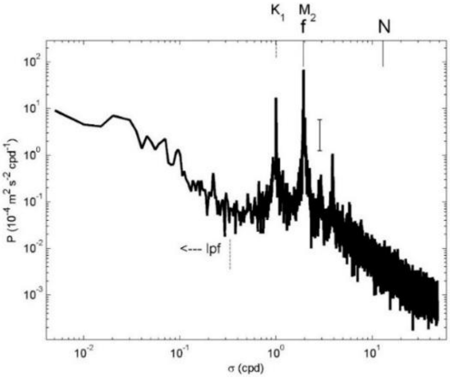

Figure 4.8 Weakly smoothed, about 10 degrees of freedom, average kinetic energy spectrum from currents of bins 2 to 4, with indications at tidal frequencies diurnal K_1 and semidiurnal M_2, inertial frequency f, and buoyancy frequency N. The lower vertical dashed line indicates the cut-off frequency for low-pass filtering.

4.3.2.4 *Short term fluctuations*

In order to determine relationships between physical factors and the resuspension of suspended material, two shorter periods of two days were analysed. Two days in December with large semi-diurnal current fluctuations were compared with two days in July with small diurnal current fluctuations, being essentially the extremes from the entire observation period.

In winter current speeds varied in a semi-diurnal pattern from 0.2 m s^{-1} to 0.7 m s^{-1}. Low current speed was correlated with a southward current direction, high currents with a northwest current direction. Peaks in the acoustic backscatter did not appear to be strictly associated with one part of the tidal cycle. Sometimes turbidity peaks appeared during slow southward current, whereas other turbidity peaks were in line with peaks in current speed (Figure 4.9). In contrast to semi-diurnal tides in winter, during summer a predominantly diurnal current pattern was observed with much smaller semi-diurnal constituents and current maxima less than half those observed for the winter season (Figure 4.9a). Highest currents in summer, as with winter, were in a northwest direction and slower currents in a southern direction. Acoustic backscatter did not correlate with the current speed in summer.

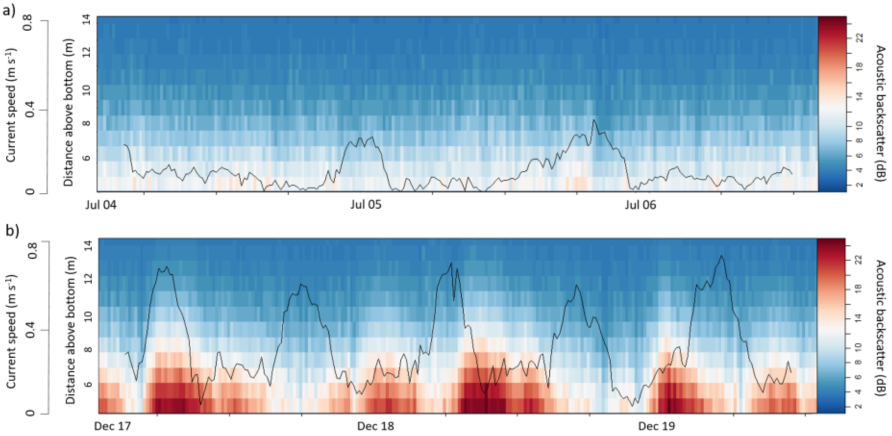

Figure 4.9 Acoustic backscatter from 4-14 mab and current speed at 7.5 m above seafloor (black line) at two days a) in summer, b) in winter.

4.3.2.5 Vertical Fluxes

Vertical downward mass fluxes showed three peaks in September 2016, December 2016 and June 2017 all exceeding 200 mg dry matter m^{-2} day^{-1}, whilst during spring and early summer mass fluxes were below 100 mg m^{-2} day^{-1} (Figure 4.10a). The carbon flux peaked in June 2017, when it exceeded 20 mg C_{org} m^{-2} day^{-1}. Comparing mass and carbon fluxes showed that the 2016 September and December peaks in mass flux were relatively low in organic carbon, indicating resuspension of material as was shown by high backscatter values, high current speeds and in the video footage. This was confirmed by the presence of large amounts of sponge spicules in the collected trap material for these periods. The $\delta^{15}N$ of the sediment trap material increased from 2.2 ‰ in July 2016 to 7.5 ‰ in June 2017 (Figure 4.10b). The $\delta^{13}C$ value was on average -24.88 ‰ (data not shown). Over the same time interval the C/N ratio decreased from 7.4 to 5.2 (Figure 4.10a). The chlorophyll-*a* concentration decreased from about 50 µg l^{-1} in July 2016 to 0 µg l^{-1} in November 2016 and stayed at 0 µg l^{-1} until June 2017 (no value for July 2017, Figure 4.10b). The chlorophyll-*a*/phaeophytin-*a* ratio was highest in July 2016 (2488) and decreased during the sampled time interval.

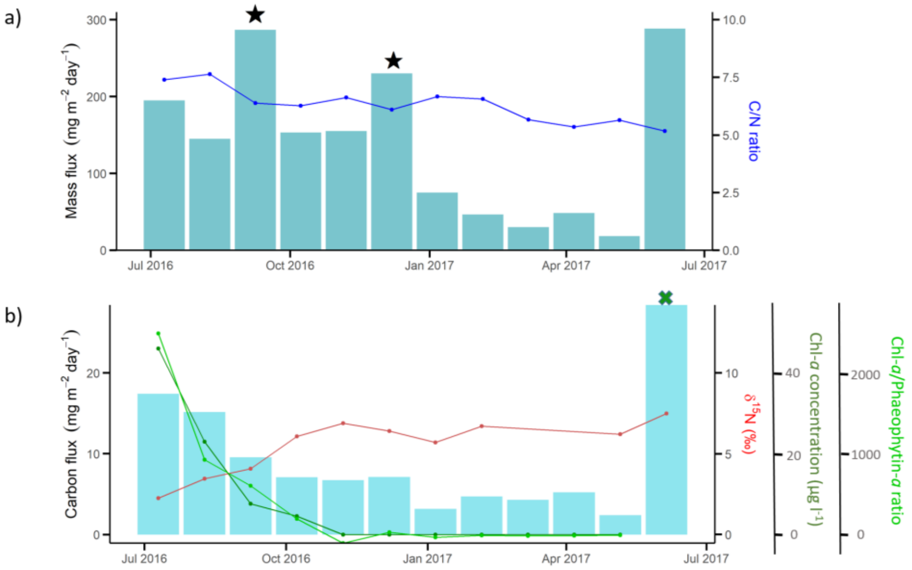

Figure 4.10 a) Vertical mass flux at the sponge ground and C/N ratio b) Carbon flux, δ^{15}N, chlorophyll-a concentration and chlorophyll-a/phaeophytin-a ratio of the sediment trap material from July 2016 to July 2017 in 30-day intervals. Stars indicate resuspension events; green cross indicates missing chlorophyll-a value.

4.4 Discussion

Deep-sea sponge grounds are hotspots of biological activity, yet their environmental requirements, in terms of hydrodynamics and food supply mechanisms are so far poorly known. This study shows the first observations of the long-term near-bed environmental conditions at a sponge ground in the Arctic. It provides insight into the variability of physical and biological conditions deep-sea sponges are experiencing throughout a year.

4.4.1 Temperature

Bottom water temperatures on the Schulz Bank summit were around 0°C during the whole 13 months of observations, which might have important implications for the benthic communities. In general low temperatures slow chemical reactions and reduce enzyme activities (Hochachka and Somero, 1968). This has a major effect on the functioning of (benthic) organisms as it controls metabolic rate and physiological processes slow down with decreasing temperature (King and Farner, 1961; Strand et al., 2017). A slower metabolism reduces energy demand in most aquatic invertebrates, where respiration rates are roughly halved with every 10 °C decrease (Q_{10} temperature coefficient = 2-3, e.g. Coma, 2002). It is known that benthic species can adapt to cold environments, which compromises extrapolation of the metabolic rates of tropical or temperate species down to cold environments (Somero, 1998). Still, the cold environment might play a role in the survival of species in this food-deprived environment due to reduced metabolism, whereas food reduction itself might also decrease the metabolic state like for example observed in fish (Yang and Somero, 1993). The upper temperature range for deep-sea sponge occurrences is not known for most species, whereas for example *Geodia barretti* (characteristic for boreal grounds) is known to survive in temperatures of up to 12 °C (Strand et al., 2017). Our long-term record showed that deep-sea sponges in Arctic grounds thrive at temperatures at least 4 °C lower than the reported temperature range of, for instance, CWCs (4-12 °C, Dodds et al., 2007; Freiwald, 2002). *Pheronema carpenteri*, a relatively well-known glass sponge, has been found over a broad temperature range of 2.7-20.9 °C (Howell et al., 2016). These thresholds imply that sponges could be more prevalent in the deep sea compared with CWSs.

4.4.2 Hydrodynamics

Density gradients play an important role in mixing processes in the ocean interior. In general, less mixing is found in a highly stratified water column. Nevertheless, baroclinic tidal waves are able to propagate along density gradients inside the ocean interior. The ability of internal waves to propagate freely depends on the turning point latitudes. At the latitude of the Schulz Bank they can only exist at a semi-diurnal frequency since diurnal internal tides cannot exist as freely propagating waves at this latitude (Lavelle and Mohn, 2010; Robertson et al., 2017). However, around Rockall Bank trapped diurnal tidal waves have been demonstrated to considerably contribute to turbulent mixing over coral mounds (van Haren et al., 2014; Cyr et al., 2016). The large diurnal tidal signal observed in our data suggests a similar mechanism is at work around Schulz Bank. In addition, the latitude of Schulz Bank is so close to the turning point latitude of M_2 internal tides that enhancement of internal tidal energy is expected (Munk, 1980).

If propagating internal tidal waves impinge on topographic features like seamounts they can be reflected or their energy can be converted into turbulence depending on the properties of the obstacle (Jalali et al., 2017). Turbulence is created by internal waves propagating upslope and interacting with the downslope flow, which remains from previous waves, resulting in wave breaking (Taylor, 1993). This can produce high local turbulence around the seamount summit (van Haren et al., 2017). At the Schulz Bank we observed strong semi-diurnal and diurnal tides which are likely the origin for high internal wave breaking, increasing local mixing and turbulence. Intensification and amplification of both turbulence and mixing at the Schulz Bank is expected to appear in areas where the bed slope is steeper than that of semi-diurnal internal tidal wave slopes of around 0.68° (Figure 4.11). Unfortunately, there was not enough fauna distribution data available to correlate the steeper slopes of the summit with an increased abundance of benthic organisms. However, it is known that steep slopes on the north-eastern summit are an area of high species abundance (Meyer et al., 2019).

We established the characteristics of the internal waves at Schulz Bank by comparing temporal and spatial measurements (see Methods): isopycnal displacements are up to >200 m and peak near-bed horizontal current velocities are up to 0.7 m s^{-1}. These velocities are much higher than found at other biologically rich Mid-Atlantic seamounts (van Haren and Gostiaux, 2012; van Haren et al., 2017) and are comparable to currents associated with internal waves at the Hawaiian ridge, which were observed to be up to 300 m in displacement (Rudnick et al., 2003), or over a cold-water coral mound at the Rockall bank, which were more than 120 m high (van Haren et al., 2014). The maximum current speeds at Schulz Bank were close to those of internal waves observed in the South China

Sea, where horizontal velocities of up to 1 m s^{-1} were found producing massive overturns of up to 500 m, which are expected to be amongst the most powerful in the world (Alford et al., 2015). Resulting turbulence in such regions can be >1000 times that of the open ocean (van Haren and Gostiaux, 2012), which is also suggested to be beneficial for CWCs (Mienis et al., 2012). Video recordings taken during highest current speed events in winter at Schulz Bank showed that these might be close to the maximum that sessile benthic fauna can endure, with some individual sponges as well as anemones already being detached from the bottom and transported laterally (Hanz, 2019).

Mixing processes due to turbulence and the vertical displacement of water with different properties are likely to be an essential driver for the local benthic fauna since they supply nutrients, oxygen, and particulate organic matter (Duineveld et al., 2004). Comparison of the baroclinic tides with SPM supply to the sponge ground in this study indicated that tidal waves might provide an alternative route for delivering nutrients from deeper water layers and possibly even fresher SPM from shallower water masses as a consequence of enhanced downward currents on short-time scales as was also observed near CWCs (Duineveld et al., 2007). Once brought into suspension by turbulent mixing, the suspended matter will be advected horizontally by the larger-scale flows. These flows are, on average, directed approximately westward over Schulz Bank. Since we did not study potential sources further away from Schulz Bank, we have no quantitative measure of the supply of organic matter to the Schulz Bank from the east. Mixing around the seamount is likely to deliver water column bacteria towards the sponge communities on the summit, which act as a food source. This process has been observed to influence the microbial community structure up to several hundreds of meters above the summit (Busch et al., 2020).

Hydrodynamic processes can also trap food particles above the seamount summit. Earlier modelling studies (Chapman and Haidvogel, 1992) showed that anti-cyclonic circulation patterns (*Taylor caps)* or *trapped waves* in the case of periodically alternating flow can arise over the summit of isolated seamounts (Haidvogel et al., 1993). These have the potential to trap sinking organic material (Mourino et al., 2001; Vilas et al., 2009), but can also affect the microbial community composition (Busch et al., 2020). Roberts et al. (2018) expected possible transient Taylor caps at the Schulz Bank. Calculations in this study with an updated larger dimension of the seamount (h= 1.9 km, L= 22 km, H= 2460 m, U= 0.14 m s^{-1}) confirms the possibility of a Taylor cap (R_o= 0.045, δ= 0.77, S= 2.55, f= 1.4 x 10^{-4} rad s^{-1}, N= 3.2 x 10^{-3} s^{-1}, calculations like stated in Roberts et al. 2018). However, evidence for a Taylor cap in the form of clear isopycnal doming, higher turbidity or increased fluorescence above the summit, as shown in Roberts et al. (2018), were not detected by the CTD transect in 2018. This likely reflects the coarse spatial resolution of the CTD transect or the timing of the CTD transect not corresponding with the main bloom period or with a Taylor cap that is transient in nature.

4.4.3 The reef effect

Benthic food availability also depends on smaller-scale processes entraining food resources in the BBL (Boudreau and Jorgensen, 2001). Particulate matter was continuously resuspended above the sponge ground as indicated by a turbid BBL throughout the year. Short-term observations showed that this BBL experiences periods where the extent of the turbidity in the BBL decreases. These periods are likely essential to replenish the BBL with new suspended (organic) matter as well as dissolved (organic) matter, bacteria (Busch et al., 2020), and nutrients, which all serve as a food source for the benthic fauna. Roberts et al. (2018) showed that water in the BBL is also replenished by water with higher DO concentration during so-called jump-relax events.

In the 5 m immediately above the bottom, currents interact with the “roughness” of the bottom created by the 3D structure of the benthic fauna and sponges (Witte et al., 1997), which creates additional small-scale turbulence, as observed at CWC reefs (Guihen et al., 2013; Mienis et al., 2019). This turbulence may play a role in the trapping and accumulation of particles in the lower benthic boundary layer. Significant differences between the current speeds below and above 5 mab (Figure 4.6) as well as in the long-term permanent turbid layer from 2-6 mab in the acoustic backscatter record (Figure 4.5) are indicating the presence of this reef effect at the Schulz Bank sponge ground.

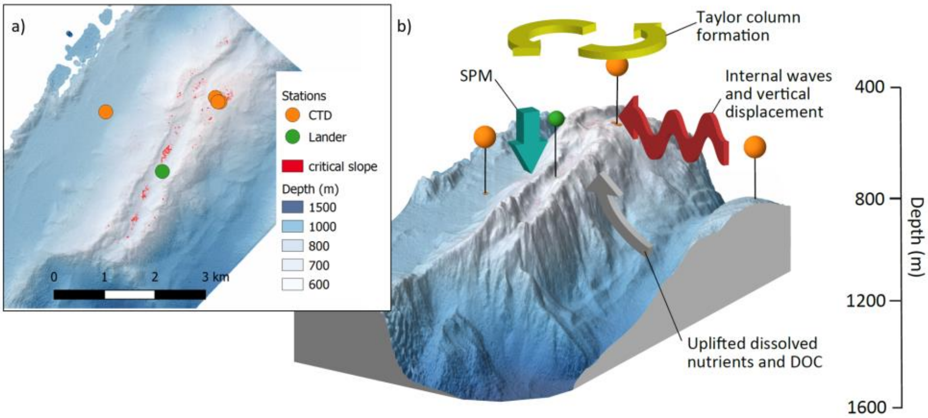

Figure 4.11 a) Summit of the Schulz Bank from multibeam echosounder data (5 m resolution) with critical slope areas for semi diurnal internal waves marked in red. The slopes were calculated over a 5x larger neighbourhood of cells to better visualize areas of critical slope, b) 3D representation of the Schulz Bank summit with dominant hydrodynamic features and food supply mechanisms indicated.

4.4.4 Fluxes of organic matter

One peak in fluorescence was observed at the end of May at the Schulz Bank summit corresponding with a high flux of organic matter. The presence of only one bloom period is typical for the Arctic region (Sverdrup, 1953). At high latitudes, the spring bloom occurs late without a subsequent fall bloom, depending on the onset of the stabilization of the upper water layer and the limited sun elevation (Wassmann et al., 1991). The Arctic summer phytoplankton bloom at the surface delivered OM of relatively high nutritional quality to the Schulz Bank sponge ground in July 2017 and especially June 2016, when $\delta^{15}N$ reached its lowest value and chlorophyll-*a* values were highest, indicating the presence of relatively fresh phytodetritus at the sponge ground (Figure 4.10). However, the C_{org} flux throughout the year was in general low during all other months. After the 2016 bloom period the C_{org} flux decreased to reach a minimum just prior to the onset of the next bloom period in June 2017. The June 2017 peak in vertical flux in our sediment trap does not seem to be composed of sinking fresh primary production because of the relatively high $\delta^{15}N$. More likely the material is derived from faecal pellets of copepods (*Calanus* sp.) which contain degraded phytodetritus (Nöthig and von Bodungen, 1989). According to Bathmann et al. (1990) copepod abundance decreases significantly after the faecal pellet pulse in June/July due to insufficient food resources and small quantities of unprocessed organic material can sink to the bottom. This would explain the relatively fresh organic matter in our sediment trap in months following the July 2016 peak in C_{org} flux (Figure 4.10). In September light intensity in the Arctic is insufficient for substantial primary production, inhibiting a second bloom and therefore there is no further delivery of fresh material to the sponge ground. After the summer period more processed (i.e. refractory) organic material was observed in the sediment trap, based on increasing $\delta^{15}N$ values and decreasing chlorophyll-*a* content, which is most likely derived from resuspended or advected sediments. Resuspension events were observed in our data when turbidity increased in the BBL from that time onwards (Figure 4.6). High turbidity events in winter are produced by resuspension of material from the bottom, which is confirmed by the fact that a large amount of spicules and a low carbon content was found in the sediment trap at these times. The combined data suggest that the benthic community on Schulz Bank depends on the food pulse of fresh material in summer refuelling the BBL with high-quality SPM, which becomes progressively more refractory and depleted over the remainder of the year.

The food delivered to the sponge ground has likely no allochthonous source since no landmasses are close enough to deliver terrestrial organic material. Terrestrially derived organic material has a higher C/N ratio (>10) and generally shows a depleted $\delta^{13}C$ signal around -27 ‰ (Knies and Martinez, 2009), compared to the values recorded here, which were showing a marine origin (C/N <10 and $\delta^{13}C$ of <26 ‰).

There are so far no data available on community carbon uptake by the sponge ground on Schulz Bank to match with the C flux measured here. Taking the estimated carbon demand of a deep-water glass sponge reef (ca. 160 m depth, ~10°C) at the Canadian coast (1800-4100 mg C m^{-2} day^{-1}, Kahn et al. 2015), the carbon input at Schulz Bank during the bloom period with the highest carbon input would provide approximately <1 % of the required carbon demand. In the Canadian sponge reefs C consumption was much higher compared to the carbon flux (460 mg m^{-2} day^{-1}). However, this estimation does not include the potential changes or adaptations in metabolism depending on depth and temperature. Even though it is difficult to compare both ecosystems, it is likely that the low carbon flux will at no time cover the carbon demand of the densely covered sponge ground of the Schulz Bank even if the actual demand is much lower than in sponge grounds of the Canadian coast. This is based on sediment trap data which presumably underestimates the vertical flux (Baker et al., 1988), which implies that the assumed carbon deficit is slightly smaller. Therefore, it is to be expected that the availability of dissolved organic matter (de Goeij et al., 2008), pelagic bacteria (Reiswig, 1975; Yahel et al., 2006) and chemosynthesis by symbiotic bacteria and archaea (Hentschel et al., 2006; Radax et al., 2012a) will play an important and supplementary role in meeting the food supply demands of the Schulz Bank sponge community (Busch et al., 2020). To enhance these processes the hydrodynamic regime will play an important role. Internal wave actions will transport water from deeper areas with higher dissolved nutrient concentrations (PO_4, NO_x, Si) towards the summit with each tidal cycle (Roberts et al., 2018). This is detectable by the temperature records measuring water from deeper or shallower regions with a difference of up to 1 °C and the calculated vertical displacement of > 200 m water depth. This can fuel the bacterial and Archean communities at the sponge ground, as well as the sponges and their own bacterial communities directly (Busch et al., 2020; de Goeij et al., 2008; Radax et al., 2012b). Turbulence at the seamount summit due to interaction of internal waves with the seamount topography is proposed as the essential factor allowing a constant replenishment of both resources (resuspended SPM and inorganic nutrients) in the BBL, resulting in a dense coverage of filter-feeding and microbially-active sponges.

4.5 Conclusion

The 1-year dataset on near-bed environmental conditions showed that sponges can withstand temporarily high current speeds (~0.7 m s^{-1}), live in temperatures around 0°C and can survive in an environment which likely does not receive sufficient food from surface waters to be able to sustain such a dense benthic ecosystem. Although we do not have quantitative evidence of the suspended matter and nutrient sources, larger-scale flows may have transported these from the east and greater depths. A major finding was that the sponge ground is located at the interface between two water masses, where strong internal tidal waves can propagate and interact with the bottom topography. Being near the M_2-turning point latitude, enhanced semi-diurnal (as well as trapped diurnal) internal tides slosh back and forth against the steep slopes causing wave breaking. This creates mixing and turbulence on the seamount summit, delivering and exchanging water with different beneficial characteristics from above and below, thereby supplying the benthic ecosystem with new resources (e.g. particulate and dissolved matter) within a semi-diurnal tidal cycle.

4.6 Acknowledgements

This research has been performed in the scope of the SponGES project, which received funding from the European Union's Horizon 2020 research and innovation programme under grant agreement No. 679849. This document reflects only the authors’ views and the Executive Agency for Small Medium-sized Enterprises (EASME) is not responsible for any use that may be made of the information it contains. Daniel Codiga is thanked for his advice on applying the MATLAB package UTide. FM is supported by the Innovational Research Incentives Scheme of the Netherlands Organisation for Scientific Research (NWO-VIDI grant no. 0.16.161.360).

4.7 Data availability

Lander and CTD data are available in PANGAEA (Hanz, 2021). The lander video data are available in the NIOZ data repository (Hanz et al.2019).

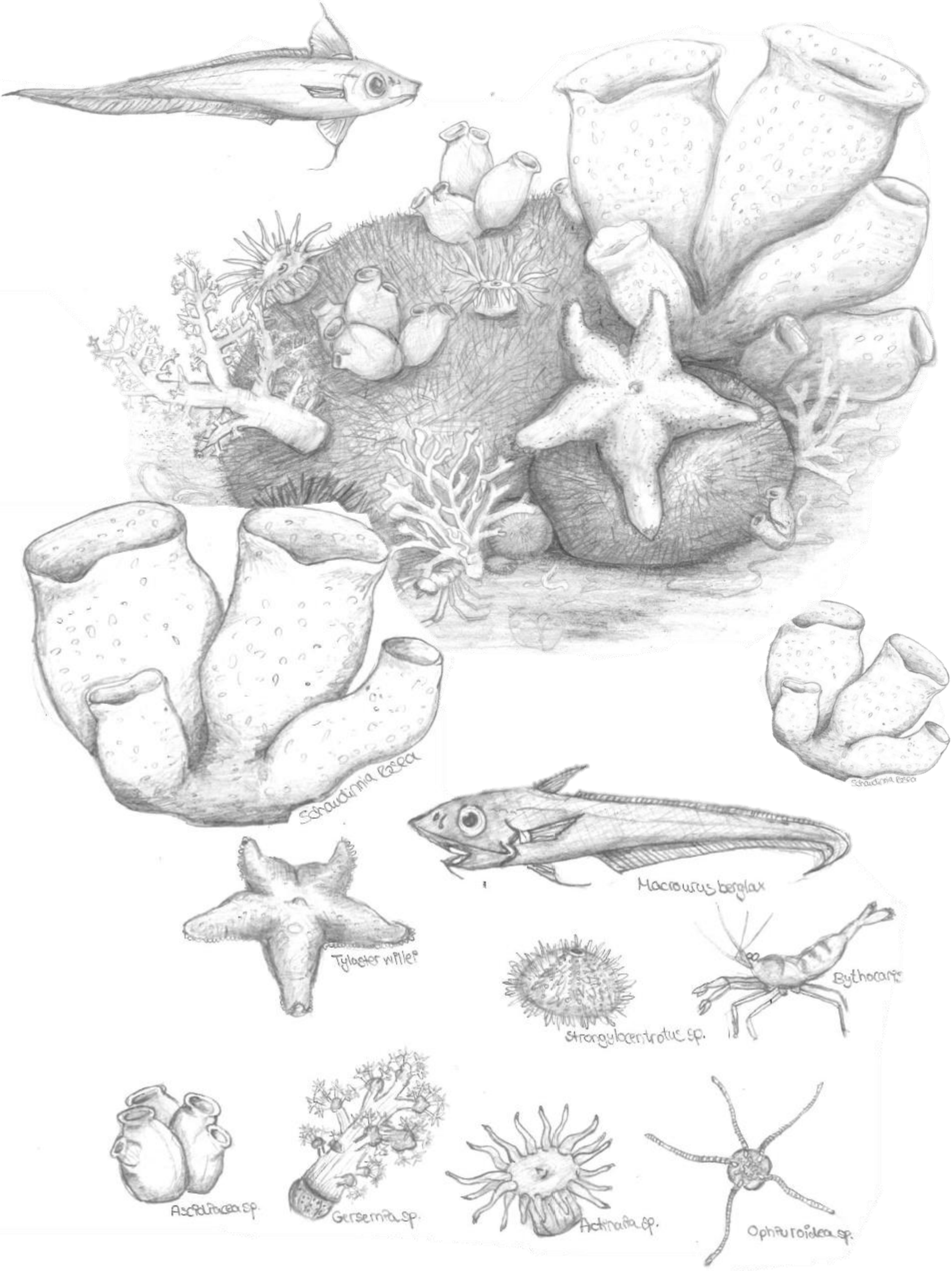
Schaudinnia rosea
Schaudinnia rosea
Macrourus berglax
Tylaster willei
Bythocaris
Strongylocentrotus sp.
Ascidiacea sp.
Gersemia sp.
Actinaria sp.
Ophiuroidea sp.

Chapter 5

Are sponges at the top and bottom of the food web in a benthic deep-sea biological hotspot?

Ulrike Hanz, Philip Riekenberg, Anna de Kluijver, Marcel van der Meer, Jack J. Middelburg, Jasper M. de Goeij, Martijn C. Bart, Erik Wurz, Ana Colaço, Gerard Duineveld, Gert-Jan Reichart, Hans-Tore Rapp† and Furu Mienis

Submitted to Functional Ecology

Picture to the left: Megafauna from the Schulz Bank seamount

Abstract

Sponge grounds are hotspots of biomass and biodiversity in the otherwise barren deep sea. It remains unknown how these ecosystems can thrive in such food limited environments since organic matter settling from the surface ocean covers only small parts of their carbon demand. In this study, the food-web interactions and potential food sources of a North Atlantic deep-sea sponge ground were identified by bulk and compound-specific stable isotope analysis of amino and fatty acids. The elevated bulk δ^{15}N values of sponges with relatively low abundance of associated microbes (LMA) is in line with a position at the top of the benthic food web, while the relatively high δ^{13}C and intermediate δ^{15}N values of high microbial abundance (HMA) sponges suggest considerable reliance on an alternate resource. Trophic positions based on amino acid δ^{15}N values placed HMA sponges at the base of the food web. Fatty acid analysis of δ^{13}C indicated transfer of sponge derived organic matter to the wider food web. Our results show that sponges drive both bottom-up and top-down processes, shunting organic carbon to higher trophic levels that would otherwise be inaccessible to other fauna. In this way, sponges are key to the sustenance of thriving deep-sea ecosystems.

5.1 Introduction

Sponges are ubiquitous in the marine environment and are among the most common megafaunal organisms in the deep sea (Tabachnick et al., 1994). They can appear solitarily or in high abundances, forming extensive sponge grounds which are found globally along continental shelves, slopes, seamounts, mid-ocean ridges and canyons (Maldonado et al., 2017). Deep-sea sponge communities are represented by demosponges (Demospongiae) and glass sponges (Hexactinellidae), which form 3-dimensional structures that can serve as substrate, refuge, and feeding ground for associated fauna as well as sponges themselves (Maldonado et al., 2017). Therefore, deep-sea sponge grounds have been recognized as hotspots of biodiversity and biomass (Buhl-Mortensen et al., 2010).

Sponges can filter up to 24m^3 seawater per kg sponge per day (Maldonado et al., 2012, Pham et al., 2019) and thereby transfer energy from the pelagic to the benthic environment. They efficiently take up particulate food (Reiswig, 1971; Yahel et al., 2007) as well as dissolved food, as shown for many shallow-water sponges (Yahel et al., 2003; de Goeij et al., 2008) and recently also for deep-sea sponges (Bart et al., 2021). Sponges on tropical coral reefs were shown to convert dissolved organic matter (DOM), which is generally not available for other heterotrophic organisms, to particulate detritus that is available to higher trophic levels, a pathway named the sponge loop (De Goeij et al., 2013). Sponges are also established as sources of dissolved inorganic nutrients to their environment (Keesing et al., 2013), but their influence on the wider food web is not yet known. In addition, top-down controlled resource recycling through sponge predation has been hypothesized as an alternative sponge loop pathway on coral reefs (Pawlik and McMurray 2019).

Nevertheless, it remains unclear how dense sponge grounds can thrive in the (particulate) food limited deep sea since the flux of suspended particulate organic matter (SPOM) from the surface ocean decreases rapidly with depth (Suess, 1980). A mismatch between SPOM influx and carbon demand has been observed at the

Canadian shelf, where sponges require seven times more carbon than is delivered by the vertical flux alone (Kahn et al., 2015). Uptake of DOM may resolve the imbalance between carbon delivery and consumption of SPOM (Maldonado et al., 2017) since DOM is by far the largest reservoir of organic C and N in the ocean (Benner et al., 1992).

Sponges are known to contain an abundant and diverse community of microbial symbionts like bacteria, fungi, yeast and archaea (Hentschel et al., 2003; Taylor et al., 2007; Webster and Taylor, 2012). Based on differences in these symbionts, sponge species are classified as high microbial abundance (HMA) sponges or low microbial abundance (LMA) sponges (Vacelet and Donadey, 1977; Hentschel et al., 2006). In HMA sponges, symbionts account for up to 60% of the biomass and have 2–4 orders of magnitude higher microbial concentrations than the surrounding seawater. LMA sponges contain much lower microbial abundances at concentrations similar to that of the ambient seawater. The turnover of DOM is generally considered to be mediated by heterotrophic microbes through the well-established microbial loop (Kirchman, 1994). Therefore, sponge-associated microbes are often suggested to play an important part in the ability of sponges to utilize DOM, but both HMA and LMA species have been found to process DOM in shallow and deep waters (de Goeij et al., 2017; Bart et al., 2021).

The full potential of sponges as drivers of carbon cycling in deep-sea ecosystems, nor their actual place in the food web, have been established to date. It remains challenging to study the specific function and contribution of sponges to the food web due to their use of multiple resources, their poorly characterized feeding strategies and the difficulty quantifying the fluxes to process these resources.

Single analyses, like bulk nitrogen and carbon isotope analyses, have been shown to provide an incomplete overview of the role of sponges in the food web. Therefore, in this study we have combined bulk and compound specific stable isotope analyses with FA biomarker analysis to elucidate the benthic food web of a sponge ground situated on an arctic seamount, the Schulz Bank. Specifically, we aimed (1) to unravel the food sources supporting a deep-sea sponge ground and (2) to characterize the role of sponges in providing food to the associated fauna.

5.2 Material and Methods

5.2.1 Study area

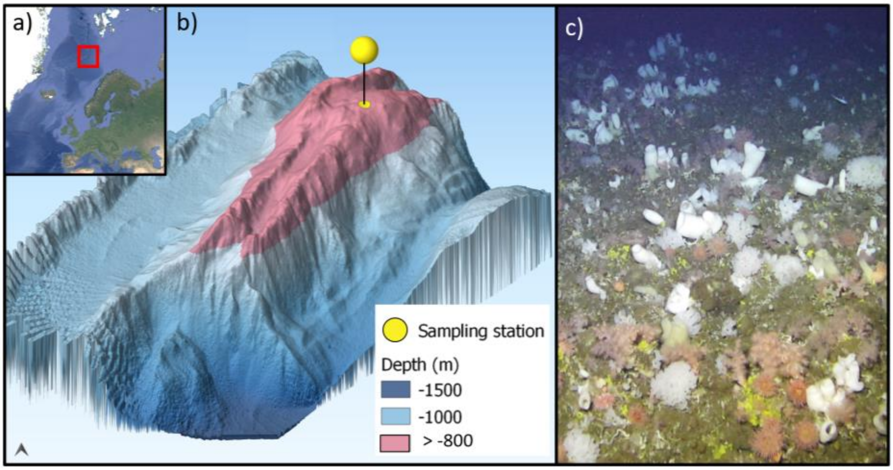

Figure 5.1 a) Overview map with the Schulz Bank indicated, b) The Schulz Bank summit, with the red area depicting the area with highest sponge abundances (Roberts et al., 2018), c) The summit is covered by a dense accumulation of sponges and associated fauna.

The sponge ground is situated on the summit of Schulz Bank (73°50’N, 7°34’E, Figure 5.1), which is part of the Arctic Mid-Ocean Ridge. The highest density of sponges and associated fauna was found on the summit between 600 and 700m water depth, forming a reef-like ecosystem (Roberts et al., 2018). The benthic fauna is growing on a thick sponge spicule layer and is dominated by hexactinellids, demosponges, ascidians, cnidarians, echinoderms and demersal fish species (Meyer et al., 2019). The primary structure-forming hexactinellid species are white, vase-shaped sponges like *Schaudinnia rosea* (LMA) (Figure 5.1c), while the demosponges are mainly represented by brown-white, round, massive sponges, like *Geodia* sp. and *Stelletta* sp. (HMA).

5.2.2 Sampling

Samples were collected during three research cruises (2016-2018) with the RV G.O. Sars. During 2016-2017 a lander was deployed at 663m inside the sponge ground for a period of one year, which was equipped with a sediment trap collecting the suspended (organic) particle flux ($SPOM_{trap}$; Roberts et al., 2018). Fauna samples were collected from within the sponge ground in 2018 during dives with the ROV ÆGIR 6000 and using an Agassiz trawl. We aimed to collect as many trophic levels as possible and divided fauna into their expected trophic positions (supplementary material, Table S5.1). Smaller fauna were collected and sampled as a whole animal, whereas for larger fauna different tissue types were sampled. Muscle tissue or complete arms/legs of the organism were preferentially sampled, depending on the size of the animal. For sponges, 2x2 cm cubes of tissue were collected from different parts of the body in order to distinguish potential tissue-related effects. As a primary food resource $SPOM_{CTD}$ was collected with a CTD rosette system at the surface (~40 m depth) and ~10 m above bottom. 10 l of bottom water and 5 l of surface water were filtered over pre-weighed, combusted (4 h at 450°C) GF/F filters (Whatman^{TM}, ~0.7µm) and kept frozen until further analysis. Additional water samples for DO13C measurements were collected from surface, intermediate and near bottom depths (2 and 0.8 m above bottom (mab). For this water was filtered over pre-combusted GF/F filters and collected in pre-combusted amber glass EPA vials. The samples were acidified with six drops of HCl (12 M) to remove inorganic C and stored in the dark (4°C).

5.2.3 Elemental and stable isotope analysis

All samples were freeze-dried before further analyses. Faunal, sediment and $SPOM_{trap}$ samples were homogenized, transferred into silver cups (8x5mm Elemental Microanalysis) and were acidified in the cups (2 mol l^{-1} HCl). $SPOM_{CTD}$ filters for particulate organic carbon

(POC) isotope analysis were exposed to a vapor of concentrated hydrochloric acid (2mol l^{-1} HCl) to remove inorganic carbonates. Samples for total nitrogen (N) isotope analysis were not acidified, but directly transferred to pressed tin capsules (12 x 5 mm, Elemental Microanalysis). The concentration and isotopic composition ($\delta^{15}N$, $\delta^{13}C$) of C_{org} and N_{total} were analysed by a Delta V Advantage isotope ratio MS coupled to a Flash 2000 Elemental Analyzer (EA-IRMS) via a Conflo IV interface (Thermo Fisher Scientific Inc.). Benzoic acid and acetanilide were used as standards for $\delta^{13}C$, and acetanilide, urea, and casein for $\delta^{15}N$. Precision based on replicate measurements were ± 0.15‰ for both $\delta^{13}C$ and $\delta^{15}N$. Differences between trophic levels were tested with a Tukey multiple pairwise-comparisons in R (R Studio 1.2.1335). The ^{13}C isotopic signature of dissolved organic carbon (DOC) was analysed using a high temperature combustion TOC (IsoTOC, Elementar GmbH, Langenselbold, Germany). Before and after the samples a set of two international standards (IAEA-600 and IAEA-CH6) were measured to calibrate ^{13}C values. A linear regression between the expected and the measured values of the standards was used to calibrate all samples vs VPDB (^{13}C; further description in the supplementary material 5.11.1).

5.2.4 Fatty acid analysis

Fatty acids (FAs) were used as compound-specific source biomarkers to unravel trophic interactions. Sponges can elongate carbon chains and introduce distinct double bonds (Gillan et al., 1988; De Goeij et al., 2008; Koopmans et al., 2015), resulting in specific long-chain FAs ($>C_{24}$) in Demosponges (Thiel et al., 1999) or C_{28} and C_{32} polyenoic FAs in Hexactinellidae (Thiel et al., 2002).

Total lipids were extracted from all samples except $SPOM_{trap}$. Between 10–50 mg fauna and spicule mat sample, 60–100 mg sponge sample, 150 mg sediment and $SPOM_{CTD}$ were extracted according to the protocol of de Kluijver (2020). An aliquot of the total lipid extract of sponges was separated into different polarity classes, from which the phospholipid (PL) fraction was further analysed.

FA methyl esters (FAMEs) were analysed in ethyl-acetate using gas chromatography with an apolar column (Agilent, Cp-sil 5 CB 25m x 0.32 mm x 0.12 µm) coupled to FID for quantification and MS for identification and isotope ratio mass spectrometer (IRMS) for $\delta^{13}C$ analysis. Gastropod, soft coral, sea urchin and starfish had very high sterol concentrations, hence the FAME fractions were purified (de Kluijver 2021). $SPOM_{surfaceCTD}$, anemone and soft coral containing wax esters were excluded from FA analysis. Since fatty acids can be metabolized and transformed by organisms only the relative abundance rather than absolute amounts were considered. The $\delta^{13}C$ values of *Geodia* sp. FAMEs represent an average of TLE and PL fraction, since those isotopic results were similar (average difference 0.7-1.1‰).

5.2.5 $\delta^{15}N$ analysis of amino acids (AA)

The compound specific AA analysis relies on the different processing of amino-nitrogen groups (Chikaraishi et al., 2009; O'Connell, 2017): trophic AAs (Asparagine, Glutamine, Alanine, Isoleucine, Leucine, Valine, Proline), source AAs (Glycine, Serine, Phenylalanine, Tyrosine, Lysine) and metabolic AA (Threonine; O'Connell 2017). The $\delta^{15}N$ value of source amino acids reflect the isotopic composition of N at the base of the food web since they fractionate minimally during metabolism resulting in only a small increase in $\delta^{15}N$ values with increased trophic level. Trophic amino acids, in contrast, undergo transamination and deamination processes and will increase in ^{15}N values with each trophic transfer relative to the source AAs (Chikaraishi et al., 2009).

Dried and homogenized tissue underwent acid hydrolysis followed by derivatization into n-pivaloyl isopropyl esters. These esters were subsequently analysed via gas chromatography-combustion isotope ratio mass spectrometry using a Thermo Trace 1310 GC attached to a Delta V Advantage isotope ratio mass spectrometer via an Isolink 2. Further details of sample preparation and the ramp and temperature schedule used during analysis are discussed in Riekenberg et al. (2020).

Compound-specific stable isotope analysis (CSIA) of individual amino acids provides independent information on the trophic level as well as the δ^{15}Nbaseline and shows the relative influence of δ^{15}Nbaseline and trophic fractionation of consumer δ^{15}N values (McClelland and Montoya, 2002; McMahon and McCarthy, 2016).

The trophic position (TP) estimation is based on the offset between the trophic AA glutamic acid (GLU) and source AA phenylalanine (PHE), and values of 7.6 and 3.4 for trophic discrimination factor and β to describe the increased ^{15}N values due to metabolism of GLU relative to PHE with each trophic transfer (McClelland and Montoya, 2002; Chikaraishi et al., 2007; O'Connell, 2017).

To assess microbial re-synthesis of amino acids, the summed variance (ΣV) value was calculated (McCarthy et al., 2007; Calleja et al., 2013) to examine the extent of heterotrophic reworking of proteinaceous material due to a range of processes including hydrolysis, uptake, de novo synthesis, salvage of AAs into new proteins and catabolism.

Details on the calculations of the TP and microbial re-synthesis can be found in the supplementary material (see 5.11.1).

5.3 Results

5.3.1 Stable carbon and nitrogen isotopes

The analysis of SPOM$_{\text{surfaceCTD}}$ showed an average δ^{15}N of 0.6 ± 0.54‰ and δ^{13}C of -26 ± 0.35‰ (mean ± SD throughout text, Figure 5.2). Isotopic ratios of SPOM$_{\text{CTD}}$ increased with depth to 2.5 ± 0.84‰ for δ^{15}N and -24.9 ± 0.8‰ for δ^{13}C. SPOM$_{\text{trap}}$ had δ^{15}N values between 2.2 and 7.5‰ with an average of 5.7‰, depending on the month of collection. The average δ^{13}C ratio of trap material (-24.9 ± 0.93‰) did not differ from that of the SPOM$_{\text{bottomCTD}}$ ($p=1$). Bulk tissue of suspension feeding fauna (primary consumers), such as tunicates, brittle stars, soft corals, small crustaceans, and anemones showed average δ^{15}N values of 10.1 ± 0.4‰ and δ^{13}C of -23 ± 0.4‰. This corresponded to trophic enrichment factors of about 5.1‰ for δ^{15}N and 2.6‰ for δ^{13}C compared to the presumed food source, here taken as $\text{SPOM}_{\text{bottomCTD}}$. The $\delta^{15}N$ values of HMA sponges (*Geodia* and *Stelleta* sp.) were similar to those of other suspension feeders (primary consumers, $p=0.9$), whereas the $\delta^{13}C$ ratio of HMA sponges was significantly enriched (about 4‰; $p=<0.001$). Secondary consumers, such as polychaeta, sea urchins, fish, and starfish had average $\delta^{15}N$ and $\delta^{13}C$ values of 13.6 ± 3.5‰ and -20.3 ± 2.6‰, respectively. The trophic enrichment from primary consumers (suspension feeders) to secondary consumers was about 3.6‰ for $\delta^{15}N$ and 2.6‰ for $\delta^{13}C$. The most common LMA sponge, *S. rosea*, showed the highest $\delta^{15}N$ value of 19.4 ± 2.3‰, corresponding to an additional trophic enrichment of 5.8‰ with respect to the secondary consumers. For the first two trophic steps, the average enrichments were 4.8 ± 1.2‰ for $\delta^{15}N$ and 2.6 ± 0‰ for $\delta^{13}C$, whereby the HMA sponges are excluded.

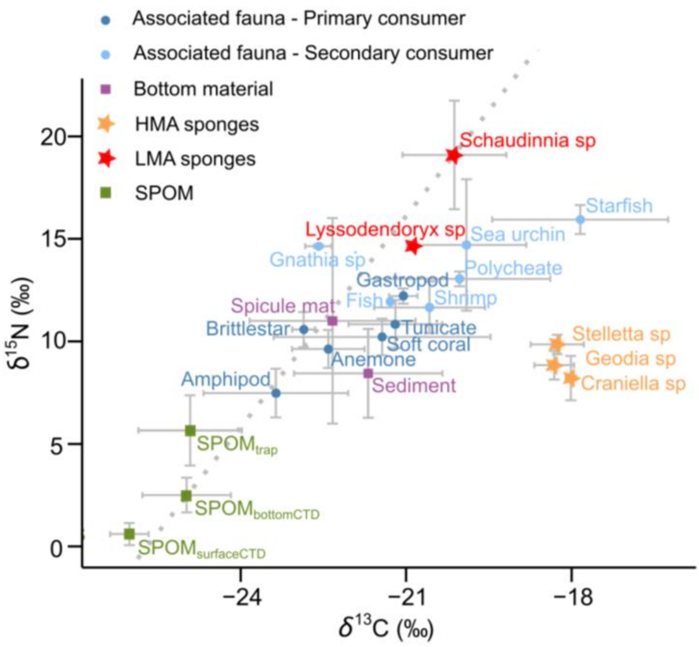

Figure 5.2 Nitrogen and carbon stable isotope ratios of bulk fauna, SPOM and bottom material ± SD. The dotted line indicates the generally anticipated enrichment in marine food webs of 3.4‰ $\delta^{15}N$ and 0.8‰ $\delta^{13}C$ (Zanden and Rasmussen 2001) with the $\text{SPOM}_{\text{bottom}}$ as the primary food source.

The isotopic signature for DO^{13}C increased with water depth, surface waters was 33.6‰ VPDB, while near bottom samples showed values of –26.8‰ at 2 mab. In the lower benthic boundary layer ^{13}C values were enriched and showed values of -16.8 ± 1.8‰ (supplementary material, Figure S5.1).

5.3.2 Compound specific nitrogen isotope analysis of amino acids (CSIA-AA)

The metabolic AA (AA$_{\text{metabolic}}$) threonine (THR) had the lowest δ^{15}N values (0.96 ± 0.28‰, Figure 5.3), with sponges and their spicule mat remaining above the total AA$_{\text{metabolic}}$ average (6.1 ± 2.9‰). The δ^{15}N of source AAs (AA$_{\text{source}}$) was on average 8.7±3‰. HMA sponges (7.2 ± 1.9‰) and SPOM$_{\text{trap}}$ (5.7 ± 2.9‰) were below the average of total AA$_{\text{source}}$, while LMA sponges and spicule mats were above the total AA$_{\text{source}}$ average. Trophic AAs (AA$_{\text{trophic}}$) had an average δ^{15}N value of 20.4 ± 7‰. The HMA sponges (12.6 ± 2.1‰) as well as the SPOM$_{\text{trap}}$ (15.6 ± 2.9‰) showed a much lower signal than all other organisms. The spicule mat material showed the highest δ^{15}N values for the AAtrophic (30.2 ± 4.6‰).

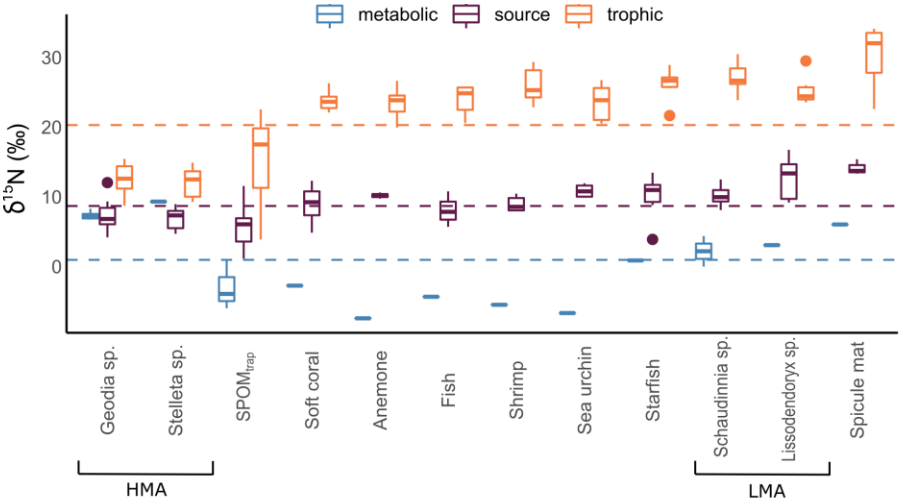

Figure 5.3 δ^{15}N of the different classes of AAs. Horizontal dotted lines indicate the average of all samples for the individual classes.

The $\delta^{15}N$ value of AA_{source} significantly differed between the $SPOM_{trap}$ and suspension feeder (p=0.055), secondary consumers (p=0.005), and LMA sponges (p=0.005). HMA sponges showed similar AA_{source} $\delta^{15}N$ values as $SPOM_{trap}$ (p=0.299). The AA_{source} $\delta^{15}N$ values of the spicule mat were significantly different from HMA (p=0.002), LMA (p=0.040), $SPOM_{trap}$ (p=<0.001) as well as secondary consumers (p=0.035).

The AA $\delta^{15}N$ values of GLU and PHE were used to calculate trophic positions (Figure 5.4). A difference of more than 0.48 can be considered as significant. The values of the HMA sponges indicate that they occupy the lowest trophic position (1.3). $SPOM_{trap}$ and most associated fauna group at the second trophic level (from 2 to 2.5), including the LMA sponges (2.4). Sea urchins (2.6) and tunicates (2.7) have a slightly higher trophic level. Fish (3.2) and shrimp (3.3), as well as spicule mat material (3.2) were found at the third trophic level.

The ΣV ranged from 0.81 to 4.12 (Figure 5.4), with the lowest heterotrophic enrichment for soft corals (0.81) and LMA sponges (1.22). $SPOM_{trap}$, sea urchins and shrimp (2-2.5), and the highest heterotrophic enrichment for the spicule mat (4.12).

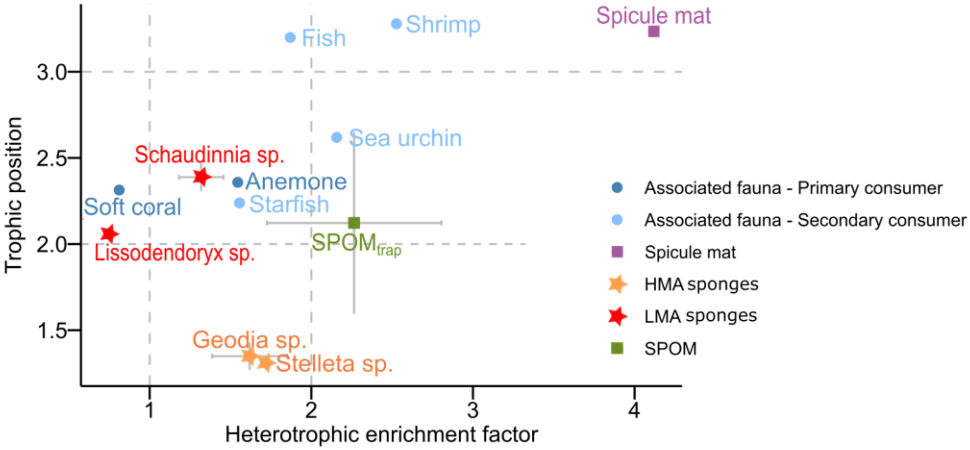

Figure 5.4 Trophic position and ∑V of the benthic fauna and spicule mat samples ± SD.

5.3.3 Fatty acid analysis

The $SPOM_{surfaceCTD}$ was dominated by algal markers (e.g 18:nω3, 20:5ω3 and 22:6ω3 (Dalsgaard et al., 2003, Kelly and Scheibling 2012), Table 5.1), accounting for 31% of all total FA, whereas $SPOM_{bottomCTD}$ contained lower proportions of algal markers and relatively more mono-unsaturated and straight FA. The spicule mat had a high diversity in FA and contained mostly typical sponge FAs. Anemones included high concentrations of zooplankton markers (20:1 and 22:1; Kelly and Scheibling, 2012), which are also present in most of the associated fauna, except tunicates. Soft coral included octocoral FA markers 20:4ω6 and 24:5 (Imbs et al., 2016) and brittle stars and tunicates contained substantial proportions (>1%) of bacterial markers (i-C15:0, ai-C15:0 and 18:1ω7; Dalsgaard et al., 2003; Kelly and Scheibling, 2012). The fatty acid profiles of HMA sponges are dominated by mid-chain-branched fatty acids (MBFA): me-C16:0 and me-C18:0, which are unique microbial markers of the associated microbiota of HMA sponges that are typically not found in the environment (Thiel et al., 2002). Additionally, the HMA sponges produced long chain fatty acids (LCFA), Me-24:2Δ(5,9) and 26:2Δ(5,9), which are unique for sponges (Thiel et al., 1999). The LMA sponge *S. rosea* hardly contained bacterial markers compared to the HMA sponges, but mainly LCFA, such as 30:3. Predators like sea urchins and starfish also contained substantial (>1%) bacterial markers (i-C15:0, ai-C15:0 and 18:1ω7) as well as the sponge-specific microbial markers, me-C18:0 and small amounts (<3%) LCFA. The algal-derived poly-unsaturated FA (20:5ω3 and 22:6ω3) dominated the FA of shrimp and fish.

To further constrain food sources and food-web transfers, the $\delta^{13}C$ isotopic values of the fatty acids in the HMA sponge were assessed. The bulk isotopic carbon value of HMA sponges was -18.1‰, whereas the value of SPOM was -24.9 ± 0.8‰ (Figure 5.2). The non-specific FAs in *Geodia* sp. had a weighted average isotopic value of -21.7 ± 0.8‰, the general bacterial-specific FAs -24.9 ± 0.6‰ and the sponge specific LCFAs -22.5 ± 0.2‰. The symbiont-specific MBFAs had a much higher $\delta^{13}C$ of -19.2 ± 0.6‰. The enriched isotopic signal of these mid-methyl FAs was also found in both sea urchins (-19.5‰) and starfish (-19.4‰).

Table 5.1 Dominant fatty acids (≥10% of total fatty acids) in Schulz Bank fauna and spicule mat. *<10%

Dominant fatty acids in the fauna (≥10%)		Mid-Me-c16:0	Mid-Me-C18:0	Me-24:2Δ(5,9)	26:2Δ(5,9)	30:3	C16:0	18:1ω9	18:1ω7	C18:0	20:4ω6	20:5ω3	20:1ω	22:6ω3	22:1ω	24:5 (0r6)ω3
Marker for		Sponge associated bacteria		Sponge			General	Animal	Bacteria + Algae	General	Macroalgae	Algae	Zooplankton	Algae	Zooplankton	Octocorals
Fauna	HMA sponge	x	x	x	x											
	LMA sponge					x										
	Anemone						x						x		x	
	Brittle stars						x			x		x	x			
	Fish						x			x				x		
	Gastropod									x		x	x			
	Polychaeta						x	x					x			
	Sea urchin			*	*							x	x			
	Shrimp						x	x	x			x		x		
	Soft coral										x		x			x
	Starfish			*	*							x	x			
	Tunicate						x		x							
	Spicule mat				x		x									

5.4 Discussion

We aimed to unravel the role of sponges in the food web of a biological hotspot in the dark and oligotrophic deep sea. At first glance, the bulk isotope data of the food web (Figure 5.2) show a traditional linear increase with a strong positive correlation between bulk $\delta^{15}N$ and $\delta^{13}C$ as is expected for a food web supported by a main primary source (Polunin et al., 2001). The base of the food web consists of SPOM, which is primarily consumed by suspension-feeding fauna. The following trophic position is taken by secondary consumers, such as starfish, sea urchins, and fish. However, several distinct offsets from a traditional food-chain are observed based on bulk isotope data: 1) The expected primary food source ($SPOM_{bottomCTD}$) is located at the second trophic position. 2) LMA sponges, presumably primary consumers, are observed at the top of the food web. 3) HMA sponges do not follow the linear increase of the isotopic ratios and are characterized by a much higher enrichment of $\delta^{13}C$ in comparison to other suspension feeding fauna, and 4) Trophic enrichment factors are higher than typically expected for both C and N. In the following paragraphs, these distinct offsets will be discussed:

1) The position of the primary food source at the second trophic level can be attributed to extensive zooplankton processing of phytoplankton produced during the single annual bloom occurring in the Norwegian Sea (von Bodungen et al., 1995). Consequently, the SPOM remaining and reaching the bottom has a higher $\delta^{15}N$ (2.5‰) than $SPOM_{surfaceCTD}$ (0.6‰) and includes zooplankton FA markers.

2) High $\delta^{15}N$ values were also observed for LMA sponges in other studies (Iken et al., 2001; Polunin et al., 2001; Kahn et al., 2018). A high inferred trophic level is inconsistent with their suspension feeding activities, but so far no conclusive explanation has been presented. These extremely enriched ^{15}N values either indicate that they rely on additional or altered food sources besides SPOM, or that LMA sponges internally recycle nitrogen within their sponge tissue or in the sponge microbiome. Selective uptake of microbes or uptake of microbial-derived material can affect the expected tropic enrichment (Middelburg 2014). Kahn et al., (2018) suggested that LMA sponges take up re-suspended benthic bacteria, which are enriched in $\delta^{15}N$. However, this does not explain the bulk $\delta^{15}N$-isotopic composition of spicule mats, which show the highest enrichment (11‰) and still remain more than one trophic level (-8.4‰) lower than that of the LMA sponges (19.4‰). Alternatively LMA sponges may internally recycle nutrients increasing their $\delta^{15}N$, analogous to the principle of

cannibalism in Arctic fishes (Hobson and Welch, 1995). Intense recycling of nitrogen within the sponge microbiome, which is consistent with molecular biology data (Kiran et al., 2018) and rate measurements (Rooks et al., 2020), may result in large isotopic effects with the consequence that LMA sponges obtain high $\delta^{15}N$ values.

The AA values of $\delta^{15}N$ provide additional constraints on these alternative explanations. LMA sponges in this study show a much higher $\delta^{15}N$ of $AA_{trophic}$ (27.3 ± 2.2‰, Figure 5.2) and AA_{source} (10 ± 1.6‰) than that of $SPOM_{trap}$ (15.6 ± 2.9 and 5.7 ± 2.9‰), which is consistent with our observation that the vertical flux is not the primary food source for LMA since AA_{source} should only increase by ~0.4‰ per trophic position (Chikaraishi et al., 2009). However, the impact of intense carbon and nitrogen recycling processes within the sponge microbiome might impact the isotope values of AA_{source} isotopes, e.g. via de novo synthesis of AAs by chemoautotrophs as observed for example in deep-sea corals (Middelburg et al., 2015). Based on the AA isotope analysis, sponges appear to have a similar trophic position as the associated suspension feeding fauna (Figure 5.4). This trophic position for LMA sponges is not only consistent with our knowledge on sponge physiology as primary consumers, but also appeared to be little affected by internal recycling processes that cause large and incompletely understood changes in bulk $\delta^{15}N$. Accordingly, AA isotope analysis should be considered as the preferred method to analyse deep-sea ecosystem food webs.

3) The HMA sponges clearly deviate isotopically from the linear food-chain concept, because their $\delta^{13}C$ values were strongly enriched relative to the other suspension feeding fauna. This indicates that they not only rely on SPOM, but also use another carbon source that is elevated in ^{13}C value, likely DOM. There are two main dissolved carbon sources; DOC and dissolved inorganic carbon (DIC). Recent experiments confirmed that sponges are able to take up DOC and release POC (Bart et al., 2021), which is consumed by detritivores in CWC reefs (Maier et al., 2020). The uptake of DIC or DOC might be partly mediated by the sponge microbial symbionts (Yahel et al.,

2003; De Goeij et al., 2008), although increasing evidence confirms significant direct processing of DOC by sponge cells, specifically choanocytes (i.e. filter cells; De Goeij et al., 2009; Rix et al., 2020). The metagenome of the HMA sponge *G. barretti*, for example, exhibits only a 27% sponge signature accompanied by archaea and as the main part bacteria like *Chloroflexi*, which are known for their ability to degrade abundantly present refractory DOC (Radax et al., 2012). Archaea, as well as some bacteria, are able to oxidize regenerated NH_4^+ to NO_2^-, which is then used by other microbes to oxidize NO_2^- to NO_3^- (Hoffmann et al., 2009). Oxidation of NH_4^+ generates energy that is used by chemoautotrophs to fix DIC (Wuchter et al., 2006). DIC has an elevated ^{13}C value with typical water column values of around ~0–1‰ (Griffith et al., 2012) and chemoautotrophy thus introduces a major shift towards higher $\delta^{13}C$ values. Nevertheless only relatively low fluxes of (dark) carbon fixation were found in other deep-sea sponges (van Duyl et al., 2008). The majority of the unique carbon signal is likely derived from the uptake of DOC, which is supported by a recent study that shows that DOC is, by far, the main carbon source of deep-sea HMA and LMA sponges (Leys et al., 2018; Bart et al., 2021; De Kluijver et al., 2020). Only a limited number of $DO^{13}C$ values were sampled, but water column values were comparable to values measured in the North Atlantic (-23.1 to -22.2‰; Hansell and Carlson, 2014). Future analysis of additional samples is necessary to identify possible recycling effects inside the benthic boundary layer influencing $DO^{13}C$. These values nevertheless suggests the uptake of DOC together with some chemoautotrophic fixation of DIC, which likely accounts for the elevated $\delta^{13}C$ values observed in HMA sponges.

The $\delta^{13}C$ values of the FAs in HMA sponges provide additional evidence for chemoautotrophic inputs (supplementary material, Table S5.2). FAs produced by sponge bacterial symbionts that were linked to mixotrophs (Siegl et al., 2011) show the highest isotopic enrichment (-19.2 ± 0.6‰), compared to other bacterial FAs (-24.9 ± 0.6‰) and sponge-specific LCFA had intermediate values, indicating transfer of carbon from symbionts to the sponge. However, the role of archaea on the isotopic composition of sponges remains unknown since they cannot be detected with FA analysis.

The average $\delta^{15}N$ of the $AA_{trophic}$ of HMA sponges (12.6 ± 2.1‰) is slightly lower than that of $SPOM_{trap}$ (15.6 ± 5.8‰, Figure 5.2), yet the isotopic value of $AA_{trophic}$ is expected to increase by about 7.6‰ per trophic level (Chikaraishi et al., 2009) rather than decrease in $\delta^{15}N$ relative to their food source. Also the difference between AA_{source} and $AA_{trophic}$ points towards a less processed food source for HMA sponges (+5.4‰) when compared to the $SPOM_{trap}$ (+9.8‰). Moreover, the $\delta^{15}N$ values from AAs suggests that the HMA sponges are at the base of the food web since only a very small trophic enrichment of the $AA_{trophic}$ compared to the AA_{source} was found. *Geodia* sp. (and other HMA species) can efficiently recycle N, with active ammonia assimilation, that will result in de novo synthesis of AAs (Hentschel et al., 2012).

4) The larger than expected enrichment in isotopic values between each trophic level of 4.7‰ for $\delta^{15}N$ and 2.6‰ for $\delta^{13}C$ per trophic position (Figure 5.2) is much higher than the generally expected 3.4‰ and 0.8‰ enrichments, respectively (Zanden and Rasmussen, 2001). These large trophic enrichment values are likely caused by an enhanced recycling associated with the transfer of ^{13}C-enriched carbon from the HMA sponges and transfer of ^{15}N enriched nitrogen mainly from LMA sponges towards the associated fauna. The FA analysis is in line with transfer of sponge organic matter to the associated fauna since sponge derived FAs were found in their tissue. This can also be caused by top-down processes, such as predation of associated fauna on sponges.

What is the role of sponges in food webs in the deep-sea environment? The relative abundance of the FA in consumers confirmed that sponge OM is directly transferred to the associated fauna and thereby represent an important link in this deep-sea ecosystem. Mid-branched C18:0 FA, known features of demosponges, are found in starfishes and sea urchins, which confirmed that at least these two benthic species directly feed on sponges or detritus released by sponges. Brittle stars and tunicates do not contain sponge biomarkers, whereas they contain substantial amounts of general bacterial markers, indicating that they feed on bacteria, bacteria-derived material (from sponges), or have bacterial symbionts themselves. The surveyed fish also lacks sponge biomarkers even though it is known that many fish species, like cod and halibut, feed on sponges (Randall and Hartman 1968; Mehl 1991). However, consumers may transform, catabolize or produce new FAs. For example, soft corals have distinct fatty acids, which are not found in other fauna, since they can produce FAs themselves (Imbs et al., 2016). Unfortunately trophic transfer involving archaea, which can facilitate DIC fixation, cannot be detected with this approach since they do not use FAs for their membrane phospholipids (Koga and Morii 2007).

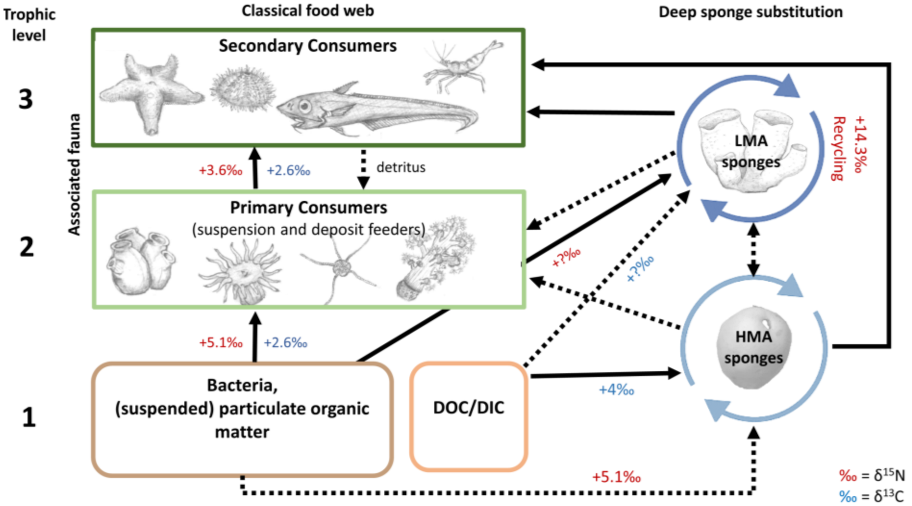

Figure 5.5 Proposed food web of the Schulz Bank sponge ground with isotopic enrichment of bulk $\delta^{15}N$ and $\delta^{13}C$, dotted arrows indicate expected interactions, which were not resolved in this study.

This study shows that deep-sea sponge grounds do not follow the classical food web structure. These ecosystems are subsidized by additional food resources entering the food web via sponges (deep sponge substitution, Figure 5.5). This addition of resources appears to be mediated by both sponge HMA and LMA sponges. HMA sponges directly aggregate DOM and their microbial symbionts utilize DIC and DOC (Bart et al., 2021) and produce detritus (De Goeij et al,. 2013). LMA sponges are also known to aggregate DOM from the water column and transfer detritus, and presumably inorganic nutrients to the associated fauna, whereas their carbon contribution might be much smaller compared to their contribution of nitrogen (Bart et al., 2021). The compound-specific isotope analysis of AA gave a more detailed and consistent picture of the food web structure compared to the classical bulk isotope analysis. Through the combination of bulk, AA and FA profiling, we elucidated major parts of this complex food web (Figure 5.5). Overall, it is likely that the Schulz Bank sponge ground is relying on particulate as well as dissolved sources and that sponges play an important role in bottom-up as well as top-down control in the food web.

5.5 Acknowledgments

This research has been performed in the scope of the SponGES project, which received funding from the European Union's Horizon 2020 research and innovation programme under grant agreement No. 679849. A.C. was supported by Fundação para a Ciência e a Tecnologia (FCT) through IF/00029/2014/CP1230/CT0002 to and through the strategic projects UID/ 05634/2020. Klaas Nierop, Desmond Eefting and Femke van Dam (Utrecht University) are acknowledged for their help with fatty acid analysis. Ronald van Bommel (NIOZ) is acknowledged for his help with the stable isotope analysis. We thank captain and crew of the G.O. Sars as well as the ROV crew for their help in obtaining the samples.

5.6 Data availability

The isotope data is available in PANGAEA (doi:10.1594/PANGAEA.923765).

5.7 Supplements

5.7.1 Methods

5.7.1.1 Analysis of the isotopic signature of DOC

The samples for DOC concentration and isotopic signature were measured using a high temperature combustion TOC (IsoTOC, Elementar GmbH, Langenselbold, Germany). The eluted CO_2 peak was pre-concentrated in a low concentration module (LCM, Elementar GmbH, Langenselbold, Germany) before entering the isotope ratio mass spectrometer (BioVision, Elementar ltd., Cheadle Hulme, UK) for the analysis of ^{13}C. Before the samples were run, blank ultra-pure water injections were monitored to check the stability of the system. 0.5 ml of the pre-acidified sample was introduced in the combustion tube of the system which was set at 760°C, a small amount of O_2 was dosed during and after the injection of the sample to completely combust the DOC into CO_2. Any access of O_2 was trapped in a copper filled reduction tube, which was set at 500°C. To minimalize possible carry over effects between the samples, the samples were measured repeatedly (5 injections) and the results of the first 2 injections are discarded. Before and after the samples a set of two international standards (IAEA-600 and IAEA-CH6) were measured to calibrate the ^{13}C values. A linear regression between the expected and the measured values of the two standards was used to calibrate all the samples vs VPDB (^{13}C).

5.7.1.2 Amino acid data processing

The trophic position (TP) estimation was based on the offset between the trophic AA glutamic acid (GLU) and source AA phenylalanine (PHE), with a large and constant increase in ^{15}N values due to metabolism of GLU relative to PHE with each trophic transfer (Chikaraishi et al.,2007; McClelland and Montoya, 2002; O´Connell, 2017):

$$\mathrm{TP} = \left(\frac{\delta^{15}\mathrm{N}_{\mathrm{GLU}} - \delta^{15}\mathrm{N}_{\mathrm{PHE}} - \beta}{\mathrm{TDF}}\right) + 1$$

where β represents the fractionation between the primary producers and their underlying basal resources at the base of the food web (β=3.4‰) and β has been found to be relatively consistent in marine primary producers (Chikaraishi et al., 2009; Nielsen et al., 2015; McMahon and McCarthy, 2016) and TDF is the trophic discrimination factor between consumer and their diet of 7.6‰.

The propagated standard analytical error for the TP is ± 0.48‰ resulting from the TDF uncertainty of ± 0.33‰ (McMahon and McCarthy, 2016) and the measurement errors from GLU (± 0.41‰) and for PHE (± 0.46‰). Therefore, robust differences in TP can be assumed when the TP difference is more than 0.48. Differences in source or trophic AAs between groups were tested by an ANOVA combined with a post hoc Tukey's test (Tukey's honest significant differences with R Studio 1.2.1335). Due to limited sample replication these statistical tests should be considered with caution.

To assess microbial re-synthesis of amino acids, the summed variance (ΣV) value was calculated (McCarthy et al., 2016). Heterotrophic reworking of proteinaceous material includes a range of processes by heterotrophic organisms. Therefore, heterotrophic processed material inherently represents a mixture of new biosynthesized AA as well as remnant material. This additional processing will increase the variance in δ^{15}N of selected AAs whereby others remain relatively unaltered. The ΣV gives the sum of variance among individual δ^{15}N values of trophic AAs (aspartic acid, glutamic acid, alanine, leucine, and proline) and can be used as a measure for total heterotrophic re-synthesis. The parameter is defined as the average deviation in the δ15N values of the trophic AAs [7, 8].

$$\Sigma\mathrm{V} = \frac{1}{n}\sum |x_{AA}|$$

where x is the deviation of each trophic AA from the average δ^{15}N of all trophic AAs and n is the total number of trophic AAs used in the calculation.

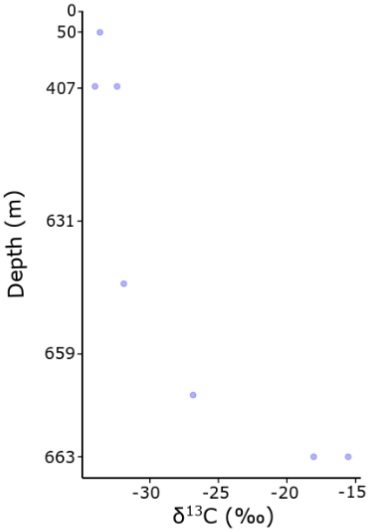

Figure S5.1 DO^{13}C (vs VPDB) isotopic values measured within the water column. Note that the y-axis is log transformed.

Table S5.1 Taxa description and category of collected fauna as well as their expected trophic position.

	Taxa	Category	Expected trophic position
Porifera	*Geodia hentschelii*	HMA sponge	Primary consumer (filter feeder)
	Geodia parva	HMA sponge	Primary consumer (filter feeder)
	Stelletta raphidiophora	HMA sponge	Primary consumer (filter feeder)
	Craniella infrequens	HMA sponge	Primary consumer (filter feeder)
	Thenea valdivae	HMA sponge	Primary consumer (filter feeder)
	Hexadella dedritifera	HMA sponge	Primary consumer (filter feeder)
	Schaudinnia rosea	LMA sponge	Primary consumer (filter feeder)
	Lissodendoryx complicata	LMA sponge	Primary consumer (filter feeder)
Cnidaria	Actiniaria	Anemone	Prim. con. (carnivorous/susp. feeder)
	Gersemia rubiformis	Soft coral	Primary con. (suspension feeder)
Echinodermata	Ophiuridaea	Brittle stars	Primary con. (suspension feeder)
	Strongylocentrotus sp.	Sea urchin	Secondary consumer (scavenger)
	Tylaster willei	Starfish 1	Secondary consumer (scavenger)
	Henricia perforata	Starfish 2	Secondary consumer (scavenger)
Chordata	*Macrourus berglax*	Fish	Secondary consumer (scavenger)
	Humphreysianum cf. sp.	Gastropoda	Primary consumer (deposit feeder)
	Ascidiacea spp.	Tunicate	Primary consumer (filter feeder)
Arthropoda	*Bythocaris* sp.	Shrimp	Secondary consumer
	Themisto cf. libellula	Crustacaea	Primary consumer (filter feeder)
	Gnathia sp.	Gnathia	Secondary consumer (parasite)

Table S5.2 Weighted average δ^{13}C isotopic values of different FA markers and bulk value in HMA sponges (*Geodia* sp.)

Fatty acid	Marker	Isotopic value
C16:0/C18:0	General	-21.7±0.8‰
i/ai15/16:1 mix/18:1 mix	Bacteria	-24.9±0.6‰
9-meC16:0/9-meC18:0	Sponge specific bacteria	-19.2±0.6‰
25:2/26:2	Sponge	-22.5±0.2‰
Bulk		-18.1±0.3‰

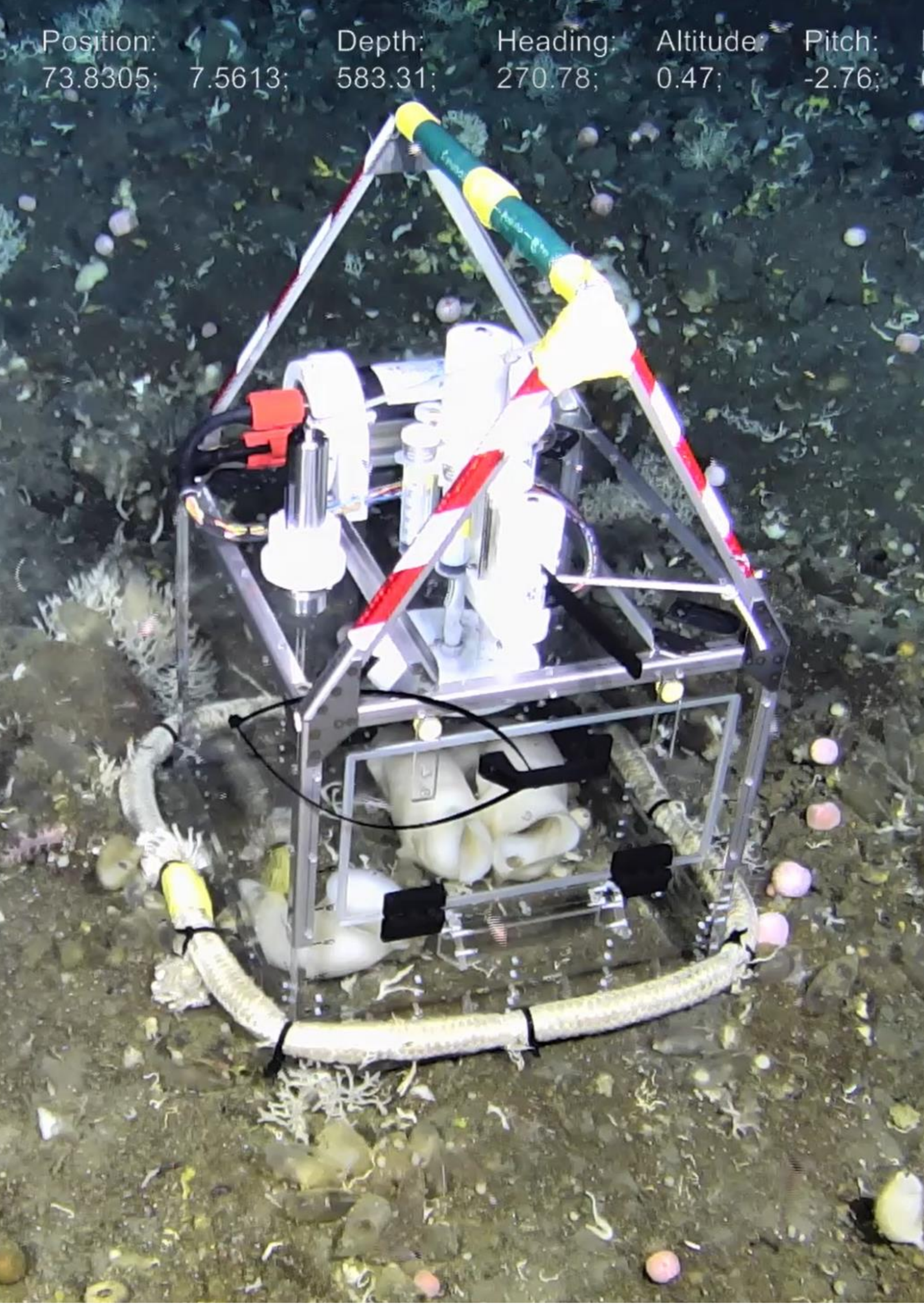
Position:
73.8305; 7.5613;
Depth:
583.31;
Heading:
270.78;
Altitude:
0.47;
Pitch:
-2.76;

Chapter 6

Oxygen uptake and inorganic nutrient dynamics in an Arctic deep-sea sponge ground: the sponge ground effect

Ulrike Hanz, Martijn Bart, Benjamin Mueller, Jasper M. de Goeij, Kathrin Busch, Emyr Martyn Roberts, David Bowers, Gert-Jan Reichart, Hans Tore Rapp†, Furu Mienis

Picture to the left: Schulz Bank sponge ground with in-situ chamber incubating *Schaudinnia rosea* ©University of Bergen

Abstract

Sponge grounds are hotspots of biomass and biodiversity in an otherwise mostly barren deep sea. However, in-situ studies focusing on the impact of deep-sea sponge dominated ecosystems on carbon and nutrient cycling are sparse. To fill this knowledge gap, in-situ incubation experiments were used to quantify oxygen, carbon and inorganic nutrient fluxes of a deep-sea sponge ground community on the Arctic Mid Oceanic Ridge. A profile pump, which also monitored hydrodynamic conditions, was deployed to quantify fluxes in the benthic boundary layer. Calculated respiration rate for the sponge ground community is 0.70 ± 0.31 mmol O_2 m^{-2} h^{-1} (mean ± SD) and driven by a high sponge biomass, which more than doubled the respiration rate. The vertical gradient in the bacterioplankton concentration within the benthic boundary layer showed a decrease of bacterioplankton towards the bottom during all deployments, which confirms a net uptake by the sponge ground community. Inorganic nutrients (NH_4^+, NO_2^-, NO_3^- and PO_4^{3-}) were released during the in-situ incubations. Incubations with a high biomass of low microbial abundance sponges showed higher fluxes of NH_4^+, NO_2^- and PO_4^{3-} compared to incubations with a high abundance of high microbial abundance sponges. Incubations with a high biomass of low microbial sponges showed a higher release of NH_4^+ , whereas high microbial sponges convert all nitrogen species into nitrate. Still, calculated C:DIN:P ratio was similar in all incubations, indicating a common food source for the sponge community. The high respiration rates and nutrient fluxes show that sponge grounds are hotspots of carbon and nutrient cycling, comparable to other deep-sea hotspots like cold-water coral reefs.

6.1 Introduction

Deep-sea benthic communities are considered to endure extreme conditions compared to ecosystems in the photic zone, since they occur in a cold, dark, and (particulate) food-limited environment (Ramirez-Llodra et al., 2010). Nevertheless, biological hotspots of high biodiversity and biomass have been found in many places of the deep ocean, as for example cold-water coral reefs, hydrothermal vent communities and deep-sea sponge grounds (Klitgaard and Tendal, 2004; Hogg et al., 2010; Roberts et al., 2006; Baker and German, 2004). Studying these ecosystems in situ remains challenging due to their inaccessibility and as a consequence the very abundant deep-sea sponge grounds are generally understudied (Hogg et al., 2010).

Deep-sea biological hotspots are commonly found in areas with enhanced water currents and strong turbulence (Roberts et al., 2018; Van Haren et al., 2017; Hanz et al., 2021; Davison et al., 2019). These high currents are often related to the interaction of tidal waves with sloping topography as has been observed on continental shelves, seamounts, mid-ocean ridges, and submarine canyons (Nycander, 2005; Levin and Sibuet, 2012; Hanz et al., 2021). Internal wave motions potentially deliver particulate and dissolved food sources towards the benthic ecosystems and replenish oxygen, particulate and dissolved organic matter (POM and DOM) in the benthic boundary layer (BBL) (Van Haren et al., 2014). This provides a source of nutrition for deep-sea ecosystems like cold-water coral reefs (CWCs), sponge grounds, their associated fauna as well as microorganisms (Ritzrau, 1996; Davies et al., 2009; Hanz et al., 2019).

Sponges are one of the most common and abundant megafaunal organisms in the deep sea, with an often scattered distribution (Tabachnick et al., 1994). In some areas they dominate the biomass of benthic ecosystems like cold-water coral reefs (Cathalot et al., 2015) or they may form sponge grounds characterized by either monospecific or mixed species assemblages (Maldonado et al., 2017a). At specific sites, sponges even create reef-like habitats through deposition of dense, tens of cm-thick, layers of skeletal needles, so-called spicule mats (Maldonado et al., 2017b; Hogg et al., 2010). Sponge grounds provide important ecosystem services by enhancing heterogeneity and provide a spawning, nursery and foraging area for many fish and invertebrate species (Maldonado et al., 2017b; Fuller and Cameron, 1998; Meyer et al., 2019; Hawkes et al., 2019). Moreover, sponges potentially create beneficial hydrodynamic conditions, influencing the water flow at the near-bed environment similar to CWC reefs (Mienis et al., 2019). In addition, sponges affect the water column in their immediate surroundings due to their ability to pump large volumes of water. This way deep-sea sponges play an important role in benthic-pelagic coupling, extensively filtering particulate organic matter (POM, e.g. bacterio and phytoplankton, e.g., Yahel et al., 2007; Kahn et al., 2015; Leys et al., 2018) from the water column. More recently, common North-Atlantic sponge species have been shown to also take up dissolved organic matter (Rix et al., 2016; Bart et al., 2021) as a major part (>90%) of their carbon diet (Bart et al., 2021). DOM is the largest potential organic food source in the ocean (Hansell et al., 2009), which is not bioavailable to most benthic fauna, whereas the ability to take up DOM in large quantities makes deep-sea sponges potentially important players in the recycling of energy in deep-sea ecosystems (Bart et al. 2021). Through the so-called sponge loop (De Goeij et al., 2013), sponges can take up dissolved organic carbon and transfer it as particulate organic matter to higher trophic levels by detrital pathways (Rix et al., 2018). Deep-sea sponges have recently been shown to be able to transfer DOM to associated fauna (Bart et al., 2021).

Additionally, sponges are able to access resources from their microbial symbionts and in turn transfer carbon and nitrogen to their symbionts, resulting in highly efficient recycling of host waste products by the microbiome (Hudspith et al., 2021). Sponges typically contain a diverse community of microbial symbionts like bacteria, fungi and archaea (e.g., Hentschel et al., 2003; Pita et al., 2018), providing the holobiont (i.e. sponge host and microbial symbionts) access to a wide variety of metabolic pathways (Taylor et al., 2007). In high microbial abundance (HMA) sponges, 20-30% of the total holobiont biomass can consist of the associated microbes, whereas low microbial abundance (LMA) sponges contain much less and smaller sized microbes with a lower diversity, more similar to that found in the ambient seawater (Hentschel et al., 2006; Moitinho-Silva et al., 2017). These microbial symbionts for example enable sponges to use chemoautotrophic pathways to generate energy from NH_4^+ and NO_2^- (Radax et al., 2012; De Kluijver et al., 2021).

In-situ community studies are needed to elucidate the integrated functioning (e.g., the cycling of carbon and nitrogen) of sponge grounds, including the associated fauna, similarly as has been done for CWC reefs (De Froe et al., 2019). To date little is known about respiration rates, exchange and fluxes of (in)organic nutrients in deep-sea sponge dominated communities.

Therefore, in this study, in-situ incubation experiments were carried out to quantify oxygen, bacterioplankton and inorganic nutrient fluxes in a dense deep-sea sponge ground at the summit of the Schulz Bank which is situated along the Arctic Mid Ocean Ridge (73°50'N, 7°34'E). A profile pump was used as an alternative means to quantify fluxes from the benthic boundary layer (from 10 cm to 2.1 m above bottom) as well as to study how the sponge ground community affects the overlying water column. The aims of this study were to (1) quantify oxygen, inorganic nutrient and bacterioplankton fluxes, (2) to measure their effect on the benthic boundary layer and (3) determine the influence of hydrodynamic conditions on fluxes.

6.2 Material and Methods

6.2.1 Study site and setting

The Schulz Bank is part of the Atlantic Mid Oceanic Ridge and is located between the Norwegian and Greenland basins (73°50'N, 7°34'E). The seamount is rising about 1900 m from the surrounding basin seafloor to the summit at around 560 m depth. The seamount has an oval shape, and its summit is orientated in a NE direction. The highest abundance of sponges and associated fauna is located on the summit at water depths between 560 and 700 m, forming a reef like ecosystem (Roberts et al., 2018). This area is dominated by soft sediments covered by a thick layer of sponge spicules (~ 20 cm), overgrown by benthic fauna (Meyer et al., 2019). On the summit an aggregation of hexactinellids and demosponges associated with other fauna dominated by ascidians (*Ascidiacea* spp.), cnidarians (soft corals), echinoderms and demersal fish species was found (Meyer et al., 2019). The primary structure-forming hexactinellid species are *Schaudinnia rosea*, *Scyphidium septentrionale*, *Trichasterina borealis*, and *Asconema foliata* (vase-shaped sponges) and the main demosponge species are *Geodia* spp., Stelletta rhaphidiophora (massive, subglobular) and *Lissodendoryx complicata* (branched) (Meyer et al., 2019). *S. rosea* is considered a LMA sponge, whereas *Geodia* spp. and *S. foliata* are considered to be HMA sponges. On the seamount flanks, sponges have a patchy distribution with a lower density and no densely overgrown spicule mats were observed (Roberts et al., 2018; Meyer et al., 2019).

The water masses at the location of the Schulz Bank are the Norwegian Atlantic Water at the surface and the Norwegian Arctic Intermediate Water from a depth of around 500 to 1000 m (Hopkins, 1991; Helland-Hansen and Nansen, 1909). The Norwegian Sea Deep Water is located below the intermediate water mass. The summit of the Schulz Bank is located at the interface between two water masses inside a local maximum of dissolved oxygen concentrations (~7 ml l^{-1}). Tidally driven waves move on this interface and interact with the seamount topography and thereby produce turbulence and mixing on the summit. (Roberts et al., 2018; Hanz et al., 2021). This mixing replenishes oxygen, food and nutrients on a semi-diurnal period in the benthic boundary layer (Hanz et al., 2021; Roberts et al., 2018).

6.2.2 Field measurements

6.2.2.1 In-situ incubations

To determine changes in concentration of oxygen, bacterioplankton and inorganic nutrients (NH_4^+, NO_3^-, NO_2^- and PO_4^{3-}) two 50 x 50 x 50 cm (125 l volume) acrylic incubation chambers (assigned labels “F” and “J”) with open bottoms were deployed for 4-6 hours at three Schulz Bank summit stations (total of six incubations, Figure 6.1b). The chambers were developed by the NIOZ Royal Netherlands Institute for Sea Research and are modified version of the chambers used by Stratmann et al. (2018). The chambers were carefully positioned at random locations with the remotely operated vehicle (ROV) Ægir 6000 during the G.O. Sars research cruise in 2017 (July 20th - August 6th 2017, Table 6.1). A lead (Pb) rope attached to the bottom of the chamber ensured that the weight of the chambers was heavy enough to submerge them up to 10 cm into the sediment. This created an enclosed chamber with negligible leakage as was tested in the laboratory. The chambers contained a stirring plate with pre-programmed stirring speeds at different time intervals to ensure homogenous mixing of water within the chamber, as well as an autosampler to take 6x60 ml water samples at preprogramed time points. The program controlling both functions was triggered by pushing a lever that was attached to the chamber with the arm of the ROV. During the incubations a dissolved oxygen sensor (Advantech-ARO-USB) continuously monitored oxygen concentrations and temperature (20 s interval).

The incubations were performed between 577 and 583 m depth (73°50’N, 7°34’E; Table 6.1) at the Schulz Bank summit. Chambers were either placed over a mixed benthic community site with obvious large sponge individual(s) or at a random mixed benthic community with only smaller sponge individuals (see Figure S6.1 in supplements). After the sampling program was started by the ROV, the stirring disc started 2-5 min before the first sample of 60 ml (t_0) was taken to ensure that water within the chamber was well mixed. During the 4 or 6 h incubations consecutive water samples (60 ml) were taken autonomously at equal time intervals (2880 to 4320 s, depending on the overall deployment time). At the end of each incubation, the chambers were carefully lifted (to avoid disturbance of samples and incubated species) and water samples, as well as major incubated sponge specimens were retrieved with the ROV.

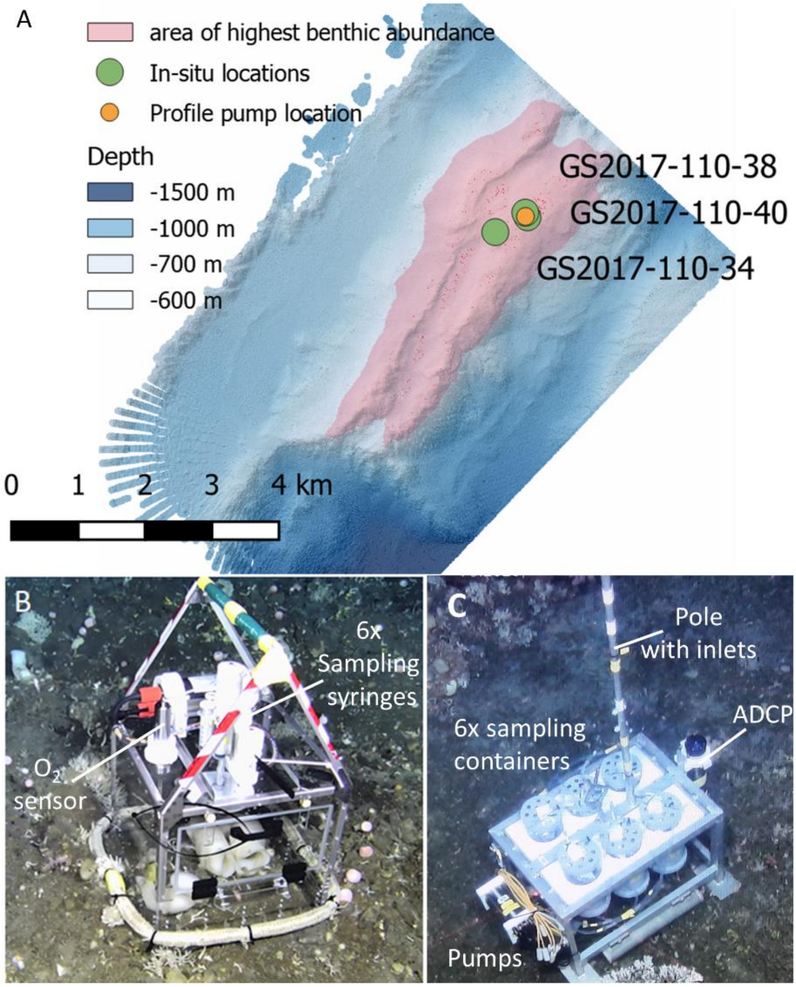

Figure 6.1 a) Map of the summit of the Schulz Bank with sampling sites of in-situ incubations (Table 6.1 for details) and profile pump deployments. Area of highest benthic fauna abundance in red, b) In-situ incubation chamber deployed inside the sponge ground, c) Profile pump deployed on the seafloor.

On board the research vessel, biomass (dripping wet weight) was assessed, later dry weight (dw) was measured in the laboratory. Water samples were processed within 2 h after recovery of the chamber and subsampled for inorganic nutrients (NH_4^+, NO_3^-, NO_2^- and PO_4^{3-}; 5 ml) and bacterial concentrations (1 ml). Benthic megafauna in the chambers was analyzed using video images made by the ROV (see Figure S6.1 in supplements).

Table 6.1 Stations and characteristics of the in-situ incubations with dry weight and wet weight of sponge biomass indicated as well as the presence of associated fauna as observed from video image analysis. Incubations with *Schaudinna rosea* being LMA sponge dominated and with *Geodia parva* being HMA sponge dominated.

No.	Station	Incubation	time (h)	Major incubated sponge species	Sponge biomass (kg ww)	Sponge biomass (g dw)	+visible megafauna	
1	GS2017-110-34	34J	4	No large sponges	<0.1	1	3x Anemones Tunicate	Low sponge biomass
2	GS2017-110-38	38F	6	No large sponges	<0.1	30	5x Tunicates Anemone *Lissodendoryx complicata*	
3	GS2017-110-40	40J	6	No large sponges	<0.1	*1*	*Lissodendoryx complicata*	
4	GS2017-110-34	34F	4	*Geodia parva*	*1.8*	357	Encrusting sponge Soft coral Tunicates	High sponge biomass
5	GS2017-110-38	38J	6	*Schaudinnia rosea* *Geodia hentscheli*	1.19 0.6	240		
6	GS2017-110-40	40F	6	*Schaudinnia rosea* *Geodia hentscheli*	2.1 0.281	303		

6.2.2.2 Profile pump

To determine small-scale variations of bacterioplankton and inorganic nutrient concentrations within the BBL, an autonomous NIOZ designed profile pump (Figure 5.1c) was deployed to (during 1.5 h) take 5 l water samples at different water depths (0.1, 0.2, 0.4, 0.8, 1.4 and 2.1 m) above the seafloor simultaneously. The profile pump consisted of an aluminium frame with six sampling bags and an Acoustic Doppler Current Profiler sensor (ADCP, Nortek Aquadopp, 2000 kHz) to measure current speed and direction. The ADCP sensor head was located at 0.7 m above bottom, measuring current speed and direction in 50 cm bins. Inlets for water sampling were attached to an aluminium pole at aforementioned, predefined heights above the bottom. Three deployments were conducted at the sponge ground during different current regimes (see Table 6.2, GS2018108-6, -16, -32). Subsamples from each sampling depth were taken in duplicate for inorganic nutrients (NH_4^+, NO_3^-, NO_2^- and PO_4^{3-}) and bacterioplankton concentration. Fluxes were calculated based on a turbulent diffusion model using current speed and concentration profiles within the BBL (see 6.2.4.2).

6.2.3 Laboratory analysis

6.2.3.1 Inorganic nutrient analysis

Samples for dissolved inorganic nutrient analysis were filtered through sterile 0.8/0.2 µm polycarbonate membrane syringe filters (Whatman Nuclepore), collected in 6 ml high-density polyethylene (HDPE) ponyvials and stored at -20 °C until further analysis. Inorganic nutrient concentrations were determined by colorimetric analyses using a QuAAtro Gas Segmented Continuous Flow Analyser (Seal Analytical Ltd., UK) simultaneously on four channels. Measurements were calibrated against standards diluted to known nutrient concentrations with low nutrient seawater. A ‘nutrient cocktail’ with PO_4^{3-} and NO^{3-} was used as a standard in every run to monitor the performance. Precision and accuracy of the standard showed between run reproducibility better than 1.5%, but typically 0.7% of its average value.

6.2.3.2 Bacterioplankton abundance analysis

Water samples (1 ml) for bacterioplankton abundance from the benthic chambers and profile pump were collected in 2 ml cryovials and fixed on board with 20 µL 25 % EM grade glutaraldehyde solution for 15 min at 4 °C. After fixation, the samples were snap frozen in liquid nitrogen and stored at -80 °C until further analysis. Bacterioplankton abundances were analyzed using a FACS Calibur flow cytometer (Becton Dickinson, San Jose, Calif.) with a 15 mW 488-nm air-cooled argon-ion laser and a standard filter setup (Brussaard, 2004). Upon thawing, samples were 2x diluted in Tris-EDTA buffer (pH 8.0, 10 mM Tris-HCl, Roche Diagnostics; 1 mM EDTA, Sigma-Aldrich) to avoid electronic coincidence and were stained with SYBR Green I (Molecular Probes; 1:10000 final concentration (Brussaard, 2004). Bacterial samples were left in the dark for 15 min at room temperature until they were analyzed for 1 min at 49 µl min^{-1}. Data was analyzed using Flowing Software 2.5.1 freeware. Samples were corrected for blanks (TE-buffer with SYBR Green I).

6.2.4 Oxygen and inorganic nutrient fluxes

6.2.4.1 In situ incubation fluxes

The oxygen flux was calculated from the difference between oxygen concentration at t0 and the oxygen concentration at the end of the incubation experiment divided by the incubation time. Fluxes of bacterioplankton abundance and inorganic nutrients were described according to its best fitting mathematical model, integrated over the entire time frame of the incubation. Initial fluxes were estimated based on the tangent of each model at t_0.

To calculate inorganic nutrients over time, a linear regression analysis was performed for each individual incubation including all time points. Therefore, fluxes were calculated from the slope of a linear regression fitted to the observed concentration change of each incubation. All fluxes were corrected for chamber volume (125 l) and the incubated surface area (0.25 m^2). The carbon consumption was estimated assuming a respiratory quotient (RQ) of 1, assuming 1 mol C respired = 1 mol O_2 removed (Bart et al., 2021; Yahel et al., 2003).

Bacterioplankton removal rates were estimated assuming a simplified exponential clearance of cells in the incubations over time, which corresponds to the observation that the benthic megafauna is dominated by filter-feeding organisms. This exponential model was fitted to each individual incubation. In order to estimate the amount of carbon delivered by bacterioplankton, we assumed 12.4 fg C for each bacterial cell, which is an average of values measured for open ocean bacteria (2-23 fg C; Fukuda et al., 1998; Bart et al., 2021).

6.2.4.2 Flux calculations in the BBL

In order to calculate the fluxes of bacterioplankton and nutrients within the benthic boundary layer, a turbulent diffusion model was used. The downward flux of bacteria and nutrients, *F*, was estimated from the vertical gradients in bacteria and nutrient concentration, *dc/dz*, observed in the profile pump data by considering

$$F = K_z \frac{dc}{dz} \ , \qquad (1)$$

where *F* is in units of bacteria $m^{-2}\ s^{-1}$ or nutrients in $\mu mol\ m^{-2}\ s^{-1}$, *c* is in bacteria m^{-3} or nutrients $\mu mol\ m^{-3}$, *z* (height above bed) is in m, and K_z is a vertical diffusion coefficient (with units $m^2\ s^{-1}$).

Assuming vertical transfer of bacteria or nutrients occurring mostly by turbulent diffusion (and assuming no density stratification in the BBL), K_z is equal to the diffusion coefficient which applies to the downward flux of horizontal momentum by turbulent diffusion. K_z can therefore be approximated as $\kappa u^* z$, where κ is the von Kármán constant (≈0.4) and u^* is the friction velocity (in m s^{-1}). This approximation captures the suppression of vertical eddies by the bed and assumes K_z increases linearly with *z*.

Substituting the above expression for K_z into (1) and rearranging gives

$$\frac{\kappa u^*}{F} dc = \frac{dz}{z} \ . \qquad (2)$$

Integrating both sides of (2), applying the boundary condition *c* = 0 at *z* = *z′*, and rearranging further gives an expression for the dependence of *c* on *z* as follows:

$$c = \frac{F}{\kappa u^*}\ln\left(\frac{z}{z\prime}\right) \qquad (3)$$

Here, z' is the height above the bed at which the concentration c falls to zero. The downward flux of bacteria (or nutrients) *F* can then be estimated from the gradient $m = \frac{F}{\kappa u^*}$ of a linear regression of *c* against ln(*z*), if the friction velocity *u** is known. Here, we determined values for *u** from the observed turbulent velocity profiles (i.e., the Aquadopp ADCP data). *u** was calculated for the three profile pump deployments (high, intermediate, and low flow) by fitting a simple parameterisation of turbulent flow to the data from the logarithmic portions of the current velocity profiles:

$$u = \frac{u^*}{\kappa}\ln\left(\frac{z}{z_0}\right) , \qquad (4)$$

where *u* is the magnitude of the horizontal current velocity and z_0 is known as the roughness length. *u** was determined from the gradients of linear regressions of *u* on ln(*z*).

Velocity profile data has been time-averaged over each 1.5 h pumping period. The first few (proximal) depth bins (up to 1.6 m) of the ADCP data returned values that indicated frame acceleration effects, and they were therefore excluded from the analysis. Friction velocity, *u** values were calculated to be of order 0.01 m s^{-1} (0.004 – 0.02 m s^{-1}) and *m* values were of order $1x10^{10}$ bacteria m^{-3} ($3.4x10^9$ – $1.7x10^{10}$ bacteria m^{-3}) or 10 to $1x10^4$ µmol m^{-3} for inorganic nutrients. Fluxes determined from these values are reported in the Results section.

Roughness length z_0, averaged over the three deployments, was 0.5 ± 0.7 m (mean ± SD). Roughness length is the height above bed at which the horizontal current speed theoretically becomes zero if we extrapolate the logarithmic part of the velocity profile downwards. In reality, a viscous sub-layer exists beneath the logarithmic turbulent layer and current speed only truly goes to zero within this sub-layer, at the bed itself. Roughness length, however, scales with bed roughness (e.g., due to grain size, bedforms, biogenic structures etc.), and the proximity of the (rather large) calculated mean z_0 to the observed larger hexactinellid sponges and other erect species (e.g. soft corals) on the Schulz Bank (~0.5 m length) is notable. This observation suggests that further investigation on the potential role of these organisms on flow regime and how they benefit from this might be rewarding.

6.3 Results

6.3.1 In-situ incubations

The summit of the Schulz Bank was characterized by the presence of a ca. 20 cm thick spicule layer, which was covered by a mixed assemblage of sponge species as well as associated megafauna like anemones, tunicates, and soft corals. Based on sponge biomass (dry weight), three incubations contained >240 g of sponge dw and the remaining three incubations contained <30 g of sponge dw (form hereon referred to as 'high' and 'low' sponge biomass respectively, Table 6.1). These incubations also contained a variable associated megafauna community like anemones and soft corals (Table 6.1). The bottom water temperature inside the incubation chambers was on average 0.15 ± 0.01 °C (mean ± SD).

6.3.1.1 Oxygen flux of in-situ incubations

The sponge community on the Schulz Bank summit respired on average 0.70 ± 0.31 mmol O_2 m^{-2} h^{-1}. The low sponge biomass incubation (no. 1) showed the lowest O_2 uptake (0.23 mmol O_2 m^{-2} h^{-1}). The high sponge biomass incubations (no. 4-6, Figure 6.2) had a significantly higher oxygen uptake (0.96 ± 0.02 mmol O_2 m^{-2} h^{-1}; Figure 6.2a) compared to incubations with a low biomass of sponges (0.44 ± 0.20, t-test, p=0.042). Hence, a high sponge biomass more than doubled the average O_2 uptake (Figure 6.2b).

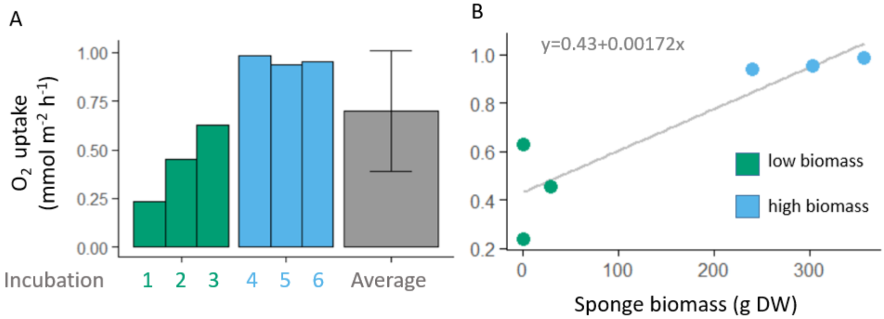

Figure 6.2 a) Oxygen uptake per incubation and average of all incubations (grey ± SD), b) Respiration per sponge biomass with a linear trend line indicating the overall increase in oxygen consumption as a function of increased biomass.

6.3.1.2 Bacterioplankton fluxes of in-situ incubations

The initial bacterioplankton concentrations at the start of the incubations ranged from 5.6 x 10^4 to 2.4 x 10^5 cells ml^{-1} (average 1.5 x 10^5 bacteria ml^{-1}, see Figure S6.2 in supplements). Bacterial uptake in the in-situ incubations did, however, not show a consistent pattern in 5 out of 6 incubations (see Figure S6.2 in supplements). A significant initial removal rate of 5.5 x10^6 bacteria m^{-2} h^{-1} ($r = 0.98$, $p < 0.01$) was found for one of the low sponge biomass incubations (no. 2), which showed a bacterioplankton carbon removal rate of 1.4 x 10^{-5} mmol C m^2 h^{-1}. Fluxes could not be calculated for the other in-situ incubations.

6.3.1.3 Nutrient flux – Inorganic nitrogen and phosphate fluxes of in-situ incubations

Fluxes for the most important inorganic nutrients (nitrogen and phosphate) were measured during the in-situ incubations. Dissolved inorganic nitrogen (DIN: sum of NH_4^+, NO_3^- and NO_2^-) was released with on average 39.9 ± 24.3 mmol DIN m^{-2} h^{-1} from the sponge community during the in-situ incubations (Figure 6.3a). The three high sponge biomass incubations showed an almost 6 times higher average release rate of DIN (29.2 ± 24.6 mmol m^{-2} h^{-1}) than low biomass incubations (4.8 ± 2.7 µmol m^{-2} h^{-1}), albeit that because of the large inter-incubation differences this offset is not significant (t-test, p=0.20). NH_4^+ was released with an average of 18.6 ± 21.1 µmol

m^{-2} h^{-1}, except that for one incubation it was not possible to calculate a flux due to a poor model fit (no.3). This incubation showed an increase, followed by a decrease in concentration, not observed in the other incubations (see Figure S6.3 in supplements). Incubations with a higher sponge biomass showed higher release of NH_4^+ (28.0 ± 23.6 µmol m^{-2} h^{-1}) compared to incubations with a lower biomass of sponges (4.63 ± 2.58 µmol m^{-2} h^{-1}), but the difference is not significant ($p = 0.23$). The variation in nutrient fluxes in the high biomass incubations differ when considering sponge type (LMA versus HMA). Incubations with a high biomass of LMA sponges (red stars, Figure 6.3) released on average 10 times more NH_4^+ (39.9 ± 16.3 µmol m^{-2} h^{-1}) than incubations with a high biomass of HMA (blue star, Figure 6.3, 4.1 µmol m^{-2} h^{-1}) or low sponge biomass (4.6 ± 2.5 µmol m^{-2} h^{-1}). NO_3^- was released in all incubations with an average of 26.6 ± 7.6 µmol m^{-2} h^{-1}. Incubations with a higher sponge biomass show a trend towards a lower release of NO_3^- (22.1 ± 5.8 µmol m^{-2} h^{-1}) compared to incubations with a lower biomass of sponges (31.2 ± 6.9 µmol m^{-2} h^{-1}, $p = 0.16$). Incubations with a high biomass of LMA sponges had on average a ~1.5 times lower release in NO_3^- (18.8 ± µmol m^{-2} h^{-1}) compared to high biomass of HMA incubations (28.7 µmol m^{-2} h^{-1}) and low sponge biomass incubations (31.1 ± 6.9 µmol m^{-2} h^{-1}).

Release of NO_2^- was relatively limited in all incubations (average of 1.3 ± 1.4 µmol m^{-2} h^{-1}, Figure 6.3d). One incubation with a low sponge biomass (no. 1) actually showed a slight uptake of NO_2^- (-0.3 µmol m^{-2} h^{-1}), with the other incubations showing modest release. Incubations with a higher biomass of sponges show a trend towards higher NO_2^- release (2.3 ± 1.1 µmol m^{-2} h^{-1}) compared to incubations with a lower biomass of sponges (0.3 ± 0.7 µmol m^{-2} h^{-1}, $p = 0.07$). Similar to NH_4^+, highest release of NO_2^- was observed in the incubations with a high biomass of LMA sponges (2.9 ± 0.9 µmol m^{-2} h^{-1}). The release was on average about double the flux of incubations with a high biomass of HMA (1.3 µmol m^{-2} h^{-1}), and 10 times the flux of low sponge biomass incubations (0.3 ± 0.7 µmol m^{-2} h^{-1}).

In general PO_4^{3-} was released in all incubations, with an average of 4.9 ± 3.4 µmol m^{-2} h^{-1} (Figure 6.3e). PO_4^{3-} fluxes did show an about 2 times higher release rate in the high sponge biomass incubations (6.6 ± 4.1 µmol m^{-2} h^{-1}) compared with low biomass incubations (3.3 ± 2.8 µmol m^{-2} h^{-1}, $p = 0.32$). Incubations with a high biomass of LMA sponges showed a 20 to 40% higher release rate of PO_4^{3-} (8.5 µmol m^{-2} h^{-1}) compared to HMA (1.9 µmol m^{-2} h^{-1}) and low sponge biomass incubations (3.5 µmol m^{-2} h^{-1}).

Unfortunately, there were not enough incubations performed to calculate if the differences between the sponge groups are significant (n=1 for HMA, n=2 for LMA, n=3 for low sponge biomass).

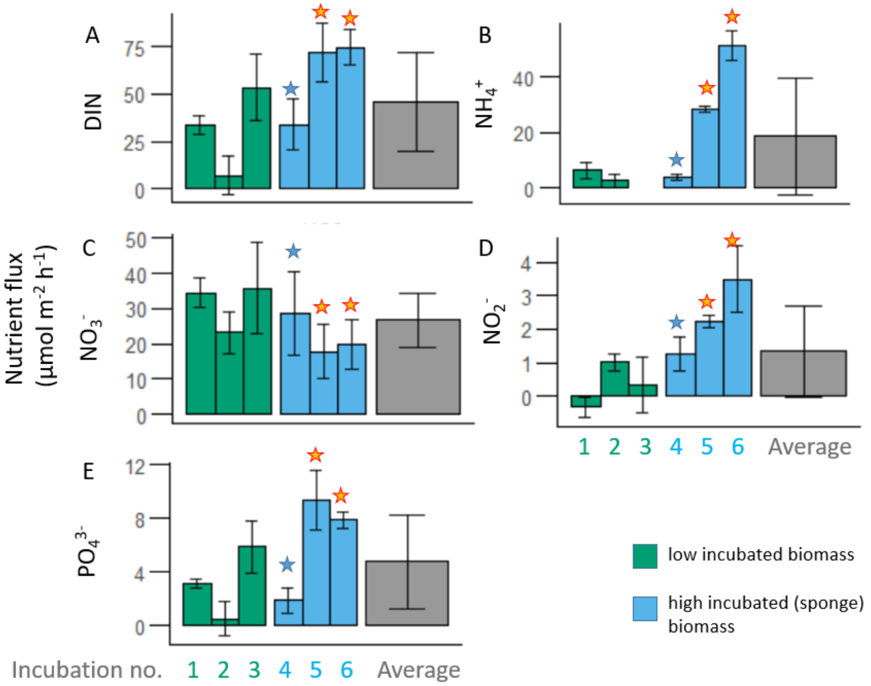

Figure 6.3 Inorganic nutrient fluxes of all incubations ± SE of linear regression, divided into incubations with a low (green) and high (blue) biomass of sponges and average of all incubations (grey ± SD). Incubations with dominantly LMA sponges are marked with a red star and incubations with HMA sponges are marked with a blue star.

The N:P ratio ($DIN:PO_4^{3-}$) in the incubations was on average 15.1:1 compared to the optimal Redfield ratio of 16:1, similar to the value of 15.3:1 which was measured for the ambient sea water (t_0, Figure 6.4, red lines). Ratios derived from the linear regression of DIN vs.

PO_4^{3-} did not differ strongly between incubations. Incubations with a high biomass of LMA sponges ($y= 7.62x + 6.73$, $r^2= 0.73$, blue values, Figure 6.4a and Figure S6.4 in supplements) were very similar to incubations with a low biomass of sponges ($y= 7.74x + 6.66$, $r^2= 0.72$, green values), whereas incubations with a high biomass of HMA sponges had a slightly higher ratio ($y= 12.7x + 2.25$, $r^2= 0.89$).

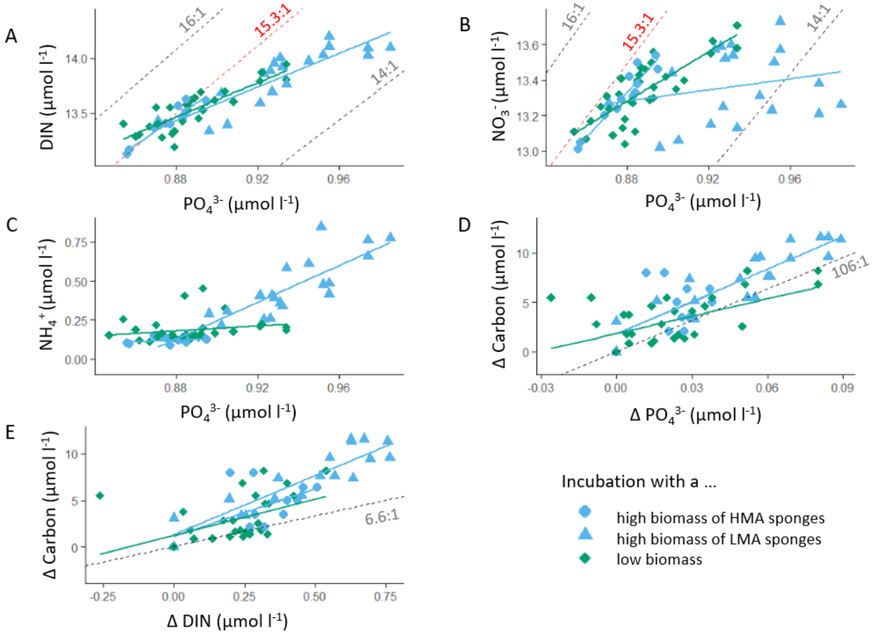

Figure 6.4 a-c) Inorganic nitrogen concentrations vs. phosphate concentration and linear regressions of three main incubation types including the optimal Redfield Ratio (16:1, dotted black line) as well as the oceanic water ratio (dotted, red line). d-e) Difference in the carbon concentration vs. difference in inorganic nutrient release and linear regressions of three main incubation types and the expected Redfield ratio.

Incubations with a high biomass of LMA sponges were also showing a 12 times higher NH_4^+: PO_4^{3-} ratio ($5.89x + 5.0$ $r^2= 0.70$, Figure 6.4c) compared to HMA sponge incubations ($y= 0.49x + 0.31$, $r^2= 0.12$) and incubations with a low biomass of sponges ($y= 0.79x + 0.52$, $r^2= 0.04$). The strongest difference in the nutrient ratios were observed in the ratio of NO_3^-: PO_4^{3-} where incubations with a high biomass of LMA sponges ($y= 1.56x + 11.9$, $r^2=0.04$) had an about 8 times lower ratio than HMA sponges ($y= 12.6x + 2.23$, $r^2=0.9$, Figure 6.4b). The ratio between carbon consumption and phosphate and DIN release were very similar between all incubations and was on average 90:1 for ΔC: ΔPO_4^{3-} (Redfield ratio = 106:1) and 10:1 for ΔC:ΔDIN (Redfield ratio 6.6:1).

6.3.2 Gradients in the benthic boundary layer and water column

Water samples were collected with a profile pump between 0.1 and 2.1 mab. The analyses were differentiated based on average current speed into 0.26 ± 0.07 m s^{-1} (in 1.2 mab, high), 0.09 ± 0.05 m s^{-1} (intermediate) and 0.05 ± 0.02 m s^{-1} (low), respectively (Table 6.2). The average temperature measured during the profile pump deployments were rather similar at 0.05 ± 0.09°C during high current speed, -0.05 ± 0.01°C during intermediate currents and 0.14 ± 0.03°C during low currents.

Table 6.2 Profile pump deployments with average near-bed environmental conditions during the sampling periods.

Profile pump deployments	Average current during sampling period in 1.6 mab (m s^{-1})	Average temperature during sampling period (°C)	Current direction during the sampling period
GS2018108-6	0.26 ± 0.07 (high)	0.05 ± 0.09	SW
GS2018108-16	0.09 ± 0.05 (intermediate)	-0.05 ± 0.01	NW
GS2018108-32	0.05 ± 0.02 (low)	0.14 ± 0.03	NE

6.3.2.1 Bacterioplankton in the benthic boundary layer

Bacterioplankton concentration was on average 1.3 x 10^5 bacteria ml^{-1} within the BBL, with no differences between the different current speeds. This concentration is in the same range as the initial bacterioplankton concentration measured for the in-situ incubation experiments (average 1.5 x 10^5 bacteria ml^{-1}, see 6.3.1.2). In the BBL towards the sponge ground a gradient was observed with decreasing bacterioplankton abundance towards the sea floor during all three deployments (Figure 6.5). During low current speed bacterioplankton abundances decreased approximately 5 % from 2.1 mab (~1.3 x 10^5

bacteria ml^{-1}) towards 0.1 mab (~1.2 x 10^5 bacteria ml^{-1}). During the intermediate current regime the change in bacteria over the same depth range was highest (~30%), decreasing to a minimum of 1 x 10^5 bacteria ml^{-1}. During high current speed the bacterial concentration decreased with about 7 % lower values being observed close to the sediment water interface.

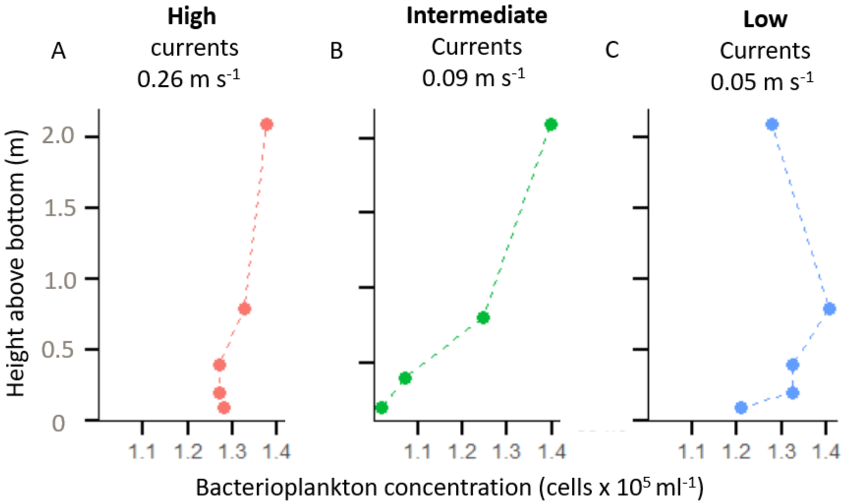

Figure 6.5 Bacterioplankton concentrations inside the benthic boundary layer during a) high, b) intermediate and c) low currents.

6.3.2.2 Inorganic nutrients in the benthic boundary layer

We were able to observe gradients in inorganic nutrient concentrations within the benthic boundary layer (Figure 6.6). The inorganic nutrient concentration profiles measured in the BBL differed depending on the current condition (Figure 6.6). The highest average NH_4^+ concentrations within the BBL were observed during the high currents (0.09 ± 0.03 µmol l^{-1}) and lowest during low current conditions (0.06 ± 0.01 µmol l^{-1}, Figure 6.6a). During all current conditions, the NH_4^+ concentration was increasing from 2.1 mab towards the bottom (0.1 mab) by on average 44 ± 7 %. The NO_3^- concentration within the BBL did not change from 2.1 mab towards the bottom at 0.1 mab (<1% difference, Figure 6.4b). The average

NO_3^- concentration within the whole BBL was highest during lowest current speed (13.6 ± 0.03 µmol l^{-1}, Figure 6.6). The average concentration of NO_2^- over the whole BBL between the different current regimes did not change (average of 0.020 ± 0.002 µmol l^{-1}, Figure 6.6c), whereas values were close to the detection limit. Only during intermediate (+65%) and high (+15%) currents the concentration of NO_2^- was higher in the lower 0.2 mab, whereas the error between duplicates was very large. The average concentration of PO_4^{3-} within the BBL did not change between the current scenarios and was on average 0.91 ± 0.01 µmol l^{-1}. The PO_4^{3-} concentration within the BBL showed a slight decrease from 2.1 mab towards the bottom (~1%). The N:P (NO_3^-: PO_4^{3-}) ratio was on average 14.9 ± 0.1 within the BBL during all current scenarios.

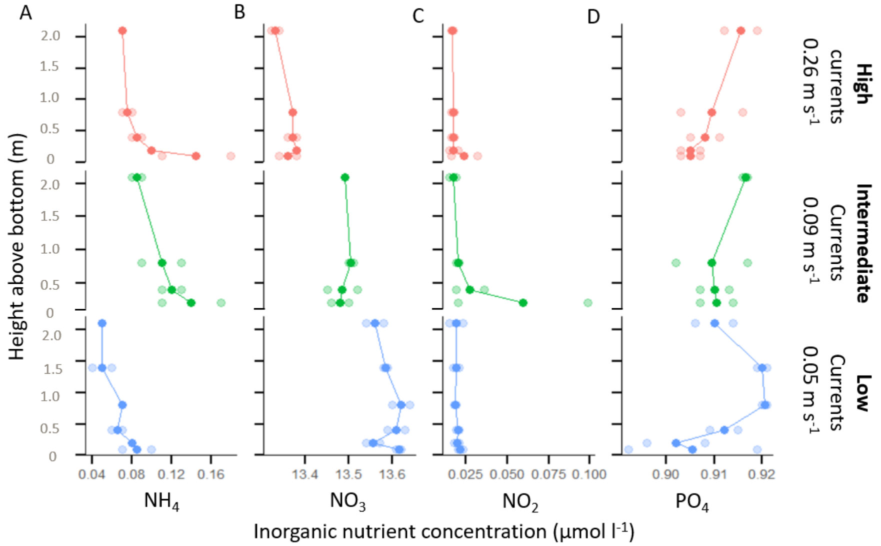

Figure 6.6 a-d) Nutrient concentrations within the BBL. Transparent dots represent technical replicates, full dots represent averages.

6.3.2.3 Bacterioplankton and nutrient fluxes by turbulent diffusion in the BBL

The drawdown of bacterioplankton and release of nutrients near the seabed was estimated from the vertical gradients in bacteria and inorganic nutrient concentrations within the BBL (Table 6.3). The average drawdown of bacterioplankton over the three deployments was 6 ± 5 x10^7 bacteria m^{-2} s^{-1}, which is close to flux at intermediate current conditions (8 x 10^7 bacteria m^{-2} s^{-1}). Higher fluxes were

observed during low speed (1 x 10^8 bacteria m^{-2} s^{-1}), and lower fluxes during the period of high flow (5 x 10^6 bacteria m^{-2} s^{-1}).

The average nutrient flux within the BBL showed a release for NH_4^+, NO_3^- and NO_2^- and suggests a net uptake for PO_4^{3-} (Table 6.3). The highest release rate for NH_4^+ was on average 305 ± 152 µmol m^{-2} h^{-1}, observed during low and intermediate current speeds, while a lower flux was observed during high current speeds. The release of NO_3^- was not consistent between all current scenarios since during intermediate currents a positive flux was measured. NO_2^- was released on average by 25 µmol m^{-2} h^{-1}. PO_4^{3-} was the only nutrient for which a net average downward flux (benthic uptake) of 68 ± 64 µmol m^{-2} h^{-1} is suggested by the profiles. The lowest uptake was measured during high current conditions (19.6 µmol m^{-2} h^{-1}) and highest during slow current speed conditions (141 µmol m^{-2} h^{-1}). Still, differences in the inorganic nutrient concentrations within the BBL, especially of NO_2^- and PO_4^{3-}, were not high, which leads towards high uncertainties of the absolute fluxes.

Table 6.3 Bacteria and nutrient fluxes within the BBL during different current conditions calculated by the diffusion model, compared to fluxes from the in-situ incubation chambers. Uptake, opposite to a release, is marked with an #.

Current conditions	**Bacterioplankton** (cells m^{-2} s^{-1})	**NH_4^+** (µmol m^{-2} h^{-1})	**NO_3^-** (µmol m^{-2} h^{-1})	**NO_2^-** (µmol m^{-2} h^{-1})	**PO_4^{3-}** (µmol m^{-2} h^{-1})
High	# 5 x 10^6	128.7	57.5	11.3	# 19.6
Intermediate	# 8 x 10^7	392.6	# 99.4	39.2	# 42.4
Slow	# 1 x 10^8	392.7	227.7	24.5	# 141.1
Average ± SD	**# 8** ± 7 x 10^7	**305** ± 152	**62** ± 163	**25** ± 14	**# 68** ± 64
From in-situ incubations	# 5.5 x 10^6 (n=1)	18.6 ± 21.1 (n=5)	26.6 ± 7.6 (n=6)	1.3 ± 1.4 (n=6)	4.9 ± 3.4 (n=6)

6.4 Discussion

6.4.1 Oxygen consumption and carbon uptake

Respiration rates of the Schulz Bank sponge ground were driven by sponge biomass (Figure 6.2), whereby the oxygen consumption ranged from 5.6 to 23.6 mmol O_2 m^{-2} day^{-1} with an average of 16.8 ± 7.4 mmol O_2 m^{-2} day^{-1}. This is comparable to other known sponge grounds, like the Norwegian Træna Coral Field (Kutti et al., 2013). Kutti et al. (2013) estimated based on an ex-situ approach that coral reef-associated sponge grounds of large demosponges in 300 m water depth respired similar amounts of oxygen (3 to 34 mmol O_2 m^{-2} day^{-1}). Also Aquatic Eddy Correlation (AEC) measurements in the same area showed slightly higher but overall comparable oxygen uptake (54 ± 5 mmol O_2 m^{-2} day^{-1}; Cathalot et al., 2015). The average oxygen consumption implies an average carbon consumption rate of 67 to 283 to on average 202 mg C m^{-2} day^{-1} or 16.8 mmol C m^{-2} day^{-1} (assuming an RQ of 1). This simplified value was used since no further information about the RQ in deep-sea ecosystems is yet available, whereas it can be expected that the value lays between 0.8 and 1.6 since it depends on the elemental composition of the substrate and the fraction of substrate that is respired (Kutti et al., 2013; Maier et al., 2020; Pham et al., 2019; Cathalot et al., 2015; Leys et al., 2018; De Kluijver et al., 2021; Tanioka and Matsumoto, 2020).

The estimated carbon demand reflects the minimal carbon requirement for respiration and does not include carbon needed for other metabolic processes like for example growth, production of secondary metabolites, turnover cells and reproduction (Bart et al., 2021). Compared to soft sediment communities in the deep sea, the carbon uptake of the Schulz Bank sponge ground community is much higher, based on actual in situ measurements. Carbon uptake falls in the same range as that of deep-sea hotspots like for example scleractinian cold-water coral reefs on the Rockall Bank, where a carbon consumption between 12 and 57 mmol C m^{-2} day^{-1} was found (De Froe et al., 2019; Oevelen et al., 2009). This cold-water coral reef occurs at a similar water depth as the Schulz Bank sponge community but thrives at a much higher temperature (7 to 9°C; van Oevelen et al., 2009; Mienis et al., 2007). Specifically temperature is an important variable to include in comparisons, since lower temperatures generally result in lower respiration rates (Coma, 2002; Dodds et al., 2007). However the sponge community at the Schulz Bank summit has a similar oxygen demand as the coral community that is living at >7°C higher temperatures.

The high metabolic activity of the sponge ground community has important implications when considering carbon cycling, and therefore benthic-pelagic coupling, on an ecosystem scale. The sponge ground community at Schulz Bank consumes as much carbon as a sponge ground inside the much shallower and warmer Norwegian Træna Coral Field (0.2 t C km-2 day^{-1}; Kutti et al., 2013) and exceeds the carbon consumption of sponge grounds at the Flemish Cap by far (0.00046 t C km^{-2} day^{-1}; Pham et al., 2019). As a result of the even higher carbon consumption of the Schulz Bank sponge ground and therefore likely also filtration capacity, we suggest that these sponge grounds play a very important role in carbon cycling in deep-sea benthic ecosystems. It also shows, that carbon cycling in the deep sea is very localized and likely depends on certain hydrodynamic conditions, which are delivering enough organic matter towards the benthic communities to support their metabolic demand (Hanz et al., 2021).

6.4.2 Carbon sources at the Schulz Bank summit

Sponge community carbon requirements need to be covered by sufficient carbon input to sustain a thriving ecosystem. Most benthic fauna relies on particulate organic matter which originates from surface ocean productivity (Ruhl et al., 2008; Smith et al., 2008). The (vertical) flux of particulate carbon supplied to the sponge ground community at the Schulz Bank was determined in an earlier study and is on average 9.3 ± 7.6 mg C m^{-2} day^{-1} (Hanz et al., 2021), which equals on average < 5% of the carbon demand (Figure 6.7). A large deficit between vertical flux and carbon demand is known for many deep-sea ecosystems, such as for example for a sponge ground at the western and eastern Canadian shelf (Kahn et al., 2015; Hanz et al., 2021) as well as for cold-water coral ecosystems (Oevelen et al., 2009). Only after the summer phytoplankton bloom period the sponge ground community of the Schulz Bank temporarily receives higher amounts of particulate carbon, with nearly 12% of the carbon demand being covered from the vertical C flux (28.4 mg C m^{-2} day^{-1}; Hanz et al., 2021), but the organic matter deficits rapidly increases during the remainder of the year.

Newer evidence suggests that also “dark energy” contributes significantly to the carbon budgets of deep sea ecosystems (Danovaro et al., 2014), which is the energy that is fixed by microbial life. These microbes rely on dissolved resources and can then act as an additional source of carbon for the food web, accounting for 19% of the total heterotrophic biomass production (Molari et al., 2013). Bacteria for example contain valuable vitamins, fatty acids and amino acids, which are essential for anabolic processes (Bart et al., 2021). The uptake of bacterioplankton in the in-situ incubations of this study could not be quantified except for one incubation, which might be due to the fact that sponges filter high amounts of water in very short time periods removing all labile parts of the bacterioplankton before we were able to capture a significant trend in bacterial densities. Ex-situ incubations of Bart et al. (2021) for example were showing at least a 2 times higher initial bacterioplankton concentration, than measured in this study. However, the bacterioplankton concentration at the beginning of the incubations was similar to the concentration within the BBL. Still, it is likely that microorganisms from the water column play an important role in the nutrition of sponges on the Schulz Bank. A decrease in bacterioplankton concentrations towards the seafloor within the BBL was consistently observed, suggesting that the sponge ground community actively depletes the surrounding water. Bacterioplankton drawdown based on these profiles showed a flux (6 ± 5 x 107 bacteria m^{-2} s^{-1}) comparable to the single flux measured by the in-situ incubation (5.5 x 106 bacteria m^{-2} s^{-1}). During high current scenarios the concentration of bacterioplankton throughout the whole BBL was higher, which indicates, that higher currents do replenish bacterioplankton in the first m above the sponge community. The bacterioplankton flux corresponds to an estimated uptake of 85.7 mg C m^{-2} day^{-1} (12.4 fg C for each bacterial cell, see 6.2.4.1), potentially covering up to 40% of the sponge ground carbon demand (202 mg C m^{-2} day^{-1}). This is a higher value than found in earlier studies, where only 5% of the sponges total carbon budget was based on bacteria, with the remainder consisting of particulate organic matter and for a major part DOC (Leys et al., 2018; Bart et al., 2021). A higher bacterioplankton flux was also observed when comparing these values with the fluxes of the in-situ incubation in this study, which showed an about 10 times lower bacterioplankton flux. The overestimation can be related to the flux calculations which are based on a turbulent diffusion model, excluding other physical and biological factors. Additionally, currents up to 1.6 m above the bottom could not be measured due to the characteristics of the setup and are therefore extrapolated for this model assuming a logarithmic vertical velocity structure of the BBL (Thomsen, 2002), which might overestimates fluxes appearing in the lower BBL.

Likely major parts of the observed deficit in carbon demand are covered by DOC, which in general cannot be taken up by benthic megafauna. Large part of the DOC in the oceans is refractory (Hansell, 2013), which also does not allow many microorganisms to access this resource. DOC is nevertheless expected to be the main source of carbon for sponges. Bart et al., 2021 showed that DOC is responsible for over 90% of the total net organic carbon removal in ex-situ experiments. Unfortunately, no DOC data is available for this study. Measuring DOC from in-situ experiments and within the BBL should have priority for future studies to be able to close the carbon budget for deep-sea sponge grounds.

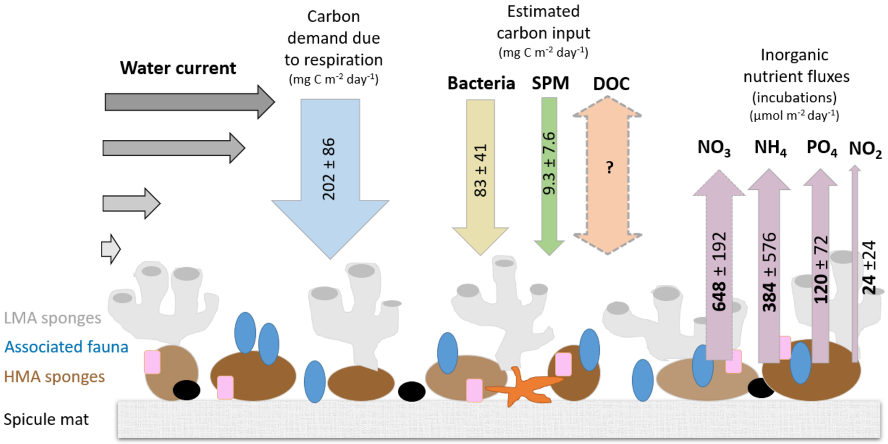

Figure 6.7 Estimated carbon and nutrient fluxes of the Schulz Bank sponge ground community.

6.4.3 Nutrient exchange

The Schulz Bank sponge ground community was shown to acts as a net source for inorganic nutrients (Figure 6.3 and 6.4). The release of DIN by the sponge ground community increased the local concentration of NO_x and NH_4^+ in the BBL, showing a "sponge ground effect" (Figure 6.4, Table 6.3). NH_4^+ was released in all in-situ incubations with an average of 18.6 ± 21.1 µmol m^{-2} h^{-1}, which is expected from invertebrates and also known from for example CWC reefs, where a very comparable flux of about 17 µmol m^{-2} h^{-1} was measured (De Froe et al., 2019).

Specific nitrogen release rates between sponge groups can be explained by the fact that the nitrogen cycle is highly associated with the activity of their associated microbes (Ward et al., 2007). Highest nitrogen releases were found in the incubations with a high biomass of LMA sponges. LMA sponges are known to convert particulate organic nitrogen to dissolved organic nitrogen and NH_4^+, which is then released into the BBL (Maldonado et al., 2012). The release of NH_4^+ was leading to a higher NH_4^+: PO_4^{3-} ratio within the incubations with a high biomass of LMA sponges, compared to the other incubations. Interestingly, the overall stoichiometry of DIN:PO_4^{3-} ratio is not influenced by this NH_4^+ efflux and incubations with a high biomass of LMA sponges and a low biomass of sponges have similar ratios. Also, the overall relation between oxygen uptake, phosphate and DIN remains the same comparing the incubations with a high biomass of LMA and HMA sponges and incubations with a low biomass of sponges. This shows that during all incubations food with similar C:N:P ratio was consumed, which suggest that they rely on the same food source. Since bacteria and POC only contribute to a maximum of 30%, this is most likely DOC (Bart et al., 2021).

The NH_4^+ that is released by LMA sponges and thereby lost to the water column is available for the efficient microbial community hosted by the HMA sponges and microbes within the water column, which use this ammonia as energy source. At the Schulz Bank the concentration of NH_4^+ in the BBL was higher closer to the bottom especially during slow current conditions. During these low current conditions water is less quickly replaced and diluted compared to high current conditions, when the NH_4^+ likely gets washed away. The release of NH_4^+ in the in-situ incubations was about 20 times smaller (15.6 ± 24.1 µmol m^{-2} h^{-1}) than the estimated average flux in the BBL (305 µmol m^{-2} h^{-1}), which might be explained by the limitations of the diffusion model, as stated above. Another major factor in a smaller release of NH_4^+ could be the incubation set-up. The released NH_4^+ might be taken up by the HMA sponges within the incubation chambers since they have the chance to recycle NH_4^+ which otherwise would be released towards the BBL, where it is not available for the HMA sponges anymore. This would indicate a major downside for the in-situ incubation chambers when measuring net community nitrogen fluxes.

In contrast to most marine animals, many HMA sponges, like for example *Geodia barretti*, are found to release NO_3^- with no significant release of NH_4^+ or NO_2^- (Leys et al., 2018; De Kluijver et al., 2020). NO_x is produced in the lower BBL by chemosynthesis by HMA sponge associated microorganisms, which stands in contrast with the low rates or even lack of nitrification in LMA species (Maldonado et al., 2012; Schläppy et al., 2010). NO_2^- and NO_3^- are released due to the oxidation of NH_4^+ for energetic purposes (called nitrification/denitrification), which is mediated by ammonia oxidizing bacteria or archaea and the nitrite oxidizing bacteria associated to the HMA sponges (Schläppy et al., 2010; Ribes et al., 2012; Van Bleijswijk et al., 2015). The release of NO_3^- is also responsible for the slightly higher DIN:PO_4^{3-} ratio in incubations with a high biomass of HMA sponges, which comes closer to the expected Redfield ratio. The concentration of NO_2^- in the BBL of the Schulz Bank sponge ground showed an increase very close to the bottom, indicating (low) nitrification processes of probably HMA sponges, which are situated close to the bottom and are overgrown by other fauna. These fluxes were not influenced by current speed, which is likely caused by the smaller influence of the hydrodynamics in the last centimeters above the bottom. Additionally aerobic sediments are known to release NO_x produced by nitrifying microorganisms in the sediment itself (Thamdrup and Dalsgaard, 2008; De Froe et al., 2019), which might take place in the probably well aerated spicule mat. Nevertheless, NO_2^- fluxes are very small and effects can lay within the variation in the data.

The in-situ incubations of this study showed also a release of PO_4^{3-} with a trend towards a higher release in the incubations with LMA sponges. In general phosphorous is an essential nutrient required by all organisms for biological synthesis and energy transfer processes (Tyrrell, 1999). Sponges release excess phosphorous in form of inorganic dissolved PO_4^{3-} if sufficient P is taken up from the particulate diet (Taylor et al., 2007; Maldonado et al., 2012). Release of PO_4^{3-} by sponges was also described in other studies, including HMA and LMA sponges (Yahel et al., 2007; Ribes et al., 2012; Taylor et al., 2007). The profile pump flux calculations on the other hand showed no clear release and even suggest net uptake of PO_4^{3-} by the benthic community. This would point towards a deficit in the availability of phosphate from the sponge diet. We do not know what is causing the difference in PO_4^{3-} fluxes between the in-situ incubations and the fluxes within the BBL, but concentration differences of PO_4^{3-} within the BBL were small which hampers quantification by the diffusion model. Flux calculations introduce an additional error, which could lead towards the differences in the net phosphate fluxes. Accordingly, the fluxes determined by the in-situ incubations probably better reflect the true sponge ground PO_4^{3-} fluxes, since no recycling processes between HMA and LMA sponges are expected.

The incubations in this study involved the integrated community including all associated benthic organisms, such as a relatively high number of anemones and tunicates (Table 6.1). Unfortunately, individual nutrient fluxes for these associated benthic species are not known so far. Nevertheless, due to the high abundance and biomass of sponges, the metabolic activity of sponges likely dominates the local carbon and nutrient cycling (Figure 6.3). This is important in food limited deep-sea ecosystems, since sponges transfer organic matter as detritus to the associated fauna (Bart et al., 2021; Maier et al., 2020). Released nitrogen by the benthic fauna might also support the growth of microorganisms in the water column above it and/or in the sponge-biome. Shallow water sponges for example are known to process bacterial food and release inorganic nutrients in the benthic boundary layer, which support for example photoautotrophic plankton (Jiménez and Ribes, 2007; De Goeij et al., 2013). Similarly, microorganisms hosted by the sponge biome might take advantage of the ammonia released by the associated fauna.

6.4.4 Role of environmental conditions at the Schulz Bank

Internal waves, that cause variability in current speed at the Schulz Bank summit as well as corresponding turbulence and mixing, constantly resuspend material like particulate matter and bacteria in the BBL, allowing filter feeding fauna to access these resources (Van Haren et al., 2014; Hanz et al., 2021). Tidal currents constantly replenish the BBL with resources like bacterioplankton, nutrients and DOM from water layers above and below (Hanz et al., 2021). Additionally, currents will transport waste products (like NH_4^+) away from the sponge community. At low current speeds a strong depletion of bacterioplankton is observed and this will be even lower towards the seafloor since currents are further weakened due to the 3D structure of the sponges, as was also observed in cold-water coral reefs (Mienis et al., 2019). During highest current speeds the bacterial concentration within the lower 1 mab was replenished as shown by increased numbers of bacteria in the entire BBL. The relative higher number of bacterioplankton can also be related to resuspension of bacteria from the spicule mat during high current speeds, as observed during a long-term lander deployment at the Schulz Bank (Hanz et al., 2021). These benthic bacteria can subsequentially be taken up by the ingestion of these resuspended particles (Kuwae and Hosokawa, 1999). Moreover, a constant water flow is needed to induce a beneficial pressure gradient across the sponge wall in order to make the pumping process for sponges more efficient and reduce the energetic costs of pumping and therefore feeding (Leys et al., 2011).

6.5 Conclusion

The Schulz Bank sponge ground community represents a hotspot of carbon and nutrient cycling in the deep sea. Even though ambient temperatures were much lower, respiration rates measured in this study were comparable to other hotspot ecosystems in the deep sea, like cold-water coral reefs. The metabolic activity of sponges dominated the local carbon and nutrient cycling of the sponge ground community, since incubations with higher biomass of sponges showed the highest respiration rates. The sponge ground community thrives at the Schulz Bank due to the specific hydrodynamic conditions that enhance organic matter transport. However, the vertical flux of organic matter cannot cover the energetic costs of respiration and therefore other carbon sources are needed to balance the carbon demand. The high drawdown of bacterioplankton from the benthic boundary layer at the sponge ground suggests that bacteria serve as one of the additional food sources for the benthic community. However, uptake of bacteria still only covers less than half of the required carbon demand. Hence, the contribution of DOC, which is in line with high uptake rates of sponges, needs further investigation in the future to close the carbon budget. The sponge ground community also affected benthic pelagic coupling at the local ecosystem scale, showing an overall release in inorganic nutrients in the benthic boundary layer. LMA sponges released the highest amounts of NH_4^+ and NO_2^-, which might form an additional energy source for chemoautotrophic microorganisms in the sponge microbiome and/or benthic boundary layer. Such a high recycling efficiency might be an essential trait to survive in a dark, deep, cold and above all food deprived deep-sea environment.

6.6 Acknowledgements

This research has been performed in the scope of the SponGES project, which received funding from the European Union's Horizon 2020 research and innovation program under grant agreement No. 679849. This document reflects only the authors' views and the Executive Agency for Small Medium-sized Enterprises (EASME) is not responsible for any use that may be made of the information it contains. FM is supported by the Innovational Research Incentives Scheme of the Netherlands Organization for Scientific Research (NWO-VIDI grant no. 0.16.161.360).

6.7 Supplements

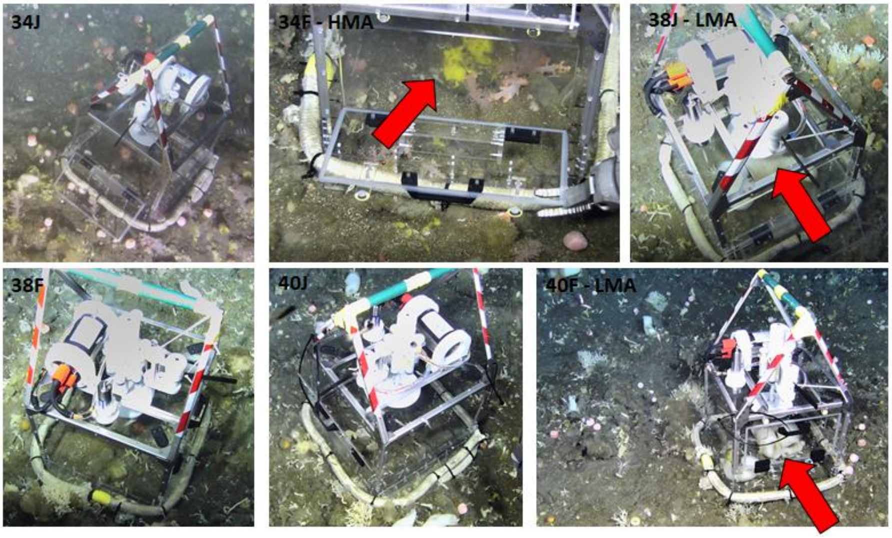

Figure S6.1 Picture of each in-situ incubation, the main incubated sponges are marked with a red arrow.

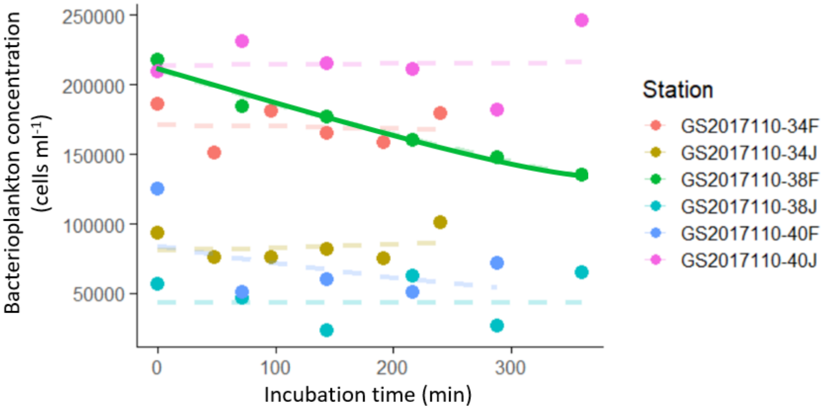

Figure S6.2 Bacterioplankton concentrations during the different in-situ incubations, with the non-significant exponential regressions as a dashed line and the incubation with a significant fit with a solid line.

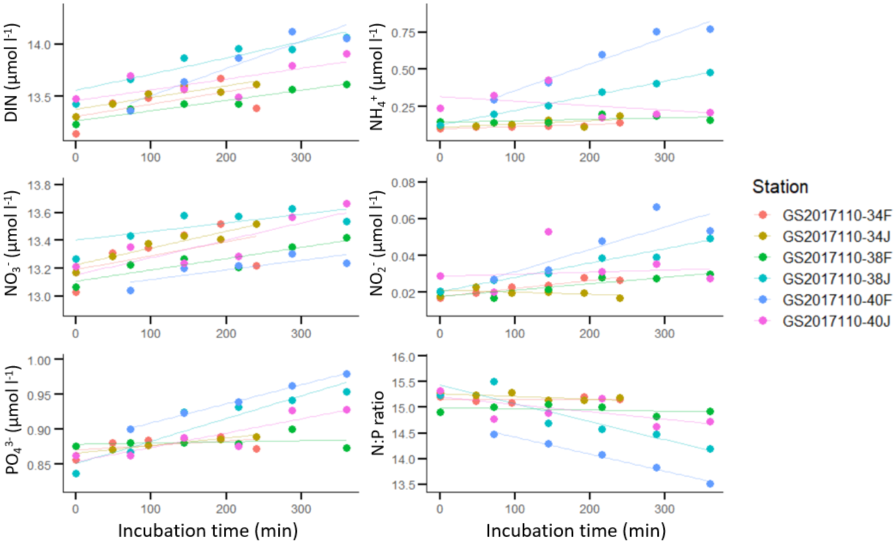

Figure S6.3 Inorganic nutrient concentrations as well as N:P ratio within the in-situ incubations as well as their linear regressions.

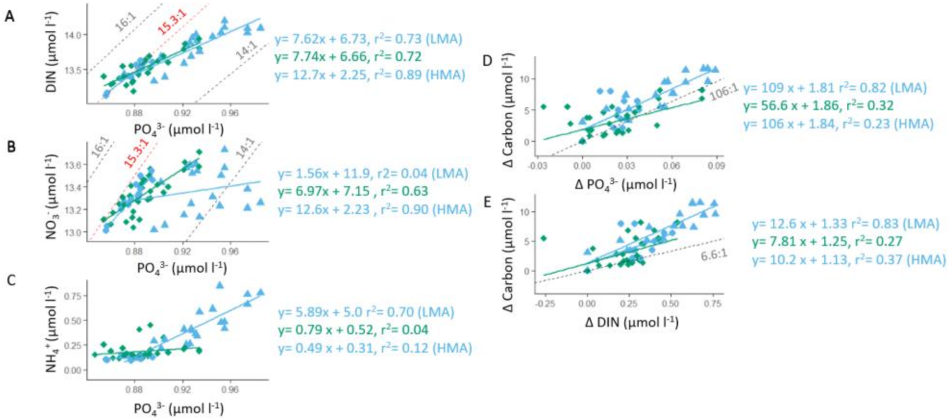

Figure S6.4 Nutrient ratios from Figure 6.4 with their linear regressions.

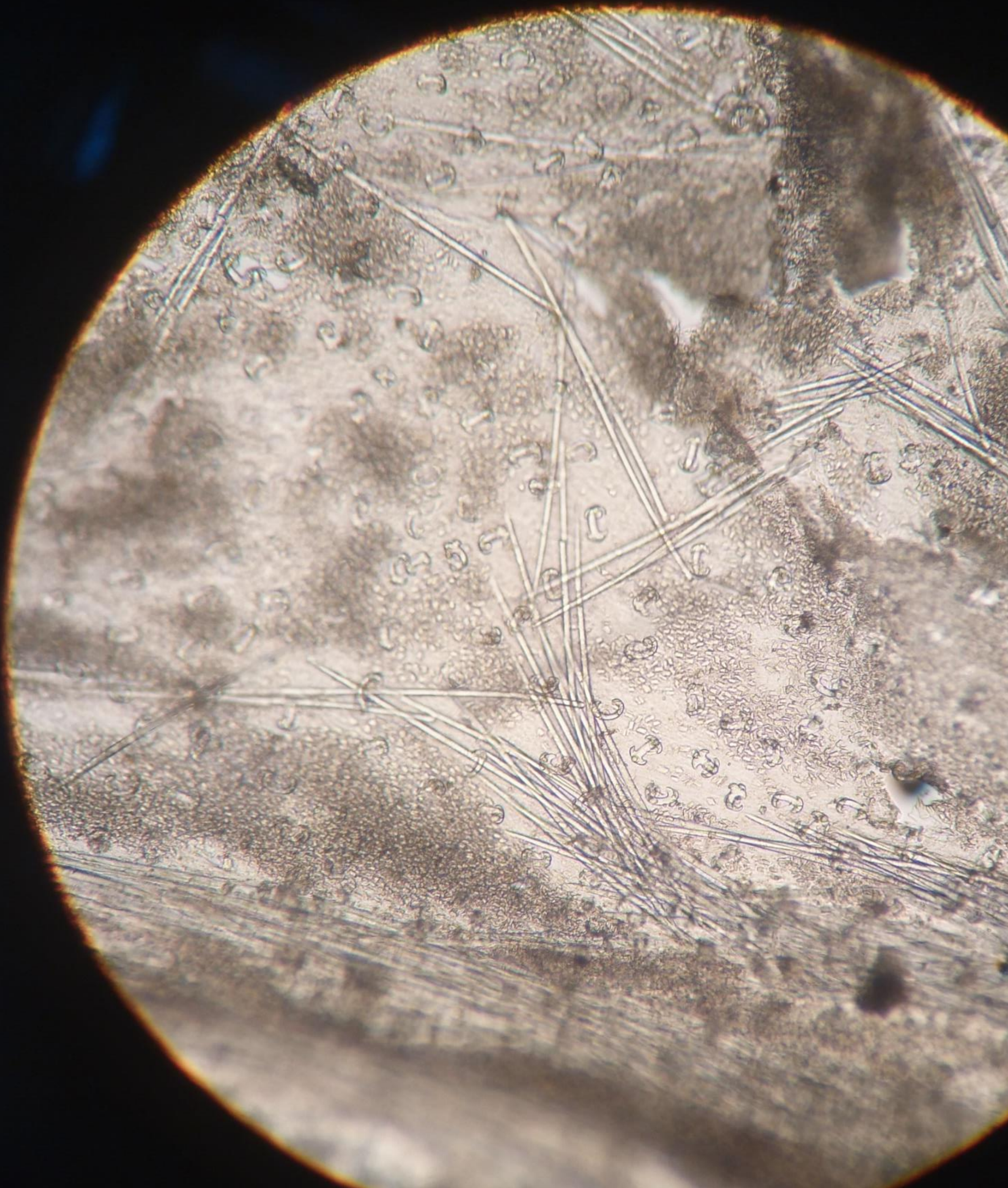

Chapter 7

Synthesis

Picture to the left: Sponge spicules under the microscope

7.1 Synthesis

Over the last few decades major advances have been made in exploring the deep ocean and gradually people are starting to appreciate the crucial role of the local ecosystem for global biology and biogeochemical cycling (York, 2018; Smith et al., 2009). Nevertheless, the most common megafaunal organism in the deep sea and one of the major players in deep-sea environments thus far received limited attention: **sponges** (Tabachnick et al., 1994). **Sponge grounds**, like cold-water coral (CWC) reefs, form oases of life in an otherwise largely barren deep sea (Maldonado et al., 2017; Roberts et al., 2006). How these biological and biogeochemical hotspots function and sustain themselves in such a food deprived environment is still ill-understood, even though it is clear that these sponges provide many goods and services for associated fauna and ultimately also humankind (see Introduction, Maldonado et al., 2017). Sponge grounds have been identified as vulnerable marine ecosystems (VMEs), being very sensitive to human impacts, on account of their longevity and expected long recovery times after disturbance (Levin et al., 2019). All these aspects make it important to increase our knowledge of deep-sea sponges, specifically in the light of the rapidly increasing environmental pressures in the deep sea as a consequence of anthropogenic activities.

This thesis aimed at unravelling the processes that drive the fascinating and vulnerable ecosystems, trying to characterize environmental conditions near and in these deep-sea sponge grounds and gain knowledge on how they function and sustain themselves. In addition, it was determined how sponge grounds influence their environment by the so-called sponge ground effect. Sponges were shown to be hotspots of carbon and nutrient cycling in the deep sea, where they take up dissolved food and transfer particulate detritus feeding their associated fauna. Results presented in this thesis show that sponges are essential members of the benthic ecosystem, and also play a major role in the benthic pelagic coupling in the deep sea. In this synthesis, I describe the natural oceanographic setting and environmental ranges of sponge grounds, comparing data from this thesis with environmental data from other areas to identify commonalities. In addition, these data are compared to other deep-sea ecosystems like CWC reefs. These comparisons suggests that sponge grounds occur in a wide range of environmental conditions and are actually very resilient to certain types of environmental stressors, which will have implications on their response to future global change. Additionally, I present a possible explanation of how sponges can overcome the carbon deficit in the food limited deep sea and how their associated fauna benefits from that.

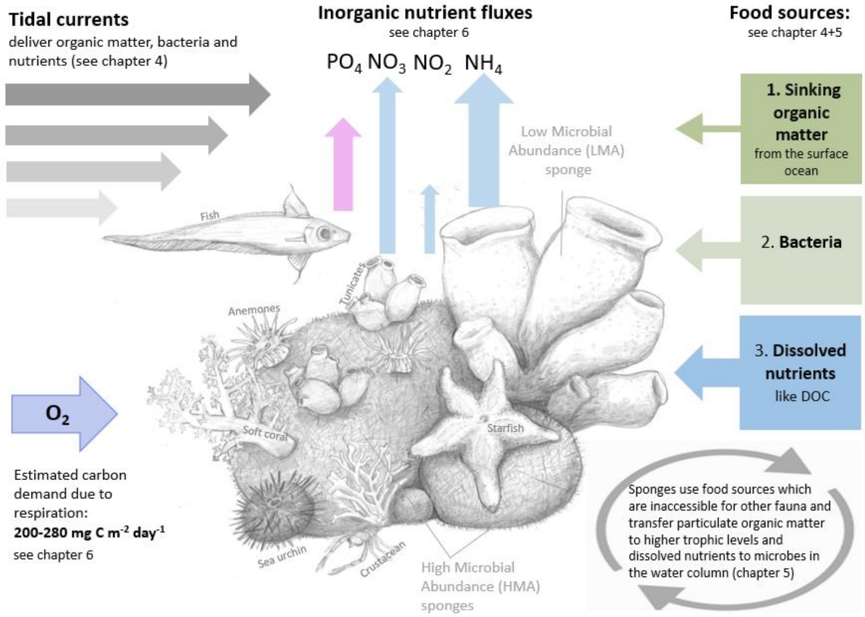

Figure 7.1 Overview of the different processes at the Schulz Bank sponge ground. Exact fluxes are presented in the indicated chapters.

7.2 Under which conditions do sponges thrive?

To improve our understanding of the environmental ranges suitable for sponge ground initiation, their sustenance and their further development it is necessary to quantify environmental conditions and variability therein over time. This helps to predict and model their distribution (Howell et al., 2016;Beazley et al., 2018) as well as shows how sponge grounds might be affected by future climate change and other anthropogenic impacts, like fisheries or deep-sea mining (Lubchenco and Petes, 2010; Millenium Assessment, 2005; Beazley et al., 2021).

For baseline studies, in-situ data collection is needed at sufficient spatial and temporal scales to identify and monitor key environmental factors and their natural variability (e.g. food supply, currents). Environmental data of sponge grounds, like currents and temperature ranges were until now mainly based on snapshots in time (like Conductivity-Temperature-Depth casts) or based on models. In this thesis, the first long-term data series were collected with bottom observatories within a monospecific (Hexactinellids) as well as a mixed sponge ground (Hexactinellids and demosponges).

The long-term temperature data collected with bottom landers showed that bottom water bathing the sponge ground ranged in temperature from -0.5 to +0.9°C in mixed grounds on the Arctic Mid-Atlantic ridge and fluctuated between 9 to 12°C, in monospecific Hexactinellid grounds on the Scotian Shelf (see Table 1). This temperature range agrees with the temperature ranges for monospecific *Geodia* sp. grounds (demosponges), which have been reported over a temperature range of −1.76°C in eastern Greenland to 10.75°C in the northeast Atlantic (Klitgaard and Tendal, 2004; Murillo et al., 2012; Cárdenas et al., 2013). An even higher temperature range (2.73 to 20.9°C, Howell et al., 2016) was modelled for the Hexactinellid species P. carpenteri, which was not yet confirmed by in-situ studies. Overall it shows that sponges can thrive in a large temperature envelope and can cope with daily, seasonal (Chapter 2, 3 and 4) as well as (inter-) annual variability of several degrees (Beazley et al., 2018). Knowledge on natural temperature ranges is not only important to predict how these ecosystems will respond to future environmental changes, but also to assess influences on metabolic rates and enzyme activities. In general low temperatures slow chemical reactions and reduce enzyme activities (Hochachka and Somero, 1968), and therefore slow down metabolic and physiological rates (Strand et al., 2017; King and Farner, 1961), which reduces the energy demand in many aquatic invertebrates (Coma, 2002). This could be beneficial for sponges that occur in food limited environments like the deep sea since respiration rates and therefore carbon demand is expected to be low (Cathalot et al., 2015). Nevertheless, the data presented in this thesis show that sponge grounds can thrive at temperatures at least 4°C lower than the until now reported temperature range for scleractinian CWCs (4 to 14.2°C; Freiwald, 2002; Dodds et al., 2007; Davies et al., 2008; Hebbeln et al., 2020) and have a comparable respiration rate (Chapter 6). This suggests that sponge grounds, which form similar oases of life in the deep sea as compared to CWCs likely can cover a larger area, specifically in the arctic regions, and potentially play a similar role as hotspots of carbon cycling.

In our studies, sponges appeared only over a relatively narrow salinity range of 34 to 35 (Table 1), typical for the deep waters of the North Atlantic (Emery and Meincke, 1986) and fall within the typical salinity range for sponge species. Knudby et al. (2013) modelled that a minimum bottom salinity was an important predictor for the distribution of *Geodia* sp., with a minimum bottom salinity tolerance of 34.3. Hexactinellid sponges on the Western Scotian Shelf were found in even lower salinities of 33.2–34.2 (Whitney et al., 2005), while so called sponge gardens were found in the Mediterranean Sea in relatively high salinity, ranging from about 35 to 38 (Sitja and Maldonado, 2014). Therefore, it is likely that salinity is not restricting the distribution of sponges in the deep sea in general and the narrow salinity range experienced in the studies of this thesis is more related to the limited variety of investigated areas.

Besides being able to live over large temperature and salinity ranges, sponges are resilient to a large range of oxygen concentrations (Table 7.1, Chapter 2-4). The investigated sponge areas at the Scotian Shelf and Schulz Bank were situated in well-oxygenated waters >3.5 to 9.1 ml l^{-1} (Table 7.1). However, along the Namibian margin sponges were the most abundant species of benthic megafauna even in oxygen concentrations of <1 ml l^{-1} (Chapter 2).

Oxygen concentrations below 2 ml l^{-1} are in general expected to be the tolerance limit for many benthic organisms, including CWCs (Fink et al., 2012; Diaz and Rosenberg, 1995). Also Leys et al. (2004) found that glass sponges were rare in regions where oxygen levels fall below 2 ml l^{-1} in coastal waters of British Colombia, Canada. The ability to survive in such low oxygen concentrations likely evolved only in some sponge species, which are adapted to oxygen minimum zones. This might be related to their microbial symbionts, which are able to perform anaerobic energy fixation, implying a mutualistic interaction between sponge cells and anaerobic microbes (Hoffmann et al., 2005). However, also thriving CWCs were found along the Angolan margin at oxygen conditions as low as 0.5 ml l^{-1} as shown in Chapter 2 (Hanz et al., 2019). Apparently, besides adaptation, stressors like low oxygen levels can be counteracted by positive environmental conditions, like sufficient food supply (Hanz et al., 2019; Hebbeln et al., 2020). The ability of sponges to thrive in anoxic and hypoxic environments and adapt to extremely low oxygen concentrations might be an indication that some sponge species will be resilient expanding oxygen minimum zones due to ongoing climate change (Helm et al., 2011; Schmidtko et al., 2017).

One of the most important factors for the distribution of nearly all sponge grounds seemed to be the position underneath an interface of two water masses, which has also been observed as an important characteristic for the occurrence of for example CWC reefs (Dullo et al., 2008). Sponges were in most areas observed underneath the interface of two water masses, for example at the Schulz Bank seamount (Hanz et al., 2021), but also on the Scotian Shelf (Hanz et al., 2021), the Western African margin (Hanz et al., 2019) the Saba Bank (Van Haren et al., 2019) and at the Azores (van Haren et al., 2017; Figure 7.2). Also Roberts et al. (2021) showed that the occurrence of the genus *Geodia* is structured by water mass distribution and mainly confined to intermediate and deep water masses.

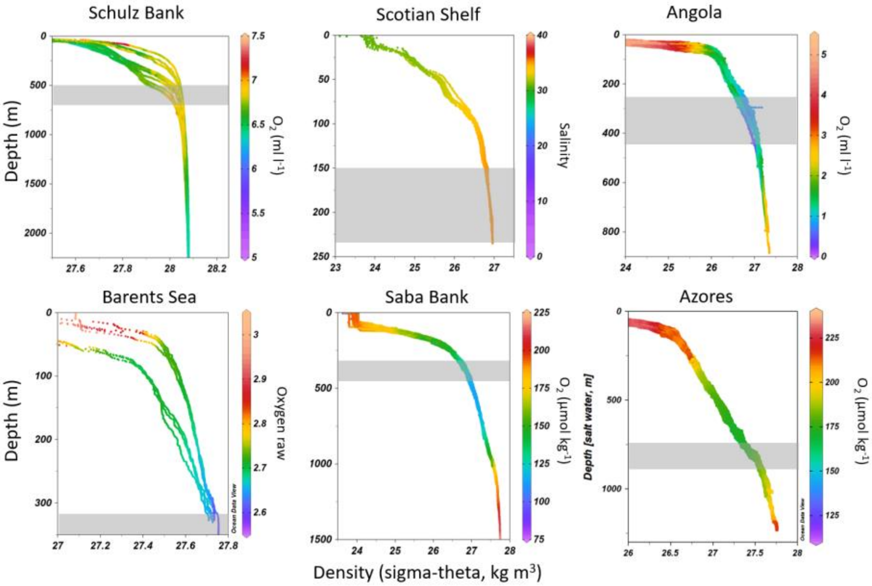

Figure 7.2 Density-Depth profiles of sponge ground regions including the oxygen concentration (or salinity if O_2 conc. was not available). Grey area is indicating the depth range of the highest sponge density.

Multiple mechanisms might explain sponge ground occurrences below the interface between two water masses: The first mechanism is related to the presence of enhanced currents, turbulence and mixing due to internal tides. Inertial waves (influenced by the Coriolis Effect) can move along the density gradients within the water column and can interact, together with the tidal flow, with the ocean floor topography, which will create internal waves (Bell Jr, 1975). These internal waves can cause large vertical movements within the water column (up to several 100 m; Klymak et al., 2012), creating zones that are influenced by water from above and below which often have different characteristics (e.g., oxygen concentration, SPOM content). The vertical water movement is creating rapid changes inside the sponge grounds in for example temperature, salinity and oxygen concentration throughout each tidal cycle. These chemical gradients are important for chemosynthetic processes or microbes within the water column as well as sponge associated microbes. Gradients in oxygen concentration were observed for example at the Namibian margin (Chapter 2), where sponges live in an anoxic environment and are likely to survive because they receive water with slightly higher oxygen concentrations from greater depths due to semi-diurnal internal tides. At the same time, they benefit from higher food concentrations from shallower water. At the Schulz Bank similar conditions were observed, where internal waves bring water with a higher suspended particulate organic matter concentration towards the sponge grounds (Chapter 4; Roberts et al., 2018). The internal waves might also play an important role in the seamount effect observed by Bush et al., 2020, where the bacterial community within the water column above the seamount is affected by the presence of the seamount, since water affected by the sponge ground is transported several hundred meter upwards.

The second mechanism is related to the presence of nepheloid layers that occur at the strong vertical density gradient associated with the interface between the water masses (Dickson and Mccave, 1986; Gardner et al., 2018). In this thesis, nepheloid layers were observed in multiple areas, for example at the Scotian Shelf (Azetsu-Scott et al., 1995), The Schulz Bank (Roberts et al., 2018) and the Angolan margin (Hanz et al., 2019). These layers can enhance food supply and availability by lateral particle transport and potentially play also a role in larval distribution (White and Dorschel, 2010; Roberts et al., 2021; Dullo et al., 2008). Food particles can be transported laterally over large distance on such density layers, delivering an additional food source to areas which are not directly located beneath regions of high primary production (Davies et al., 2009; Davison et al., 2019). The enhanced turbulences as well as the presence of a nepheloid layer might also be responsible for an increased abundance of (pelagic) microbes (Pile and Young, 2006). The general occurrence of microbes corresponds to minima in dissolved oxygen concentrations as observed in water column profiles (Figure 7.2), related to relatively high rates of aerobic organic matter degradation (Orcutt et al., 2011). It is not completely resolved why higher rates of heterotrophic prokaryotic production can be found in this zone, but one possible factor could be the availability of particulate organic carbon (POC) versus dissolved organic carbon (DOC) (Hansell and Ducklow, 2003; Arıstegui et al., 2002).

In many places, sponge grounds were found in areas with intensified bottom currents and mixing (Rice et al., 1990; Van Haren et al., 2017; Davison et al., 2019). The average currents around the sponge grounds in our studies were very similar in all areas and varied between 0.12 to 0.14 m s^{-1}, whereas temporary maximum currents of 0.72 and 0.47 m s^{-1} were reached in the benthic boundary layer (BBL) at the Schulz Bank and Scotian Shelf sponge ground, respectively (Table 7.1). These maximum current speeds seem to be at the limit of what sponges can endure, since several sponges were observed to be dislocated and overthrown during peak current conditions, as observed by the video recordings of the landers at the Schulz Bank (Chapter 4) and the Scotian Shelf (Chapter 3). High current speed events were caused by different processes: On the Scotian Shelf and Namibian margin strongest currents were observed during surface storm events, which were reaching the seafloor, producing extreme turbidity in the BBL (Chapter 2 and 3). At the Schulz Bank and the Azores seamounts high currents and turbulence were mainly related to the interaction of internal tides with the sloping topography of the seamount (Chapter 4; van Haren et al., 2017). This interaction produced internal waves of up to 200 m height at the Schulz Bank, creating a dynamic environment on the summit of the seamount. Such strong currents seem to play an essential role for sponge grounds, since they were observed to deliver and replenish the BBL with potential food resources and oxygen (Chapter 2 and 6). Additionally, sponges in general are known to rely on currents for the uptake of food, since the energetic costs of pumping are less when currents create pressure gradients around the sponge (Vogel, 1977; Leys et al., 2011). Uptake of microorganisms and particulate organic matter (POM) is accordingly likely facilitated during times currents are invigorated, which induce a pressure gradient across the sponge wall making the pumping process for sponges more efficient. Still, this effect is clearly limited to current levels not yet having damaging effects due to high current speeds or high particle loads (Leys et al., 2011).

Based on the above can be concluded that the appearance of sponge grounds is less relying on certain temperatures, salinities or oxygen concentrations but rather on the favourable hydrodynamic conditions supplying the sponge ground with beneficial conditions and sufficient food.

Table 7.1 Environmental characteristics inside the different sponge dominated areas, *=Reigstad et al. 2006, **van Haren et al. 2019

	Schulz Bank mixed assemblages	**Barents Sea** *Geodia sp. grounds*	**Canada** *Vazella sp. ground*	**Caribbean** *Hexactinellid* grounds	**Azores** *Pheronema carpenteri*
Temperature (°C)	-0.5-0.9	5.2- 5.6	9 -12	11.8-13.4	9-12
Ø Depth (m)	600-700	300	100-200	350	750-850
Dissolved O_2 (mg l^{-1}) (ml l^{-1})	12-13 8.4-9.1 (69% saturation)	12 8.4 (90% saturation)	5-8 3.5-5.6 (69% saturation)	5-5.2 3.5 (44% saturation)	3.9-4.1 2.8 (61–65% saturation)
Salinity	34.9	35	34-35	36	35.6-35.7
Current (m s^{-1})	Ø = 0.14 Max. 0.72	Ø = 0.13 Max. 0.25	Ø = 0.12 Max. 0.47	Ø = 0.03 Max. 0.09	Ø = 0.04 Max. 0.4
Height internal tides (m)	>200	Ca. 50	Ca. 50	50-100**	
Vertical C flux (mg C m^{-2} d^{-1})	2-29	25-400*	69–422	--	--
Nutrients (µmol l^{-1})	Ø Si = 7.7 Ø NO_3 = 13.7 Ø NH_4 = 0.10	Ø Si = 5.5 Ø NO_3=12.2 Ø NH_4=0.12	Ø Si = 15.6 ØNO_3=16.85 Ø NH_4 = 1.5	Ø Si = 5.6 Ø NO_3 =~ 10	--

7.3 How do sponges survive in the "food limited" deep sea?

It remains largely unknown how ecosystems thriving in the deep sea are able to sustain themselves, since heterotrophic organisms are relying on the limited vertical flux of sinking organic matter which is escaping recycling on the way down from the surface ocean (Turley, 2002; Arístegui et al., 2009).

During long-term lander deployments of our studies, the vertical flux of organic matter on the Scotian Shelf and the Schulz Bank was measured (Chapter 3 and 4). In both areas only one single peak in vertical organic matter flux was observed, which was associated with the summer phytoplankton bloom. Fluxes varied substantially between both areas (Figure 7.2), which might be connected to the distance to the surface productive layer, which determines how much of the organic matter will be remineralized during the downward transport. Stable nitrogen isotope signatures revealed that organic matter is recycled many times, becoming increasingly refractory over the year following a spring/summer bloom. For the Scotian Shelf the vertical flux could be compared with respiration rates measured in ex-situ studies (Bart et al., 2020), where on average less than 30% of the required carbon can be delivered by the vertical flux (Figure 7.3). The incubation studies of the Schulz Bank (Chapter 6) showed through in-situ respiration measurements within the sponge community, a (particulate) carbon deficit of about 95%. These carbon budgets, however, only consider vertical POC flux and the minimal respiratory carbon demand (Figure 7.3). Imbalances in carbon budgets between delivered carbon and carbon required for survival have also been reported for other sponge grounds (Kahn et al., 2015) as well as CWC reefs (Oevelen et al., 2009; Kahn et al., 2015).

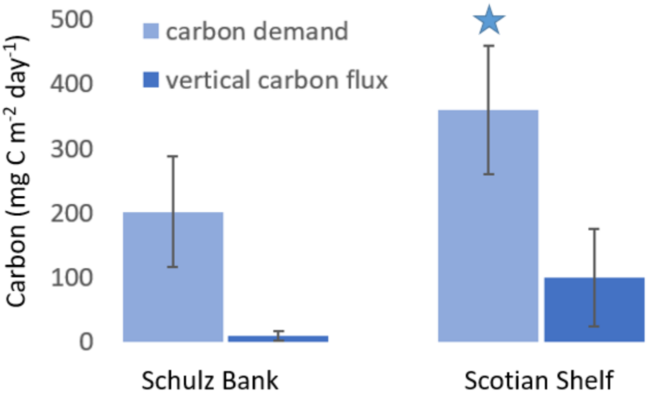

Figure 7.3 Carbon demand estimate from average community respiration (light blue) vs. average vertical (particulate) carbon flux during the year measured by sediment traps (dark blue) in the two main research areas. The value marked with a star is derived from ex-situ incubation experiments of Bart et al., 2021.

The observed carbon deficit implies that sponges are somehow able to take advantage of other food sources, such as for instance dissolved carbon resources like bacterioplankton and/or DOC (Bart et al., 2021). Because the associated fauna in sponge grounds are likely not able to use such food sources this makes them an essential link in the local recycling of carbon and nitrogen (Chapter 5). Depletion of bacteria in the BBL at the Schulz Bank indicated that the living sponge community takes up 10s of millions of bacteria per square meter of bed per second (Chapter 6), which could account for a major part of the sponge ground carbon demand. The well-aerated spicule mat underlying the sponge grounds might serve as an additional source for microorganisms next to the pelagic microorganism, especially since it is periodically resuspended due to the semi-diurnal tides. Still, also this would only add to enhanced recycling and not be a fundamentally different food source. The third potential primary source for microbial food for the sponges are the associated microbes inside their tissue (Rix et al., 2020).

Nevertheless, the main carbon source for sponges (and their associated microorganisms) in the deep sea is expected to be DOC. It is well established, that DOC comprises the major part of the carbon source for sponges in tropical reef systems as well as the deep sea, whereas it is not available for most other benthic megafauna (Mueller et al., 2014; De Goeij et al., 2008; Yahel et al., 2003; Bart et al., 2021; Maier et al., 2020). DOC is very abundant in the deep ocean, yet expected to be mainly refractory (Hansell and Carlson, 2002). The uptake of recalcitrant fractions of DOC by sponges were so far only observed in shallow water sponges associated to mangroves, where recalcitrant carbon, although not even available for microbes in the surrounding environment, was used by sponges, giving sponges a competitive advantage (Hunting et al., 2010). Such uptake of refractory DOC might play an important role on the Schulz Bank sponge ground as well. Relatively enriched δ^{13}C isotopic values were observed in HMA sponges (-18‰), pointing towards isotopically enriched carbon sources, which might be DOC and DIC (Chapter 5). DOC in the North Atlantic is expected to have slightly more depleted water column values around -23.1 to -22.2‰ (Hansell and Carlson, 2014) and can therefore not be the solely driver of the isotopic composition of HMA sponges. Additionally DIC must contribute to the carbon budget, since DIC is the only known food source so far that has very enriched ^{13}C values with typical water column values of around ~0–1‰ (Griffith et al., 2012). Additional investigations are needed to confirm active uptake of DIC through chemosynthetic bacteria and/or taumarchea, which would require stable carbon isotope labelling experiments in which the different fluxes are quantified.

Based on the above, it can be concluded that sponges potentially access a variety of carbon sources in contrast to most of their associated fauna and likely can adapt their diet based on availability of resources. Irrespective of these different sources it is clear that these sponges somehow form the basis of the local thriving ecosystem and act as a kind of primary producer. The current perception of the “food limited” deep sea should be revised with the ability of sponges to take up multiple carbon sources which allows them to colonize areas that are otherwise not suitable due to limited or refractory food. Their flexibility in using different food sources might also play an important role in their ability to adapt to changing conditions and potentially also to the ongoing global change.

7.4 What is the role of sponges in benthic pelagic coupling?

Sponges play important roles in the benthic pelagic coupling due to their extremely high water filtration rate and therefore are key grazers in many benthic habitats (Yahel et al., 2006). Sponges remove dissolved and particulate organic matter from the water column and release, as a consequence of its oxidation, inorganic nutrients and particulate detritus to the benthic environment (Maier et al., 2020; Bart et al., 2021). By this they have an important role in carbon (Cathalot et al., 2015) and nitrogen cycling (Rooks et al., 2020; Maldonado et al., 2012). For the first time it was shown in this thesis how much (particulate) nutrients are taken up and how much and which (dissolved) nutrients are released into the benthic boundary layer by deep-sea sponge grounds. The release of different nitrogen substances in sponges can be explained by the fact that the nitrogen cycle is highly associated with the activity of their associated microbes (Ward et al., 2007). LMA sponges are known to convert particulate organic nitrogen to mainly NH_4^+, similar to other animals (Maldonado, Ribes et al., 2012). HMA sponges on the other hand are known to release NO_3^- with no significant release of NH_4^+ or NO_2^- (Leys et al., 2018; De Kluijver et al., 2020). NO_2^- and NO_3^- are released due to the further oxidation of NH_4^+ for energetic purposes (called nitrification/denitrification), which is mediated by ammonia oxidizing bacteria or archaea and the nitrite oxidizing bacteria associated to the HMA sponges (Schläppy et al., 2010; Ribes et al., 2012; Van Bleijswijk et al., 2015). In Chapter 6 the fluxes of inorganic nitrogen and phosphate from a deep-sea sponge ground were quantified using in-situ incubation experiments. The sponge ground was in general observed to be a NH_4^+ and NO_x source. Release rates were related to a high incubated biomass of either HMA or LMA sponges. Especially incubations with a high biomass of LMA sponges showed a trend towards a higher release of inorganic nutrients like NH_4^+ and NO_2^-. Similar observations were made in incubation studies and integrative models of high and low microbial abundance sponges (Hoffmann et al., 2009; Bart et al., 2021; De Kluijver et al., 2020). Interestingly we could also observe a higher release of PO_4^{3-} in incubations with a high biomass of LMA sponges, which might be related to a in general higher heterotrophic metabolism as indicated by the high changes in the N:P ratio during the incubation experiments (Chapter 6). Another explanation could be that other metabolic processes, involving phosphorus, either for the HMA or LMA sponges might take place, that are not known so far.

In addition, it was observed that the benthic boundary layer above the sponge ground was enriched in inorganic nitrogen and slightly depleted in PO_4^{3-}. Inorganic nitrogen can fuel microorganisms inside the BBL since metabolic activities of microorganisms in the deep sea depend on the availability and speciation of electron donors (oxidizable compounds) and acceptors (reducible compounds; Froelich et al., 1979). It is possible that the growth of microbes is limited by the availability of carbon as an electron donor, since big parts of the available POC are likely taken up by the suspension feeding fauna and DOC is not readily available (Arıstegui et al., 2002). Processes like nitrification and anammox can therefore be exploited for metabolic energy (Orcutt et al., 2011) especially in regions where they are not limited and constantly refuelled by sponges. Studies already suggested that roughly one-third of global ocean primary production occurs in the aphotic pelagic ocean (Del Giorgio and Duarte, 2002) and one of the sources of this autotrophy in the deep sea is likely nitrification (Wuchter et al., 2006). Nevertheless, the factors determining growth rates of deep-water prokaryotic communities are still unclear. However, if the sponge community provides dissolved resources for microbes in the pelagic environment and these microbes are again taken up by the sponges and associated fauna, they are an indispensable part of the highly efficient recycling processes. This is essential for the nutrition of these deep-sea ecosystems and might also be important in for example CWC reefs, where sponges can be very abundant (Rix et al., 2018).

In how far the released nutrients influence the surrounding water column above the investigated BBL is still unclear. If the released nitrogen is brought all the way up to the surface, for instance during periods of deep winter mixing or internal wave motions, they could trigger phytoplankton blooms as happen on the Scotian Shelf, where the phytoplankton bloom is started by the upwelling of deeper waters (Chapter 3). This emphasizes the role of sponges as local source of nutrients by being able to process refractory organic matter, even to a regional level. Busch et al. (2020) for example found indications that bacterial communities around a sponge ground are distinctly influenced even several hundreds of meters above a sponge ground itself. Since sponge grounds and especially also sponges as a member of other ecosystems are very common in the whole North Atlantic (see Figure 1.4), they might even be of global importance in benthic-pelagic coupling.

7.5 Are sponges important as a food source for other benthic organisms?

The investigated sponge grounds showed differences in their species composition, where the *Vazella pourtalesii* sponge ground harbours a monospecific aggregation of LMA sponges (Chapter 3) and the Schulz Bank a mixed ground with both HMA and LMA species (Chapter 4-6). Even though major differences in the flux of organic matter were observed and therefore availability of particulate food (Figure 7.3), the food web structure was very similar (Figure 7.4). Especially the $\delta^{15}N$ ratio of LMA sponges and the $\delta^{13}C$ of HMA sponges showed in all ecosystems unexpectedly high values, which were also found in other sponge species but so far without a solid explanation (Kahn et al., 2018; Duineveld et al., 2007). Irrespective of the source of this isotopic signal, the unusual position of sponges in the food web allows tracing back transfer of food from the sponges to the associated fauna. Direct evidence that sponges act as a food source for their associated fauna was collected by video recordings, where sea urchins and starfish were observed to pray on sponges (Chapter 4). Sponges are taking up recalcitrant fractions of carbon and nitrogen and produce detritus, which they provide as a further enriched carbon and nitrogen source to the associated fauna. A general transfer of detritus to the associated fauna is known for shallow water sponges, the so called the sponge loop (De Goeij et al., 2013) and was also observed in CWC reefs (Rix et al., 2018; Maier et al., 2020). The transfer of isotopically enriched detritus to the associated fauna on the Schulz Bank of both LMA and HMA sponges can explain the high isotopic enrichment per trophic level of the associated fauna (Chapter 5, Figure 7.3). Enriched δ^{13}C values of the associated fauna are occurring in the Barents Sea sponge grounds, where mainly HMA sponges were observed, but not in the *Vazella pourtalesii* grounds, where enrichments are not expected as a high abundance or biomass of HMA sponges do not occur (Figure 7.4). Accordingly, at the *Vazella pourtalesii* grounds no enrichment in δ^{15}N is observed in the associated fauna, suggesting a lack in transfer of enriched material. Still, more data is needed to confirm these theories, including the collection of additional species as well as dissolved food resources (DOC and DIC).

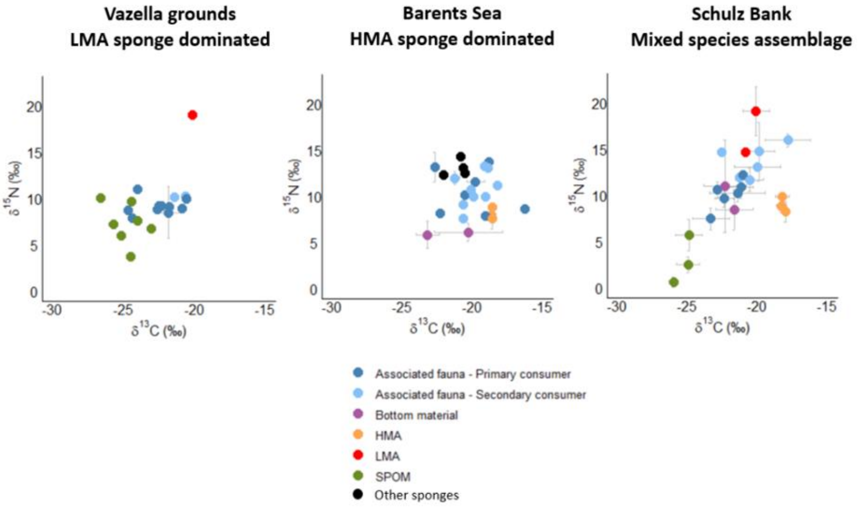

Figure 7.4 Bulk isotopes of δ^{15}N and δ^{13}C in three different sponge grounds.

These results as well as the fatty acid analysis of Chapter 5 emphasize that sponges play a unique and pivotal role in deep-sea food webs by providing an (important) additional source of carbon and nitrogen to the associated fauna at the base of the local food web. These results imply that sponges likely drive both bottom-up and top-down processes, shunting organic carbon to higher trophic levels. In this way, sponges are key to the sustenance of thriving deep-sea ecosystems and might play an important role in systems where they occur as associated fauna (e.g., CWC reefs; Rix et al., 2016; Hadas et al., 2006; Van Duyl et al., 2008).

7.6 Future threats for deep-sea sponges

It is very well known and can be directly observed in many locations that shallow water coral reefs suffer from the various impacts of anthropogenic pressure and climate change (Wilkinson, 1999). Effects on deep-sea ecosystems are, however, much more difficult to observe and baseline studies about a “healthy” appearance of these systems often simply do not exist. Nevertheless, it is very likely that deep-sea sponge grounds are impacted by the same stressors as other marine biodiversity hotspots. It is predicted that **circulation patterns and water mass properties** in the North Atlantic Ocean will change due to rising atmospheric greenhouse gasses that are bringing significant changes in terms of water column oxygenation, temperature, pH and food supply (Sweetman et al., 2017). According to Puerta et al. (2020), this might expose sponge grounds to critical changes in water temperature (+2°C), reduce organic carbon fluxes by up to 50%, which will influence dissolved oxygen concentrations (>5%; Puerta et al., 2020). Projected changes in the Atlantic Meridional Overturning Circulation due to climate change will change the distribution pattern and location of water masses and their interfaces (Yan et al., 2018). This might hence also influence sponge grounds situated below the interface of two water masses (like described in Chapter 4), influencing the occurrence of internal waves and associated turbulence, which has implications for the benthic-pelagic coupling and the food supply towards the sponge grounds (Roberts et al., 2021; Hanz et al., 2021).

With a changing climate an additional threat for sponge grounds on continental margins or shallower seamounts might be **more severe**

(surface) storm events, that are expected to occur more often (Knutson et al., 2010; Yang et al., 2020; Caesar et al., 2018). Sponges are often linked to areas associated with strong bottom currents, close to the maximum strength that they can stay attached to the substrate. Stronger and more frequent storm events would create even high currents, which physically damage sponges as was already observed in our studies in the Emerald Basin (Chapter 3) and indirectly at the Schulz Bank (Chapter 4). Additionally, surface storms can increase the load of resuspended material in the deep ocean (Sanchez-Vidal et al., 2012), which can impair the filtering ability of sponges (Tompkins-Macdonald and Leys, 2008). Severe storms are therefore not only a threat for example shallower coral reefs (Wilkinson, 1999) but likely also for deep-sea sponge grounds.

One of the main anthropogenic impacts, that is not connected to the climate, is the effect **fisheries** can have on sponge grounds. Fishery brings two negative effects: The first is bottom-contact fishing gear is stirring up sediment, which can negatively affect sponges even kilometres away from the original source of disturbance (Grant et al., 2018). Sponges will arrest their filtration activity during periods of high resuspension since particles can clog the aquiferous system of sponges and therefore have negative effects on their survival (see Chapter 3; Tompkins-Macdonald and Leys, 2008). The second, more direct threat, is however the physical damage of the fragile megabenthic species by bottom contact gear, which is able to wipe out complete sponge grounds in relatively short time periods (Pham et al., 2019). This will have major impacts on the biodiversity and functioning of these ecosystems which can further lead to economic losses that are even higher than the obtained gain due to the market value of fish catch, like estimated for example on the Flemish Cap (Pham et al., 2019).

A similar danger that is directly related to anthropogenic activities is **deep-sea mining**. Deep-sea mining activities might release high amounts of (toxic) suspended material to the water column during the process of the extraction and discharge of tailings and efflux below (Sharma, 2015). This will again negatively influence the pumping efficiency of sponges (see Chapter 3 for details). Therefore, the protection of fragile sponge grounds and other ecosystems needs to be taken into account when considering possible negative effects of planned future mining activities.

However, our data have shown that sponges have broad natural ranges of for example temperature, oxygen concentrations, current speeds as well as that they can endure (temporarily) high concentrations of suspended material. This also has important implications on their response to future changes like global warming, deoxygenation or increased load or particles in the water column. They are able to adapt to extreme environments, whereby sponges seem more resilient than for instance CWCs. For example, due to their wide temperature tolerance, sponges can occupy larger surface areas in the deep sea, specifically the extremely cold temperature regions like the Arctic (Chapter 4). A first modelling study of *Vazella* sp. showed that they might be winners during climate change since they are likely able to occupy larger areas along the Scotian Shelf (Beazley et al., 2018; Beazley et al., 2021).

Studies showed that glass sponges were abundant at various stages of the Paleozoic (540–250 Mya) and Mesozoic (250–65 Mya) eras (Brunton and Dixon, 1994) and survived significant global events like for example the transition from the Triassic to Jurassic period 200 Mya ago, which was characterized by mass extinction events including many coral species (Kiessling and Simpson, 2011). Glass sponges nevertheless persisted on these geologically relevant time scales (millions of years; Delecat et al., 2011). This shows that sponges are able to adapt during times of extreme change in environmental conditions, in contrast to many of the calcifying organisms like corals, which were likely negatively affected by ocean acidification events (Kiessling and Simpson, 2011). Sponge species might also be able to adapt and occupy habitats that are lost for other species due to deoxygenation, like seen on the Namibian margin (Chapter 2). There, sponges are the main megafaunal organisms in the nearly anoxic zones on the Namibian margin where living corals disappeared. Similar patterns might be observable in habitats that experience warming or other stressors associated with global change, where sponges can outcompete other organisms due to their broad adaptation mechanisms (Bell et al., 2013).

Nevertheless, most deep-sea ecosystems are often living in a fragile equilibrium, which can quickly change if even single factors become stressors, like observed at the Namibian margin. There CWC died probably due to small changes in the oxygen concentration, whereas they are still thriving some kilometres further towards the North (Chapter 2). Therefore, changes in environmental conditions might have negative consequences also for sponge species that are long-lived and slow growing and might not be able to adapt or shift their distributional range.

Sponges in sponge grounds might be like the water for the oasis in the dessert: A key factor that allows their associated fauna to appear in high biomass and biodiversity by providing them a habitat and food source in the otherwise barren deep sea. Sponge grounds have an underappreciated high economic value for humankind (Pham et al., 2019), provide essential ecosystem services in the deep sea (Bell, 2008). It is necessary to further extend our knowledge about the goods and services these sponge grounds provide for humankind before we risk losing such an important member of the ocean ecosystem.

8. References

Addamo, A. M., A. Vertino, J. Stolarski, R. García-Jiménez, M. Taviani and A. Machordom (2016) Merging scleractinian genera: the overwhelming genetic similarity between solitary *Desmophyllum* and colonial *Lophelia*. BMC evolutionary biology 16(1): 108.

Ahmed, M. (2020) Introduction to Modern Climate Change. Andrew E. Dessler: Cambridge University Press, 2011, 252 pp, ISBN-10: 0521173159. The Science of the Total Environment 734: 139397.

Althaus, F., A. Williams, T. Schlacher, R. Kloser, M. Green, B. Barker, N. Bax, P. Brodie and M. Schlacher-Hoenlinger (2009) Impacts of bottom trawling on deep-coral ecosystems of seamounts are long-lasting. Marine Ecology Progress Series 397: 279-294.

Anderson, C., Dobson, F., Perrie, W., Smith, P., Toulany, B., and Schwing, F. (1989). Storm response in the coastal ocean: The oceanographic component of the Canadian Atlantic Storms Program (CASP). Eos, Transactions American Geophysical Union 70, 562-572.

Arıstegui, J., C. M. Duarte, S. Agustı, M. Doval, X. A. Álvarez-Salgado and D. A. Hansell (2002) Dissolved organic carbon support of respiration in the dark ocean. Science 298(5600): 1967-1967.

Arístegui, J., J. M. Gasol, C. M. Duarte and G. J. Herndld (2009) Microbial oceanography of the dark ocean's pelagic realm. Limnology and Oceanography 54(5): 1501-1529.

Armstrong, C. W., G. K. Vondolia, N. S. Foley, L.-A. Henry, K. Needham and A. Ressurreição (2019) Expert assessment of risks posed by climate change and anthropogenic activities to ecosystem services in the deep North Atlantic. Frontiers in Marine Science 6: 158.

Azetsu-Scott, K., Johnson, B.D., and Petrie, B. (1995). An intermittent, intermediate nepheloid layer in Emerald Basin, Scotian Shelf. Continental shelf research 15, 281-293.

Baker, E. T., H. B. Milburn, and D. A. Tennant (1988), Field assessment of sediment trap efficiency under varying flow conditions, *Journal of Marine Research*, *46*(3), 573-592.

Baker, E. T. and C. R. German (2004) On the global distribution of hydrothermal vent fields. Mid-Ocean Ridges: Hydrothermal Interactions Between the Lithosphere and Oceans, Geophys. Monogr. Ser 148: 245-266.

Bart, M. C., A. de Kluijver, S. Hoetjes, S. Absalah, B. Mueller, E. Kenchington, H. T. Rapp and J. M. de Goeij (2020). Differential processing of dissolved and particulate organic matter by deep-sea sponges and their microbial symbionts. Scientific reports 10(1): 1-13.

Bart, M. C., M. Hudspith, H. T. Rapp, P. F. Verdonschot and J. M. de Goeij (2021) A deep-sea sponge loop? sponges transfer dissolved and particulate organic carbon and nitrogen to associated fauna. Frontiers in Marine Science 8:229.

Bart, M. C., B. Mueller, T. Rombouts, C. van de Ven, G. J. Tompkins, R. Osinga, C. Brussaard, B. MacDonald, A. Engel, H. T. Rapp and J. M. de Goeij (2021) Dissolved organic carbon (DOC) is essential to balance the metabolic demands of North-Atlantic deep- sea sponges. Limnol Oceanogr, 66: 925-938. doi:10.1002/lno.11652

Barthel, D., and J. Gutt (1992), Sponge associations in the eastern Weddell Sea, *Antarctic Science*, *4*(2), 137-150.

Barthel, D., O. Tendal and H. Thiel (1996) A wandering population of the hexactineliid sponge *Pheronema carpenteri* on the continental slope off morocco, Northwest Africa. Marine Ecology 17(4): 603-616.

Bathmann, U. V., R. Peinert, T. T. Noji, and B. V. Bodungen (1990) Pelagic origin and fate of sedimenting particles in the Norwegian Sea, *Progress in Oceanography*, *24*(1-4), 117-125.

Beazley, L.I., Kenchington, E.L., Murillo, F.J., and Sacau, M.D.M. (2013) Deep-sea sponge grounds enhance diversity and abundance of epibenthic megafauna in the Northwest Atlantic. ICES Journal of Marine Science 70, 1471-1490.

Beazley, L., Kenchington, E., Yashayaev, I., and Murillo, F.J. (2015) Drivers of epibenthic megafaunal composition in the sponge grounds of the Sackville Spur, northwest Atlantic. Deep Sea Research Part I: Oceanographic Research Papers 98, 102-114.

Beazley, L., Z. Wang, E. Kenchington, I. Yashayaev, H. T. Rapp, J. R. Xavier, F. J. Murillo, D. Fenton and S. Fuller (2018) Predicted distribution of the glass sponge *Vazella pourtalesi* on the Scotian Shelf and its persistence in the face of climatic variability. PloS one 13(10): e0205505.

Beazley, L., E. Kenchington, F. J. Murillo, D. Brickman, Z. Wang, A. J. Davies, E. M. Roberts and H. T. Rapp (2021) Climate change winner in the deep sea? Predicting the impacts of climate change on the distribution of the glass sponge *Vazella pourtalesii*. Marine Ecology Progress Series 657: 1-23.

Bell, J. J. (2008) The functional roles of marine sponges. Estuarine, coastal and shelf science 79(3): 341-353.

Bell, J. J., S. K. Davy, T. Jones, M. W. Taylor and N. S. Webster (2013) Could some coral reefs become sponge reefs as our climate changes? Global change biology 19(9): 2613-2624.

Bell, J.J., Mcgrath, E., Biggerstaff, A., Bates, T., Bennett, H., Marlow, J., and Shaffer, M. (2015) Sediment impacts on marine sponges. Marine pollution bulletin 94, 5-13.

Bell Jr, T. (1975) Topographically generated internal waves in the open ocean. Journal of Geophysical Research 80(3): 320-327.

Benner, R., J. D. Pakulski, M. McCarthy, J. I. Hedges and P. G. Hatcher (1992) Bulk chemical characteristics of dissolved organic matter in the ocean. Science 255(5051): 1561-1564.

Bett, B. and A. Rice (1992) The influence of hexactinellid sponge (*Pheronema carpenteri*) spicules on the patchy distribution of macrobenthos in the porcupine seabight (bathyal ne atlantic). Ophelia 36(3): 217-226.

Billett, D., R. Lampitt, A. Rice and R. Mantoura (1983) Seasonal sedimentation of phytoplankton to the deep-sea benthos. Nature 302(5908): 520-522.

Boehlert, G. W. and A. Genin (1987) A review of the effects of seamounts on biological processes. Seamounts, islands, and atolls: 319-334.

Boudreau, B. P., and B. B. Jorgensen (2001) The benthic boundary layer: Transport processes and biogeochemistry, Oxford University Press.

Boutton, T. W. (1991) Stable carbon isotope ratios of natural materials: II. Atmospheric, terrestrial, marine, and freshwater environments, Carbon isotope techniques, 1, 173.

Boyd, P. W., H. Claustre, M. Levy, D. A. Siegel and T. Weber (2019) Multi-faceted particle pumps drive carbon sequestration in the ocean. Nature 568(7752): 327-335.

Buesseler, K. O., C. H. Lamborg, P. W. Boyd, P. J. Lam, T. W. Trull, R. R. Bidigare, J. K. Bishop, K. L. Casciotti, F. Dehairs and M. Elskens (2007) Revisiting carbon flux through the ocean's twilight zone. Science 316(5824): 567-570.

Buhl-Mortensen, L., A. Vanreusel, A. J. Gooday, L. A. Levin, I. G. Priede, P. Buhl-Mortensen, H. Gheerardyn, N. J. King and M. Raes (2010) Biological structures as a source of habitat heterogeneity and biodiversity on the deep ocean margins. Marine Ecology 31(1): 21-50.

Bunt, J.A., Larcombe, P., and Jago, C.F. (1999) Quantifying the response of optical backscatter devices and transmissometers to variations in suspended particulate matter. Continental shelf research 19, 1199-1220.

Breitburg, D., Levin, L. A., Oschlies, A., Grégoire, M., Chavez, F. P., Conley, D. J., Garçon, V., Gilbert, D., Gutiérrez, D., and Isensee, K. (2018) Declining oxygen in the global ocean and coastal waters, Science, 359, eaam7240.

Brooke, S., and Ross, S. W. (2014) First observations of the cold-water coral *Lophelia pertusa* in mid-Atlantic canyons of the USA, Deep Sea Research Part II: Topical Studies in Oceanography, 104, 245-251.

Brunton, F. R. and O. A. Dixon (1994) Siliceous sponge-microbe biotic associations and their recurrence through the Phanerozoic as reef mound constructors. Palaios 9(4): 370-387.

Brussaard, C. P. (2004) Optimization of procedures for counting viruses by flow cytometry. Applied and Environmental Microbiology 70(3):1506-1513.

Busch, K., U. Hanz, F. Mienis, B. Müller, A. Franke, E. M. Roberts, H. T. Rapp and U. Hentschel (2020) On giant shoulders: How a seamount affects the microbial community composition of seawater and sponges. Biogeosciences, 17, 3471–3486, doi:10.5194/bg-17-3471-2020.

Caesar, L., S. Rahmstorf, A. Robinson, G. Feulner and V. Saba (2018) Observed fingerprint of a weakening Atlantic Ocean overturning circulation. Nature 556(7700): 191-196.

Cairns, S. D. (2007) Deep-water corals: an overview with special reference to diversity and distribution of deep-water scleractinian corals, Bulletin of Marine Science, 81, 311- 322.

Calleja, M. L., F. Batista, M. Peacock, R. Kudela and M. McCarthy (2013) Changes in compound specific $\delta^{15}N$ amino acid signatures and D/L ratios in marine dissolved organic matter induced by heterotrophic bacterial reworking. Marine Chemistry 149: 32-44.

Canadell, J. G., C. Le Quéré, M. R. Raupach, C. B. Field, E. T. Buitenhuis, P. Ciais, T. J. Conway, N. P. Gillett, R. Houghton and G. Marland (2007) Contributions to accelerating atmospheric CO_2 growth from economic activity, carbon intensity, and efficiency of natural sinks. Proceedings of the national academy of sciences 104(47): 18866-18870.

Carlson, D.F., Muscarella, P.A., Gildor, H., Lipphardt Jr, B.L., and Fredj, E. (2010) How useful are progressive vector diagrams for studying coastal ocean transport? Limnology and Oceanography: Methods 8, 98-106.

Carr, M.-E., and Kearns, E. J. (2003) Production regimes in four Eastern Boundary Current systems, Deep Sea Research Part II: Topical Studies in Oceanography, 50, 3199-3221.

Cathalot, C., Van Oevelen, D., Cox, T.J., Kutti, T., Lavaleye, M., Duineveld, G., and Meysman, F.J. (2015) Cold-water coral reefs and adjacent sponge grounds: Hotspots of benthic respiration and organic carbon cycling in the deep sea. Frontiers in Marine Science 2, 37.

Cárdenas, P., H. T. Rapp, A. B. Klitgaard, M. Best, M. Thollesson and O. S. Tendal (2013) Taxonomy, biogeography and DNA barcodes of *Geodia* species (Porifera, Demospongiae, Tetractinellida) in the Atlantic boreo-arctic region. Zoological Journal of the Linnean Society 169(2): 251-311.

Carlson, C. A., D. A. Hansell, N. B. Nelson, D. A. Siegel, W. M. Smethie, S. Khatiwala, M. M. Meyers and E. Halewood (2010) Dissolved organic carbon export and subsequent remineralization in the mesopelagic and bathypelagic realms of the North Atlantic basin. Deep Sea Research Part II: Topical Studies in Oceanography 57(16): 1433-1445.

Cathalot, C., D. Van Oevelen, T. J. Cox, T. Kutti, M. Lavaleye, G. Duineveld and F. J. Meysman (2015) Cold-water coral reefs and adjacent sponge grounds: Hotspots of benthic respiration and organic carbon cycling in the deep sea. Frontiers in Marine Science 2: 37.

Cavan, E. L., Trimmer, M., Shelley, F., and Sanders, R. (2017) Remineralization of particulate organic carbon in an ocean oxygen minimum zone, Nature communications, 8, 14847.

Chapman, P., and Shannon, L. (1985) The Benguela ecosystem, Part II. Chemistry and related processes. Oceanography and Marine Biology. An Annual Review, 23, 183-251.

Chapman, P., and Shannon, L. (1987) Seasonality in the oxygen minimum layers at the extremities of the Benguela system, South African Journal of Marine Science, 5, 85-94.

Chapman, D. C., and D. B. Haidvogel (1992) Formation of Taylor caps over a tall isolated seamount in a stratified ocean, *Geophysical & Astrophysical Fluid Dynamics*, *64*(1- 4), 31-65.

Chen, C., Huang, H., Beardsley, R.C., Xu, Q., Limeburner, R., Cowles, G.W., Sun, Y., Qi, J., and Lin, H. (2011) Tidal dynamics in the Gulf of Maine and New England Shelf: An application of FVCOM. Journal of Geophysical Research: Oceans 116.

Chikaraishi, Y., Y. Kashiyama, N. O. Ogawa, H. Kitazato and N. Ohkouchi (2007) Metabolic control of nitrogen isotope composition of amino acids in macroalgae and gastropods: implications for aquatic food web studies. Marine Ecology Progress Series 342: 85-90.

Chikaraishi, Y., N. O. Ogawa, Y. Kashiyama, Y. Takano, H. Suga, A. Tomitani, H. Miyashita, H. Kitazato and N. Ohkouchi (2009) Determination of aquatic food-web structure based on compound-specific nitrogen isotopic composition of amino acids. Limnology and Oceanography: methods 7(11): 740-750.

Chu, J.W., and Leys, S.P. (2010) High resolution mapping of community structure in three glass sponge reefs (Porifera, Hexactinellida). Marine Ecology Progress Series 417, 97-113.

Chun, C. (1903) Aus den Tiefen des Weltmeeres, Fischer.

Clark, M. R., A. A. Rowden, T. Schlacher, A. Williams, M. Consalvey, K. I. Stocks, et al. (2010) The ecology of seamounts: structure, function, and human impacts, *Annual Review of Marine Science*, *2*, 253-278.

Coma, R. (2002) Seasonality of in situ respiration rate in three temperate benthic suspension feeders. Limnology and Oceanography 47(1): 324-331.

Codiga, D. L. (2011) *Unified tidal analysis and prediction using the UTide Matlab functions*, Graduate School of Oceanography, University of Rhode Island Narragansett, RI.

Coma, R. (2002) Seasonality of in situ respiration rate in three temperate benthic suspension feeders, *Limnology and Oceanography*, *47*(1), 324-331.

Conway, K. W., J. V. Barrie, and M. Krautter (2005) Geomorphology of unique reefs on the western Canadian shelf: sponge reefs mapped by multibeam bathymetry, *Geo-Marine Letters*, *25*(4), 205-213.

Costello, M. J., McCrea, M., Freiwald, A., Lundälv, T., Jonsson, L., Bett, B. J., van Weering, T. C., de Haas, H., Roberts, J. M., and Allen, D. (2005) Role of cold-water *Lophelia pertusa* coral reefs as fish habitat in the NE Atlantic, in: Cold- water corals and ecosystems, Springer, Heidelberg, 771-805.

Culwick, T., J. Phillips, C. Goodwin, E. J. Rayfield, and K. R. Hendry (2020) Sponge Density and Distribution Constrained by Fluid Forcing in the Deep Sea, *Frontiers in Marine Science*, *7*, 395.

Cyr, F., Van Haren, H., Mienis, F., Duineveld, G., and Bourgault, D. (2016) On the influence of cold-water coral mound size on flow hydrodynamics, and vice versa. Geophysical Research Letters 43, 775-783.

Dalsgaard, J., M. St John, G. Kattner, D. Muller-Navarra and W. Hagen (2003) Fatty acid trophic markers in the pelagic marine environment. Advances in Marine Biology 46: 225-340.

Danovaro, R., P. V. Snelgrove and P. Tyler (2014) Challenging the paradigms of deep-sea ecology. Trends in ecology & evolution 29(8): 465-475.

Davies, A. J., Wisshak, M., Orr, J. C., and Roberts, J. M. (2008) Predicting suitable habitat for the cold-water coral *Lophelia pertusa* (Scleractinia), Deep Sea Research Part I: Oceanographic Research Papers, 55, 1048-1062.

Davies, A. J., G. C. Duineveld, M. S. Lavaleye, M. J. Bergman, H. van Haren and J. M. Roberts (2009) Downwelling and deep-water bottom currents as food supply mechanisms to the cold-water coral *Lophelia pertusa* (Scleractinia) at the Mingulay Reef Complex. Limnology and Oceanography 54(2): 620-629.

Davies, A. J., G. C. Duineveld, T. C. van Weering, F. Mienis, A. M. Quattrini, H. E. Seim, J. M. Bane and S. W. Ross (2010) Short-term environmental variability in cold-water coral habitat at Viosca Knoll, Gulf of Mexico. Deep Sea Research Part I: Oceanographic Research Papers 57(2): 199-212.

Davies, A. J., and Guinotte, J. M. (2011) Global habitat suitability for framework-forming cold-water corals, PloS one, 6, e18483.

Davison, J. J., H. van Haren, P. Hosegood, N. Piechaud and K. L. Howell (2019) The distribution of deep-sea sponge aggregations (Porifera) in relation to oceanographic processes in the Faroe-Shetland Channel. Deep Sea Research Part I: Oceanographic Research Papers 146: 55-61.

de Froe, E., L. Rovelli, R. N. Glud, S. R. Maier, G. Duineveld, F. Mienis, M. Lavaleye and D. van Oevelen (2019) Benthic oxygen and nitrogen exchange on a cold-water coral reef in the North-East Atlantic Ocean. Frontiers in Marine Science 6: 665.

de Haas, H., Mienis, F., Frank, N., Richter, T. O., Steinacher, R., De Stigter, H., Van der Land, C., and Van Weering, T. C. (2009) Morphology and sedimentology of (clustered) cold-water coral mounds at the south Rockall Trough margins, NE Atlantic Ocean, Facies, 55, 1-26.

de Goeij, J. M., H. van den Berg, M. M. van Oostveen, E. H. Epping and F. C. Van Duyl (2008) Major bulk dissolved organic carbon (DOC) removal by encrusting coral reef cavity sponges. Marine Ecology Progress Series 357: 139-151.

de Goeij, J. M., L. Moodley, M. Houtekamer, N. M. Carballeira and F. C. Van Duyl (2008) Tracing ^{13}C-enriched dissolved and particulate organic carbon in the bacteria-containing coral reef sponge *Halisarca caerulea*: Evidence for DOM-feeding. Limnology and Oceanography 53(4): 1376-1386.

de Goeij, J., A. De Kluijver, F. Van Duyl, J. Vacelet, R. Wijffels, A. De Goeij, J. Cleutjens and B. Schutte (2009) Cell kinetics of the marine sponge *Halisarca caerulea* reveal rapid cell turnover and shedding. Journal of Experimental Biology 212(23): 3892-3900.

de Goeij, J. M., D. Van Oevelen, M. J. Vermeij, R. Osinga, J. J. Middelburg, A. F. de Goeij and W. Admiraal (2013) Surviving in a marine desert: the sponge loop retains resources within coral reefs. Science 342(6154): 108-110.

de Goeij, J. M., M. P. Lesser and J. R. Pawlik (2017) Nutrient fluxes and ecological functions of coral reef sponges in a changing ocean. Climate change, ocean acidification and sponges. Cham, Springer: 373-410).

de Kluijver, A., M. C. Bart, D. V. Oevelen, J. M. De Goeij, S. Leys, S. R. Maier, M. Maldonado, K. Soetaert, S. Verbiest and J. J. Middelburg (2020) An integrative model of carbon and nitrogen metabolism in a common deep-sea sponge (*Geodia barretti*). Frontiers in Marine Science 7: 1131.

de Kluijver, A. (2020) Fatty acid analysis sponges. Digital repository for research protocols, protocols.io, Digital repository for research protocols, protocols.io.

Del Giorgio, P. A. and C. M. Duarte (2002) Respiration in the open ocean. Nature 420(6914): 379-384.

Delecat, S., G. Arp and J. Reitner (2011) Aftermath of the Triassic–Jurassic boundary crisis:spiculite formation on drowned Triassic Steinplatte reef-slope by communities of hexactinellid sponges (northern calcareous Alps, Austria). Advances in Stromatolite Geobiology, Springer: 355-390.

de Mol, B., P. Van Rensbergen, S. Pillen, K. Van Herreweghe, D. Van Rooij, A. McDonnell, V. Huvenne, M. Ivanov, R. Swennen and J. Henriet (2002) Large deep-water coral banks in the Porcupine Basin, southwest of Ireland. Marine Geology 188(1-2): 193-231.

Department of Fisheries and Oceans (2020) Canadian wave data ID44150 - La Have Bank, in: 2006/03/01 to 2020/01/14. Department of Fisheries and Oceans Canada.

Diaz, R. J. and R. Rosenberg (1995) Marine benthic hypoxia: a review of its ecological effects and the behavioural responses of benthic macrofauna. Oceanography and marine biology. An annual review 33: 245-203.

Dickson, R. and I. McCave (1986) Nepheloid layers on the continental slope west of Porcupine Bank. Deep Sea Research Part A. Oceanographic Research Papers 33(6): 791-818.

Dodds, L., J. Roberts, A. Taylor and F. Marubini (2007) Metabolic tolerance of the cold-water coral *Lophelia pertusa* (Scleractinia) to temperature and dissolved oxygen change. Journal of Experimental Marine Biology and Ecology 349(2): 205-214.

Dodds, L., Black, K., Orr, H., and Roberts, J. (2009) Lipid biomarkers reveal geographical differences in food supply to the cold-water coral *Lophelia pertusa* (Scleractinia), Marine Ecology Progress Series, 397, 113-124.

Drinkwater, K., Petrie, B., and Smith, P. (Year) Climate variability on the Scotian Shelf during the 1990s, in: ICES Mar. Sci. Symp, 40-49.

Drinkwater, K., Petrie, B., and Sutcliffe Jr, W. (1979) Seasonal geostrophic volume transports along the Scotian Shelf. Estuarine and Coastal Marine Science 9, 17-27.

Duineveld, G., M. Lavaleye and E. Berghuis (2004) Particle flux and food supply to a seamount cold-water coral community (Galicia Bank, NW Spain).Marine Ecology ProgressSeries 277: 13-23.

Duineveld, G. C. A., M. S. S. Lavaleye, M. I. N. Bergman, H. De Stigter and F. Mienis (2007) Trophic structure of a cold-water coral mound community (Rockall Bank, NE Atlantic) in relation to the near-bottom particle supply and current regime. Bulletin of Marine Science 81(3): 449-467.

Dullo, W.-C., S. Flögel and A. Rüggeberg (2008) Cold-water coral growth in relation to the hydrography of the Celtic and Nordic European continental margin. Marine Ecology Progress Series 371: 165-176.

Eisele, M., Frank, N., Wienberg, C., Hebbeln, D., Correa, M. L., Douville, E., and Freiwald, A. (2011) Productivity controlled cold-water coral growth periods during the last glacial off Mauritania, Marine Geology, 280, 143-149.

Emery, W. and J. Meincke (1986) Global water masses-summary and review. Oceanologica acta 9(4): 383-391.

EMODnet Bathymetry Consortium (2016), EMODnet Digital Bathymetry (DTM), *EMODnet Bathymetry. doi*, *10*.

Farrow, G. E., J. P. Syvitski and V. Tunnicliffe (1983) Suspended particulate loading on the macrobenthos in a highly turbid fjord: Knight Inlet, British Columbia. Canadian Journal of Fisheries and Aquatic Sciences 40(S1): s273-s288.

Fink, H. G., C. Wienberg, D. Hebbeln, H. V. McGregor, G. Schmiedl, M. Taviani and A. Freiwald (2012) Oxygen control on Holocene cold-water coral development in the eastern Mediterranean Sea. Deep Sea Research Part I: Oceanographic Research Papers 62: 89-96.

Flögel, S., Dullo, W.-C., Pfannkuche, O., Kiriakoulakis, K., and Rüggeberg, A. (2014) Geochemical and physical constraints for the occurrence of living cold-water corals, Deep Sea Research Part II: Topical Studies in Oceanography, 99, 19-26.

Forbes, E. and E. Forbes (1844) Report on the Mollusca and Radiata of the Aegean Sea, and on their distribution, considered as bearing on geology.

Frederiksen, R., A. Jensen and H. Westerberg (1992) The distribution of the scleractinian coral *Lophelia pertusa* around the Faroe Islands and the relation to internal tidal mixing. Sarsia 77(2): 157-171.

Freiwald, A. (2002) Reef-Forming Cold-Water Corals. Ocean Margin Systems. G. Wefer, D. S. M. Billett, D. Hebbeln et al. Heidelberg, Spinger Verlag: 365-385.

Freiwald, A., J. H. Fossa, A. Grehan, T. Koslow and J. M. Roberts (2004) Cold-water coral reefs: out of sight-no longer out of mind, UNEP-WCMC.

Freiwald, A., Beuck, L., Rüggeberg, A., Taviani, M., Hebbeln, D., and Participants, R. V. M. C. M. (2009) The white coral community in the central Mediterranean Sea revealed by ROV surveys, Oceanography, 22, 58-74.

Froelich, P. N., G. Klinkhammer, M. L. Bender, N. Luedtke, G. R. Heath, D. Cullen, P. Dauphin, D. Hammond, B. Hartman and V. Maynard (1979) Early oxidation of organic matter in pelagic sediments of the eastern equatorial Atlantic: suboxic diagenesis. Geochimica et cosmochimica acta 43(7): 1075-1090.

Fugate, D. C., and C. T. Friedrichs (2002), Determining concentration and fall velocity of estuarine particle populations using ADV, OBS and LISST, *Continental Shelf Research*, *22*(11-13), 1867-1886.

Fuller, S. and P. Cameron (1998) Marine benthic seascapes: fishermen's perspectives. Mar. Issues Comm. Spec. Publ. Can.(3): 68.

Fuller, S. D. (2011) Diversity of marine sponges in the Northwest Atlantic.

Gage, J. D. and P. A. Tyler (1991). Deep-sea biology: a natural history of organisms at the deep-sea floor, Cambridge University Press.

Gardner, W., Richardson, M., Hinga, K., and Biscaye, P. (1983). Resuspension measured with sediment traps in a high-energy environment. Earth and Planetary Science Letters 66, 262-278.

Gardner, W. D., M. J. Richardson, A. V. Mishonov and P. E. Biscaye (2018) Global comparison of benthic nepheloid layers based on 52 years of nephelometer and transmissometer measurements. Progress in Oceanography 168: 100-111.

Garrett, C., and Laurent, L.S. (2002) Aspects of deep ocean mixing. Journal of oceanography 58, 11-24.

Gatien, M.G. (1976) A study in the slope water region south of Halifax. Journal of the Fisheries Board of Canada 33, 2213-2217.

Geissler, W., Schwenk, T., and Wintersteller, P. (2013) Walvis Ridge Passive-Source Seismic Experiment (WALPASS) – Cruise No. MSM20/1 – January 06 – January 15, 2012 - Cape Town (South Africa) – Walvis Bay (Namibia), DFG-Senatskommission für Ozeanographie, MARIA S. MERIAN-Berichte, MSM20/1, 54 pp.

Gili, J. M. and R. Coma (1998) Benthic suspension feeders: their paramount role in littoral marine food webs. Trends in Ecology & Evolution 13(8): 316-321.

Gillan, F. T., I. L. Stoilov, J. E. Thompson, R. W. Hogg, C. R. Wilkinson and C. Djerassi (1988) Fatty acids as biological markers for bacterial symbionts in sponges. Lipids 23(12): 1139-1145.

Gooday, A. J. (2002) Biological responses to seasonally varying fluxes of organic matter to the ocean floor: a review, *Journal of Oceanography*, *58*(2), 305-332.

Gori, A., Grover, R., Orejas, C., Sikorski, S., and Ferrier-Pagès, C. (2014) Uptake of dissolved free amino acids by four cold-water coral species from the Mediterranean Sea, Deep Sea Research Part II: Topical Studies in Oceanography, 99, 42-50.

Gostiaux, L., and H. Van Haren (2010) Extracting meaningful information from uncalibrated backscattered echo intensity data, *Journal of Atmospheric and Oceanic Technology*, *27*(5), 943-949.

Govenar, B. (2012) Energy transfer through food webs at hydrothermal vents: Linking the lithosphere to the biosphere. Oceanography 25(1): 246-255.

Grant, J., Volckaert, F., and Roberts-Regan, D.L. (1987) Resuspendable organic matter in Nova Scotian shelf and slope sediments. Continental Shelf Research 7, 113-1138.

Grant, N., E. Matveev, A. S. Kahn and S. P. Leys (2018) Suspended sediment causes feeding current arrests in situ in the glass sponge *Aphrocallistes vastus*. Marine environmental research 137: 111-120.

Grant, N., Matveev, E., Kahn, A., Archer, S., Dunham, A., Bannister, R., Eerkes-Medrano, D., and Leys, S.P. (2019) Effect of suspended sediments on the pumping rates of three species of glass sponge in situ. Marine Ecology Progress Series 615, 79-100.

Grasmueck, M., Eberli, G. P., Viggiano, D. A., Correa, T., Rathwell, G., and Luo, J. (2006) Autonomous underwater vehicle (AUV) mapping reveals coral mound distribution, morphology, and oceanography in deep water of the Straits of Florida, Geophysical Research Letters, 33.

Gray, J.S., Wu, R.S.-S., and Or, Y.Y. (2002) Effects of hypoxia and organic enrichment on the coastal marine environment. Marine ecology progress series 238, 249-279.

Greenberg, D.A., Loder, J.W., Shen, Y.S., Lynch, D.R., and Naimie, C.E. (1997) Spatial and temporal structure of the barotropic response of the Scotian Shelf and Gulf of Maine to surface wind stress: A model-based study. Journal of Geophysical Research-Oceans 102, 20897-20915.

Griffith, D. R., A. P. McNichol, L. Xu, F. A. McLaughlin, R. W. Macdonald, K. A. Brown and T. I. Eglinton (2012) Carbon dynamics in the western Arctic Ocean: insights from full-depth carbon isotope profiles of DIC, DOC, and POC. Biogeosciences 9(3): 1217-1224.

Guihen, D., M. White, and T. Lundälv (2013) Boundary layer flow dynamics at a cold-water coral reef, *Journal of sea research*, *78*, 36-44.

Hadas, E., M. Shpigel and M. Ilan (2009) Particulate organic matter as a food source for a coral reef sponge. Journal of Experimental Biology 212(22): 3643-3650.

Hadas, E., D. Marie, M. Shpigel and M. Ilan (2006) Virus predation by sponges is a new nutrient-flow pathway in coral reef food webs. Limnology and Oceanography 51(3): 1548-1550.

Haidvogel, D. B., A. Beckmann, D. C. Chapman, and R.-Q. Lin (1993) Numerical simulation of flow around a tall isolated seamount. Part II: Resonant generation of trapped waves, *Journal of physical oceanography*, *23*(11), 2373-2391.

Han, G., Hannah, C.G., Loder, J.W., and Smith, P.C. (1997) Seasonal variation of the three-dimensional mean circulation over the Scotian Shelf. Journal of Geophysical Research: Oceans 102, 1011-1025.

Han, G., and Loder, J.W. (2003) Three-dimensional seasonal-mean circulation and hydrography on the eastern Scotian Shelf. Journal of Geophysical Research: Oceans 108.

Hannah, C.G., Shore, J.A., Loder, J.W., and Naimie, C.E. (2001) Seasonal circulation on the western and central Scotian Shelf. Journal of Physical Oceanography 31, 591-615.

Hansell, D. and C. A. Carlson (2002) Biogeochemistry of marine dissolved organic matter. Amsterdam, Academic Press.

Hansell, D. A. and H. Ducklow (2003) Bacterioplankton distribution and production in the bathypelagic ocean: Directly coupled to particulate organic carbon export? Limnology and Oceanography 48(1): 150-156.

Hansell, D. A., C. A. Carlson, D. J. Repeta and R. Schlitzer (2009) Dissolved organic matter in the ocean: A controversy stimulates new insights. Oceanography 22(4): 202-211.

Hansell, D. A. (2013) Recalcitrant dissolved organic carbon fractions. Annual Review of Marine Science 5:421-445.

Hansell, D. A. and C. A. Carlson (2014) Biogeochemistry of marine dissolved organic matter, Academic Press.

Hanz, U., C. Wienberg, D. Hebbeln, G. Duineveld, M. Lavaleye, K. Juva, W.-C. Dullo, A. Freiwald, L. Tamborrino and G.-J. Reichart (2019) Environmental factors influencing benthic communities in the oxygen minimum zones on the Angolan and Namibian margins. Biogeosciences (BG) 16: 4337-4356.

Hanz, U., Mienis, F. (2019) Video: High current event at an Arctic deep-sea sponge ground, doi:10.25850/nioz/7b.b.t.

Hanz, U. (2021) Vertical fluxes of organic matter over an annual cycle at an Arctic deep-sea sponge ground. PANGAEA.

Hanz, U. (2021) Long-term monitoring of near-bottom physical properties at an Arctic deep-sea sponge ground, edited, PANGAEA, doi:10.1594/PANGAEA.927956.

Hanz, U. (2021) Physical oceanography during G. O. Sars cruise GS2018108 to an Arctic deep-sea sponge ground in 2018, edited, PANGAEA, doi:10.1594/PANGAEA.927946.

Hanz, U. (2021) Vertical fluxes of organic matter over an annual cycle at an Arctic deep-sea sponge ground. edited, PANGAEA, doi:10.1594/PANGAEA.927955.

Hanz, U., L. Beazley, E. Kenchington, G. Duineveld, H. T. Rapp and F. Mienis (2021) Seasonal variability in near-bed environmental conditions in the *Vazella pourtalesii* glass sponge grounds of the Scotian Shelf. Frontiers in Ecology and the Environment.

Hanz, U., E. M. Roberts, G. Duineveld, A. Davies, H. Van Haren, H. T. Rapp, G.-J. Reichart and F. Mienis (2021) Long–term observations reveal environmental conditions and food supply mechanisms at an Arctic deep-sea sponge ground. Journal of Geophysical Research.

Harris, P. T. and T. Whiteway (2011) Global distribution of large submarine canyons: Geomorphic differences between active and passive continental margins. Marine Geology 285(1-4): 69-86.

Hawkes, N., M. Korabik, L. Beazley, H. T. Rapp, J. R. Xavier and E. Kenchington (2019) Glass sponge grounds on the Scotian Shelf and their associated biodiversity. Marine Ecology Progress Series 614: 91-109.

Hebbeln, D., C. Wienberg, P. Wintersteller, A. Freiwald, M. Becker, L. Beuck, C. Dullo, G. Eberli, S. Glogowski and L. Matos (2014) Environmental forcing of the Campeche cold-water coral province, southern Gulf of Mexico. Biogeosciences 11(7): 1799.

Hebbeln, D., C. Wienberg, W.-C. Dullo, A. Freiwald, F. Mienis, C. Orejas and J. Titschack (2020) Cold-water coral reefs thriving under hypoxia. Coral Reefs: 1-7.

Hebbeln, D., Wienberg, C., Wintersteller, P., Freiwald, A., Becker, M., Beuck, L., Dullo, W.-C., Eberli, G., Glogowski, S., and Matos, L. (2014) Environmental forcing of the Campeche cold-water coral province, southern Gulf of Mexico, Biogeosciences (BG), 11, 1799-1815.

Hebbeln, D., Wienberg, C., Bender, M., Bergmann, F., Dehning, K., Dullo, W.-C., Eichstädter, R., Flöter, S., Freiwald, A., Gori, A., Haberkern, J., Hoffmann, L., João, F., Lavaleye, M., Leymann, T., Matsuyama, K., Meyer-Schack, B., Mienis, F., Moçambique, I., Nowald, N., Orejas, C., Ramos Cordova, C., Saturov, D., Seiter, C., Titschack, J., Vittori, V., Wefing, A.-M., Wilsenack, M., and Wintersteller, P. (2017) ANNA Cold-Water Coral Ecosystems off Angola and Namibia - Cruise No. M122 - December 30, 2015 - January 31, 2016 - Walvis Bay (Namibia)-Walvis Bay (Namibia), METEOR-Berichte, M122 https://doi.org/10.2312/cr_m122.

Hedgpeth, J. W. (1957) Classification of marine environments. Treatise on marine ecology and paleoecology 50: 17-28.

Helm, K. P., N. L. Bindoff and J. A. Church (2011) Observed decreases in oxygen content of the global ocean. Geophysical Research Letters 38(23).

Helland-Hansen, B. and F. Nansen (1909) The Norwegian Sea: its physical oceanography based upon the Norwegian researches 1900-1904, Det Mallingske Bogtrykkeri.

Henrich, R., M. Hartmann, J. Reitner, P. Schäfer, A. Freiwald, S. Steinmetz, et al. (1992) Facies belts and communities of the Arctic Vesterisbanken Seamount (central Greenland Sea), Facies, 27(1), 71.

Henry, L.-A., and Roberts, J. M. (2007) Biodiversity and ecological composition of macrobenthos on cold-water coral mounds and adjacent off-mound habitat in the bathyal Porcupine Seabight, NE Atlantic, Deep Sea Research Part I: Oceanographic Research Papers, 54, 654-672.

Henry, L.-A., and Roberts, J. M. (2017) Global Biodiversity in Cold-Water Coral Reef Ecosystems, in: Marine Animal Forests, Springer, 235-256.

Hentschel, U., L. Fieseler, M. Wehrl, C. Gernert, M. Steinert, J. Hacker and M. Horn (2003) Microbial diversity of marine sponges. Sponges (Porifera). Berlin, Heidelberg, Springer: 59-88).

Hentschel, U., K. M. Usher, and M. W. Taylor (2006) Marine sponges as microbial fermenters, FEMS microbiology ecology, 55(2), 167-177.

Hentschel, U., J. Piel, S. M. Degnan and M. W. Taylor (2012) Genomic insights into the marine sponge microbiome. Nature Reviews Microbiology 10(9): 641-654.

Herzig, P. M. and M. D. Hannington (1995) Polymetallic massive sulfides at the modern seafloor a review. Ore Geology Reviews 10(2): 95-115.

Hessler, R. R. and H. L. Sanders (1967) Faunal diversity in the deep-sea. Deep Sea Research and Oceanographic Abstracts, Elsevier.

Hill, P.R., and Bowen, A.J. (1983). Modern sediment dynamics at the shelf-slope boundary off Nova Scotia.

Hochachka, P. and G. Somero (1968) The adaptation of enzymes to temperature. Comparative biochemistry and physiology 27(3): 659-668.

Hobson, K. A. and H. E. Welch (1995) Cannibalism and trophic structure in a high Arctic lake: insights from stable-isotope analysis. Canadian Journal of Fisheries and Aquatic Sciences 52(6): 1195-1201.

Hoffmann, F., O. Larsen, V. Thiel, H. T. Rapp, T. Pape, W. Michaelis and J. Reitner (2005) An anaerobic world in sponges. Geomicrobiology Journal 22(1-2): 1-10.

Hoffmann, F., R. Radax, D. Woebken, M. Holtappels, G. Lavik, H. T. Rapp, M. L. Schläppy, C. Schleper and M. M. Kuypers (2009) Complex nitrogen cycling in the sponge *Geodia barretti*. Environmental Microbiology 11(9): 2228-2243.

Hogg, M., O. Tendal, K. Conway, S. Pomponi, R. Van Soest, J. Gutt, M. Krautter and J. Roberts (2010) Deep-seas Sponge grounds: reservoirs of biodiversity. UNEP-WCMC Biodiversity 32.

Holm-Hansen, O., C. J. Lorenzen, R. W. Holmes, and J. D. Strickland (1965) Fluorometric determination of chlorophyll, *ICES Journal of Marine Science*, *30*(1), 3-15.

Hosegood, P. and H. van Haren (2004) Near-bed solibores over the continental slope in the Faeroe-Shetland Channel. Deep Sea Research Part II: Topical Studies in Oceanography 51(25-26): 2943-2971.

Hosegood, P., W. Nimmo-Smith, R. Proud, K. Adams and A. Brierley (2019) Internal lee waves and baroclinic bores over a tropical seamount shark 'hot-spot'. Progress in Oceanography 172: 34-50.

Hopkins, T. S. (1991) The GIN Sea—A synthesis of its physical oceanography and literature review 1972–1985, *Earth-Science Reviews*, *30*(3-4), 175-318.

Hovland, M. (2008) Deep-water coral reefs: Unique biodiversity hot-spots, Springer Science & Business Media.

Howell, K.-L., N. Piechaud, A.-L. Downie and A. Kenny (2016) The distribution of deep-sea sponge aggregations in the North Atlantic and implications for their effective spatial management. Deep Sea Research Part I: Oceanographic Research Papers 115: 309- 320.

Hudspith, M., L. Rix, M. Achlatis, J. Bougoure, P. Guagliardo, P. L. Clode, N. S. Webster, G. Muyzer, M. Pernice and J. M. de Goeij (2021) Subcellular view of host–microbiome nutrient exchange in sponges: insights into the ecological success of an early metazoan–microbe symbiosis. Microbiome 9(1): 1-15.

Hunting, E. R., J. M. de Goeij, M. Asselman, R. W. van Soest and H. G. van der Geest (2010) Degradation of mangrove-derived organic matter in mangrove associated sponges. Bulletin of Marine Science 86(4): 871-877.

Huthnance, J. M. (1995) Circulation, exchange and water masses at the ocean margin: the role of physical processes at the shelf edge. Progress in Oceanography 35(4): 353-431.

Iken, K., T. Brey, U. Wand, J. Voigt and P. Junghans (2001) Food web structure of the benthic community at the Porcupine Abyssal Plain (NE Atlantic): a stable isotope analysis. Progress in Oceanography 50(1-4): 383-405.

Imbs, A. B., D. A. Demidkova and T. N. Dautova (2016) Lipids and fatty acids of cold-water soft corals and hydrocorals: a comparison with tropical species and implications for coral nutrition. Marine biology 163(10): 202.

Jakobsson, M., L. Mayer, B. Coakley, J. A. Dowdeswell, S. Forbes, B. Fridman, et al. (2012) The international bathymetric chart of the Arctic Ocean (IBCAO) version 3.0, *Geophysical Research Letters*, *39*(12).

Jalali, M., A. VanDine, V. K. Chalamalla and S. Sarkar (2017) Oscillatory stratified flow over supercritical topography: Wave energetics and turbulence. Computers & Fluids 158: 39-48.

Jeansson, E., A. Olsen, and S. Jutterström (2017) Arctic intermediate water in the Nordic Seas, 1991–2009, *Deep Sea Research Part I: Oceanographic Research Papers*, *128*, 82-97.

Ji, R., Chen, C., Franks, P.J., Townsend, D.W., Durbin, E.G., Beardsley, R.C., Lough, R.G., and Houghton, R.W. (2006) The impact of Scotian Shelf Water “cross-over” on the plankton dynamics on Georges Bank: a 3-D experiment for the 1999 spring bloom. Deep Sea Research Part II: Topical Studies in Oceanography 53, 2684-2707.

Jiménez, E. and M. Ribes (2007) Sponges as a source of dissolved inorganic nitrogen: nitrification mediated by temperate sponges. Limnology and Oceanography 52(3): 948-958.

Junker, T., Mohrholz, V., Siegfried, L., and van der Plas, A.(2017) Seasonal to interannual variability of water mass characteristics and currents on the Namibian shelf, Journal of Marine Systems, 165, 36-46.

Kahn, A. S., G. Yahel, J. W. Chu, V. Tunnicliffe and S. P. Leys (2015) Benthic grazing and carbon sequestration by deep-water glass sponge reefs. Limnology and Oceanography 60(1): 78-88.

Kahn, A. S., J. W. Chu and S. P. Leys (2018) Trophic ecology of glass sponge reefs in the Strait of Georgia, British Columbia. Scientific reports 8(1): 756.

Karstensen, J., Stramma, L., and Visbeck, M. (2008) Oxygen minimum zones in the eastern tropical Atlantic and Pacific oceans, Progress in Oceanography, 77, 331-350.

Kato, Y., K. Fujinaga, K. Nakamura, Y. Takaya, K. Kitamura, J. Ohta, R. Toda, T. Nakashima and H. Iwamori (2011) Deep-sea mud in the Pacific Ocean as a potential resource for rare-earth elements. Nature geoscience 4(8): 535-539.

Keesing, J. K., J. Strzelecki, J. Fromont and D. Thomson (2013) Sponges as important sources of nitrate on an oligotrophic continental shelf. Limnology and Oceanography 58(6): 1947-1958.

Kelly, J. R. and R. E. Scheibling (2012) Fatty acids as dietary tracers in benthic food webs. Marine Ecology Progress Series 446: 1-22.

Kiessling, W. and C. Simpson (2011) On the potential for ocean acidification to be a general cause of ancient reef crises. Global Change Biology 17(1): 56-67.

King, J. R. and D. S. Farner (1961) Energy metabolism, thermoregulation and body temperature. Biology and comparative physiology of birds 2: 215-288.

Kiran, G. S., S. Sekar, P. Ramasamy, T. Thinesh, S. Hassan, A. N. Lipton, A. Ninawe and J. Selvin (2018) Marine sponge microbial association: towards disclosing unique symbiotic interactions. Marine environmental research 140: 169-179.

Kirchman, D. (1994) The uptake of inorganic nutrients by heterotrophic bacteria." Microbial Ecology 28(2): 255-271.

Kiriakoulakis, K., E. Stutt, S. J. Rowland, A. Vangriesheim, R. S. Lampitt, and G. A. Wolff (2001) Controls on the organic chemical composition of settling particles in the Northeast Atlantic Ocean, *Progress in oceanography*, *50*(1-4), 65-87.

Kiriakoulakis, K., Fisher, E., Wolff, G. A., Freiwald, A., Grehan, A., and Roberts, J. M. (2005) Lipids and nitrogen isotopes of two deep-water corals from the North-East Atlantic: initial results and implications for their nutrition, in: Cold-water corals and ecosystems, edited by: Freiwald, A. a. R., J.M. (eds.), Springer, Heidelberg, 715-729.

Kiriakoulakis, K., Freiwald, A., Fisher, E., and Wolff, G. (2007) Organic matter quality and supply to deep-water coral/mound systems of the NW European Continental Margin, International Journal of Earth Sciences, 96, 159-170.

Klitgaard, A. B. and O. S. Tendal (2004) Distribution and species composition of mass occurrences of large-sized sponges in the northeast Atlantic. Progress in Oceanography 61(1): 57-98.

Klymak, J. M., S. Legg, M. H. Alford, M. Buijsman, R. Pinkel and J. D. Nash (2012) The direct breaking of internal waves at steep topography. Oceanography 25(2): 150-159.

Knies, J., and P. Martinez (2009) Organic matter sedimentation in the western Barents Sea region: Terrestrial and marine contribution based on isotopic composition and organic nitrogen content, *Norwegian Journal of Geology/Norsk Geologisk Forening*, *89*.

Knudby, A., E. Kenchington and F. J. Murillo (2013) Modeling the distribution of *Geodia* sponges and sponge grounds in the Northwest Atlantic. PloS one 8(12).

Knutson, T. R., J. L. McBride, J. Chan, K. Emanuel, G. Holland, C. Landsea, I. Held, J. P. Kossin, A. Srivastava and M. Sugi (2010) Tropical cyclones and climate change. Nature geoscience 3(3): 157-163.

Koga, Y. and H. Morii (2007) Biosynthesis of ether-type polar lipids in archaea and evolutionary considerations. Microbiology and Molecular Biology Reviews 71(1): 97-120.

Koopmans, M., P. van Rijswijk, H. T. Boschker, H. Marco, D. Martens and R. H. Wijffels (2015) Seasonal variation of fatty acids and stable carbon isotopes in sponges as indicators for nutrition: Biomarkers in sponges identified. Marine biotechnology 17(1): 43-54.

Kopte, R., Brandt, P., Dengler, M., Tchipalanga, P., Macuéria, M., and Ostrowski, M. (2017) The Angola Current: Flow and hydrographic characteristics as observed at 11° S, Journal of Geophysical Research: Oceans, 122, 1177-1189.

Kostianoy, A., and Lutjeharms, J. (1999) Atmospheric effects in the Angola-Benguela frontal zone, Journal of Geophysical Research: Oceans, 104, 20963-20970.

Krause-Jensen, D. and C. M. Duarte (2016) Substantial role of macroalgae in marine carbon sequestration. Nature Geoscience 9(10): 737-742.

Kraay, G. W., Zapata, M., and Veldhuis, M. J. (1992) Separation of Chlorophylls c1c2, and c3 of marine Phytoplankton by Reverse Phase C18 high Performance liquid Chromatography 1, Journal of Phycology, 28, 708-712.

Kutti, T., R. J. Bannister and J. H. Fosså (2013) Community structure and ecological function of deep-water sponge grounds in the Traenadypet MPA—Northern Norwegian continental shelf. Continental Shelf Research 69:21-30.

Kutti, T., Bannister, R.J., Fosså, J.H., Krogness, C.M., Tjensvoll, I., and Søvik, G. (2015) Metabolic responses of the deep-water sponge *Geodia barretti* to suspended bottom sediment, simulated mine tailings and drill cuttings. Journal of experimental marine biology and ecology 473, 64-72.

Kutti, T., Fosså, J.H., and Bergstad, O.A. (2015). Influence of structurally complex benthic habitats on fish distribution. Marine Ecology Progress Series 520, 175-190.

Kuwae, T., and Hosokawa, Y. (1999). Determination of abundance and biovolume of bacteria in sediments by dual staining with 4′, 6-diamidino-2-phenylindole and acridine orange: relationship to dispersion treatment and sediment characteristics. Appl. Environ. Microbiol. 65, 3407-3412.

Lacharité, M., and Metaxas, A. (2017) Hard substrate in the deep ocean: how sediment features influence epibenthic megafauna on the eastern Canadian margin. Deep Sea Research Part I: Oceanographic Research Papers 126, 50-61.

Lampitt, R., and A. Antia (1997) Particle flux in deep seas: regional characteristics and temporal variability, *Deep Sea Research Part I: Oceanographic Research Papers*, *44*(8), 1377-1403.

Lavelle, J. W. and C. Mohn (2010) Motion, commotion, and biophysical connections at deep ocean seamounts. Oceanography 23(1): 90-103.

Le Guilloux, E., Olu, K., Bourillet, J.-F., Savoye, B., Iglésias, S., and Sibuet, M. (2009) First observations of deep-sea coral reefs along the Angola margin, Deep Sea Research Part II: Topical Studies in Oceanography, 56, 2394-2403.

Le Moigne, F. A. C. (2019) Pathways of organic carbon downward transport by the oceanic biological carbon pump. Frontiers in Marine Science 6: 634.

Levin, L. A., Huggett, C. L., and Wishner, K. F. (1991) Control of deep-sea benthic community structure by oxygen and organic-matter gradients in the eastern Pacific Ocean, Journal of Marine Research, 49, 763-800.

Levin, L. A. and M. Sibuet (2012) Understanding continental margin biodiversity: a new imperative. Annual Review of Marine Science 4: 79-112.

Levin, L. A., B. J. Bett, A. R. Gates, P. Heimbach, B. M. Howe, F. Janssen, A. McCurdy, H. A. Ruhl, P. Snelgrove and K. I. Stocks (2019) Global observing needs in the deep ocean. Frontiers in Marine Science 6: 241.

Levitus, S., J. I. Antonov, T. P. Boyer, O. K. Baranova, H. E. Garcia, R. A. Locarnini, A. V. Mishonov, J. Reagan, D. Seidov and E. S. Yarosh (2012) World ocean heat content and thermosteric sea level change (0–2000 m), 1955–2010. Geophysical Research Letters 39(10).

Leys, S., K. Wilson, C. Holeton, H. Reiswig, W. Austin and V. Tunnicliffe (2004) Patterns of glass sponge (Porifera, Hexactinellida) distribution in coastal waters of British Columbia, Canada. Marine Ecology Progress Series 283: 133-149.

Leys, S.P., Mackie, G.O., and Reiswig, H.M. (2007) The biology of glass sponges. Advances in marine biology 52, 1-145.

Leys, S. P., G. Yahel, M. A. Reidenbach, V. Tunnicliffe, U. Shavit and H. M. Reiswig (2011) The sponge pump: the role of current induced flow in the design of the sponge body plan. PloS one 6(12).

Leys, S., A. Kahn, J. Fang, T. Kutti and R. Bannister (2018) Phagocytosis of microbial symbionts balances the carbon and nitrogen budget for the deep-water boreal sponge *Geodia barretti*. Limnology and Oceanography 63(1): 187-202.

Li, Y.Z., He, R.Y., and Mcgillicuddy, D.J. (2014) Seasonal and interannual variability in Gulf of Maine hydrodynamics: 2002-2011. Deep-Sea Research Part Ii-Topical Studies in Oceanography 103, 210-222.

Loder, J.W., Han, G., Hannah, C.G., Greenberg, D.A., and Smith, P.C. (1997) Hydrography and baroclinic circulation in the Scotian Shelf region: winter versus summer. Canadian Journal of Fisheries and Aquatic Sciences 54, 40-56.

Lubchenco, J. and L. E. Petes (2010) The interconnected biosphere: science at the ocean's tipping points. Oceanography 23(2): 115-129.

Lutjeharms, J., and Stockton, P. (1987) Kinematics of the upwelling front off southern Africa, South African Journal of Marine Science, 5, 35-49.

Maier, S. R., T. Kutti, R. J. Bannister, J. K.-H. Fang, P. van Breugel, P. van Rijswijk and D. van Oevelen (2020) Recycling pathways in cold-water coral reefs: Use of dissolved organic matter and bacteria by key suspension feeding taxa. Scientific reports 10(1): 1-13.

Mariotti, A., Gadel, F., and Giresse, P. (1991) Carbon isotope composition and geochemistry of particulate organic matter in the Congo River (Central Africa): application to the study of Quaternary sediments off the mouth of the river, Chemical Geology: Isotope Geoscience Section, 86, 345-357.

Maldonado, M., Giraud, K., and Carmona, C. (2008). Effects of sediment on the survival of asexually produced sponge recruits. Marine Biology 154, 631-641.

Maldonado, M., Ribes, M., and Van Duyl, F.C. (2012). Nutrient fluxes through sponges: biology, budgets, and ecological implications. Advances in marine biology 62, 113- 182.

Maldonado, M., R. Aguilar, J. Blanco, S. García, A. Serrano, and A. Punzón (2015) Aggregated clumps of lithistid sponges: A singular, reef-like bathyal habitat with relevant paleontological connections, *PloS one*, *10*(5), e0125378.

Maldonado, M., Aguilar, R., Bannister, R.J., Bell, J.J., Conway, K.W., Dayton, P.K., Díaz, C., Gutt, J., Kelly, M., Kenchington, E.L., Leys, S.P., Pomponi, S., Rapp, H.T., Rützler, K., Tendal, O.S., Vacelet, J., and Young, C.M. (2017) Sponge grounds as key marine habitats: a synthetic review of types, structure, functional roles, and conservation concerns. Marine Animal Forests: The Ecology of Benthic Biodiversity Hotspots, 145-183.

Maldonado, M., Beazley, L., Lopez-Acosta, M., Kenchington, E., Casault, B., Hanz, U., and Mienis, F. (2020) Massive silicate utilization facilitated by a benthic- pelagic coupled feedback sustains deep-sea sponge aggregations. Limnology and Oceanography.

Martin, J. H., G. A. Knauer, D. M. Karl and W. W. Broenkow (1987) VERTEX: carbon cycling in the northeast Pacific. Deep-Sea Research 34(2): 267-285.

Mayer, L., M. Jakobsson, G. Allen, B. Dorschel, R. Falconer, V. Ferrini, G. Lamarche, H. Snaith and P. Weatherall (2018) The Nippon Foundation—GEBCO seabed 2030 project: The quest to see the world's oceans completely mapped by 2030. Geosciences 8(2): 63.

McCarthy, M. D., R. Benner, C. Lee and M. L. Fogel (2007) Amino acid nitrogen isotopic fractionation patterns as indicators of heterotrophy in plankton, particulate, and dissolved organic matter. Geochimica et Cosmochimica Acta 71(19): 4727-4744.

McClelland, J. W. and J. P. Montoya (2002) Trophic relationships and the nitrogen isotopic composition of amino acids in plankton. Ecology 83(8): 2173-2180.

Mclellan, H. (1957) On the distinctness and origin of the slope water off the Scotian Shelf and its easterly flow south of the Grand Banks. Journal of the Fisheries Board of Canada 14, 213-239.

McMahon, K. W. and M. D. McCarthy (2016) Embracing variability in amino acid δ^{15}N fractionation: mechanisms, implications, and applications for trophic ecology. Ecosphere 7(12): e01511.

Mehl, S. (1991) The Northeast Arctic cod stock's place in the Barents Sea ecosystem in the 1980s: an overview. Polar research 10(2): 525-534.

Meisel, S., Struck, U., and Emeis, K. C. (2011) Nutrient dynamics and oceanographic features in the central Namibian upwelling region as reflected in δ^{15}N-signals of suspended matter and surface sediments, Fossil Record, 14, 153-169.

Menzies, R. J., R. Y. George and G. T. Rowe (1973) Abyssal environment and ecology of the world oceans. Wiley.

Meyer, H., E. Roberts, H. Rapp and A. Davies (2019) Spatial patterns of arctic sponge ground fauna and demersal fish are detectable in autonomous underwater vehicle (AUV) imagery. Deep Sea Research Part I: Oceanographic Research Papers 153: 103137.

Middelburg, J. (2014) Stable isotopes dissect aquatic food webs from the top to the bottom. Biogeosciences 11(8): 2357.

Middelburg, J. J., C. E. Mueller, B. Veuger, A. I. Larsson, A. Form and D. Van Oevelen (2015) Discovery of symbiotic nitrogen fixation and chemoautotrophy in cold-water corals. Scientific reports 5: 17962.

Mienis, F., H. De Stigter, M. White, G. Duineveld, H. De Haas and T. Van Weering (2007) Hydrodynamic controls on cold-water coral growth and carbonate-mound development at the SW and SE Rockall Trough Margin, NE Atlantic Ocean. Deep Sea Research Part I: Oceanographic Research Papers 54(9): 1655-1674.

Mienis, F., De Stigter, H., De Haas, H., and Van Weering, T. (2009) Near-bed particle deposition and resuspension in a cold-water coral mound area at the Southwest Rockall Trough margin, NE Atlantic, Deep Sea Research Part I: Oceanographic Research Papers, 56, 1026-1038, 2009.

Mienis, F., Duineveld, G., Davies, A., Ross, S., Seim, H., Bane, J., and Van Weering, T. (2012) The influence of near-bed hydrodynamic conditions on cold-water corals in the Viosca Knoll area, Gulf of Mexico. Deep Sea Research Part I: Oceanographic Research Papers 60, 32-45.

Mienis, F., Duineveld, G., Davies, A., Lavaleye, M., Ross, S., Seim, H., Bane, J., Van Haren, H., Bergman, M., and De Haas, H. (2014) Cold-water coral growth under extreme environmental conditions, the Cape Lookout area, NW Atlantic, Biogeosciences, 11, 2543.

Mienis, F., T. Bouma, R. Witbaard, D. van Oevelen, and G. Duineveld (2019) Experimental assessment of the effects of cold water coral patches on water flow, *Marine Ecology Progress Series*, *609*, 101-117.

Miller, R. J., Hocevar, J., Stone, R. P., and Fedorov, D. V. (2012) Structure-forming corals and sponges and their use as fish habitat in Bering Sea submarine canyons, PLoS One, 7, e33885.

Millenium Ecosystem Assessment (2005) Ecosystems and Human Well-Being: Synthesis. Washington, DC, Island Press.

Mills, E., and Fournier, R. (1979) Fish production and the marine ecosystems of the Scotian Shelf, eastern Canada. Marine Biology 54, 101-108.

Mills, D. B., Francis, W. R., Vargas, S., Larsen, M., Elemans, C. P., Canfield, D. E., and Wörheide, G. (2018) The last common ancestor of animals lacked the HIF pathway and respired in low-oxygen environments, eLife, 7, e31176.

Mohn, C., A. Rengstorf, M. White, G. Duineveld, F. Mienis, K. Soetaert and A. Grehan (2014) Linking benthic hydrodynamics and cold-water coral occurrences: A high-resolution model study at three cold-water coral provinces in the NE Atlantic. Progress in Oceanography 122: 92-104.

Moitinho-Silva, L., G. Steinert, S. Nielsen, C. C. P. Hardoim, Y.-C. Wu, G. P. McCormack, S. López-Legentil, R. Marchant, N. Webster, T. Thomas and U. Hentschel (2017) Predicting the HMA-LMA Status in Marine Sponges by Machine Learning. Frontiers in Microbiology 8(752).

Molari, M., Manini, E., & Dell'Anno, A. (2013) Dark inorganic carbon fixation sustains the functioning of benthic deep-sea ecosystems. Global Biogeochemical Cycles, 27(1), 212-221.

Mooers, C. N. (1976) Overview of the physical dynamics of the continental margin/ Exposé sommaire de la dynamique physique de la marge continentale. Hydrological Sciences Journal 21(3): 467-471.

Mohrholz, V., Bartholomae, C., Van der Plas, A., and Lass, H. (2008) The seasonal variability of the northern Benguela undercurrent and its relation to the oxygen budget on the shelf, Continental Shelf Research, 28, 424-441.

Mohrholz, V., Eggert, A., Junker, T., Nausch, G., Ohde, T., and Schmidt, M. (2014) Cross shelf hydrographic and hydrochemical conditions and their short term variability at the northern Benguela during a normal upwelling season, Journal of Marine Systems, 140, 92-110.

Montoya, J. P. (2007) Natural abundance of ^{15}N in marine planktonic ecosystems, Stable isotopes in Ecology and Environmental Science, 176.

Morganti, T., R. Coma, G. Yahel and M. Ribes (2017) Trophic niche separation that facilitates co-existence of high and low microbial abundance sponges is revealed by in situ study of carbon and nitrogen fluxes. Limnology and Oceanography 62(5): 1963-1983.

Mortensen, P. B., T. Hovland, J. H. Fosså and D. M. Furevik (2001) Distribution, abundance and size of *Lophelia pertusa* coral reefs in mid-Norway in relation to seabed characteristics. Journal of the Marine Biological Association of the United Kingdom 81(4): 581-597.

Mosch, T., Sommer, S., Dengler, M., Noffke, A., Bohlen, L., Pfannkuche, O., Liebetrau, V., and Wallmann, K. (2012) Factors influencing the distribution of epibenthic megafauna across the Peruvian oxygen minimum zone, Deep Sea Research Part I: Oceanographic Research Papers, 68, 123-135.

Mountain, D.G. (2012) Labrador slope water entering the Gulf of Maine—response to the North Atlantic Oscillation. Continental Shelf Research 47, 150-155.

Mourino, B., E. Fernández, P. Serret, D. Harbour, B. Sinha, and R. Pingree (2001) Variability and seasonality of physical and biological fields at the Great Meteor Tablemount (subtropical NE Atlantic), *Oceanologica acta*, *24*(2), 167-185.

Mueller, B., J. M. de Goeij, M. J. Vermeij, Y. Mulders, E. van der Ent, M. Ribes and F. C. van Duyl (2014) Natural diet of coral-excavating sponges consists mainly of dissolved organic carbon (DOC). PloS one 9(2): e90152.

Mueller, C., A. Larsson, B. Veuger, J. Middelburg and D. Van Oevelen (2014). Opportunistic feeding on various organic food sources by the cold-water coral *Lophelia pertusa*. Biogeosciences 11(1): 123.

Mullins, H. T., Thompson, J. B., McDougall, K., and Vercoutere, T. L. (1985) Oxygen-minimum zone edge effects: evidence from the central California coastal upwelling system, Geology, 13, 491-494.

Murillo, F. J., P. D. Muñoz, J. Cristobo, P. Ríos, C. González, E. Kenchington and A. Serrano (2012) Deep-sea sponge grounds of the Flemish Cap, Flemish Pass and the Grand Banks of Newfoundland (Northwest Atlantic Ocean): distribution and species composition. Marine Biology Research 8(9): 842-854.

Murillo, F. J., E. Kenchington, G. Tompkins, L. Beazley, E. Baker, A. Knudby and W. Walkusz (2018) Sponge assemblages and predicted archetypes in the eastern Canadian Arctic. Marine Ecology Progress Series 597: 115-135.

Nöthig, E.-M., and B. von Bodungen (1989), Occurrence and vertical flux of faecal pellets of probably protozoan origin in the southeastern Weddell Sea (Antarctica), *Marine Ecology Progress Series*, 281-289.

Nycander, J. (2005) Generation of internal waves in the deep ocean by tides. Journal of Geophysical Research: Oceans 110(C10).

O'Connell, T. C. (2017) 'Trophic' and 'source' amino acids in trophic estimation: a likely metabolic explanation. Oecologia 184(2): 317-326.

Odum, H.T. (1971) Environment, power and society. New York, USA, Wiley-Interscience.

Orcutt, B. N., J. B. Sylvan, N. J. Knab and K. J. Edwards (2011) Microbial ecology of the dark ocean above, at, and below the seafloor. Microbiol. Mol. Biol. Rev. 75(2): 361-422.

Paull, C., A. Neumann, B. Am Ende, W. Ussler Iii and N. Rodriguez (2000) Lithoherms on the Florida–Hatteras slope. Marine Geology 166(1-4): 83-101.

Pawlik, J. R. and S. E. McMurray (2019) The emerging ecological and biogeochemical importance of sponges on coral reefs. Annual review of marine science 12: 315-337.

Pedrosa-Pàmies, R., M. Conte, J. Weber and R. Johnson (2019) Hurricanes enhance labile carbon export to the deep ocean. Geophysical Research Letters 46(17-18): 10484-10494.

Perdue, E. M., and Koprivnjak, J.-F. (2007) Using the C/N ratio to estimate terrigenous inputs of organic matter to aquatic environments, Estuarine, Coastal and Shelf Science, 73, 65-72.

Petrie, B., and Drinkwater, K. (1993) Temperature and salinity variability on the Scotian Shelf and in the Gulf of Maine 1945–1990. Journal of Geophysical Research: Oceans 98, 20079-20089.

Petrie, B., and Yeats, P. (2000) Annual and interannual variability of nutrients and their estimated fluxes in the Scotian Shelf-Gulf of Maine region. Canadian Journal of Fisheries and Aquatic Sciences 57, 2536-2546.

Pham, C. K., F. J. Murillo, C. Lirette, M. Maldonado, A. Colaço, D. Ottaviani and E. Kenchington (2019) Removal of deep-sea sponges by bottom trawling in the Flemish Cap area: conservation, ecology and economic assessment. Scientific reports 9(1): 1-13.

Pichevin, L., Bertrand, P., Boussafir, M., and Disnar, J.-R. (2004) Organic matter accumulation and preservation controls in a deep sea modern environment: an example from Namibian slope sediments, Organic Geochemistry, 35, 543-559.

Pile, A.J., and Young, C.M. (2006) The natural diet of a hexactinellid sponge: benthic–pelagic coupling in a deep-sea microbial food web. Deep Sea Research Part I: Oceanographic Research Papers 53, 1148-1156.

Pile, A. J. and C. M. Young (2006) The natural diet of a hexactinellid sponge: benthic–pelagic coupling in a deep-sea microbial food web. Deep Sea Research Part I: Oceanographic Research Papers 53(7): 1148-1156.

Pita, L., L. Rix, B. M. Slaby, A. Franke and U. Hentschel (2018) The sponge holobiont in a changing ocean: from microbes to ecosystems. Microbiome 6(1): 46.

Polunin, N., B. Morales-Nin, W. Pawsey, J. E. Cartes, J. K. Pinnegar and J. Moranta (2001) Feeding relationships in Mediterranean bathyal assemblages elucidated by stable nitrogen and carbon isotope data. Marine Ecology Progress Series 220: 13-23.

Poole, R., and Tomczak, M. (1999) Optimum multiparameter analysis of the water mass structure in the Atlantic Ocean thermocline, Deep Sea Research Part I: Oceanographic Research Papers, 46, 1895-1921.

Puerta, P., C. Johnson, M. Carreiro-Silva, L.-A. Henry, E. Kenchington, T. Morato, G. Kazanidis, J. L. Rueda, J. Urra and S. Ross (2020) Influence of Water Masses on the Biodiversity and Biogeography of Deep-Sea Benthic Ecosystems in the North Atlantic. Frontiers in Marine Science 7: 239.

Radax, R., F. Hoffmann, H. T. Rapp, S. Leininger, and C. Schleper (2012) Ammonia-oxidizing archaea as main drivers of nitrification in cold-water sponges, *Environmental Microbiology*, *14*(4), 909-923.

Radax, R., T. Rattei, A. Lanzen, C. Bayer, H. T. Rapp, T. Urich, and C. Schleper (2012) Metatranscriptomics of the marine sponge *Geodia barretti*: tackling phylogeny and function of its microbial community, *Environmental Microbiology*, *14*(5), 1308-1324.

Rae, C. D. (2005) A demonstration of the hydrographic partition of the Benguela upwelling ecosystem at 26° 40'S, African Journal of Marine Science, 27, 617-628

Ramirez-Llodra, E., A. Brandt, R. Danovaro, B. De Mol, E. Escobar, C. German, L. Levin, P. Arbizu, L. Menot and P. Buhl-Mortensen (2010) Deep, diverse and definitely different: unique attributes of the world's largest ecosystem. Biogeosciences 7(9): 2851-2899.

Ramirez-Llodra, E., P. A. Tyler, M. C. Baker, O. A. Bergstad, M. R. Clark, E. Escobar, L. A. Levin, L. Menot, A. A. Rowden and C. R. Smith (2011) Man and the last great wilderness: human impact on the deep sea. PLoS one 6(8).

Ramirez-Llodra, E. (2020). Deep-Sea Ecosystems: Biodiversity and Anthropogenic Impacts. The Law of the Seabed, Brill Nijhoff: 36-60.

Ramos, A., Sanz, J. L., Ramil, F., Agudo, L. M., and Presas-Navarro, C. (2017) The Giant Cold-Water Coral Mounds Barrier Off Mauritania, in: Deep-Sea Ecosystems Off Mauritania, edited by: Ramos, A., Ramil, F, Sanz, JL (Eds.), Springer, 481-525.

Randall, J. E. and W. Hartman (1968) Sponge-feeding fishes of the West Indies. Marine Biology 1(3): 216-225.

Reiswig, H. M. (1971) Particle feeding in natural populations of three marine demosponges. The Biological Bulletin 141(3): 568-591.

Reiswig, H. M. (1975) Bacteria as food for temperate-water marine sponges, *Canadian Journal of Zoology*, *53*(5), 582-589.

Ribes, M., E. Jiménez, G. Yahel, P. López-Sendino, B. Díez, R. Massana, J. Sharp and R. Coma (2012) Functional convergence of microbes associated with temperate marine sponges. Environmental microbiology 14(5): 1224-1239.

Rice, A., M. Thurston and A. New (1990) Dense aggregations of a hexactinellid sponge, *Pheronema carpenteri*, in the Porcupine Seabight (northeast Atlantic Ocean), and possible causes. Progress in Oceanography 24(1-4): 179-196.

Riekenberg, P. M., M. van der Meer and S. Schouten (2020) Practical considerations for improved reliability and precision during determination of δ^{15}N values in amino acids using a single combined oxidation–reduction reactor. Rapid Communications in Mass Spectrometry 34(14): e8797.

Ritzrau, W. (1996) Microbial activity in the benthic boundary layer: small-scale distribution and its relationship to the hydrodynamic regime. Journal of Sea Research 36(3-4): 171-180.

Rix, L., J. M. de Goeij, D. van Oevelen, U. Struck, F. A. Al-Horani, C. Wild, and M. S. Oevelen, D. v., G. Duineveld, M. Lavaleye, F. Mienis, K. Soetaert and C. H. Heip (2009) The cold-water coral community as hotspot of carbon cycling on continental margins: A food-web analysis from Rockall Bank (northeast Atlantic). Limnology and Oceanography 54(6): 1829-1844.

Rix, L., J. M. De Goeij, C. E. Mueller, U. Struck, J. J. Middelburg, F. C. Van Duyl, F. A. Al-Horani, C. Wild, M. S. Naumann and D. Van Oevelen (2016) Coral mucus fuels the sponge loop in warm-and cold-water coral reef ecosystems. Scientific reports 6: 18715.

Rix, L., J. M. de Goeij, D. van Oevelen, U. Struck, F. A. Al-Horani, C. Wild and M. S. Naumann (2018) Reef sponges facilitate the transfer of coral-derived organic matter to their associated fauna via the sponge loop. Marine Ecology Progress Series 589: 85-96.

Rix, L., M. Ribes, R. Coma, M. T. Jahn, J. M. de Goeij, D. van Oevelen, S. Escrig, A. Meibom and U. Hentschel (2020) Heterotrophy in the earliest gut: a single-cell view of heterotrophic carbon and nitrogen assimilation in sponge- microbe symbioses. The ISME Journal 14(10): 2554-2567.

Roberts, E., Mienis, F., Rapp, H., Hanz, U., Meyer, H., and Davies, A. (2018) Oceanographic setting and short-timescale environmental variability at an Arctic seamount sponge ground. Deep Sea Research Part I: Oceanographic Research Papers 138, 98-113.

Roberts, E., D. Bowers, H. Meyer, A. Samuelsen, H. Rapp and P. Cárdenas (2021) Water masses constrain the distribution of deep-sea sponges in the North Atlantic Ocean and Nordic Seas. Marine Ecology Progress Series 659: 75-96.

Roberts, J. M., A. J. Wheeler and A. Freiwald (2006) Reefs of the deep: the biology and geology of cold-water coral ecosystems. Science 312(5773): 543-547.

Roberts, J. M., A. Wheeler, A. Freiwald and S. Cairns (2009) Cold-water corals: the biology and geology of deep-sea coral habitats, Cambridge University Press.

Robertson, R., J. Dong, and P. Hartlipp (2017) Diurnal Critical latitude and the latitude dependence of internal tides, internal waves, and mixing based on Barcoo seamount, *Journal of Geophysical Research: Oceans*, *122*(10), 7838-7866.

Rogers, A. (1994) The biology of seamounts. Advances in marine biology, Elsevier. 30: 305- 350.

Rogers, A. (2004) The biology, ecology and vulnerability of deep-water coral reefs, IUCN Gland.

Rooks, C., J. K.-H. Fang, P. T. Mørkved, R. Zhao, H. T. Rapp, J. R. Xavier and F. Hoffmann (2020) Deep-sea sponge grounds as nutrient sinks: denitrification is common in boreo-Arctic sponges. Biogeosciences 17(5): 1231-1245.

Rowe, G. T. and N. Staresinic (1979) Sources of organic matter to the deep-sea benthos. Ambio Special Report: 19-23.

Rudels, B., E. Fahrbach, J. Meincke, G. Budéus, and P. Eriksson (2002), The East Greenland Current and its contribution to the Denmark Strait overflow, *ICES Journal of Marine Science*, *59*(6), 1133-1154.

Ruhl, H. A. (2008) Community change in the variable resource habitat of the abyssal northeast Pacific, Ecology, 89, 991-1000.

Ruhl, H. A., J. A. Ellena and K. L. Smith (2008) Connections between climate, food limitation, and carbon cycling in abyssal sediment communities. Proceedings of the National Academy of Sciences 105(44): 17006-17011.

Rudnick, D. L., T. J. Boyd, R. E. Brainard, G. S. Carter, G. D. Egbert, M. C. Gregg, et al. (2003) From tides to mixing along the Hawaiian Ridge, *science*, *301*(5631), 355-357.

Sanchez-Vidal, A., M. Canals, A. M. Calafat, G. Lastras, R. Pedrosa-Pàmies, M. Menéndez, R. Medina, B. Hereu, J. Romero and T. Alcoverro (2012) Impacts on the deep-sea ecosystem by a severe coastal storm. PLoS one 7(1): e30395.

Sanders, H. (1969) Benthic marine diversity and the stability-time hypothesis, Brookhaven Symposia in Biology, 71-81.

Sars, G. O. and M. Sars (1872) On Some Remarkable Forms of Animal Life from the Great Deeps Off the Norwegian Coast, Brøgger & Christie.

Schläppy, M.-L., S. I. Schöttner, G. Lavik, M. M. Kuypers, D. de Beer and F. Hoffmann (2010) Evidence of nitrification and denitrification in high and low microbial abundance sponges. Marine biology 157(3): 593-602.

Schlitzer, R. (2015), Ocean data view, edited.

Schmidtko, S., L. Stramma and M. Visbeck (2017) Decline in global oceanic oxygen content during the past five decades. Nature 542(7641): 335-339.

Schroeder, W. (2002) Observations of *Lophelia pertusa* and the surficial geology at a deep-water site in the northeastern Gulf of Mexico, Hydrobiologia, 471, 29-33.

Shannon, L., Boyd, A., Brundrit, G., and Taunton-Clark, J. (1986) On the existence of an El Niño-type phenomenon in the Benguela system, Journal of Marine Research, 44, 495-520, 1986.

Shannon, L., Agenbag, J., and Buys, M. (1987) Large-and mesoscale features of the Angola-Benguela front, South African Journal of Marine Science, 5, 11-34.

Shannon, L., and Nelson, G. (1996) The Benguela: large scale features and processes and system variability, in: The South Atlantic, Springer, Berlin, Heidelberg, 163-210.

Shannon, L. (2001) Benguela Current, Ocean Currents: A Derivative of Encyclopedia of Ocean Sciences, 23-34.

Sharma, R. (2015) Environmental issues of deep-sea mining. Procedia Earth and Planetary Science 11: 204-211.

Sibuet, M. and K. Olu-Le Roy (2002) Cold seep communities on continental margins: structure and quantitative distribution relative to geological and fluid venting patterns. Ocean margin systems, Springer: 235-251.

Siegl, A., J. Kamke, T. Hochmuth, J. Piel, M. Richter, C. Liang, T. Dandekar and U. Hentschel (2011) Single-cell genomics reveals the lifestyle of Poribacteria, a candidate phylum symbiotically associated with marine sponges. The ISME journal 5(1): 61-70.

Sitja, C. and M. Maldonado (2014) New and rare sponges from the deep shelf of the Alboran Island (Alboran Sea, Western Mediterranean). Zootaxa 3760(2): 141-179.

Smetacek, V. (1984) The supply of food to the benthos, in *Flows of energy and materials in marine ecosystems*, edited, pp. 517-547, Springer.

Smith, C. R. and A. R. Baco (2003) Ecology of whale falls at the deep-sea floor. Oceanography and marine biology 41: 311-354.

Smith, C. R., F. C. De Leo, A. F. Bernardino, A. K. Sweetman and P. M. Arbizu (2008) Abyssal food limitation, ecosystem structure and climate change. Trends in Ecology & Evolution 23(9): 518-528.

Smith, K. L., H. A. Ruhl, B. J. Bett, D. S. M. Billett, R. S. Lampitt and R. S. Kaufmann (2009) Climate, carbon cycling, and deep-ocean ecosystems. Proceedings of the National Academy of Sciences 106(46): 19211-19218.

Smith, K. L., H. A. Ruhl, C. L. Huffard, M. Messié and M. Kahru (2018) Episodic organic carbon fluxes from surface ocean to abyssal depths during long-term monitoring in NE Pacific. Proceedings of the National Academy of Sciences 115(48): 12235-12240.

Smith, P.C. (1978) Low-frequency fluxes of momentum, heat, salt, and nutrients at the edge of the Scotian Shelf. Journal of Geophysical Research: Oceans 83, 4079-4096.

Smith, P.C., Petrie, B., and Mann, C. (1978) Circulation, variability, and dynamics of the Scotian Shelf and slope. Journal of the Fisheries Board of Canada 35, 1067-1083.

Sokolova, I.M., Frederich, M., Bagwe, R., Lannig, G., and Sukhotin, A.A. (2012) Energy homeostasis as an integrative tool for assessing limits of environmental stress tolerance in aquatic invertebrates. Marine Environmental Research 79, 1-15.

Somero, G. (1998), Adaptation to cold and depth: contrasts between polar and deep-sea animals, *Cold ocean physiology*, *66*, 33-57.

Song, H., Ji, R., Stock, C., Kearney, K., and Wang, Z. (2011) Interannual variability in phytoplankton blooms and plankton productivity over the Nova Scotian Shelf and in the Gulf of Maine. Marine Ecology Progress Series 426, 105-118.

Strand, R., Whalan, S., Webster, N.S., Kutti, T., Fang, J.K.-H., Luter, H.M., and Bannister, R. (2017) The response of a boreal deep-sea sponge holobiont to acute thermal stress. Scientific reports 7, 1-12.

Strand, R., S. Whalan, N. S. Webster, T. Kutti, J. K.-H. Fang, H. M. Luter and R. Bannister (2017) The response of a boreal deep-sea sponge holobiont to acute thermal stress. Scientific reports 7(1): 1660.

Stratmann, T., L. Mevenkamp, A. K. Sweetman, A. Vanreusel and D. van Oevelen (2018) Has phytodetritus processing by an abyssal soft-sediment community recovered 26 years after an experimental disturbance? Frontiers in Marine Science 5: 59.

Suess, E. (1980) Particulate organic carbon flux in the oceans—surface productivity and oxygen utilization. Nature 288(5788): 260.

Sverdrup, H. (1953) On conditions for the vernal blooming of phytoplankton, *J. Cons. Int. Explor. Mer*, *18*(3), 287-295.

Sweetman, A. K., A. R. Thurber, C. R. Smith, L. A. Levin, C. Mora, C.-L. Wei, A. J. Gooday, D. O. Jones, M. Rex and M. Yasuhara (2017) Major impacts of climate change on deep- sea benthic ecosystems. Elem Sci Anth 5: 4.

Tabachnick, K., R. Van Soest, M. van Kempen Th and J. Braekamn (1994) Distribution of recent Hexactinellida. Sponges in Time and Space. Rotterdam: Balkema: 225-232.

Tahey, T., Duineveld, G., Berghuis, E., and Helder, W. (1994) Relation between sediment-water fluxes of oxygen and silicate and faunal abundance at continental shelf, slope and deep-water stations in the northwest Mediterranean, Marine Ecology Progress Series, 119-130.

Tamborrino, L., Wienberg, C., Titschack, J., Wintersteller, P., Mienis, F., Freiwald, A., Orejas, C., Dullo, W.-C., Haberkern, J., and Hebbeln, D. (2019) Mid-Holocene extinction of cold-water corals on the Namibian shelf steered by the Benguela Upwelling System. *Geology*, *47*(12), 1185-1188.

Tanioka, T. and K. Matsumoto (2020) Stability of marine organic matter respiration stoichiometry. Geophysical Research Letters 47(1): e2019GL085564.

Taviani, M., Remia, A., Corselli, C., Freiwald, A., Malinverno, E., Mastrototaro, F., Savini, A., and Tursi, A. (2005) First geo-marine survey of living cold-water *Lophelia* reefs in the Ionian Sea (Mediterranean basin), Facies, 50, 409-417.

Taylor (1923) Experiments on the motion of solid bodies in rotating fluids. Proceedings of the Royal Society of London. Series A 104(725): 213-218.

Taylor, J. R. (1993) Turbulence and mixing in the boundary layer generated by shoaling internal waves, *Dynamics of Atmospheres and Oceans*, *19*(1-4), 233-258.

Taylor, M. W., R. T. Hill, J. Piel, R. W. Thacker and U. Hentschel (2007) Soaking it up: the complex lives of marine sponges and their microbial associates. The ISME Journal 1(3): 187.

Team, R. C (2017) A language and environment for statistical computing [Internet]. Vienna, Austria.

Thamdrup, B. and T. Dalsgaard (2008) Nitrogen cycling in sediments. Microbial ecology of the oceans 2: 527-568.

Thiel, V., M. Blumenberg, J. Hefter, T. Pape, S. Pomponi, J. Reed, J. Reitner, G. Wörheide and W. Michaelis (2002) A chemical view of the most ancient metazoa–biomarker chemotaxonomy of hexactinellid sponges. Naturwissenschaften 89(2): 60-66.

Thiel, V., A. Jenisch, G. Wörheide, A. Löwenberg, J. Reitner and W. Michaelis (1999) Mid-chain branched alkanoic acids from “living fossil” demosponges: a link to ancient sedimentary lipids? Organic geochemistry 30(1): 1-14.

Thiem, Ø., E. Ravagnan, J. H. Fosså and J. Berntsen (2006) Food supply mechanisms for cold- water corals along a continental shelf edge. Journal of Marine Systems 60(3-4): 207-219.

Thomsen, L. (2002). The benthic boundary layer. Ocean margin systems, Springer: 143-155.

Thurber, A. R., A. K. Sweetman, B. E. Narayanaswamy, D. O. Jones, J. Ingels and R. Hansman (2014) Ecosystem function and services provided by the deep sea. Biogeosciences 11(14): 3941-3963.

Titschack, J., Baum, D., De Pol-Holz, R., Lopez Correa, M., Forster, N., Flögel, S., Hebbeln, D., and Freiwald, A. (2015) Aggradation and carbonate accumulation of Holocene Norwegian cold-water coral reefs, Sedimentology, 62, 1873-1898.

Tjensvoll, I., Kutti, T., Fosså, J.H., and Bannister, R. (2013) Rapid respiratory responses of the deep-water sponge *Geodia barretti* exposed to suspended sediments. Aquatic Biology 19, 65-73.

Tompkins-MacDonald, G. J. and S. P. Leys (2008) Glass sponges arrest pumping in response to sediment: implications for the physiology of the hexactinellid conduction system. Marine Biology 154(6): 973.

Townsend, D., and Ellis, W. (2010) Primary production and nutrient cycling on the Northwest Atlantic continental shelf. Carbon and nutrient fluxes in continental margins: A global synthesis, 234-248.

Townsend, D.W., Thomas, A.C., Mayer, L.M., Thomas, M.A., and Quinlan, J.A. (2006). Oceanography of the northwest Atlantic continental shelf (1, W). The sea: the global coastal ocean: interdisciplinary regional studies and syntheses 14, 119-168.

Turley, C. (2002) The importance of 'marine snow'. Microbiol. Today 29: 177-179.

Tyrrell, T., and Lucas, M. I. (2002) Geochemical evidence of denitrification in the Benguela upwelling system, Continental Shelf Research, 22, 2497-2511.

Urrego-Blanco, J., and Sheng, J. (2014). Study on subtidal circulation and variability in the Gulf of St. Lawrence, Scotian Shelf, and Gulf of Maine using a nested-grid shelf circulation model. Ocean Dynamics 64, 385-412.

Vacelet, J. and C. Donadey (1977) Electron microscope study of the association between some sponges and bacteria. Journal of experimental marine Biology and Ecology 30(3): 301-314.

van Bleijswijk, J., C. Whalen, G. Duineveld, M. Lavaleye, H. Witte and F. Mienis (2015) Microbial assemblages on a cold-water coral mound at the SE Rockall Bank (NE Atlantic): interactions with hydrography and topography. Biogeosciences Discussions 12(2).

von Bodungen, B., A. Antia, E. Bauerfeind, O. Haupt, W. Koeve, E. Machado, I. Peeken, R. Peinert, S. Reitmeier and C. Thomsen (1995) Pelagic processes and vertical flux of particles: an overview of a long-term comparative study in the Norwegian Sea and Greenland Sea. Geologische Rundschau 84(1): 11-27.

van Duyl, F. C., J. Hegeman, A. Hoogstraten and C. Maier (2008) Dissolved carbon fixation by sponge–microbe consortia of deep water coral mounds in the northeastern Atlantic Ocean. Marine Ecology Progress Series 358: 137-150.

Vangriesheim, A., Springer, B., and Crassous, P. (2001) Temporal variability of near-bottom particle resuspension and dynamics at the Porcupine Abyssal Plain, Northeast Atlantic. Progress in Oceanography 50, 123-145.

van Haren, H., Oakey, N., and Garrett, C. (1994) Measurements of internal wave band eddy fluxes above a sloping bottom. Journal of Marine Research 52, 909-946.

van Haren, H., and L. Gostiaux (2012) Detailed internal wave mixing above a deep-ocean slope, *Journal of Marine Research*, *70*(1), 173-197.

van Haren, H., Mienis, F., Duineveld, G.C., and Lavaleye, M.S. (2014). High-resolution temperature observations of a trapped nonlinear diurnal tide influencing cold-water corals on the Logachev mounds. Progress in Oceanography 125, 16-25.

van Haren, H., U. Hanz, H. de Stigter, F. Mienis and G. Duineveld (2017) Internal wave turbulence at a biologically rich Mid-Atlantic seamount. PloS one 12(12): e0189720.

van Haren, H., G. Duineveld and F. Mienis (2019) Internal wave observations off Saba Bank. Frontiers in Marine Science 5: 528.

van Oevelen, D.., Duineveld, G., Lavaleye, M., Mienis, F., Soetaert, K., and Heip, C. H. (2009) The cold-water coral community as hotspot of carbon cycling on continental margins: A food-web analysis from Rockall Bank (northeast Atlantic), Limnology and Oceanography, 54, 1829- 1844.

van Soest, R. W. and M. S. Lavaleye (2005) Diversity and abundance of sponges in bathyal coral reefs of Rockall Bank, NE Atlantic, from boxcore samples. Marine Biology Research 1(5): 338-349.

van Soest, R. W., Cleary, D. F., de Kluijver, M. J., Lavaleye, M. S., Maier, C., and van Duyl, F. C. (2007) Sponge diversity and community composition in Irish bathyal coral reefs, Contributions to Zoology, 76.

Vilas, J., J. Arístegui, K. Kiriakoulakis, G. Wolff, M. Espino, I. Polo, et al. (2009) Seamounts and organic matter—Is there an effect? The case of Sedlo and Seine Seamounts: Part 1. Distributions of dissolved and particulate organic matter, *Deep Sea Research PartII: Topical Studies in Oceanography*, *56*(25), 2618-2630.

Vogel, S. (1977) Current-induced flow through living sponges in nature. Proceedings of the National Academy of Sciences 74(5): 2069-2071.

Ward, B. B., D. G. Capone and J. P. Zehr (2007) What's new in the nitrogen cycle? Oceanography 20(2): 101-109.

Wainright, S.C. (1987) Stimulation of heterotrophic microplankton production by resuspended marine sediments. Science 238, 1710-1712.

Wakeham, S. G., J. I. Hedges, C. Lee, and T. K. Pease (1993) Effects of poisons and preservatives on the composition of organic matter in a sediment trap experiment, *Journal of marine research*, *51*(3), 669-696.

Wassmann, P., R. Peinert, and V. Smetacek (1991) Patterns of production and sedimentation in the boreal and polar Northeast Atlantic, *Polar Research*, *10*(1), 209-228.

Webster, N. S. and M. W. Taylor (2012) Marine sponges and their microbial symbionts: love and other relationships. Environmental microbiology 14(2): 335-346.

Welschmeyer, N. A., and Lorenzen, C. J. (1985) Chlorophyll budgets: Zooplankton grazing and phytoplankton growth in a temperate fjord and the Central Pacific Gyres, Limnology and Oceanography, 30, 1-21.

Wheeler, A. J., Beyer, A., Freiwald, A., De Haas, H., Huvenne, V., Kozachenko, M., Olu-Le Roy, K., and Opderbecke, J. (2007) Morphology and environment of cold-water coral carbonate mounds on the NW European margin, International Journal of Earth Sciences, 96, 37-56.

White, M., C. Mohn, H. de Stigter and G. Mottram (2005) Deep-water coral development as a function of hydrodynamics and surface productivity around the submarine banks of the Rockall Trough, NE Atlantic. Cold-water corals and ecosystems. J. R. A Freiwald, Springer, Heidelberg: 503-514.

White, M. and B. Dorschel (2010) The importance of the permanent thermocline to the cold water coral carbonate mound distribution in the NE Atlantic. Earth and Planetary Science Letters 296(3-4): 395-402.

White, M., Wolff, G. A., Lundälv, T., Guihen, D., Kiriakoulakis, K., Lavaleye, M., and Duineveld, G. (2012) A Freiwald, JM Roberts, Cold-water coral ecosystem (Tisler Reef, Norwegian Shelf) may be a hotspot for carbon cycling, Marine Ecology Progress Series, 465, 11-23.

Whitney, F., K. Conway, R. Thomson, V. Barrie, M. Krautter and G. Mungov (2005) Oceanographic habitat of sponge reefs on the Western Canadian Continental Shelf. Continental Shelf Research 25(2): 211-226.

Wienberg, C., and Titschack, J.: Framework-forming scleractinian cold-water corals through space and time (2017) a late Quaternary North Atlantic perspective, Ros-si S, Bramanti L, Gori A, Orejas C, Marine Animal Forests: the Ecology of Benthic Biodiversity Hotspots, Springer, 699-732 pp.

Wienberg, C., Titschack, J., Freiwald, A., Frank, N., Lundälv, T., Taviani, M., Beuck, L., Schröder-Ritzrau, A., Krengel, T., and Hebbeln, D. (2018) The giant Mauritanian cold-water coral mound province: Oxygen control on coral mound formation, Quaternary Science Reviews, 185, 135-152.

Wilkinson, C. R. (1999) Global and local threats to coral reef functioning and existence: review and predictions. Marine and Freshwater Research 50(8): 867-878.

Wilson, J. (1979) ‘Patch’ development of the deep-water coral *Lophelia pertusa* (L.) on Rockall Bank, Journal of the Marine Biological Association of the United Kingdom, 59, 165-177.

Witte, U. (1996) Seasonal reproduction in deep-sea sponges-triggered by vertical particle flux? Marine Biology 124(4): 571-581.

Witte, U., T. Brattegard, G. Graf, and B. Springer (1997) Particle capture and deposition by deep-sea sponges from the Norwegian-Greenland Sea, *Marine Ecology Progress Series*, *154*, 241-252.

Wuchter, C., B. Abbas, M. J. Coolen, L. Herfort, J. van Bleijswijk, P. Timmers, M. Strous, E. Teira, G. J. Herndl and J. J. Middelburg (2006) Archaeal nitrification in the ocean. Proceedings of the National Academy of Sciences 103(33): 12317-12322.

Wunsch, C. (1975) Deep ocean internal waves: What do we really know? Journal of Geophysical Research 80, 339-343.

Yahel, G., D. I. Eerkes-Medrano and S. P. Leys (2006) Size independent selective filtration of ultraplankton by hexactinellid glass sponges. Aquatic Microbial Ecology 45(2): 181-194.

Yahel, G., J. H. Sharp, D. Marie, C. Häse and A. Genin (2003) In situ feeding and element removal in the symbiont-bearing sponge *Theonella swinhoei*: Bulk DOC is the major source for carbon. Limnology and Oceanography 48(1): 141-149.

Yahel, G., F. Whitney, H. M. Reiswig, D. I. Eerkes-Medrano and S. P. Leys (2007) In situ feeding and metabolism of glass sponges (Hexactinellida, Porifera) studied in a deep temperate fjord with a remotely operated submersible. Limnology and oceanography 52(1): 428-440.

Yan, X., R. Zhang and T. R. Knutson (2018) Underestimated AMOC variability and implications for AMV and predictability in CMIP models. Geophysical Research Letters 45(9): 4319-4328.

Yang, T.-H., and G. N. Somero (1993), Effects of feeding and food deprivation on oxygen consumption, muscle protein concentration and activities of energy metabolism enzymes in muscle and brain of shallow-living (Scorpaena guttata) and deep-living (*Sebastolobus alascanus*) scorpaenid fishes, *Journal of Experimental Biology*, *181*(1), 213-232.

Yang, Y., V. Maselli, A. Normandeau, D. J. W. Piper, M. Z. Li, D. C. Campbell, T. Gregor and S. Gao (2020) Latitudinal Response of Storm Activity to Abrupt Climate Change During the Last 6,500 Years. Geophysical Research Letters 47(19): e2020GL089859.

Yesson, C., M. R. Clark, M. L. Taylor and A. D. Rogers (2011) The global distribution of seamounts based on 30 arc seconds bathymetry data. Deep Sea Research Part I: Oceanographic Research Papers 58(4): 442-453.

York, A. (2018) Marine biogeochemical cycles in a changing world. Nature Reviews Microbiology 16(5): 259-259.

Zabel, M., Boetius, A., Emeis, K.-C., Ferdelman, T. G., and Spieß, V. (2012) Process Studies in the Eastern South Atlantic –Cruise No. M76– Cape Town (South Africa) – Walvis Bay (Namibia), DFG Senatskommission für Ozeanographie, METEOR-Berichte, M76, 180 pp.

Zanden, M. J. V. and J. B. Rasmussen (2001) Variation in $\delta^{15}N$ and $\delta^{13}C$ trophic fractionation: implications for aquatic food web studies. Limnology and oceanography 46(8): 2061-2066.


PELAGIA

8. Appendices

Picture: RV Pelagia in the harbour of Horta, Azores

Contributing authors

Ana Colaço University of the Azores, Horta, Portugal

Anna de Kluijver Department of Earth Sciences, Utrecht University, Utrecht, Netherlands

André Freiwald Department for Marine Research, Senckenberg Institute, Wilhelmshaven, Germany

Andrew Davies Department of Biological Science, University of Rhode Island, Kingston, RI, USA

Benjamin Mueller Freshwater and Marine Ecology, Institute for Biodiversity and Ecosystem Dynamics, University of Amsterdam, Amsterdam, The Netherlands

Claudia Wienberg MARUM–Center for Marine Environmental Sciences, University of Bremen, Bremen, Germany

David Bowers Bangor University, School of Ocean Sciences, Anglesey, UK

Dierk Hebbeln MARUM–Center for Marine Environmental Sciences, University of Bremen, Bremen, Germany

Ellen Kenchington Fisheries and Oceans Canada (DFO), Bedford Institute of Oceanography, Dartmouth, NS, Canada

Emyr Martyn Roberts Department of Biological Sciences and K.G. Jebsen Centre for Deep-sea Research, University of Bergen, Bergen, Norway

Erik Wurz Wageningen University and Research, Department of Animal Sciences, Wageningen, Netherlands

Furu Mienis NIOZ-Royal Netherlands Institute for Sea Research, Den Burg, Texel, Netherlands

Gerard Duineveld NIOZ-Royal Netherlands Institute for Sea Research, Den Burg, Texel, Netherlands

Gert-Jan Reichart NIOZ-Royal Netherlands Institute for Sea Research, Den Burg, Texel, Netherlands and Department of Earth Sciences, Utrecht University, Utrecht, Netherlands

Hans Tore Rapp† Department of Biology and K.G. Jebsen Centre for Deep Sea Research, University of Bergen, Bergen, Norway

Hans van Haren NIOZ-Royal Netherlands Institute for Sea Research, Den Burg, Texel, Netherlands

Jack J. Middelburg Department of Earth Sciences, Utrecht University, Utrecht, Netherlands

Jasper M. de Goeij Freshwater and Marine Ecology, Institute for Biodiversity and Ecosystem Dynamics, University of Amsterdam, Amsterdam, The Netherlands

Kathrin Busch GEOMAR Helmholtz Centre for Ocean Research Kiel, Kiel, Germany

Katriina Juva GEOMAR Helmholtz Centre for Ocean Research Kiel, Kiel, Germany

Leonardo Tamborrino MARUM–Center for Marine Environmental Sciences, University of Bremen, Bremen, Germany

Lindsay Beazley Fisheries and Oceans Canada (DFO), Bedford Institute of Oceanography, Dartmouth, NS, Canada

Marc Lavaleye NIOZ-Royal Netherlands Institute for Sea Research, Den Burg, Texel, Netherlands

Marcel van der Meer NIOZ-Royal Netherlands Institute for Sea Research, Den Burg, Texel, Netherlands

Martijn C. Bart Freshwater and Marine Ecology, Institute for Biodiversity and Ecosystem Dynamics, University of Amsterdam, Amsterdam, The Netherlands

Philip Riekenberg NIOZ-Royal Netherlands Institute for Sea Research, Den Burg, Texel, Netherlands

Sascha Flögel GEOMAR Helmholtz Centre for Ocean Research Kiel, Kiel, Germany

Wolf-Christian Dullo GEOMAR Helmholtz Centre for Ocean Research Kiel, Kiel, Germany

Bibliography

Hanz, U., Bart, M., Mueller, B., de Goeij, J. M., Busch, K., Roberts, E.M., Bowers, D., Reichart, G.-J., Rapp, H.T., Mienis, F. **(in preparation)** Oxygen uptake and inorganic nutrient dynamics in an Arctic deep-sea sponge ground: the sponge ground effect.

Hanz, U., Riekenberg, P., de Kluijver, A., van der Meer, M., Middelburg, J.J., de Goeij, J.M., Bart, M.C., Wurz, E., Colaço, A., Duineveld, G., Reichart, G.-J., Rapp, H.T., Mienis, F. **(in review)** Are sponges at the top and bottom of the food web in a benthic deep-sea biological hotspot? Functional Ecology.

Liu, F., Daewel, U., Samuelsen, A., Brune, S., **Hanz, U.**, Pohlmann, H., Baehr, J., Schrum, C. **(accepted)** Can environmental conditions at North Atlantic deep-sea habitats be predicted several years ahead? ---- Taking sponge habitats as an example. Frontiers in Marine Science.

Hanz, U., Roberts, E. M., Duineveld, G., Davies, A., Rapp, H.T., Reichart, G.-J., Mienis, F. **(2021)** Long–term observations at an Arctic deep-sea sponge ground reveal important food supply mechanisms. Journal of Geophysical Research: Oceans, 126(3), e2020JC016776, doi:10.1029/2020JC016776

Hanz, U., Beazley, L., Kenchington, E., Duineveld, G., Rapp, H-T., Mienis, F. **(2021)** Seasonal variability in near-bed environmental conditions in the *Vazella pourtalesii* glass sponge grounds of the Scotian Shelf. Frontiers in Marine Science, doi:10.3389/fmars.2020.597682

de Kluijver, A., Nierop, K. G., Morganti, T. M., Bart, M. C., Slaby, B. M., **Hanz, U.**, de Goeij, J. M., Mienis, F., and Middelburg, J. J. **(2021)** Bacterial precursors and unsaturated long-chain fatty acids are biomarkers of North-Atlantic demosponges, PloS one, 16(1), e0241095, doi:10.1371/journal.pone.0241095

Maldonado, M., Beazley, L., López-Acosta, M., Kenchington, E., Casault, B., **Hanz, U.**, Mienis, F. **(2020)** Massive silicon utilization facilitated by a benthic-pelagic coupled feedback sustains deep-sea sponge aggregations. Limnology and Oceanography, doi:10.1002/lno.11610.

Busch, K., **Hanz, U.**, Mienis, F., Müller, B., Franke, A., Roberts, E.M., Rapp, H.T., Hentschel, U. **(2020)** On giant shoulders: How a seamount affects the microbial community composition of seawater and sponges. Biogeosciences, 17, 3471-3486, doi:10.5194/bg-17-3471-2020.

Hanz, U., Wienberg, C., Hebbeln, D., Duineveld, G., Lavaleye, M., Juva, K., Dullo, W.-C., Freiwald, A., Tamborrino, L., Reichart, G.-J., Flögel, S. and Mienis, F. **(2019)** Environmental factors influencing cold-water coral ecosystems in the oxygen minimum zones on the Angolan and Namibian margins. Biogeosciences (BG), 16 (22). pp. 4337-4356. doi: 10.5194/bg-16-4337-2019

Roberts, E. M., Mienis, F., Rapp, H. T., **Hanz, U.**, Meyer, H. K., & Davies, A. J. **(2018)** Oceanographic setting and short-timescale environmental variability at an Arctic seamount sponge ground. Deep Sea Research Part I: Oceanographic Research Papers, 138. doi: 10.1016/j.dsr.2018.06.007

Van Haren, H., **Hanz, U.**, de Stigter, H., Mienis, F., Duineveld, G. **(2017)** Internal wave turbulence at a biologically rich Mid-Atlantic seamount. PloS one, 12(12), e0189720. doi: 10.1371/journal.pone.0189720

Picture next page: *Geodia barretti* on board of the RV GO Sars


0 1 2 3 4 5 6 7 8 9 10 11 12 13 14 15 16 17 18 19 20 21 22 23 24 25
10 cm

Acknowledgements

Writing a thesis is a lot of work, which I could never have done alone. Therefore I would like to thank my co-authors as well as some other people for their support:

First of all I would like to thank my supervisor **Furu**. You made all of this possible. Thanks for choosing me as your PhD and trusting me through all these years. You gave me the possibility to go on so many cruises, conferences and meetings and introduced me to many amazing scientists. Without you all these great collaborations would have never happened. I think, I had one of the best PhDs that anyone could imagine. We always had a great time during the field work and conferences. Thank you also for teaching me to be more patient and to be more precise with a lot of things, that really helped me also in other parts of my life. And of course, thank you for teaching me about the deep sea with its cold-water coral reefs and sponge grounds, you have been a great inspiration.

A big thanks also to my promotor **Gert-Jan** who always gave me valuable insight into the geological aspects of my work. You always trusted us with what we are doing and gave us the freedom to do all of the science we wanted. Especially your comments and skills about writing nice, logical and comprehensive texts helped my manuscripts a lot.

Thank you also to **Gerard**. You are officially retired now, but you still have an open ear for any questions and with your infinite knowledge about the benthos of the North Atlantic you helped me a lot. You also have the magic skill to find every hidden weakness in a manuscript and help to improve it. **Marc**, thank you also for always helping with the identification of every benthic animal there might be in our oceans.

I thank the **dissertation committee** for reading and evaluating my thesis.

Without the **European Union** and their science program this project would have never existed. And since sometimes people don’t see the benefits of being a member of the EU, here you have one. Thank you for funding the SponGES project. A special thanks I would like to give to the project leader Hans Tore. He initiated the SponGES project due to his passion for sponges but he was unfortunately taken from us much too early. Nevertheless his legacy will proceed since he managed to bring all of us together to do science and showed us how cool sponges can be. We will never forget him and his positive energy.

A really big thank you also to all my **SponGES colleagues**. I was always looking forward to our amazing cruises, conferences and meetings. A special thanks I would like to give to **Martijn**. You started with me as the next generation of Furu and Jasper. Unfortunately you were situated in Amsterdam, but that didn’t stop us from working together on our projects. You were always there for me, when something was not working out or when I wanted to complain about our supervisors (which of course never happened). I will never forget our writing retreat on the Azores and our adventures in Colombia. Not many people can say that they were hiking through the jungle of Colombia, were swimming in Vulcanic ponds in the middle of the Atlantic and were collecting sponges from the seafloor of the Arctic deep sea with their colleague. Thanks also to **Erik** (the Viking), it was always a pleasure to work with you since you always have a funny comment to give. I hope you will manage to teach the new generation of Dutch scientist how to properly dive (don’t forget the snorkel!). Thank you also to the rest of the Dutch crew: **Jasper, Ben, Erik, Anna, Jack**. You teached me a lot about sponges, their metabolism and their fatty acids. Thanks also to the different teams of our project (some but not all): The (former) UK crew, **Martyn and Andy (& David)**. You both are the most funny people I know. Thank you for always making me laugh so much. Thanks also to the Canadian crew**, Ellen, Javier and Lindsay**, the Geomar crew, **Katrin, Beate and Ute**, the Spanish crew (especially the master of silicate - **Manuel**), the Azores team and the (former) Norwegian team, **Joana, Hans-Tore, Heidi**. And of course everyone else of this project that I didn’t mention here. You all have been a great inspiration.

A big thanks also to my NIOZ PhD colleagues: **Sofia**, thank you for all the good times we had in the Potvis and the rest of the world. Our best adventure were definitely (so far) to travel through Colombia and flying to New York for Christmas shopping. You are not only the best shopping buddy in the world, but also a great soul that is always a pleasure to spend time with. **Stanley**, you are the coolest Asian I know. You were my office neighbour, which always supplied me with snacks. Without you, I would probably have starved during my PhD. You teached us the magic of hotpot and other Asian food, which fed us during many evenings in the Potvis. Actually when I think about you, I think about food. Spareribs in the 12 Balcken or Lobster in New York City, we always found the best stuff. **Siham**, you are energetic like a nuclear explosion, but in a positive way. Thank you for always bringing some happy energy. **Sabine,** thanks for the fun we had, especially on the cruise to the Azores, but also the climbing and swimming in Den Helder. **Eveline**, thank you for being the best office mate I could have wished for. **Linda**, my Bonn buddy, thank you for introducing me to everything on Texel and to “Darwins choice”, it’s still my favourite game. You showed me how to have a different view on things and how we can make the world every day a bit better. I hope you are next with your defence. **Sarina**, thank you for all the good times we had in the Potvis and on Texel. I will never forget our swimming sessions, concerts on Texel and of course - Frank Turner. **Simone**, weird coincidences brought you on my Potvis couch. Since then, we had a lot of good times together. I hope we will enjoy some more real Austrian Schnitzel, Spritzer, cocktails in the Caribbean or relaxing times in the Texel spa in the future. Thanks for complaining with me about the world, I think you are the only person that can complain as much as I do. **Marcel and Philip**, thanks for your nice ideas and the help with all my isotopic questions. You guys are definitely the masters of isotopes. **Nadine**, thank you for all the nice conversations about science. I hope we keep on celebrating our accepted papers with champagne in the future! **Hans**, we met each other at the North Pole and since then we had many nights with a lot of beer - from the winch room to the Potvis bar. Where do we meet next? A special thanks also for bringing this super cool

student to the NIOZ, I kept him. A big thanks also to my other NIOZ colleagues, co-authors, technicians and all the Potvis people that I meet during the years. Some but not all in random order: **Milou, Onno, Jonathan, Coral, Ella, Sandra, Evert, Katriina, Matthijs, Rick, Esmee, Hans, Loes, Magda, Evaline, Lise, Lennart, Sharyn, Karel, Piet, Bob, Ronald, Kristin, Indah, Szabina, Sabine, Femke, Laurent, Matthew, Peter, Alice, Wim, Laura, Michelle, Rob, Geert-Jan, Henko, Jan-Berend, Judith, Fons, Marc and all of the ones I didn't name here because I temporarily don't remember**. And not to forget my student **Django**, thanks for helping me with the analyses. And thanks to all the **dogs (Kiko, Almond, Pili and many more)** that I took care of during my time in the Potvis, you were great mental support animals. I will always have some spare bacon for you.

Thanks also to the **NIOZ workshop**. You can literally build everything and you are always open to help with fun projects with some deep sea monsters. I think every institute should have a workshop like yours. Thanks also to the **crew of the RV Pelagia and all the other research vessels** I have been on. You guys (and girls) were not only always super helpful but we also had a lot of fun during the cruises and in the harbours. Without you, we would (probably) be lost and couldn't do any research.

Last but not least I would like to thank my family. **David**, I met you right at the beginning of my PhD and and since then you never left again (only temporarily for Antarctica). We had a lot of fun in the NIOZ and many amazing adventures together (South America, US, Caribbean,..) and we probably will have many more in the future. You always supported me in everything I am doing and I am incredibly thankful for all of this. I am sure it is not always (super) easy with me but I hope you also enjoy every moment we have together as much as I do. Without you, my PhD might not have been as crazy, fun and successful. And of course, thanks to **Vivi**, my little baby. You were born at the end of my PhD and keep me busy during the hours I am not working. You add so much meaning to everything and I hope you will also like the oceans (and sponges!) in the future. I will teach you about the deep sea very soon.

Ein großes Danke auch an meine **Mama** and meinen **Papa**, ihr wart wirklich immer für mich da und habt mich immer unterstützt. Es ist gut zu wissen, dass ich bei euch immer ein Zuhause habe. Danke auch an den Rest von meiner ganzen Familie. Ihr habt nicht immer verstanden was ich so mache aber wart trotzdem interessiert an meinen Expeditionsgeschichten. Ich hoffe es ist euch jetzt klar geworden, dass ich nicht immer nur „in Urlaub“ war, sondern tatsächlich Wissenschaft auf meinen ganzen Expeditionen betrieben habe😉.

Und ein großes Danke auch an alle meine Freunde, die nichts mit der Wissenschaft am Hut haben: **Motte, Caro, Ben, Don, Sandra, Marie, Rosa, Fabian, Ornella, Hendrik, Jan** und viele andere. Ihr habt immer interessiert zugehört wenn ich Geschichten von meinen Expeditionen und der Tiefsee erzählt habe. Ich bin so froh euch zu haben und dass ich mit euch ab und zu die Wissenschaft vergessen kann.

Thank you also to my new supervisor, **Moritz**, and my current working group at the Alfred Wegener Institute for giving me the chance to go on with science. I am looking forward to work with you in the coming years.

Thanks


RV Pelagia 2016


RV G.O. Sars 2017


CCGS Hudson 2018


RV G.O. Sars 2018


Saba Bank 2018

About the author

Ulrike Beatrix Hanz was born on the 01. April 1989 in Bonn, Germany. She enrolled in the Bachelor of Science Biology at the University of Bonn and wrote her thesis on “Verification of the interaction of Xin-repeat proteins with potential binding partners”. Since the exclusive lab-work during her Bachelor thesis did not fulfil her passion for exploring the world, she enrolled at the same time for the Master course “Tropical ecology”, which included an expedition to the Brazilian jungle. Because of this expedition, she decided to continue in an ecological field even though many people warned her about the job prospects. This led her to start her Master in Biological Oceanography at the GEOMAR-Helmholtz-Centre for Ocean Research/Christian Albrechts-University Kiel, where she discovered her passion for seagoing research during her Master thesis on “Structure of benthic communities from the Kattegat in relation to environmental drivers and historical data”. Since the warnings about job prospects were not groundless, she additionally completed the Master of Science in Agricultural Science/ Crop Science while she was witing for a matching PhD position. During that time, she also attended an expedition to the Arctic Ocean including a visit to the North Pole, which reinforced her to stay in Marine Science. In the beginning of 2016, she finally started a PhD at the NIOZ-Netherlands Institute for Sea Research on Texel in the EU-SponGES project, where she investigated deep-sea sponge grounds in the North Atlantic. During her PhD she attended seven research cruises all over the North Atlantic and collected valuable information about the physical, chemical and environmental conditions around deep-sea sponge grounds and how these underestimated animals are able to influence their environment.